PULSED POWER SYSTEM
脈衝功率系統

Po-Yu Chang

Institute of Space and Plasma Sciences, National Cheng Kung University

2024 Fall Semester

Thursday 9:10-12:00

Lecture 12

http://capst.ncku.edu.tw/PGS/index.php/teaching/

Online courses:

https://nckucc.webex.com/nckucc/j.php?MTID=mf87b10f22c1e36d5c4b2337e60d8a847

2024/12/26 updated

問卷調查

Grading

- Homework (Quizzes) – 30 % => 10 %
  - Design of each component of a pulsed-power system
- Final presentations – 70 % => 90 %
  - Design of a pulsed-power system – 35 %. => 45 %
    Presentation on 1/2.
  - Applications of pulsed-power system – 35 %. => 45 %
    Presentation on 1/9.

Final presentations on 1/2: design a Marx generator

姓名	V_{cap} (kV)	C (μF)	V_{out} (kV)
張元耀	30	5	600
廖梓翔	40	2	800
畢永葳	50	1	1000
賴柏佑	30	5	450
張書熏	40	2	600
林伯鴻	50	1	750
張博傑	30	5	300
雷子霆	40	2	400
李禎祐	50	1	500
林宴丞	30	5	750

- **Please send me your slides before class beginning at 9:10.**

Final presentations on 1/2: design a Marx generator

1. Based on the given capacitors and output voltage, please design a Marx generator.
2. Based on the Paschen's curve, please design the proper (control) spark-gap switch.
3. Please design a proper high-voltage generator that can trigger the control spar-gap switch.

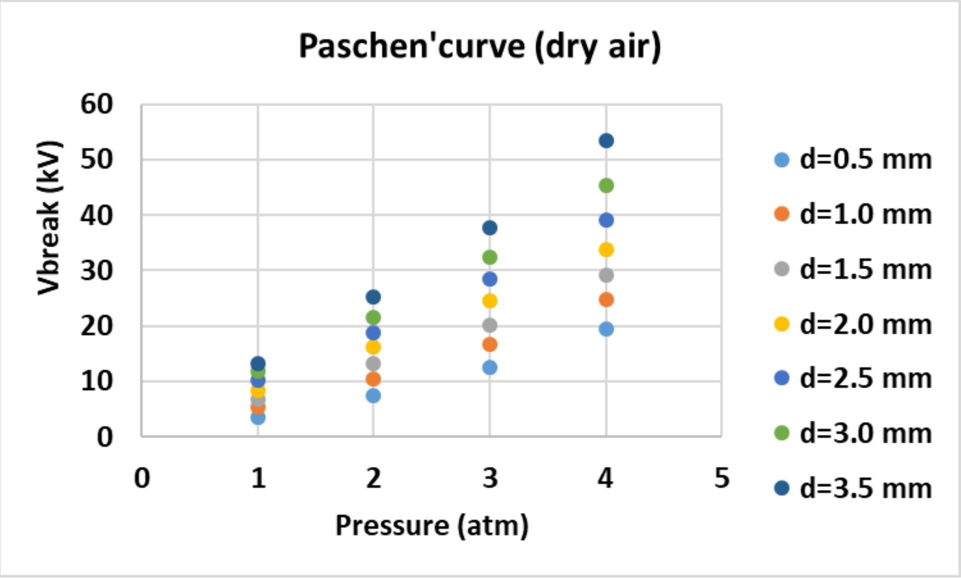

4. Please design an intermediate capacitor that can compress the pulse output.
5. Please design a proper voltage divider that can measure the output of the Marx generator using a scope that can read a highest voltage of 5 V.

Final presentations on 1/9: Applications of pulsed-power system

- 10 mins for each person
- Grading:
  - Time Score (2 points)
    - < 8 mins: 0 points
    - 8~9 mins: 1 points
    - 9~11 mins: 2 points
    - 11~12 mins: 1 points
    - >12 mins: 0 points
  - Pulsed-power related (2 points)
  - Understand the physics (10 points)
  - Presentation skill (10 points)
  - Slides (10 points)

Outlines

- Switches
  - Closing switches: the switching process is associated with voltage breakdown across an initially insulant element.
  - Opening switches: the switching process is associated with a sudden growth of its impedance.
- **Pulse-forming lines**
  - Blumlein line
  - Pulse-forming network
  - **Pulse compressor**
- Pulse transmission and transformation

Capacitor load

- **Pulse compression scheme: a charged capacitor can transfer almost all of its energy to an uncharged capacitor if connected through an inductor.**
- **Output voltage can be doubled in a peaking circuit.**

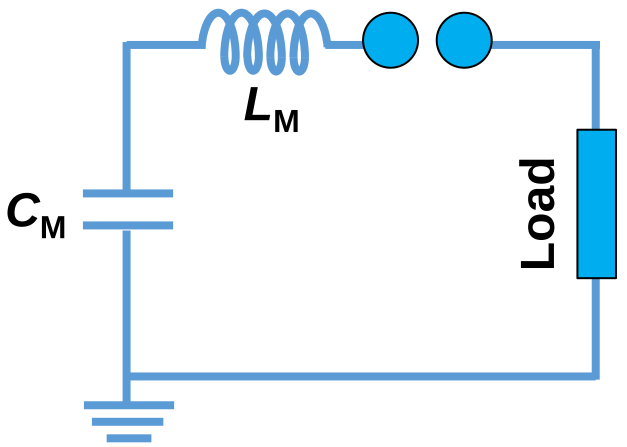

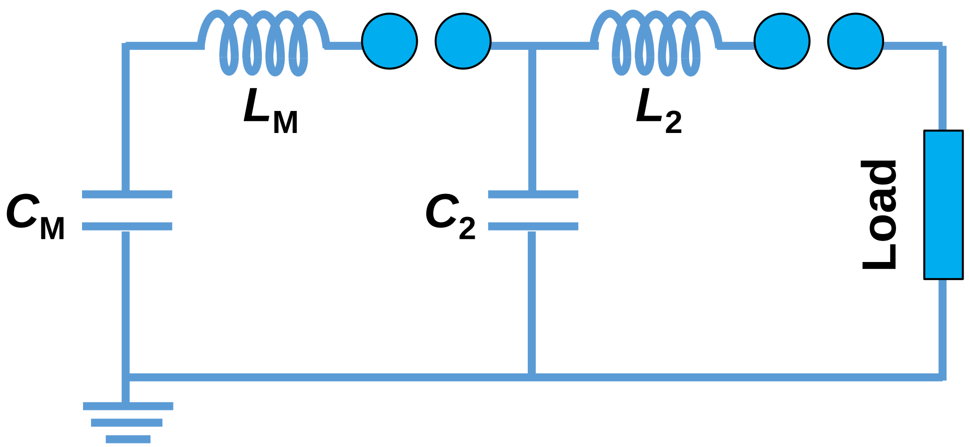

$$I_0 = \frac{V_0}{\sqrt{L_M/C_M}} \quad \omega_0 = \frac{1}{\sqrt{L_M C_M}}$$

$$I_2 = \frac{V_0}{\sqrt{L_2/C_2}} \quad \omega_2 = \frac{1}{\sqrt{L_2 C_2}}$$

$L_M > L_2$ => $I_M < I_2$ $\quad \omega_M < \omega_2$ $\quad T_M > T_2$

Capacitor load

$$V_1 - L_M \frac{\mathrm{dI}}{\mathrm{dt}} = V_2$$

$$V_1 = V_M - \frac{1}{C_M}\int I\,\mathrm{d}t \qquad V_M = \mathrm{NV_0}$$

$$V_2 = \frac{1}{C_2}\int I\,\mathrm{d}t$$

$$V_M - \frac{1}{C_M}\int I\,\mathrm{d}t - L_M\frac{\mathrm{dI}}{\mathrm{dt}} = \frac{1}{C_2}\int I\,\mathrm{d}t$$

$$-\frac{1}{C_M}I - L_M\frac{d^2I}{\mathrm{dt}^2} = \frac{1}{C_2}I \qquad L_M\frac{d^2I}{\mathrm{dt}^2} + \left(\frac{1}{C_M}+\frac{1}{C_2}\right)I = 0$$

$$\frac{d^2I}{\mathrm{dt}^2} + \frac{1}{L_M C_{\mathrm{eff}}}I = 0 \qquad \frac{1}{C_{\mathrm{eff}}} = \frac{1}{C_M} + \frac{1}{C_2} \qquad \omega = \sqrt{\frac{1}{L_M C_{\mathrm{eff}}}}$$

$$I = \alpha\sin(\omega t) + \beta\cos(\omega t)$$

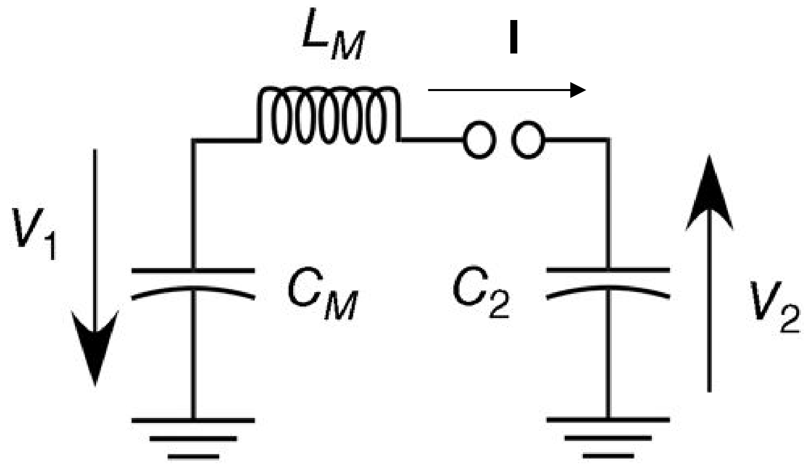

Capacitor load

$$I = \alpha\sin(\omega t) + \beta\cos(\omega t)$$

$$I(t=0) = 0 => \beta = 0$$

$$I = \alpha\sin(\omega t)$$

$$\frac{dI}{dt} = \alpha\omega\cos(\omega t)$$

$$L_M \frac{dI}{dt}\bigg|_{t=0} = L_M\alpha\omega = V_M \qquad \alpha = \frac{V_M}{L_M\omega}$$

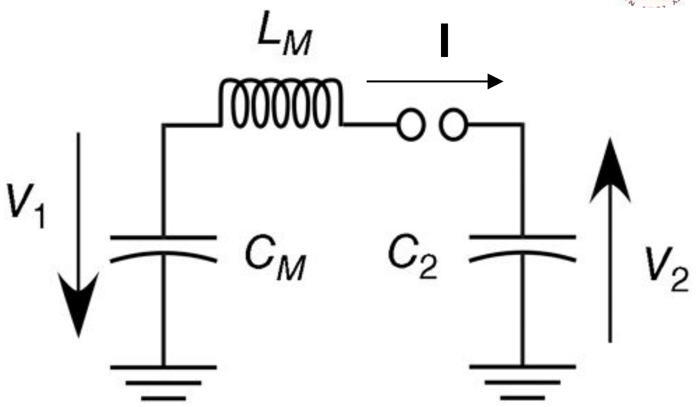

$$I(t) = \frac{V_M}{L\omega}\sin(\omega t)$$

$$V_1 = V_M - \frac{1}{C_M}\int_0^t \frac{V_M}{L\omega}\sin(\omega t)\,dt = V_M - \frac{V_M C_2}{C_M + C_2}[1 - \cos(\omega t)]$$

$$V_2 = \frac{1}{C_2}\int_0^t \frac{V_M}{L\omega}\sin(\omega t)\,dt = \frac{V_M C_M}{C_M + C_2}[1 - \cos(\omega t)] \qquad \frac{V_2}{V_M}\bigg|_{max} = \frac{2C_M}{C_M + C_2}$$

for $C_2 \sim C_M, \frac{V_2}{V_M} \sim 1$

Pulse compression scheme: $C_2 \sim C_M$

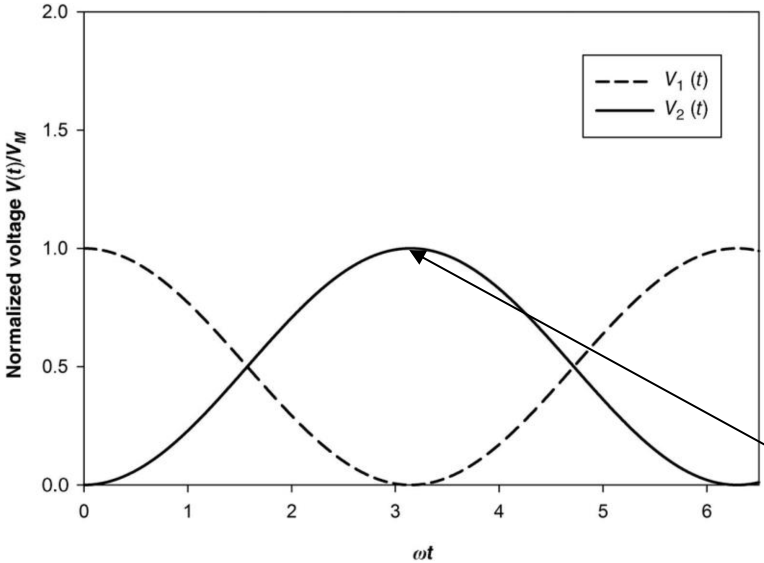

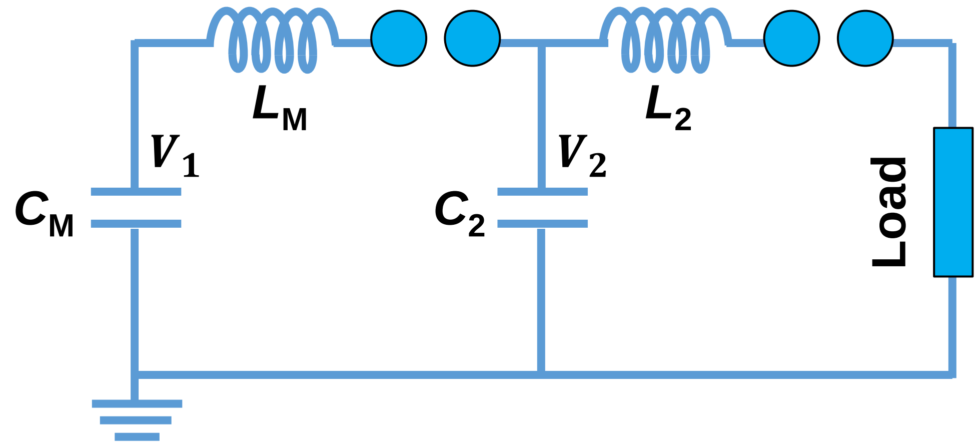

Energy is fully transferred to the 2nd cap, i.e., intermediate storage capacitor.

$$V_1 = V_M - \frac{V_M C_2}{C_M + C_2}[1 - \cos(\omega t)] \approx V_M - \frac{V_M}{2}[1 - \cos(\omega t)]$$

$$V_2 = \frac{V_M C_M}{C_M + C_2}[1 - \cos(\omega t)] \approx \frac{V_M}{2}[1 - \cos(\omega t)]$$

$$\text{For } t = \frac{\pi}{\omega}, \qquad V_1 \approx 0, \qquad V_2 \approx V_M$$

Water is commonly used as the dielectric material for the intermediate capacitor

$$C = \frac{2\pi\epsilon_r\epsilon_0}{\ln(b/a)} l \qquad \text{For } \frac{b}{a} = \frac{1}{0.9} \approx 1.1$$

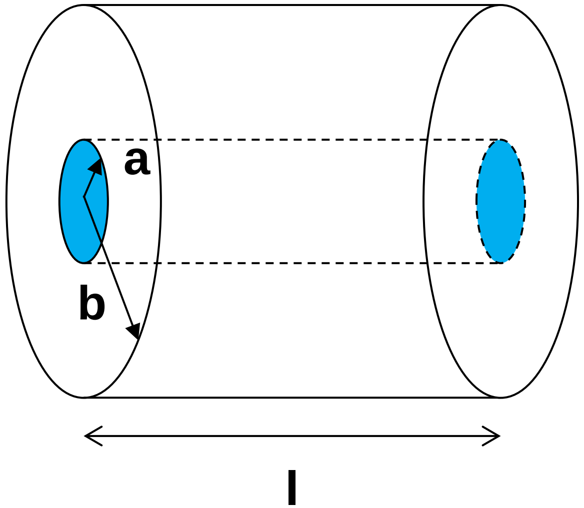

- **The gap between two cylinders need to be able to handle the high voltage.**

$$\text{Air: } \epsilon_r = 1 => \frac{C}{l} = 0.5 \times 10^{-9}\, F/m$$

$$\text{Water: } \epsilon_r = 80 => \frac{C}{l} = 4 \times 10^{-8}\, F/m$$

Ex: KALIF, bipolar Marx generator, charged up to ±100 kV. $V_{M,out}$=5 MV.

$$C_M = \frac{0.5\mu\text{F}}{25} = 25\text{nF}$$

$$\text{Using air: } \quad \text{l} = \frac{25 \times 10^{-9}}{0.5 \times 10^{-9}} = 50 \text{ m}$$

$$\text{Using water: } \quad \text{l} = \frac{25 \times 10^{-9}}{4 \times 10^{-8}} = 0.625 \text{ m}$$

Intermediate storage capacitors can be used to compress the pulse

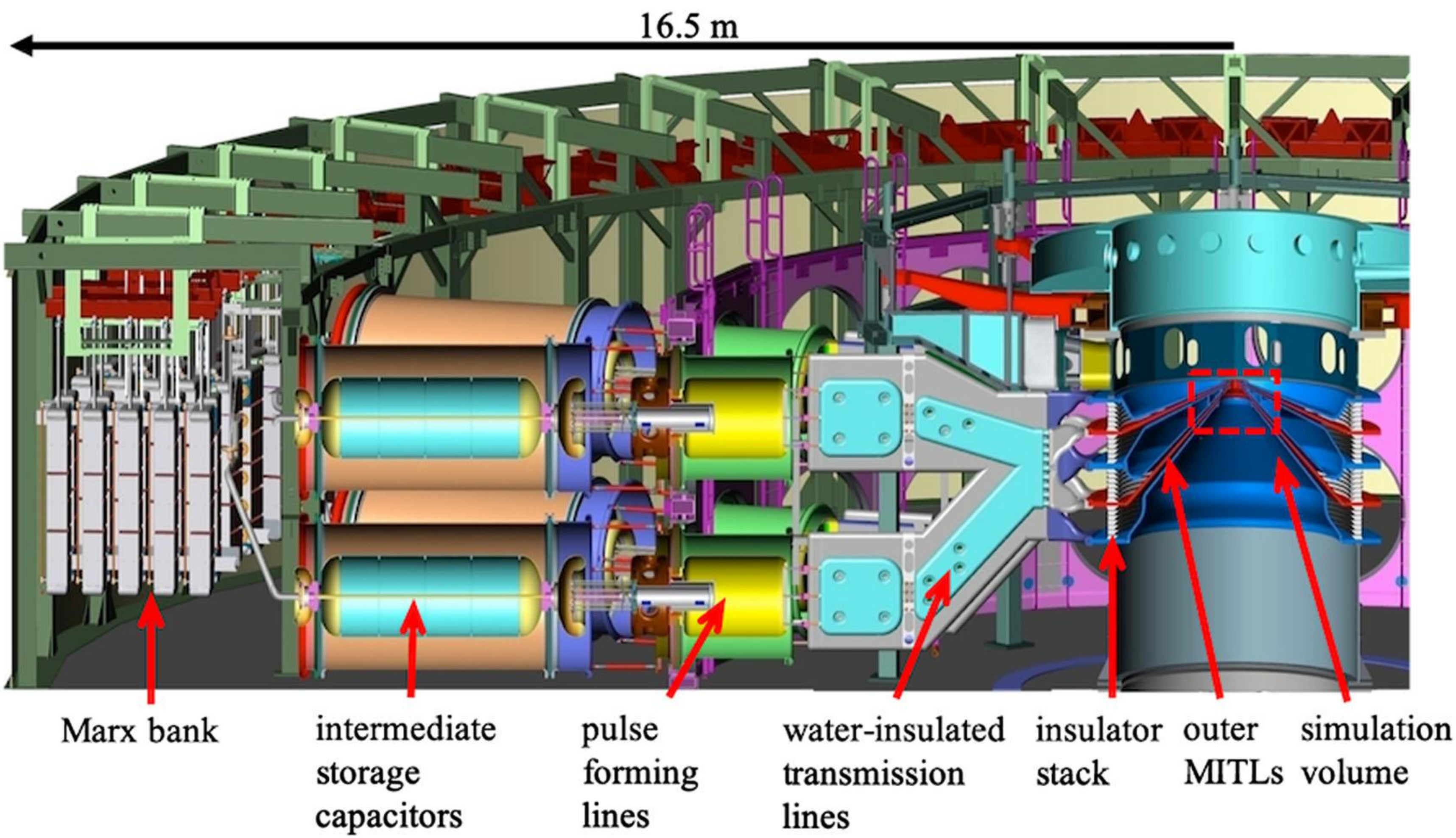

Outlines

- Switches
  - Closing switches: the switching process is associated with voltage breakdown across an initially insulant element.
  - Opening switches: the switching process is associated with a sudden growth of its impedance.
- Pulse-forming lines
  - Blumlein line
  - Pulse-forming network
  - Pulse compressor
- **Pulse transmission and transformation**

Insulating interface separating the vacuum section and the liquid dielectric is needed

- **Some tasks in science and technology required brightness of intense pulsed radiation > 100 TW/cm^2-Sr. With E > 1 MJ, electric power > 100 TW, electric power flux density > 100TW/m^2 are needed.**
- **Vacuum environment is required.**
- **High-voltage pulse must enter a vacuum vessel hosting the source through an insulating interface separating the liquid dielectric from the vacuum section.**

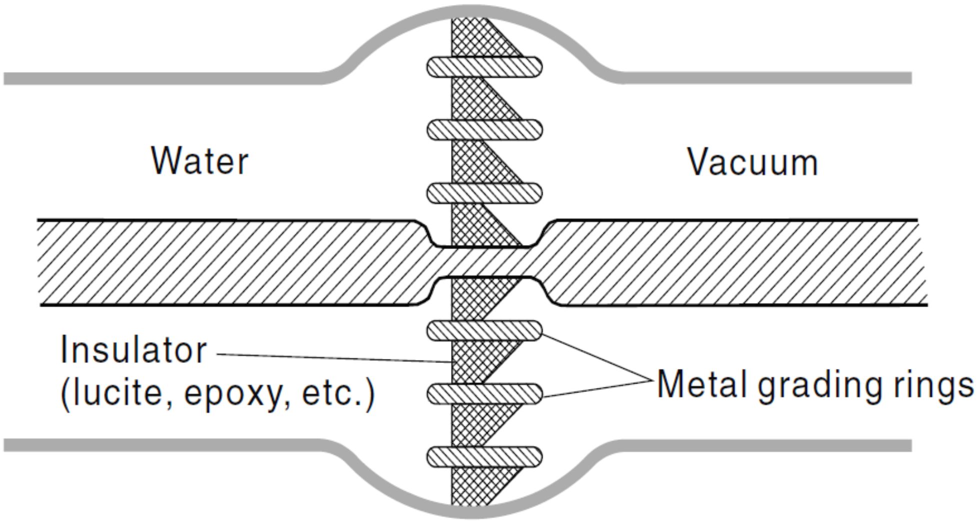

The interface consists of insulating rings separated by metallic grading rings

- **The metal grading rings are used to distribute the potential homogeneously over the interface on the vacuum surface.**
- **The metallic and dielectric rings are sealed to hold the high vacuum either by O-rings or by Metal-to-dielectric bond.**
- **Sparking on the surface on the vacuum side is more important.**
- **Electrons may be produced by field emission on metallic surfaces.**

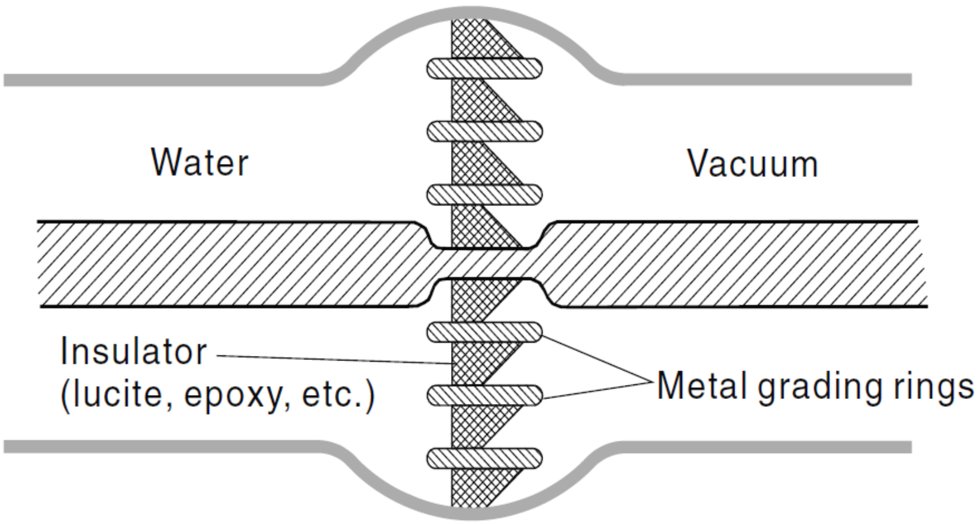

The side surface of the dielectric material is tilted to prevent flash over

- **Out gassing: gas from the "absorbs" released by electron bombardment.**
- **Electron avalanches may occur with the tangential electric field from the space charge on insulator.**

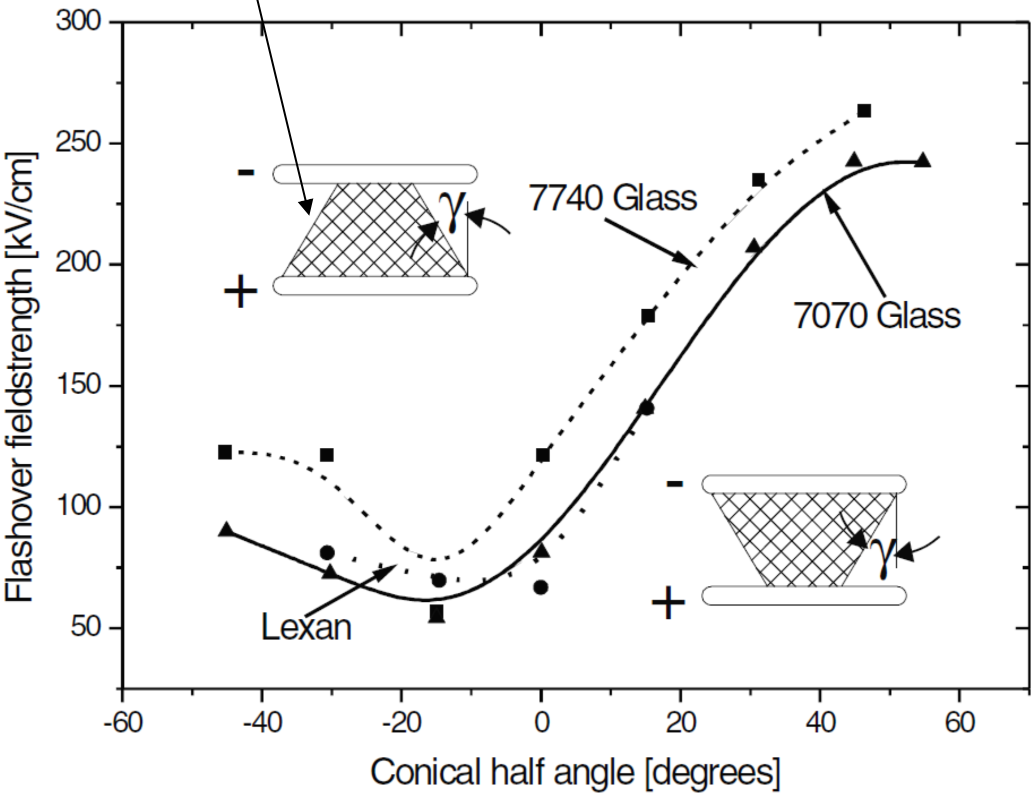

- **Dielectric-vacuum interface is the weakest element of a high-voltage pulse line under E-field stress.**

$$E_{\mathrm{DB}} = \frac{7 \times 10^5}{t^{1/6} A^{1/10}} (V/m)$$

- **t: time when E > 87% E_{max}.**
- **For t=10 ns, E_{max}=20MV/m, Max power density that can be delivered is 1 TW/m^2.**

Self-magnetic insulation

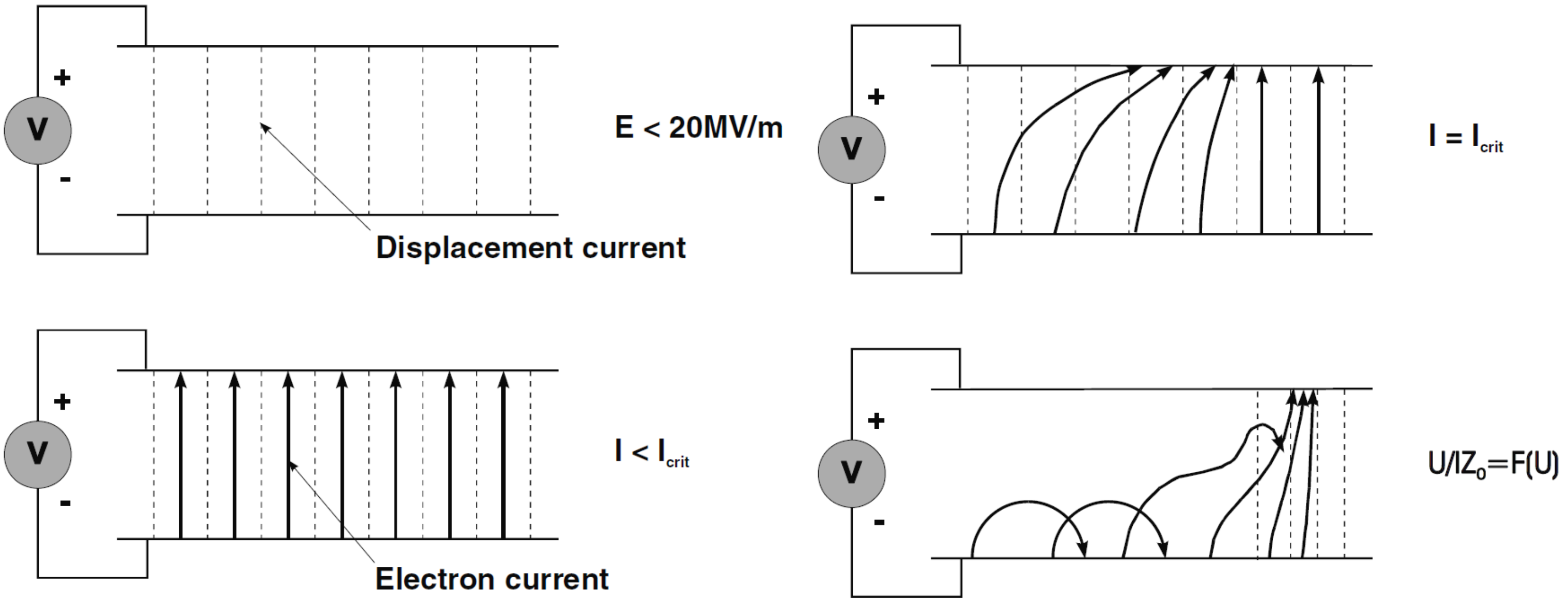

- For E > 20 MV/m, homogeneous plasma layer is generated within a few nanosecond.
- For $I > I_{crit}$, electron orbits can no longer reach the anode => more and more sections are insulated. => An electron sheath forms on the negative conductor.

Electromagnetic shock wave is formed

- **The propagation velocity of the loss front is less than the speed of light, c.**
- **As long as the voltage ramp remains below the breakdown threshold, the wave propagates at the speed of light.**

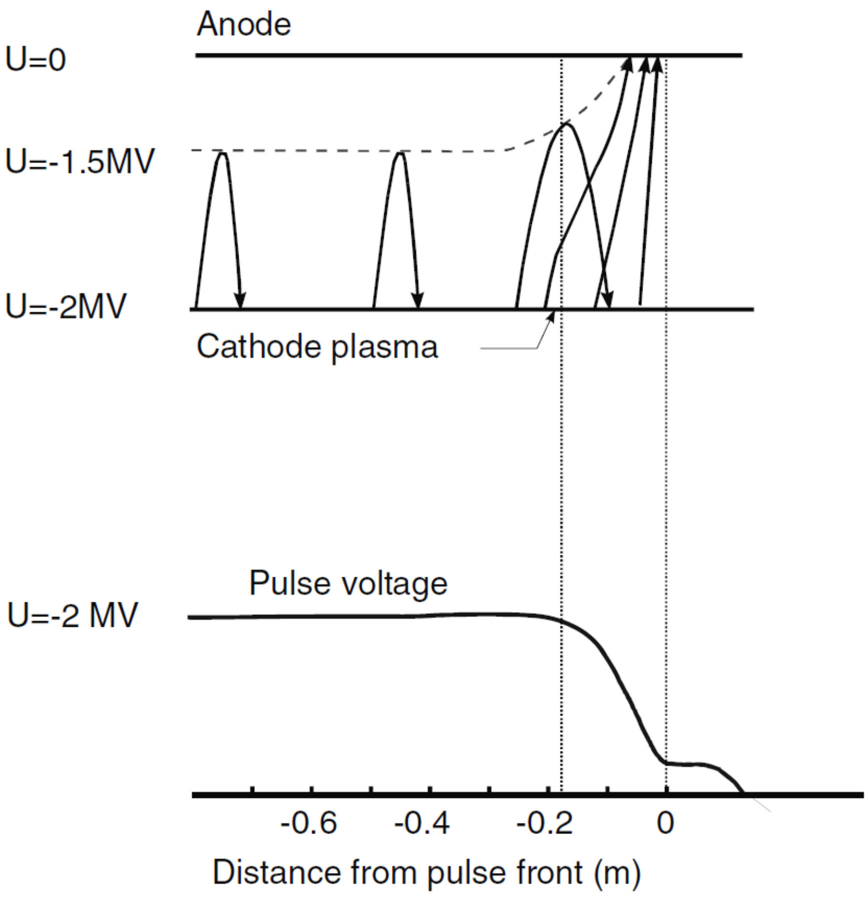

Pulse transformers

- **High-voltage transformers: used for transformation of current, voltage, impedance, polarity inversion, insulation and coupling between circuits at different potentials.**
- **Based on magnetic coupling between two conducting circuits.**
- **Perfect or ideal transformer: no ohmic losses, no eddy currents, without hysteresis and stray field => magnetic flux goes completely through both the primary and second coil.**
- **Faraday's law:**

$$U_1 = N_1 \frac{d\phi}{dt}$$

$$U_2 = -N_2 \frac{d\phi}{dt}$$

$$\frac{U_2}{U_1} = -\frac{N_2}{N_1}$$

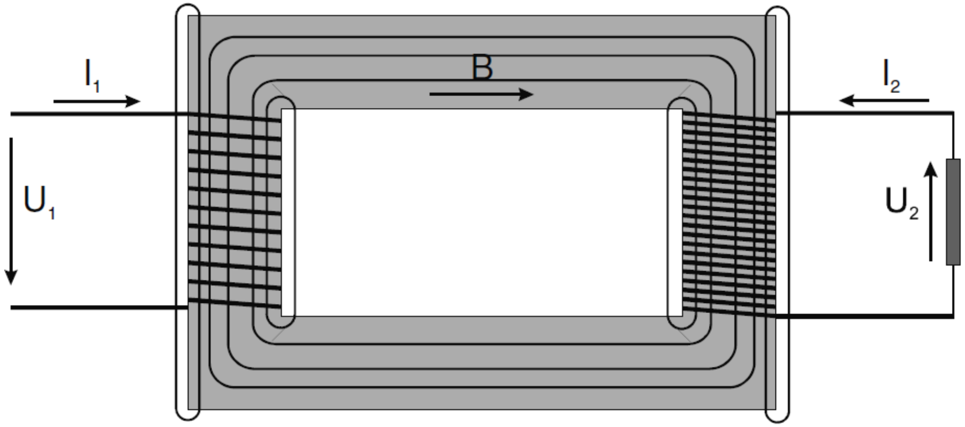

The transformer rise the voltage but reduce the current

$$U_1 = N_1 \frac{d\phi}{dt} \qquad \frac{U_2}{U_1} = -\frac{N_2}{N_1}$$

$$U_2 = -N_2 \frac{d\phi}{dt}$$

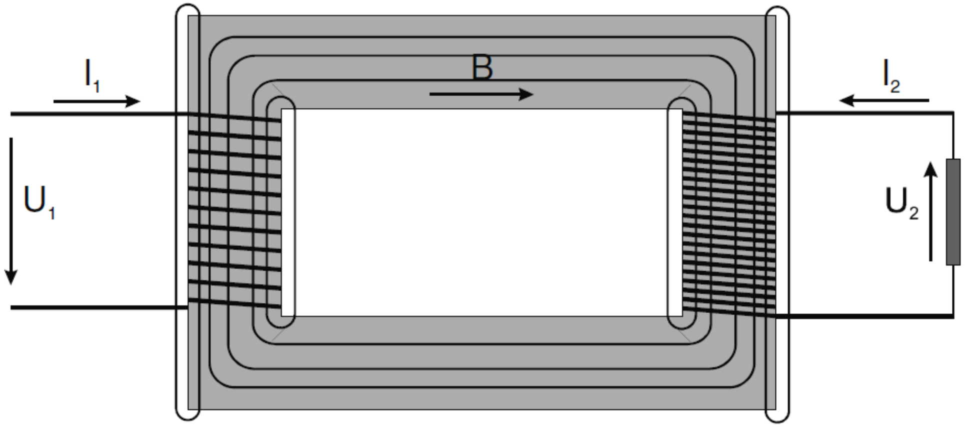

- For open circuit, i.e. secondary coil is open => ϕ is caused by i_1 only:

$$i_{10} = \frac{U_1}{i\omega L_1}$$

- If a load of complex impedance Z is connected to the secondary coil:

$$i_2 = \frac{U_2}{Z} \qquad N_2 i_2 = N_1 i_1{}'$$

Additional flux from the secondary coil is compensated from primary coil.

$$i_1{}' = i_{10} + i_1{}' = i_{10} - \frac{N_2}{N_1} i_2 \qquad \text{Power} = (i_1{}' - i_{10}) U_1 = -\frac{N_2}{N_1} i_2 U_1 = i_2 U_2$$

- If $i_{10} << \frac{N_2 i_2}{N_1}$ => $i_1 = -\frac{N_2}{N_1} i_2$

Rectifier

- **Half-wave rectifier:**

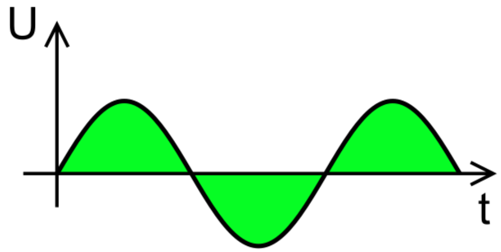

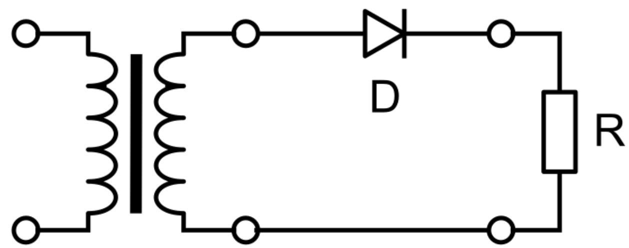

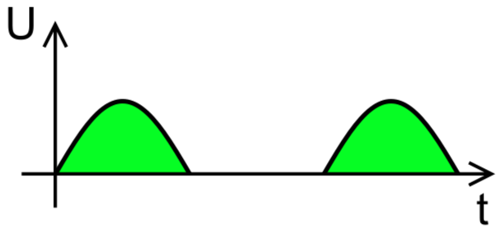

- **Center-tapped full-wave rectifier:**

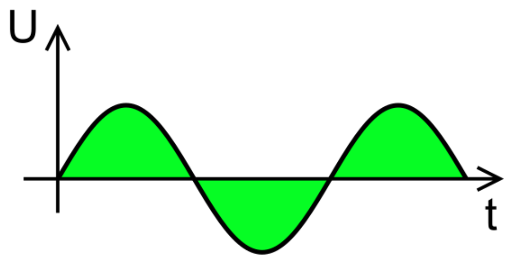

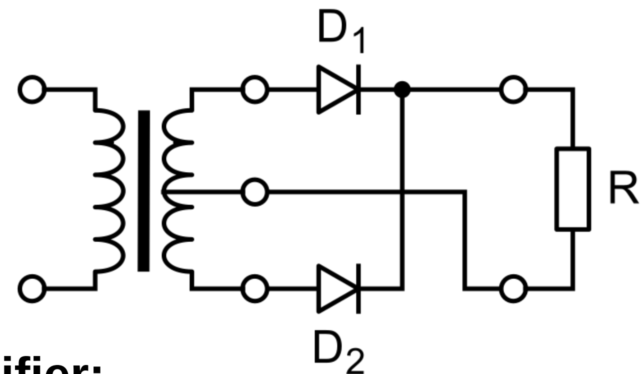

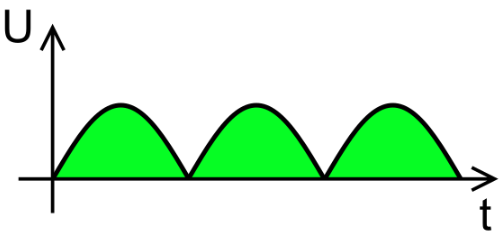

- **Full-wave bridge rectifier:**

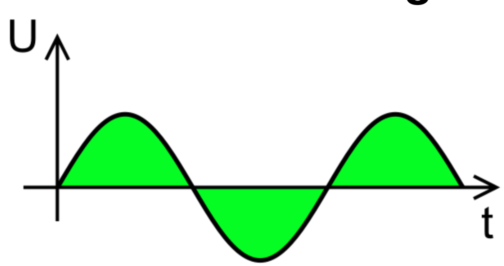

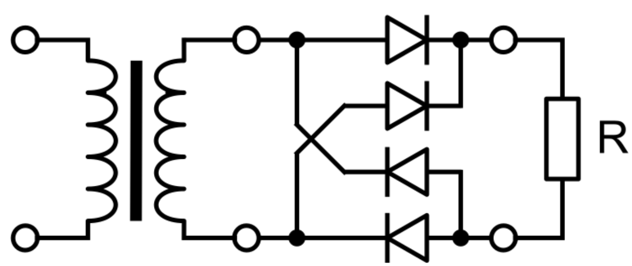

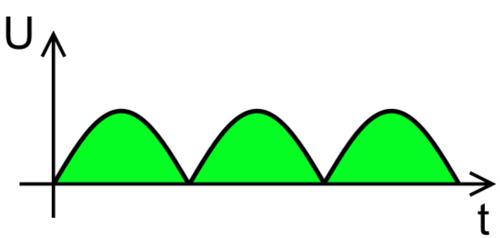

https://zh.wikipedia.org/wiki/%E6%95%B4%E6%B5%81%E5%99%A8

Full-wave rectifier with smoothing capacitor

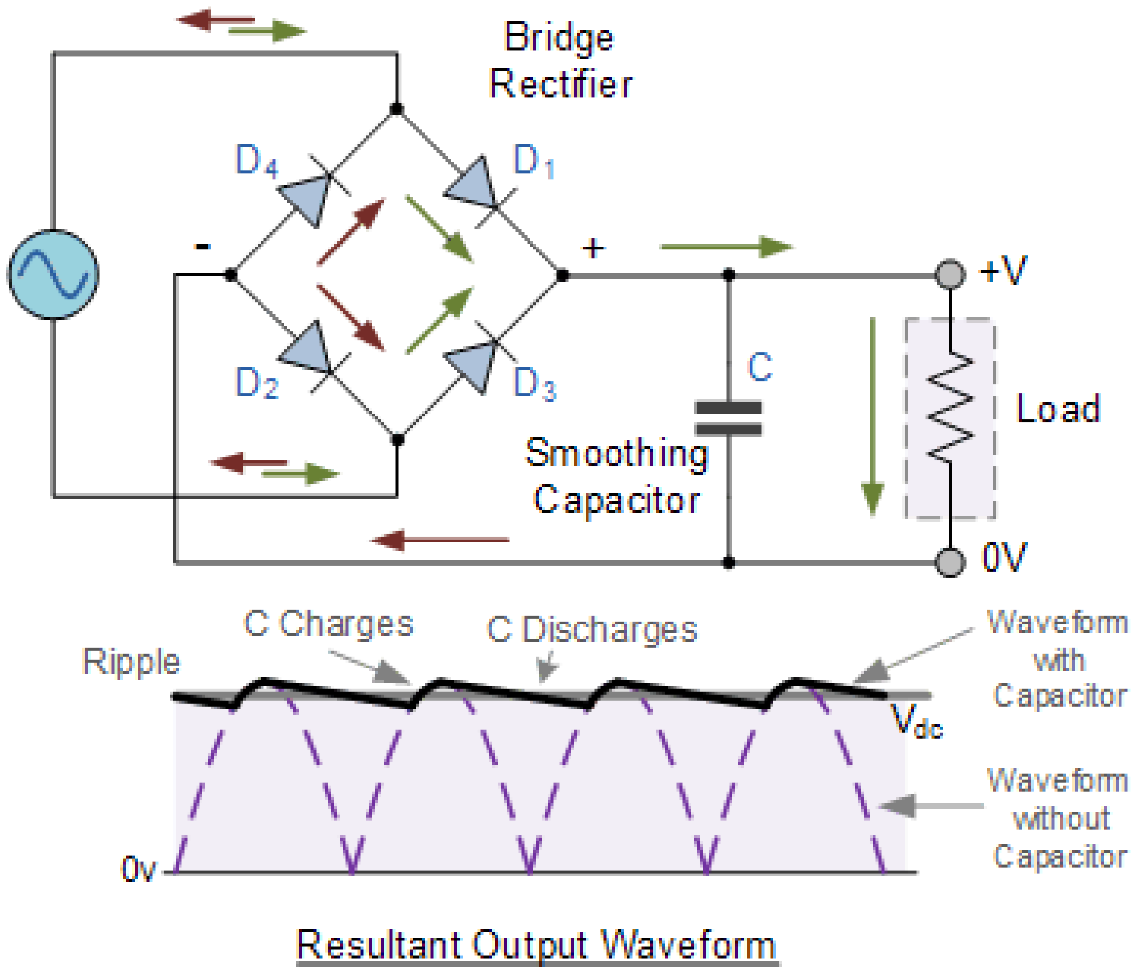

https://electronics.stackexchange.com/questions/363454/smoothing-a-full-wave-rectifier-voltage

Dual output

- **Positive cycle:**

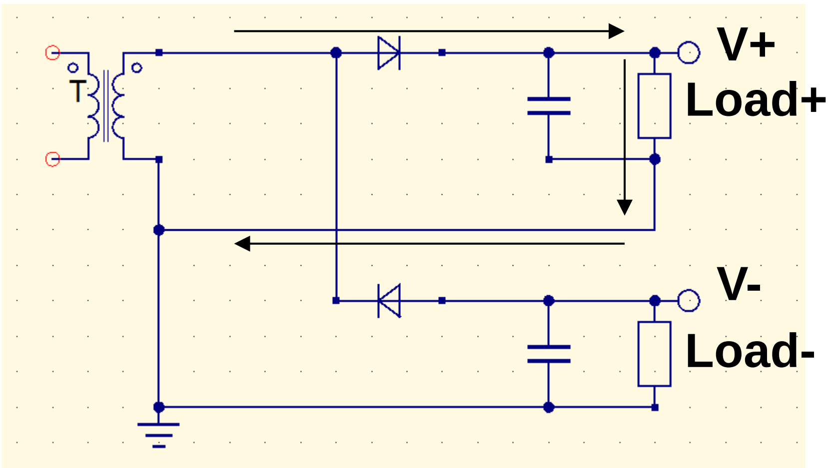

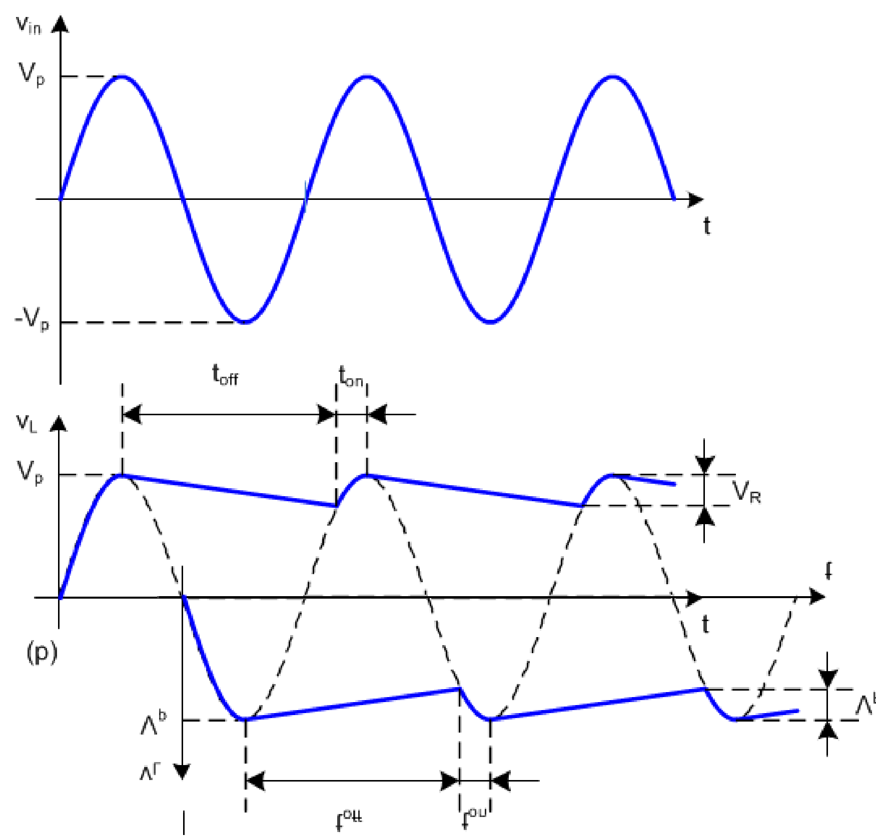

- **Negative cycle:**

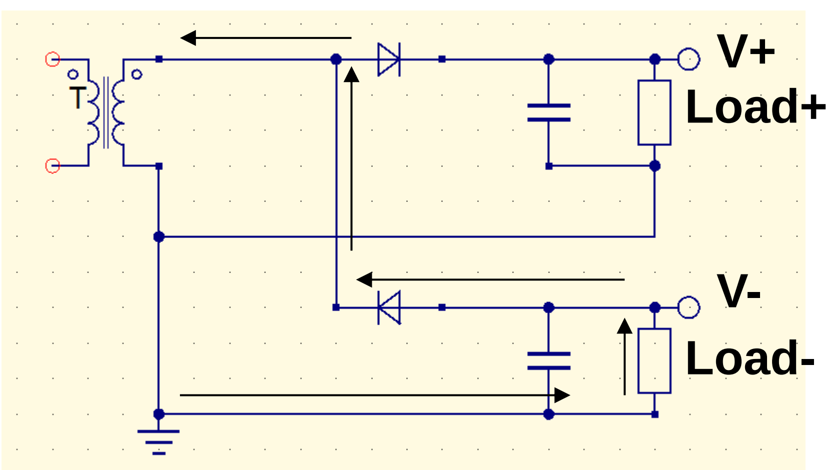

http://www.electroniccircuits.be/?page_id=267

Voltage multiplier (Cockcroft–Walton (CW) generator)

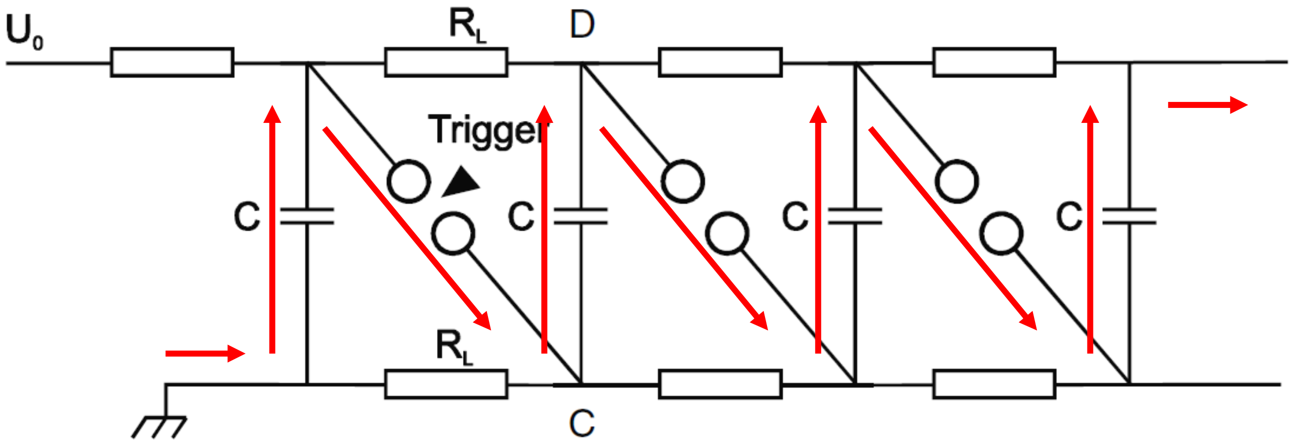

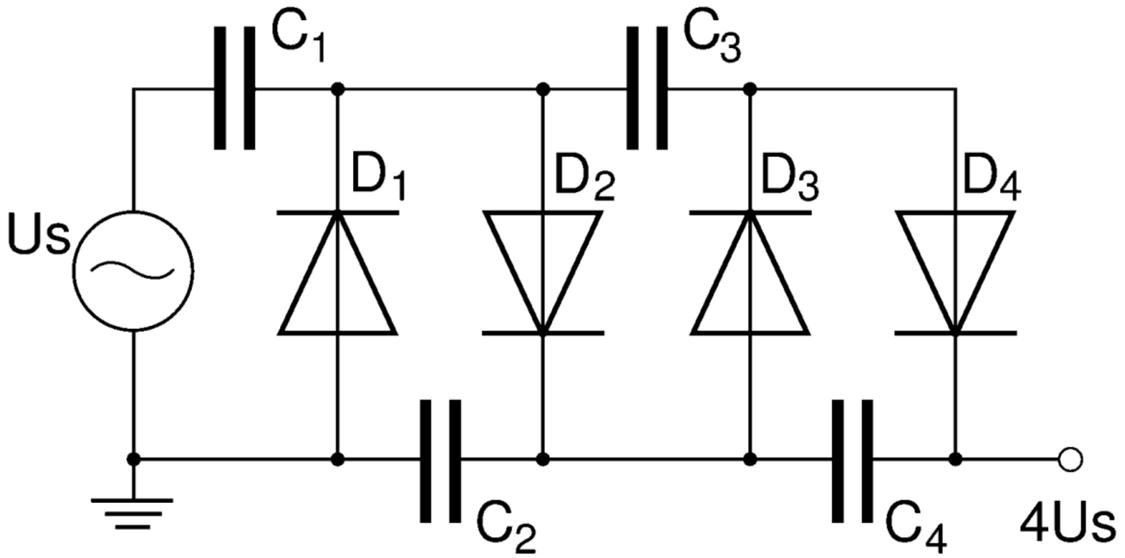

https://en.wikipedia.org/wiki/Voltage_multiplier

Voltage multiplier (Cockcroft–Walton (CW) generator)

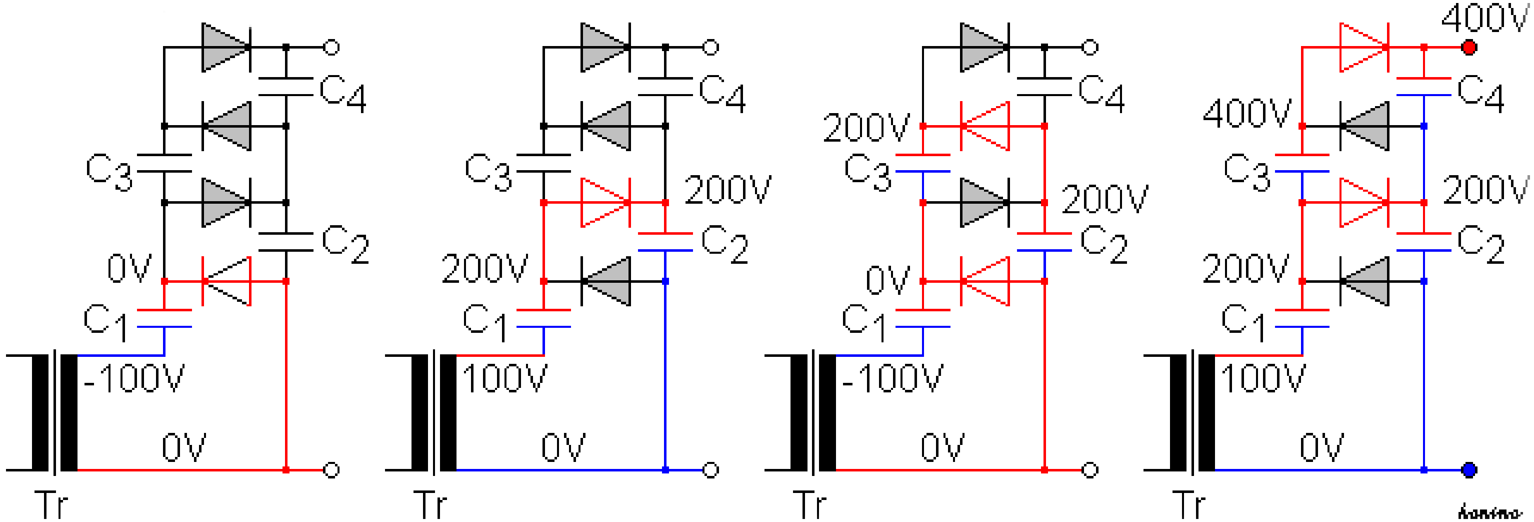

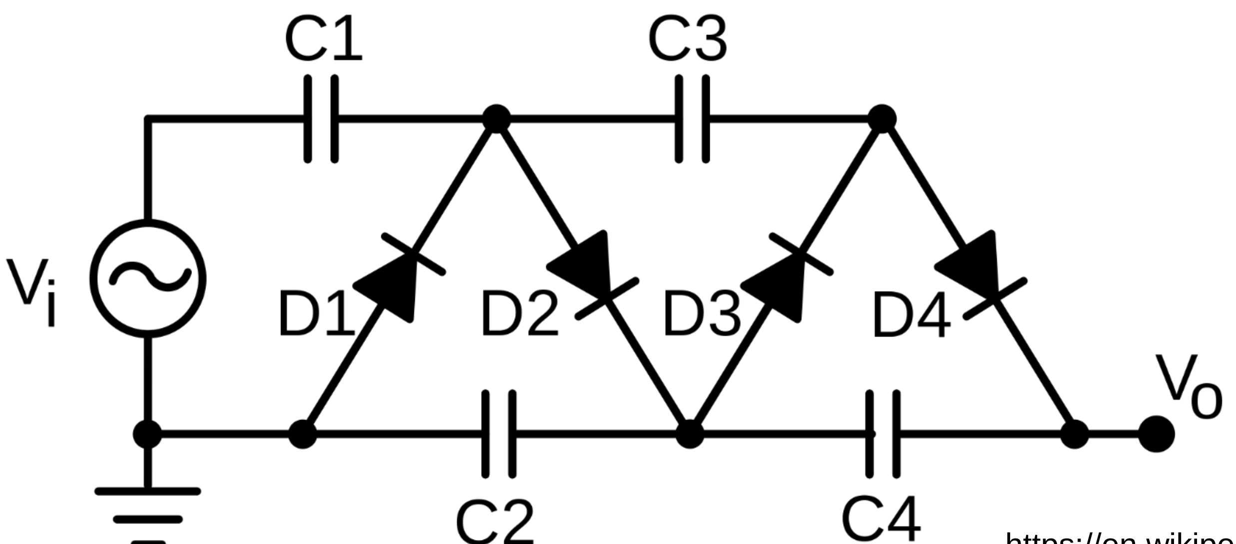

https://en.wikipedia.org/wiki/Voltage_multiplier

Dual-output

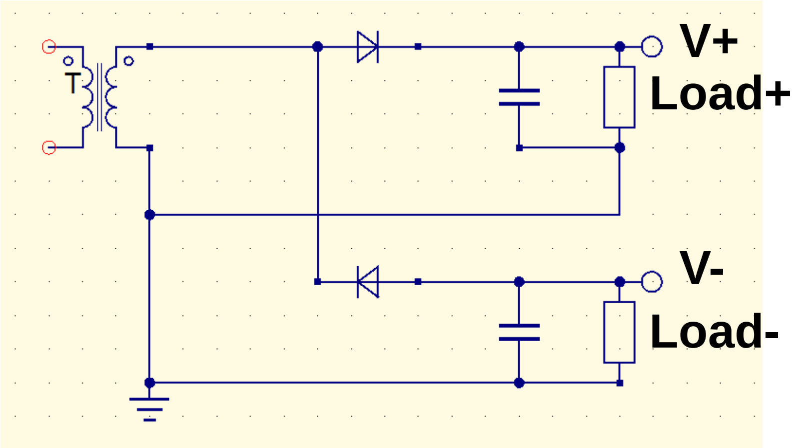

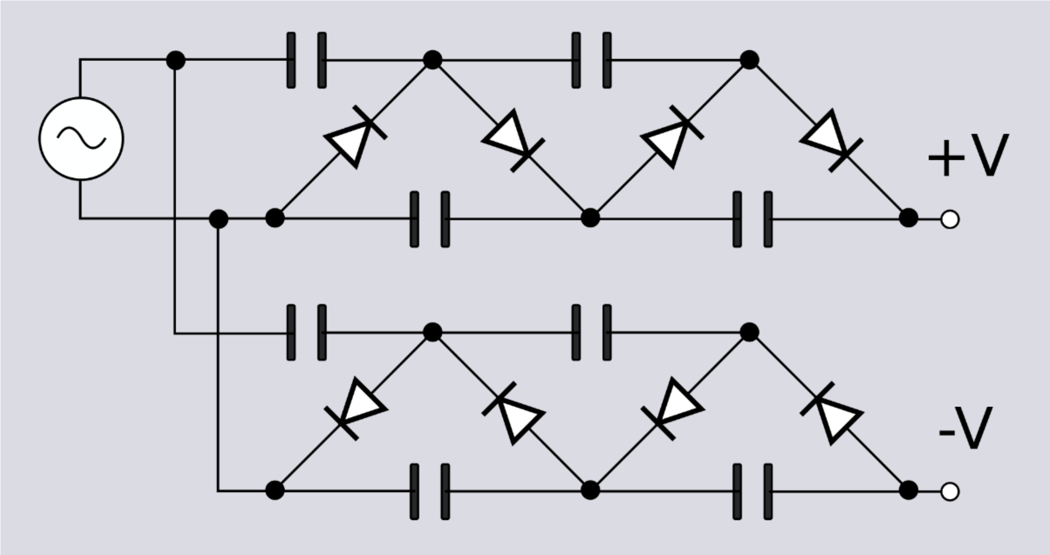

https://en.wikipedia.org/wiki/Voltage_multiplier

Internal of a magnetron

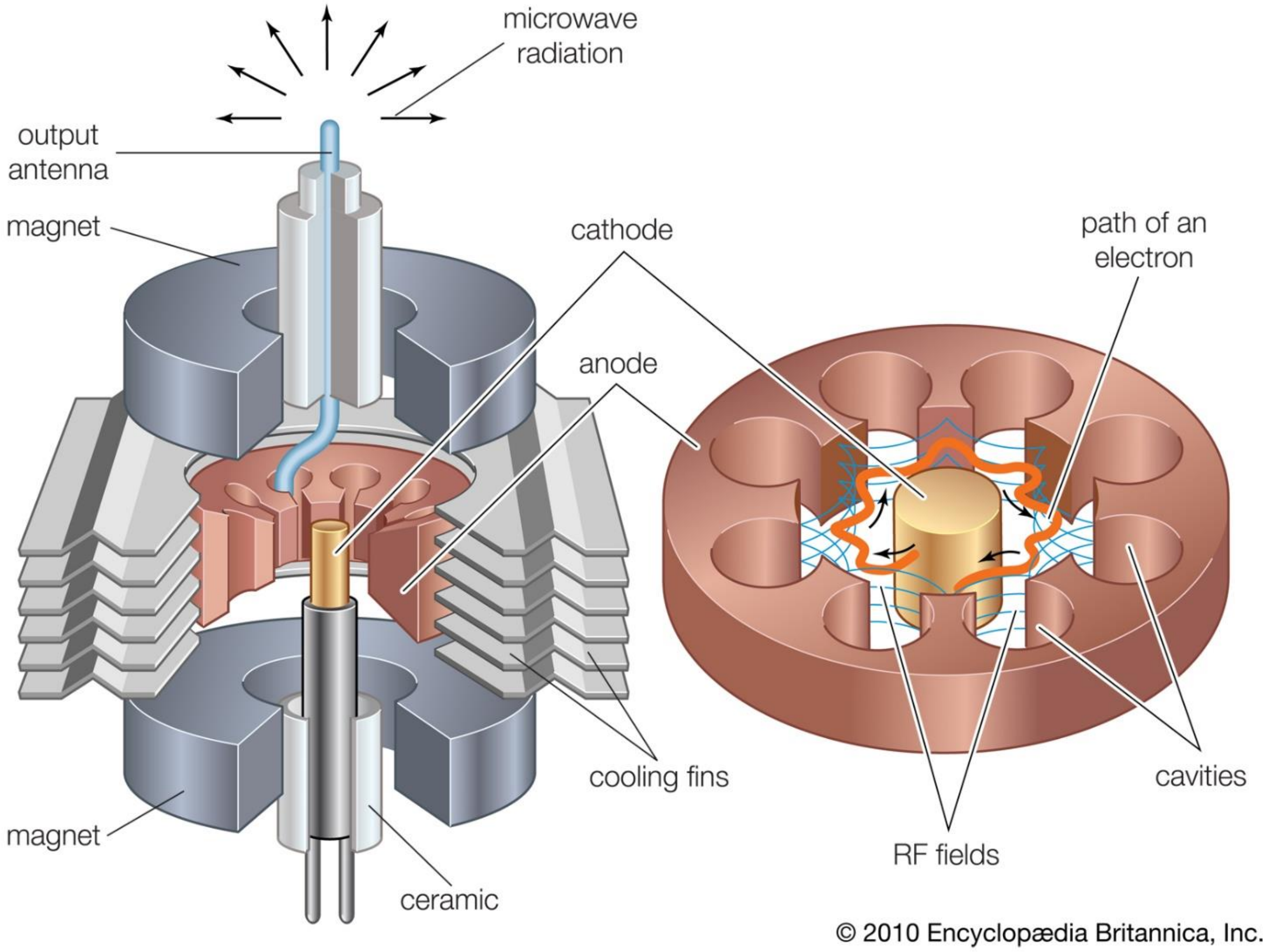

https://kids.britannica.com/students/article/electron-tube/106024/media?assemblyId=137

Magnetron is a forced oscillation driven by electrons between the gap

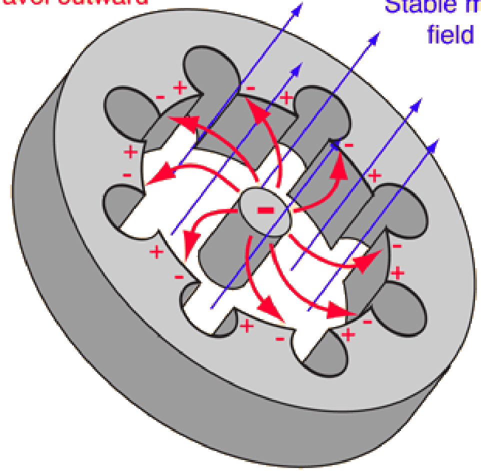

Electrons from a hot filament would travel radially to the outside ring if it were not for the magnetic field. The magnetic force deflects them in the sense shown and they tend to sweep around the circle. In so doing, they "pump" the natural resonant frequency of the cavities. The currents around the resonant cavities cause them to radiate electromagnetic energy at that resonant frequency.

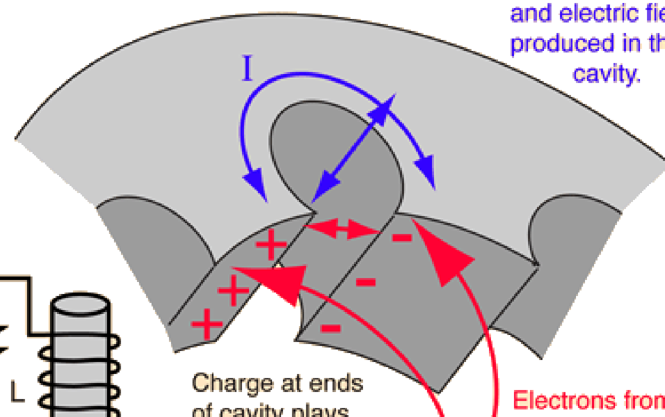

The cavity exhibits a resonance analogous to a parallel resonant circuit.

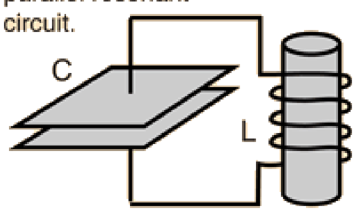

$$f_{resonance} \approx \frac{1}{2\pi}\sqrt{\frac{1}{LC}}$$

http://hyperphysics.phy-astr.gsu.edu/hbase/Waves/magnetron.html

Magnetron schematic diagram

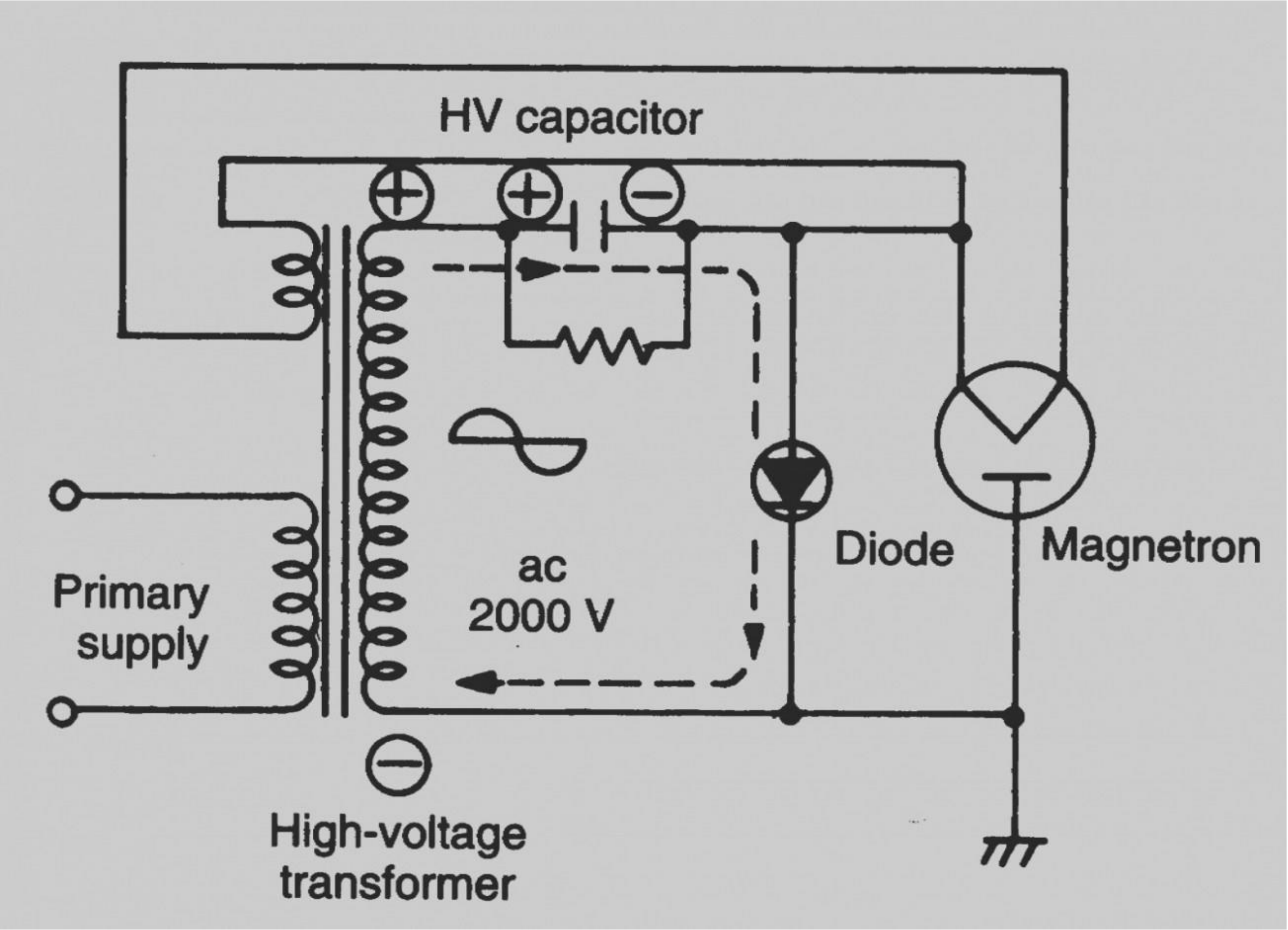

http://www.sciencemadness.org/talk/viewthread.php?tid=154071

Magnetron schematic diagram

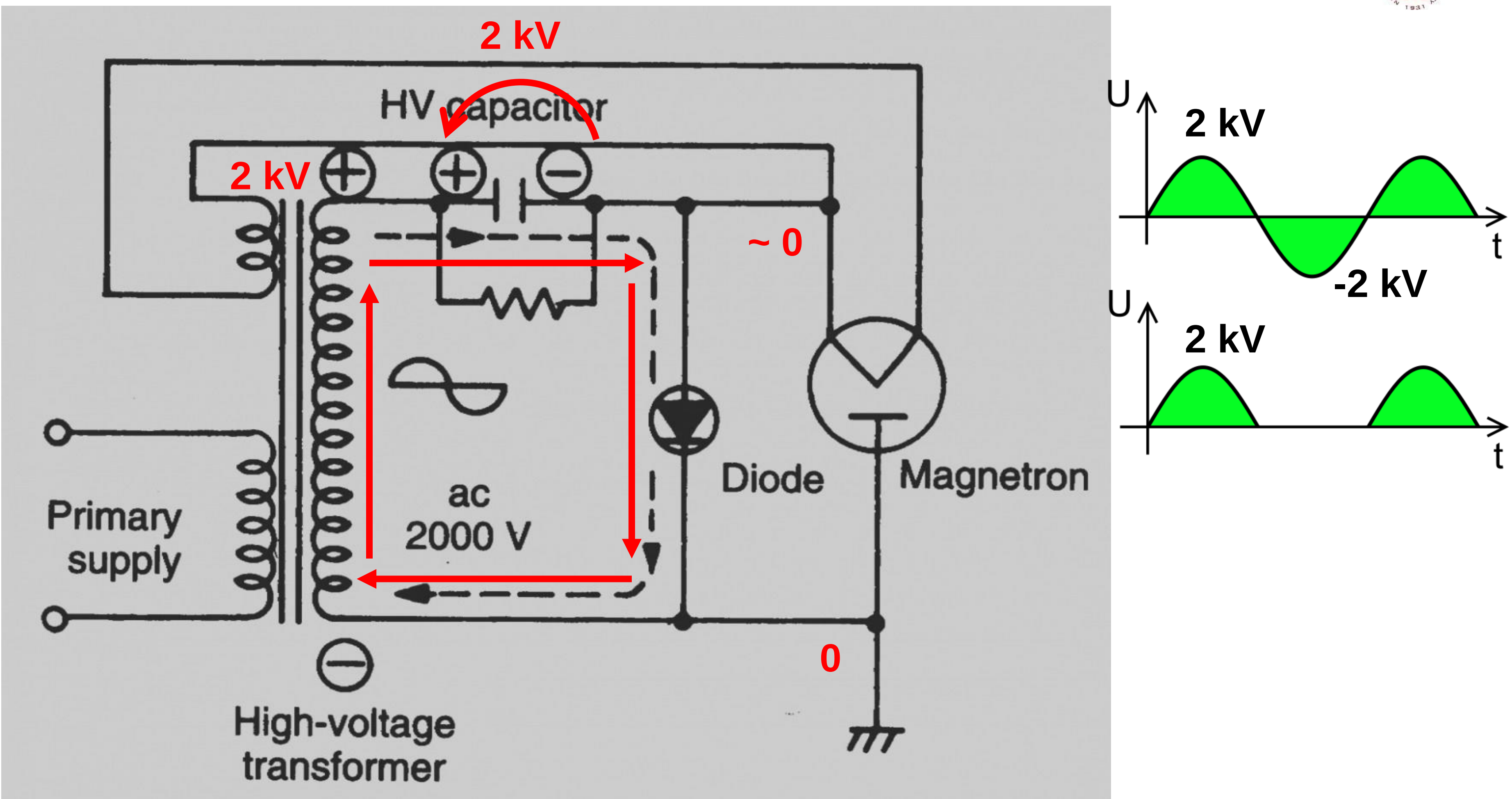

http://www.sciencemadness.org/talk/viewthread.php?tid=154071

Magnetron schematic diagram

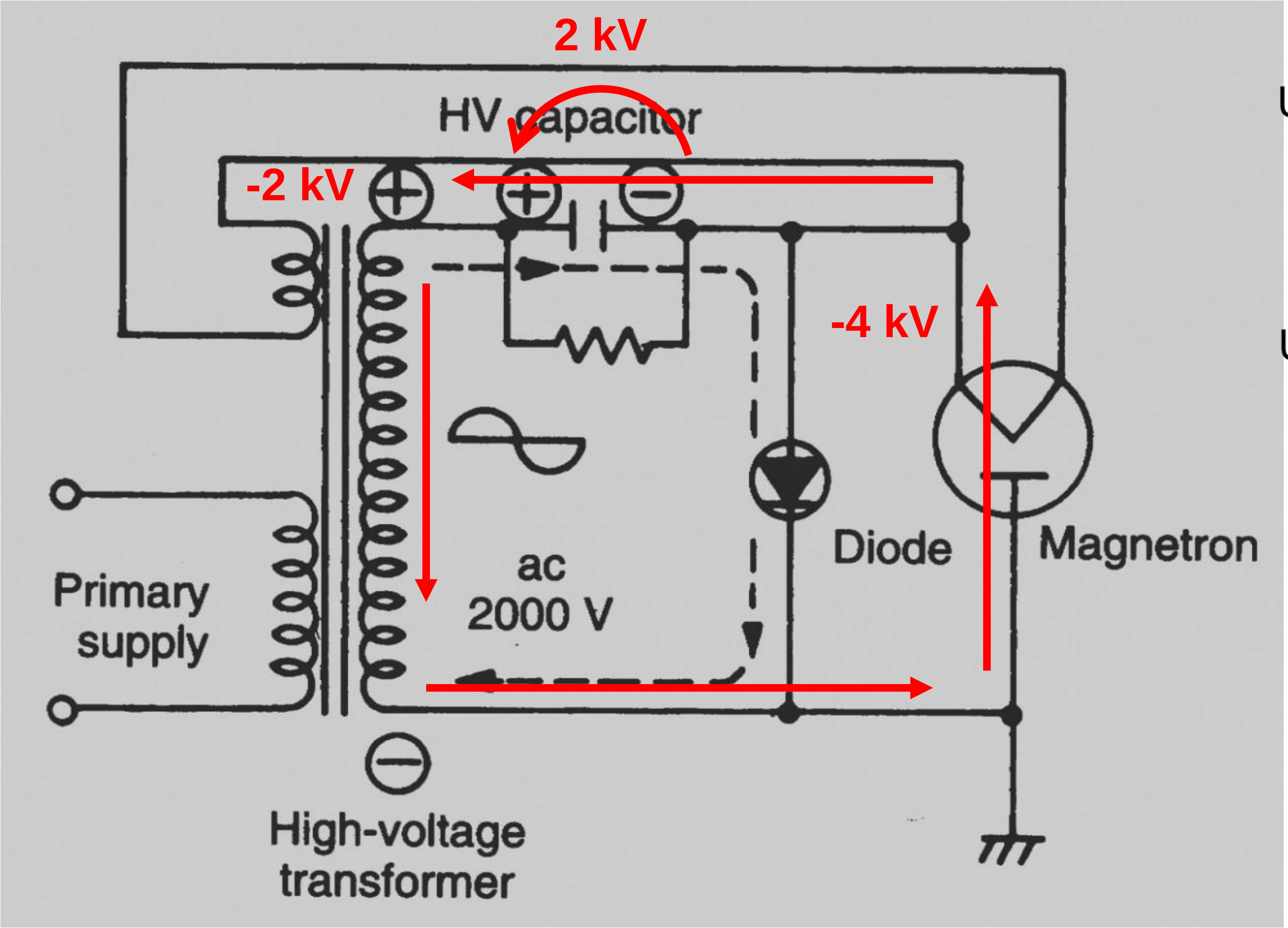

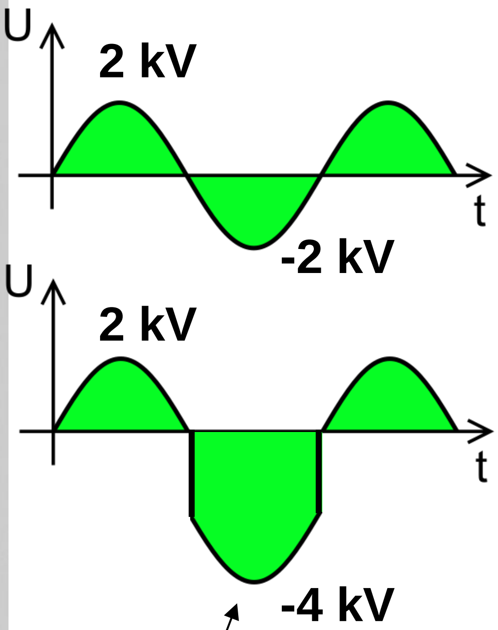

Microwave is generated.

http://www.sciencemadness.org/talk/viewthread.php?tid=154071

Pulse generator using H-bridge inverter

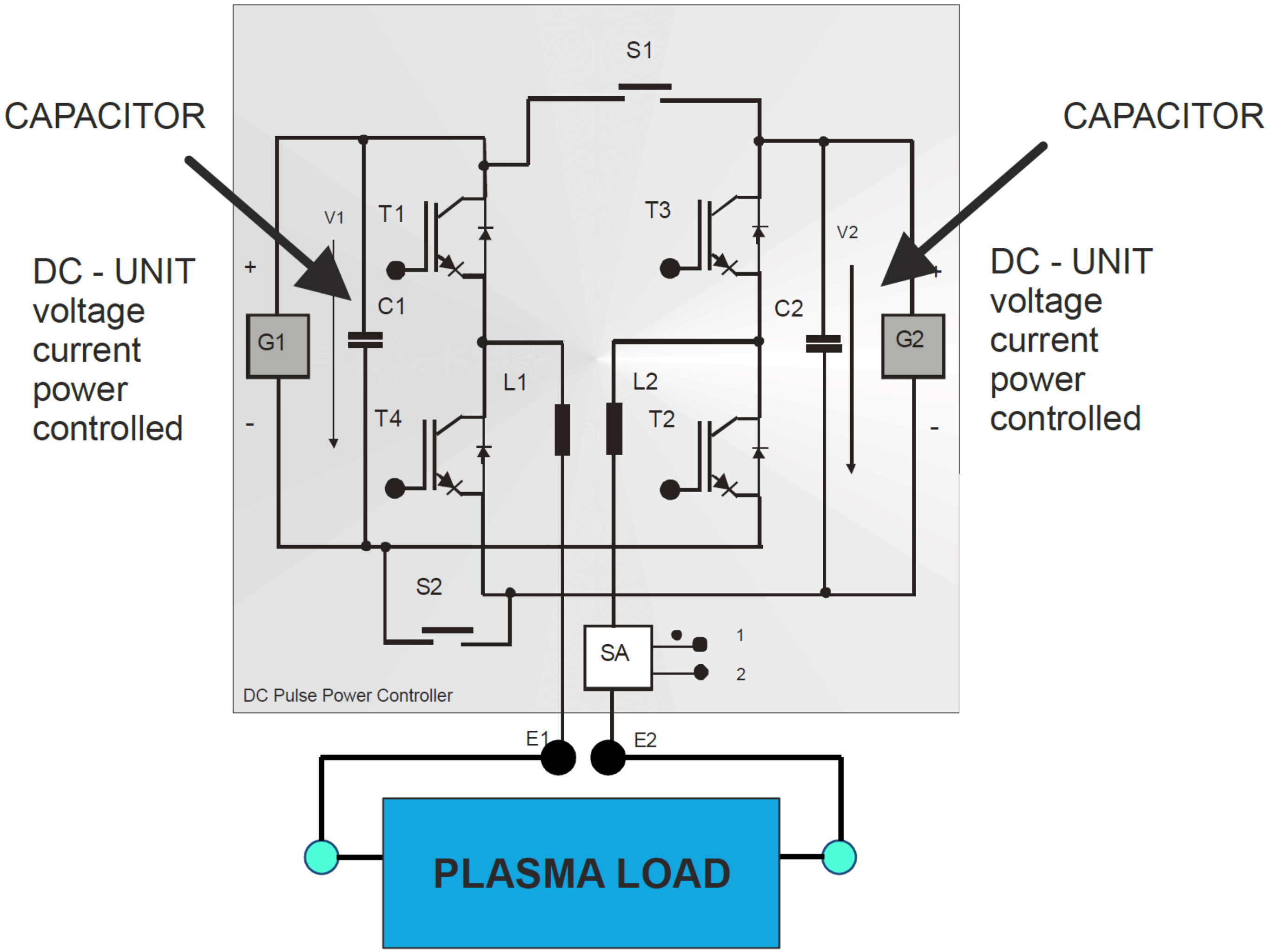

Pulse generator using H-bridge inverter

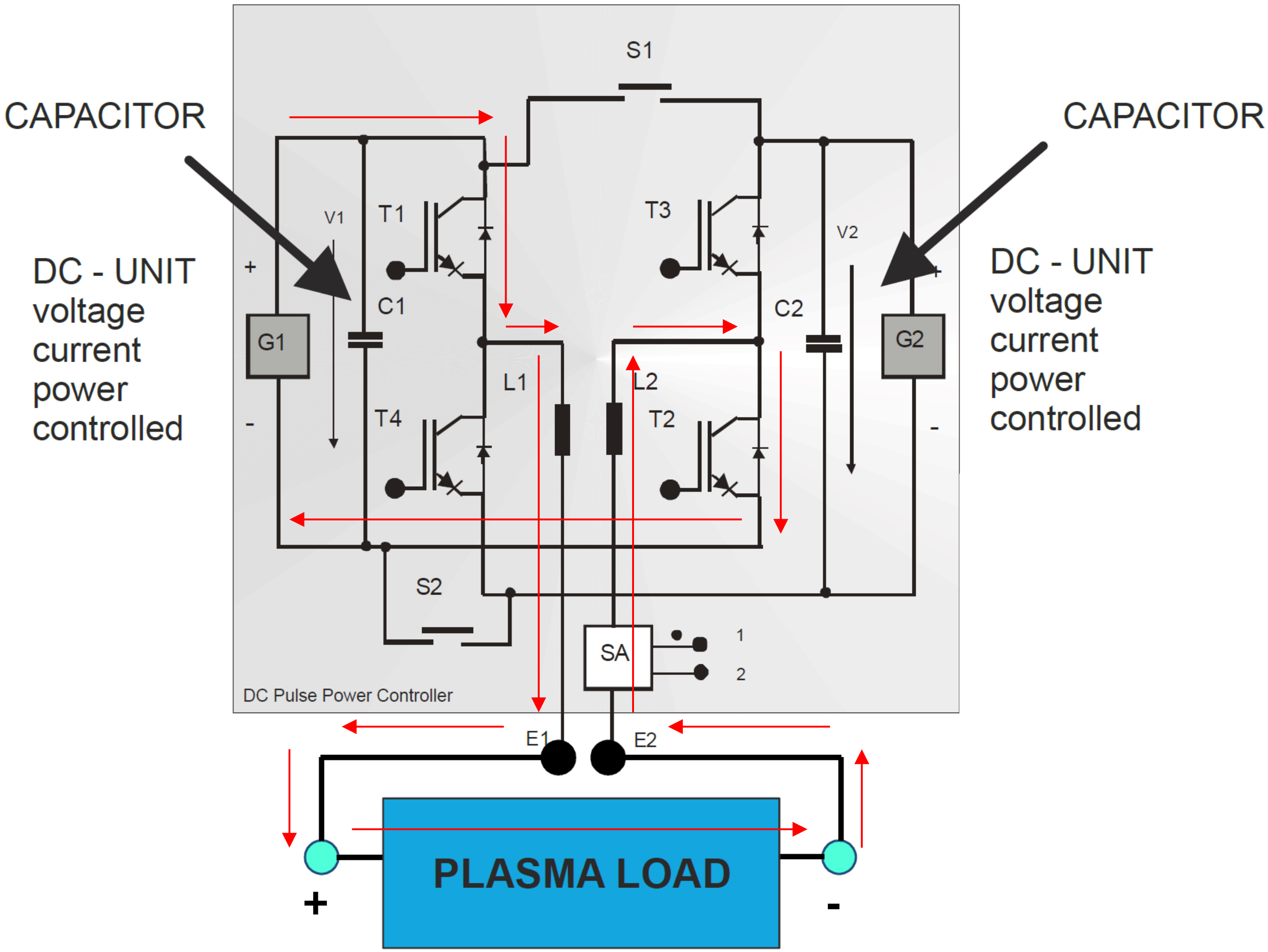

Pulse generator using H-bridge inverter

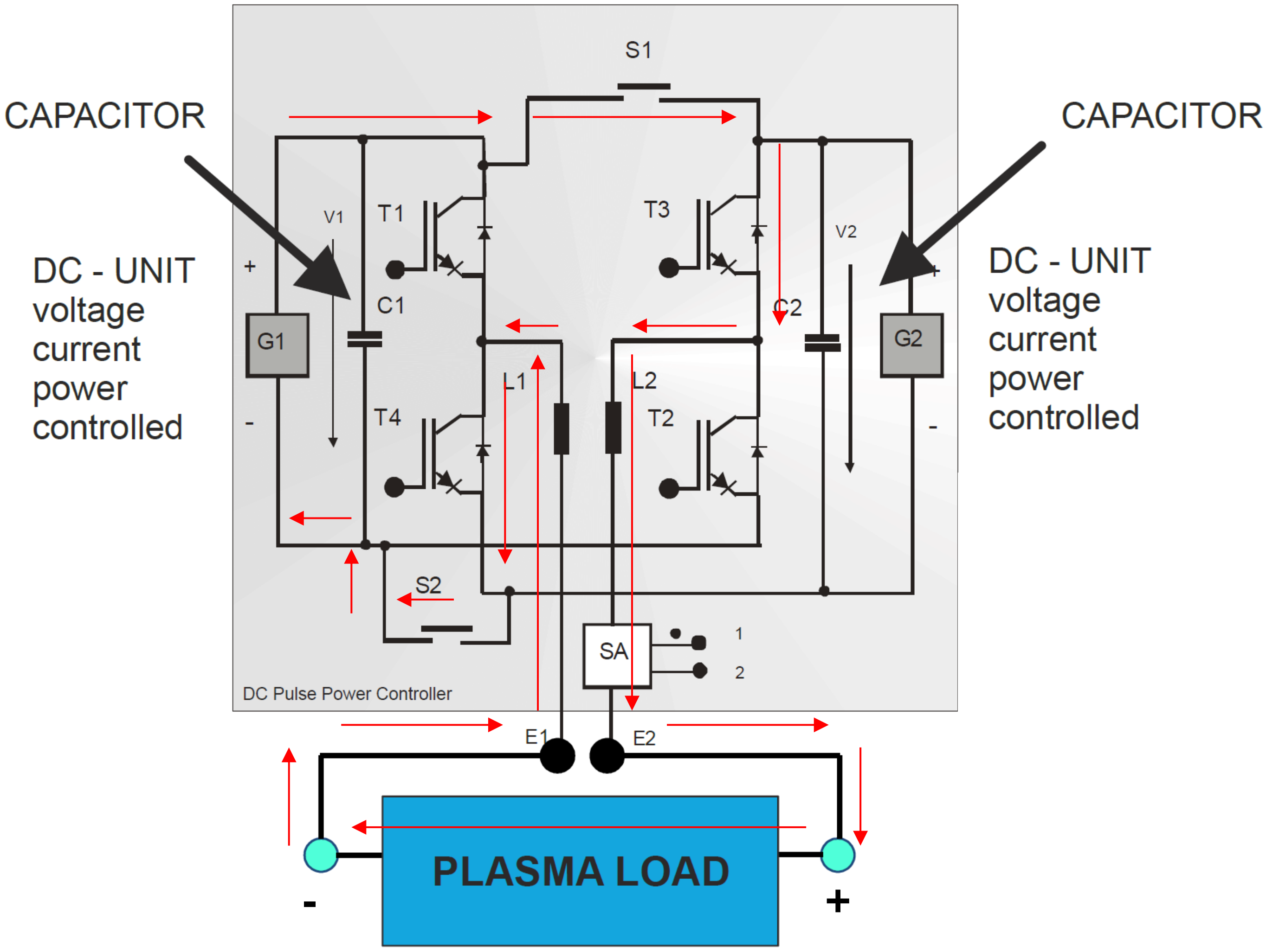

Pulse generator using DC power supply

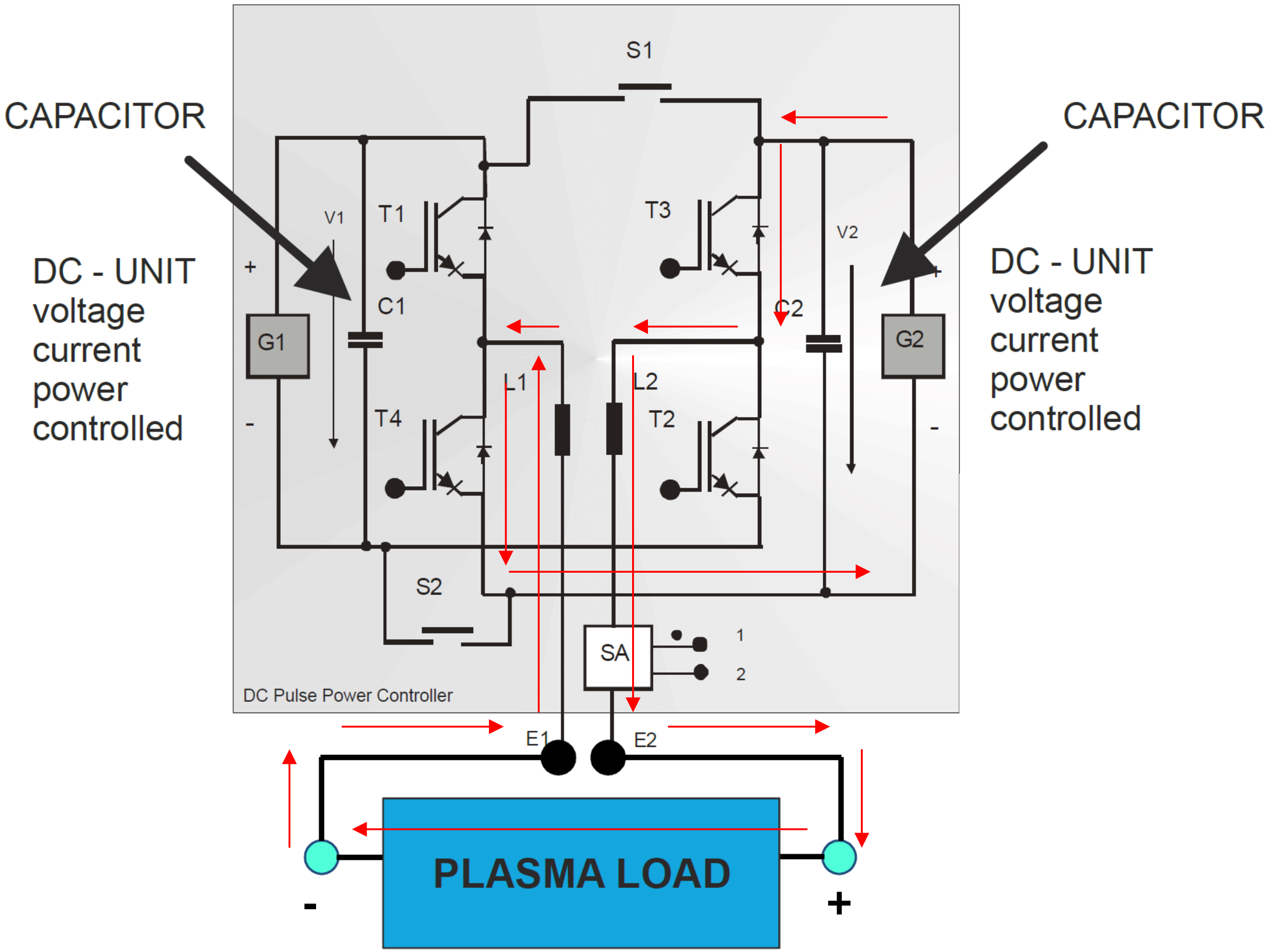

Pulse generator

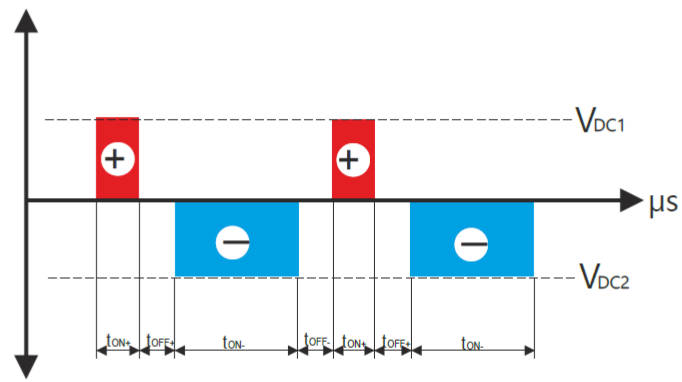

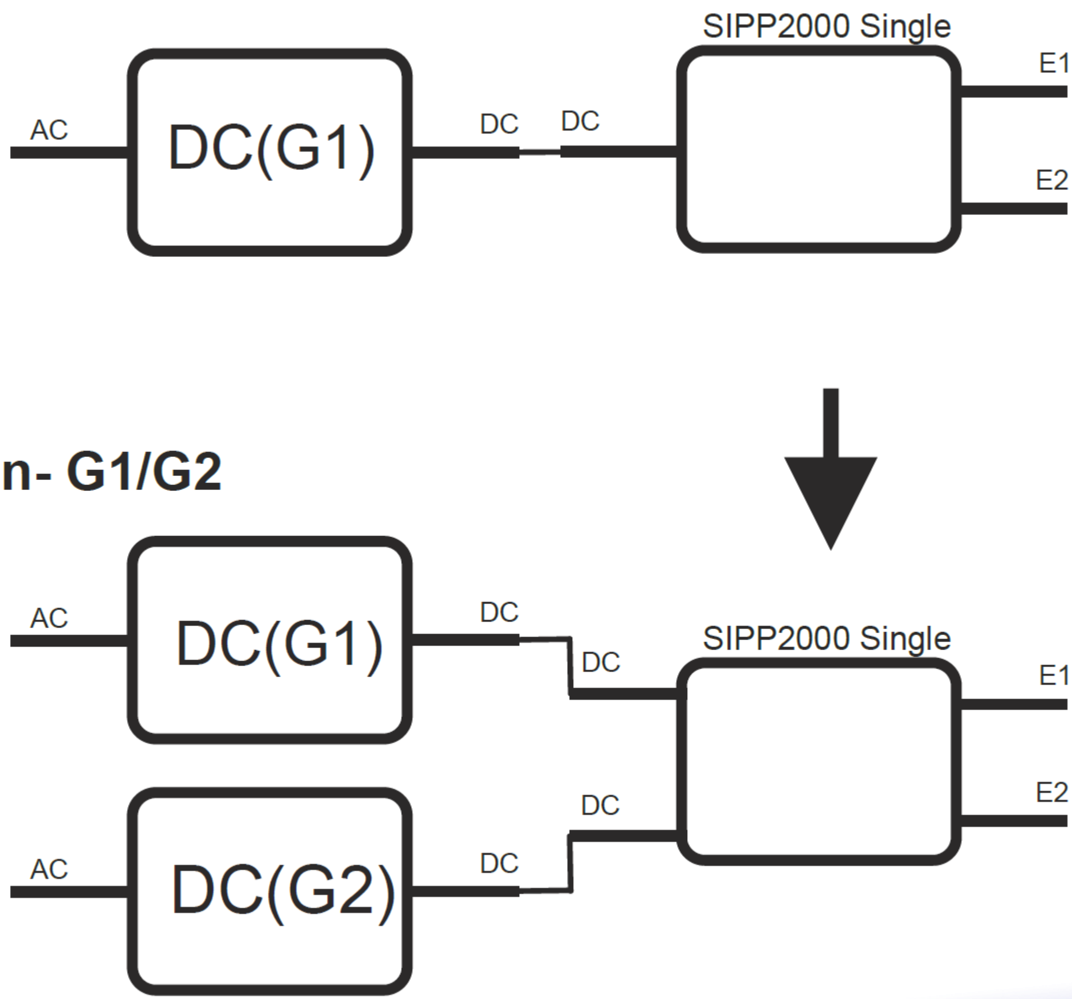

ASYMMETRIC : S1/S2 open- G1/G2

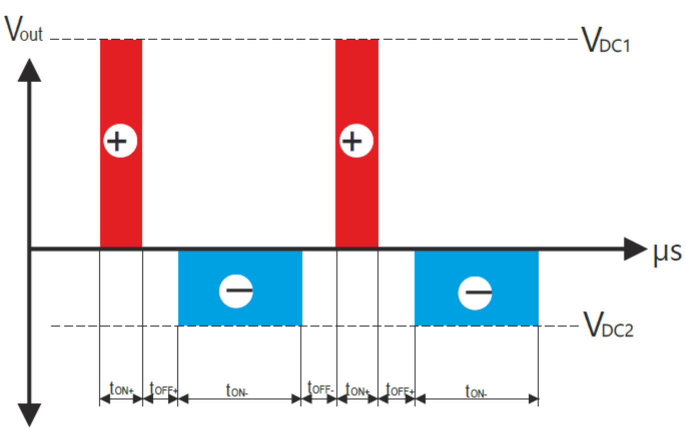

High-frequency switch mode power supply

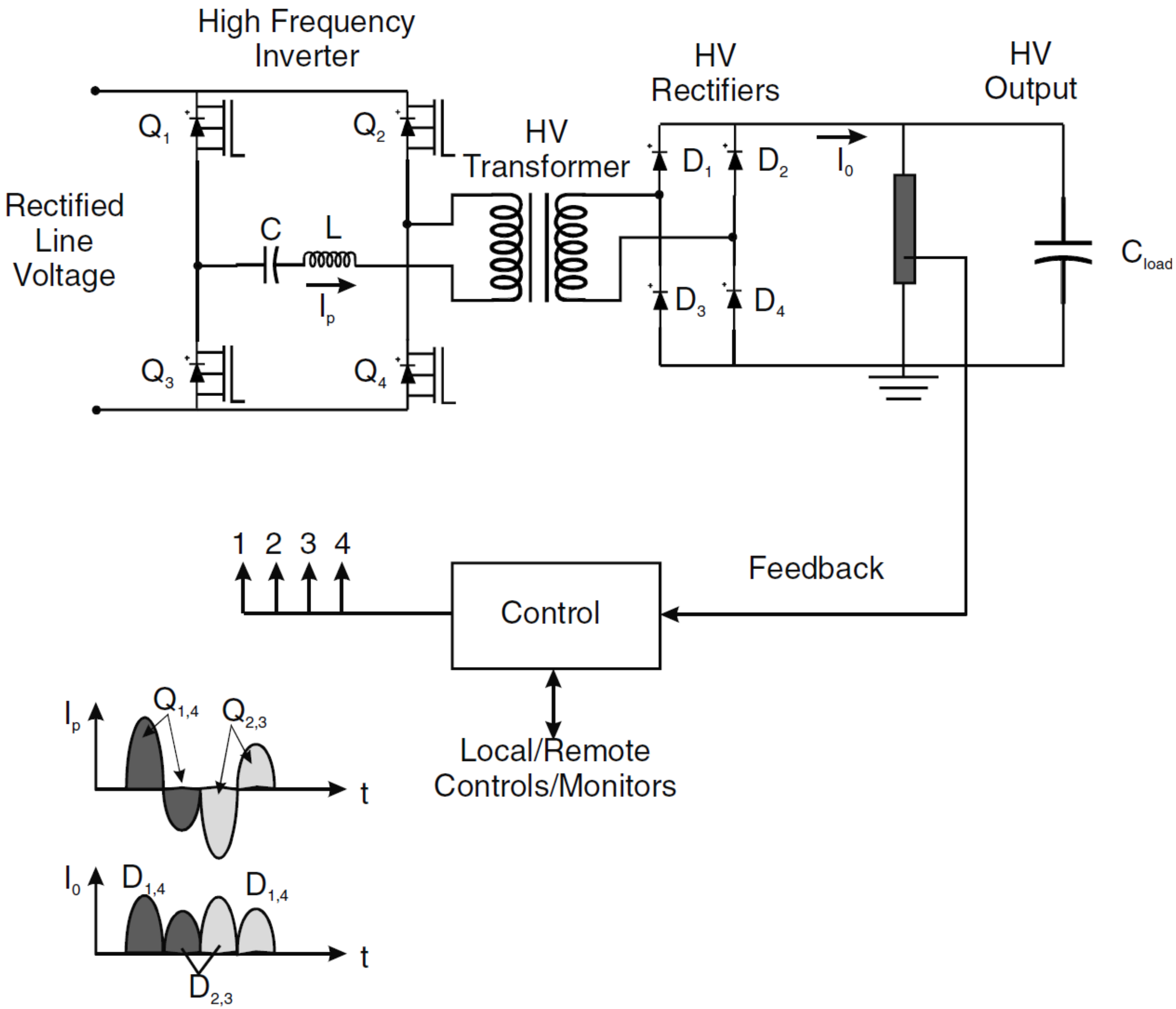

A tokamak is a device to achieve nuclear fusion via confinement plasma using magnetic field

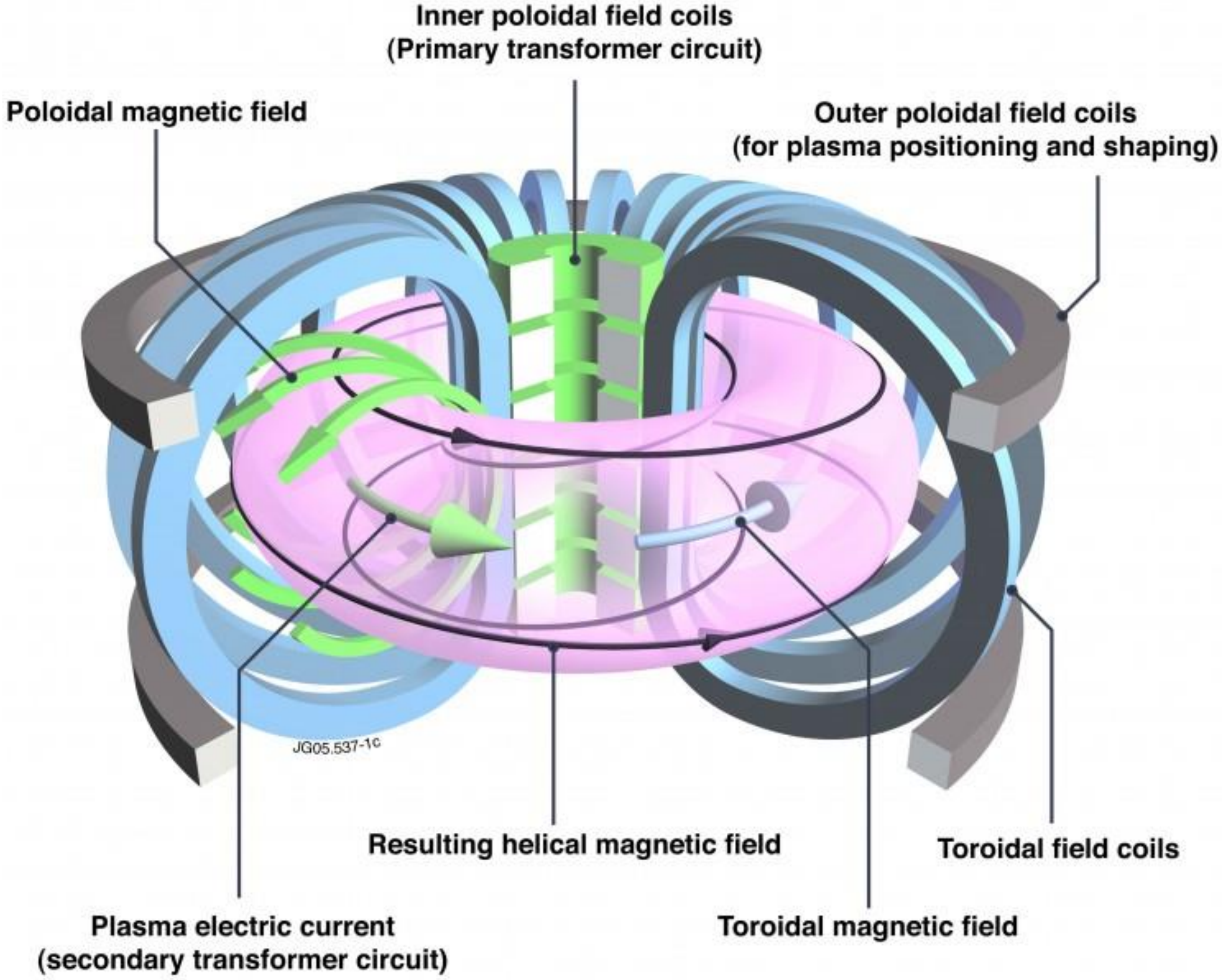

https://www.euro-fusion.org/2011/09/tokamak-principle-2/

Currents with specific profiles needed to be provided to drive coils in Tokamaks to confine the plasma

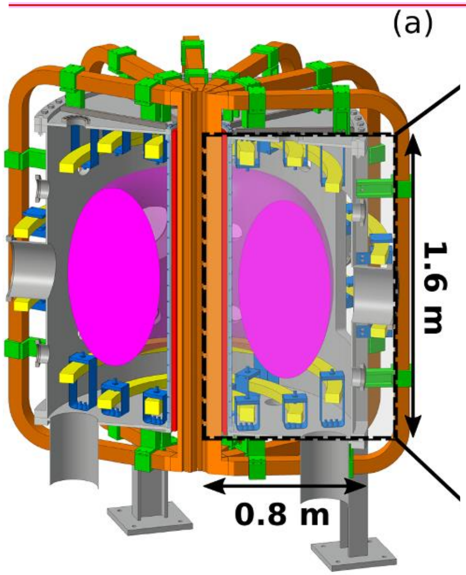

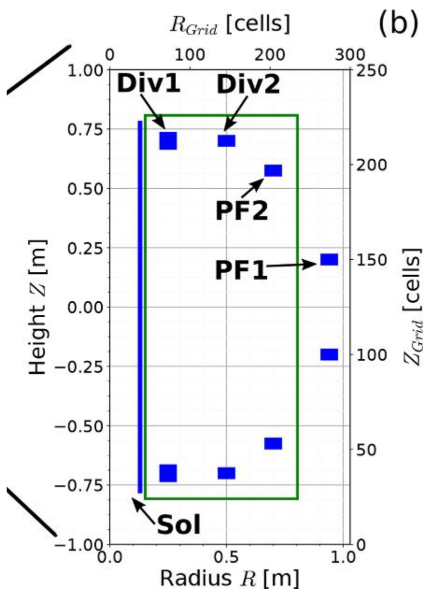

- **Currents of SMART**

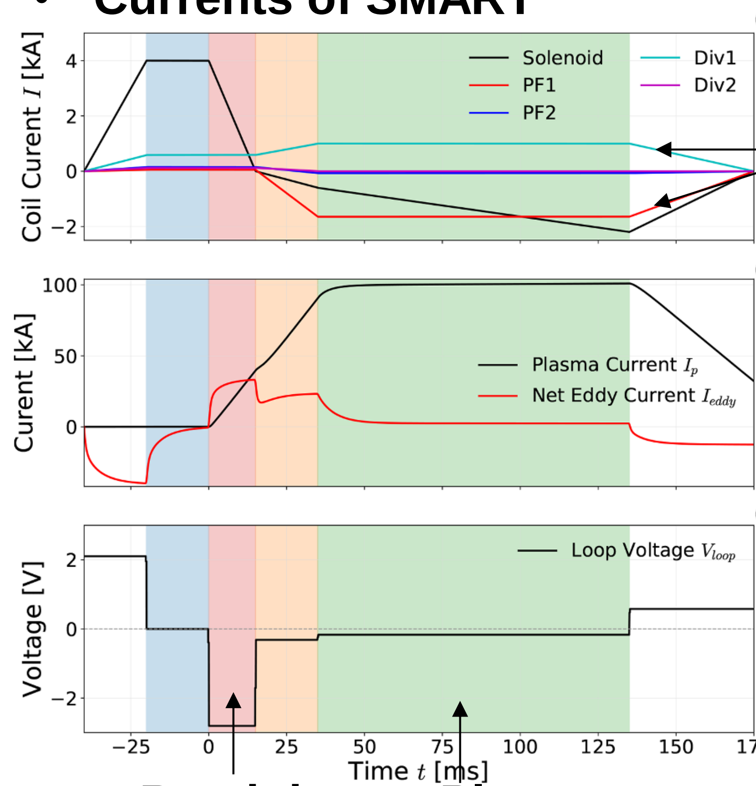

Equilibrium state can be achieved with poloidal field coils.

Breakdown **Plasma current is driven.**

- **The current of the CS will be determined by the required breakdown voltage and plasma current.**

S. J. Doyle, etc., Fusion Eng. Des. **171**, 112706 (2021)

An H-bridge combining pulse width modulation technique will be used to provide the controllable currents

- **H-bridge configuration provides the capability of reversing the current direction:**

- **Pulse width modulation provides the capability of controllable currents**

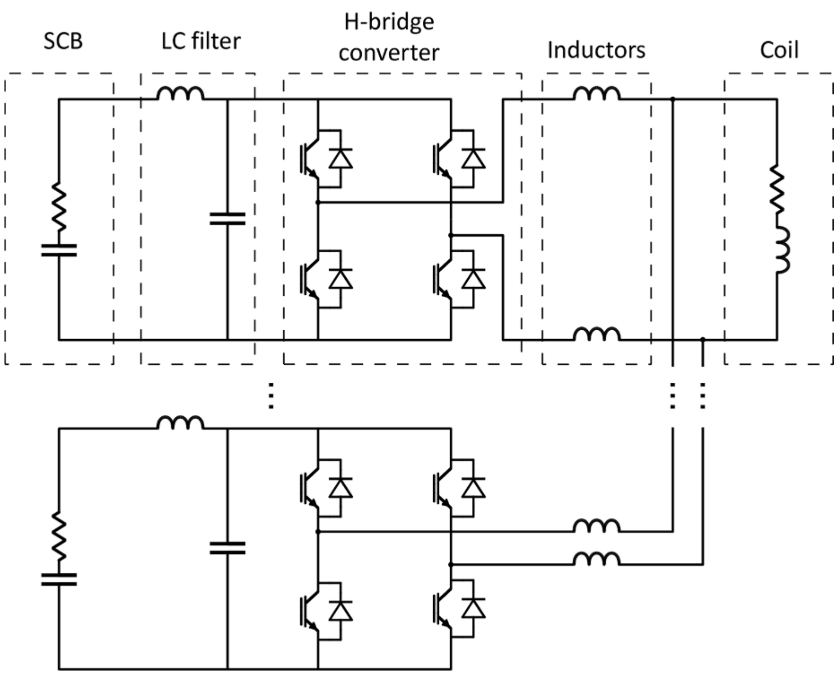

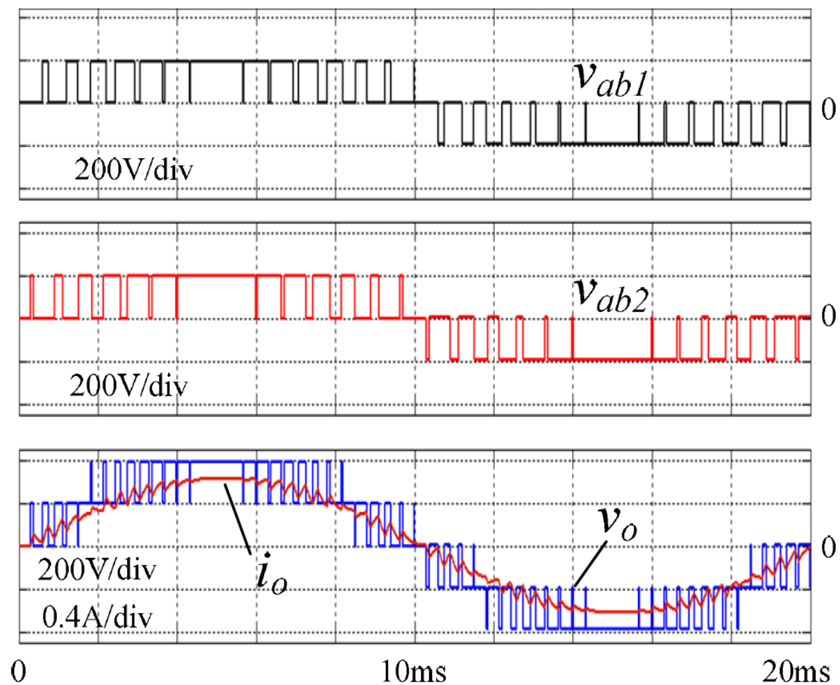

M. Agredano-Torres, etc., Fusion Eng. Des. **168**, 112683 (2021)
C. Boonmee and Y. Kumsuwan, 2012 15th International Power Electronics and Motion Control Conference, Novi Sad, Serbia, 2012, pp. LS8c.3-1

The output voltage is controlled by the status of switches S1~S4

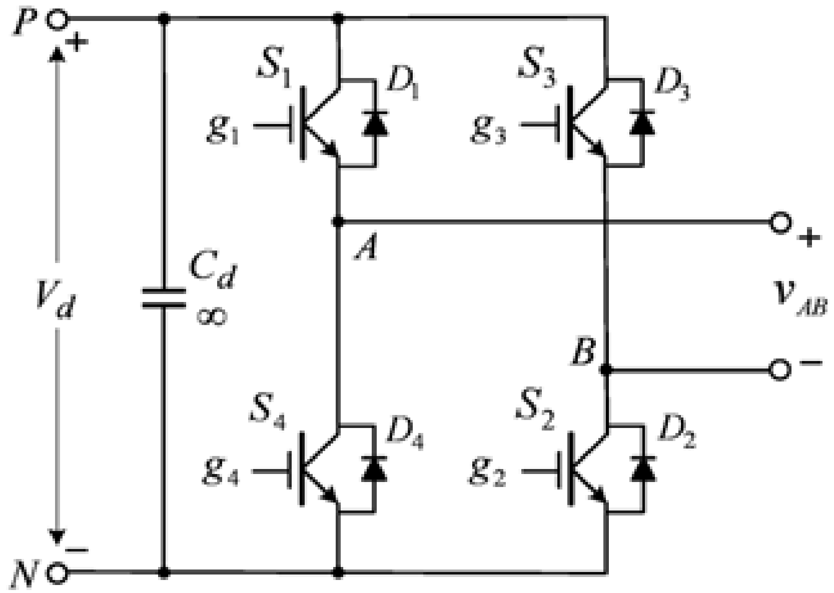

- **S_1/S_2 ON; S_3/S_4 Off: $V_{AB} = V_d$.**
- **S_1/S_2 Off; S_3/S_4 ON: $V_{AB} = -V_d$.**
- **S_1/S_2 ON; S_3/S_4 ON: $V_{AB} = 0$.**

A. Namboodiri & H. S. Wani, I. J. Innovative Research in Sci. & Tech. 1, 2349 (2014)

Bipolar Modulation Scheme

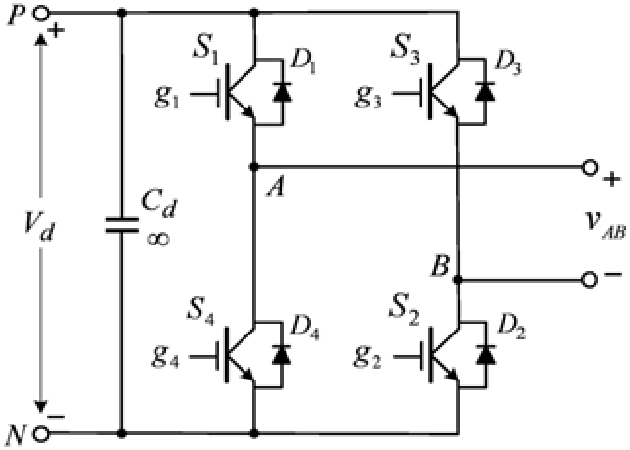

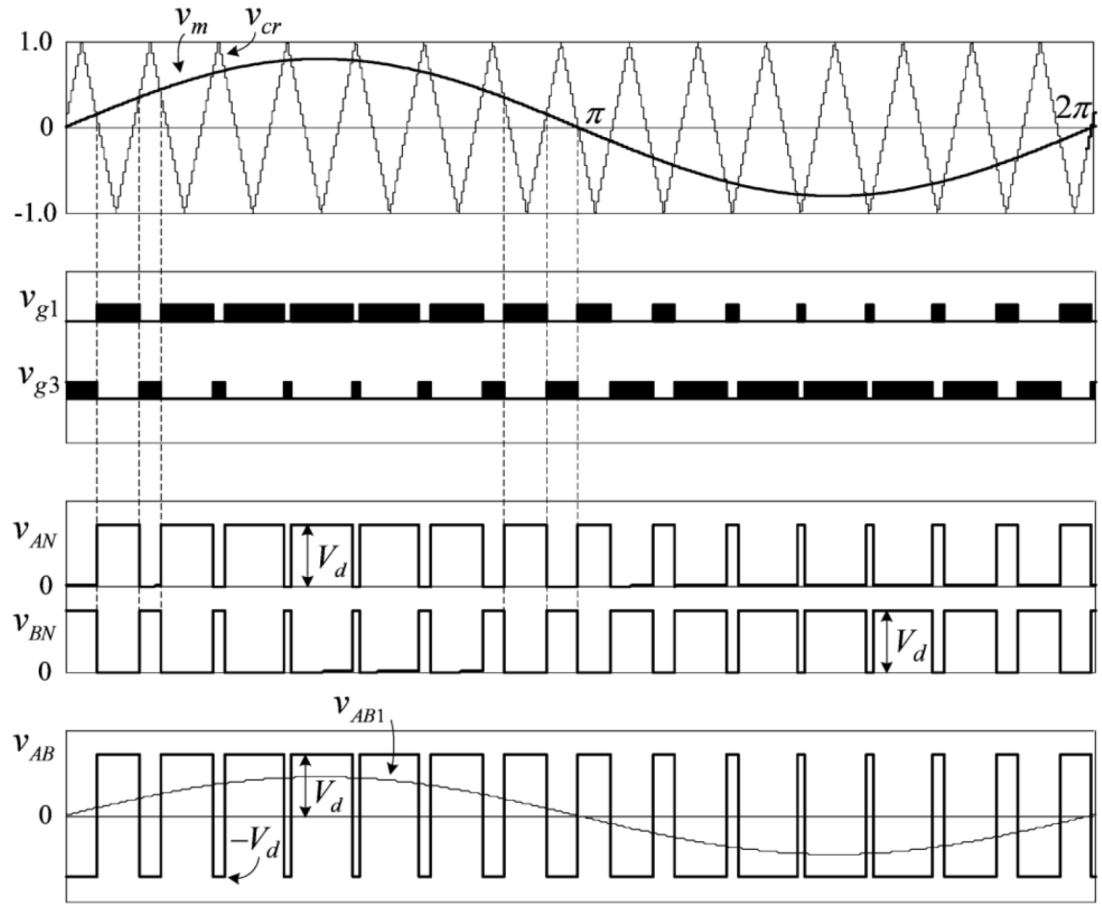

- S_1/S_2 ON; S_3/S_4 Off: $V_{AB} = V_d$.
- S_1/S_2 Off; S_3/S_4 ON: $V_{AB} = -V_d$.
- S_1/S_2 ON; S_3/S_4 ON: $V_{AB} = 0$.

A. Namboodiri & H. S. Wani, I. J. Innovative Research in Sci. & Tech. 1, 2349 (2014)

Unipolar Modulation Scheme

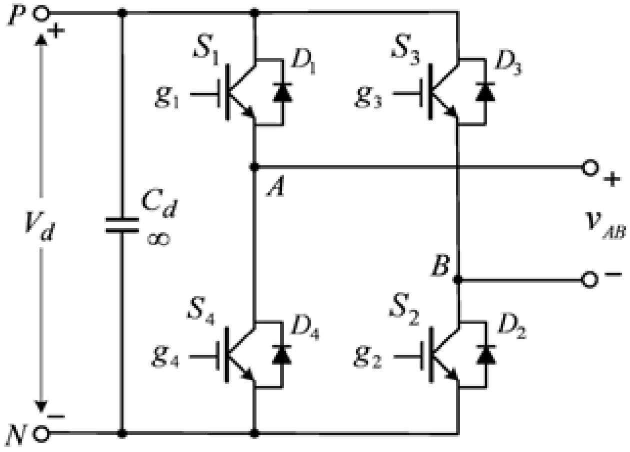

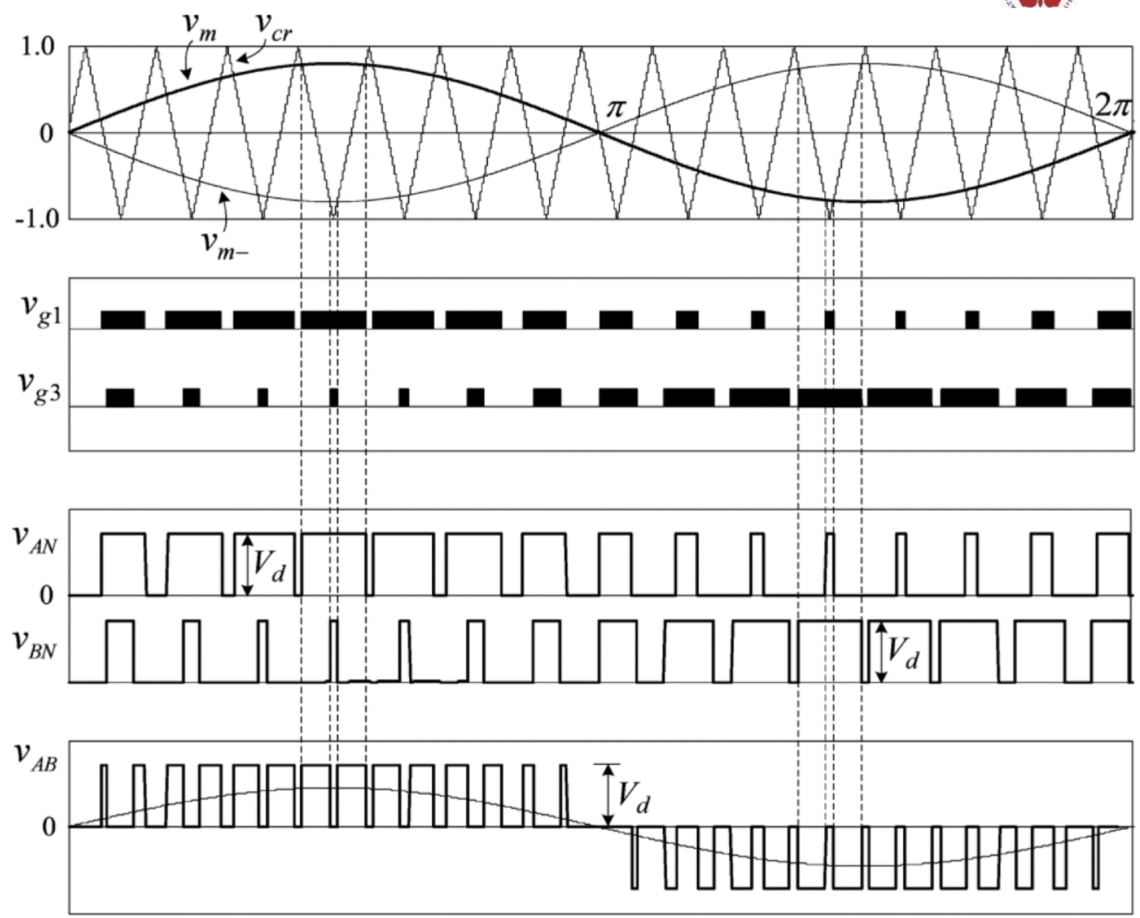

- S_1/S_2 ON; S_3/S_4 Off: $V_{AB} = V_d$.
- S_1/S_2 Off; S_3/S_4 ON: $V_{AB} = -V_d$.
- S_1/S_2 ON; S_3/S_4 ON: $V_{AB} = 0$.

A. Namboodiri & H. S. Wani, I. J. Innovative Research in Sci. & Tech. 1, 2349 (2014)

Simulation using bipolar modulation scheme

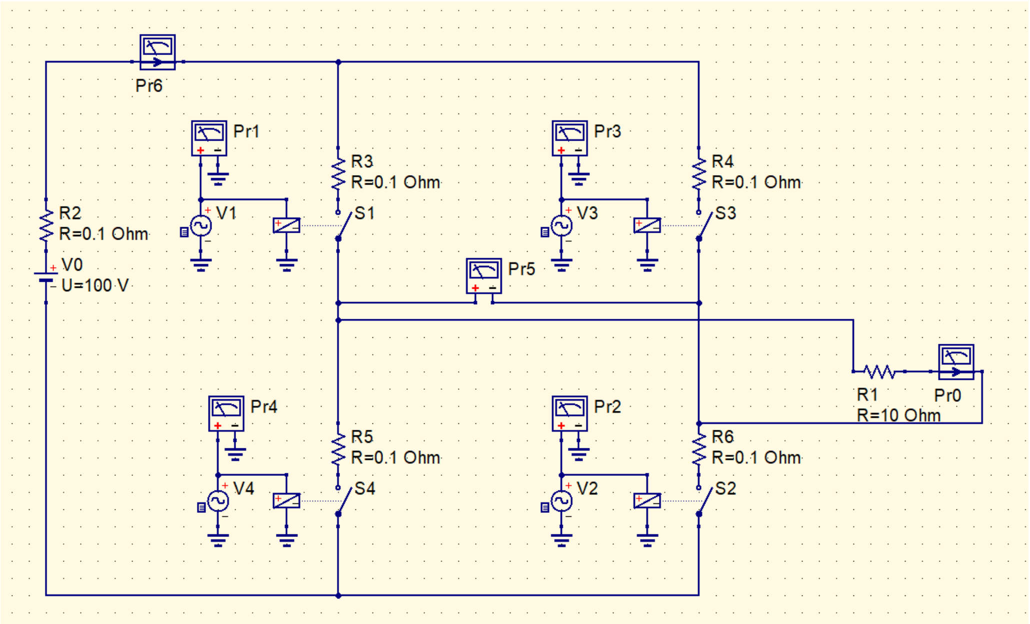

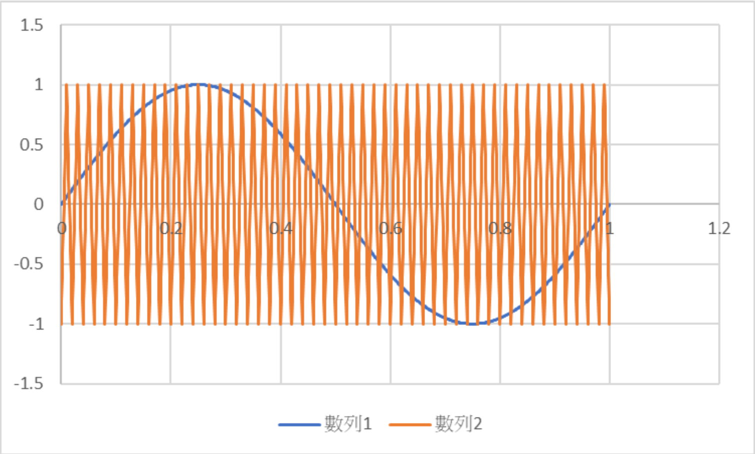

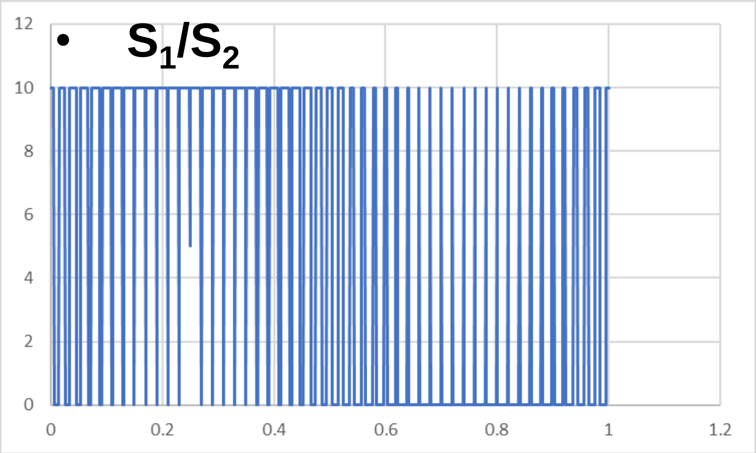

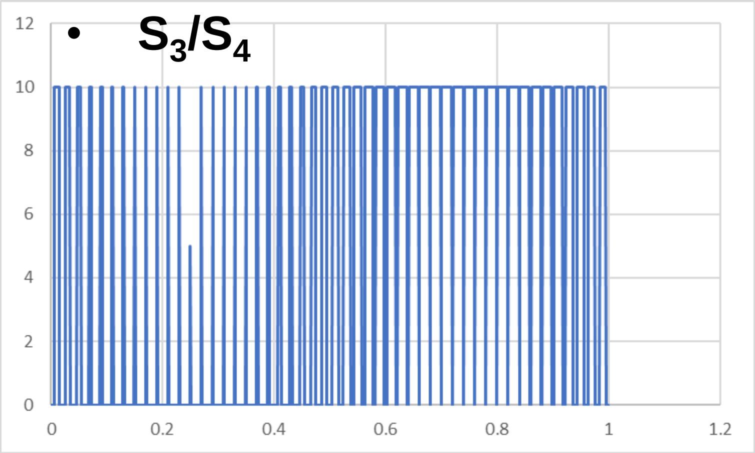

Simulation using bipolar modulation scheme

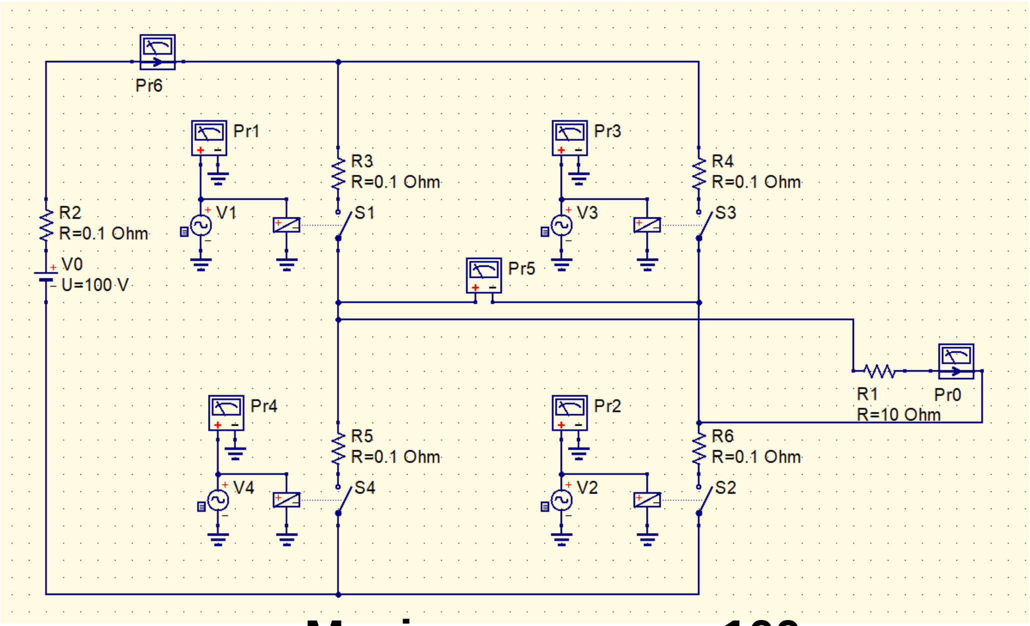

- **Raw data**

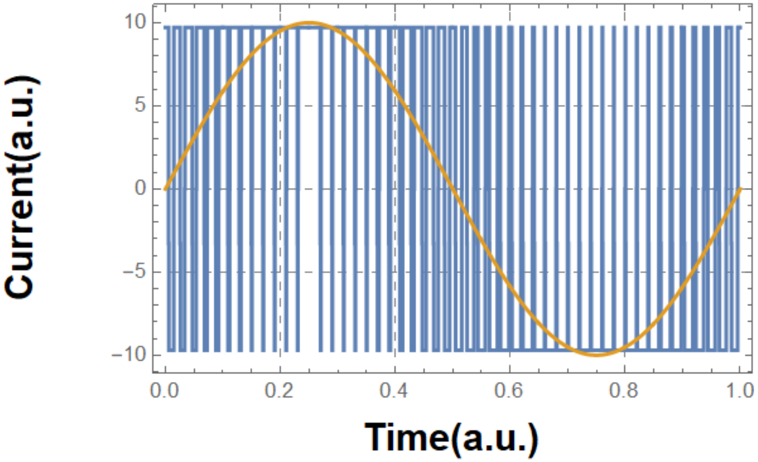

- **Moving average = 100**

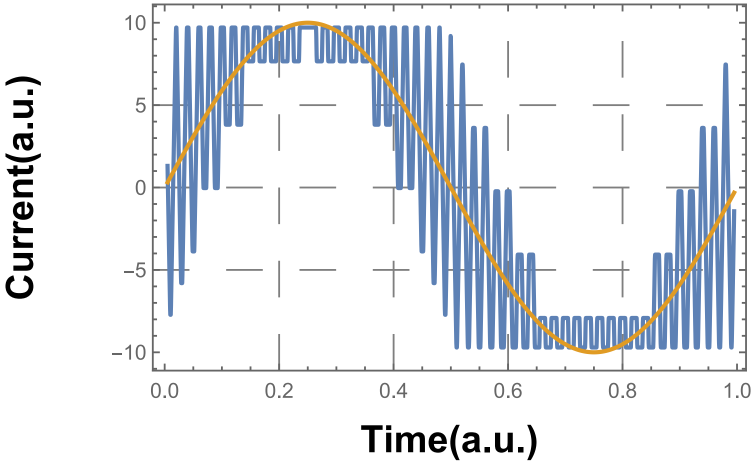

- **Moving average = 1000**

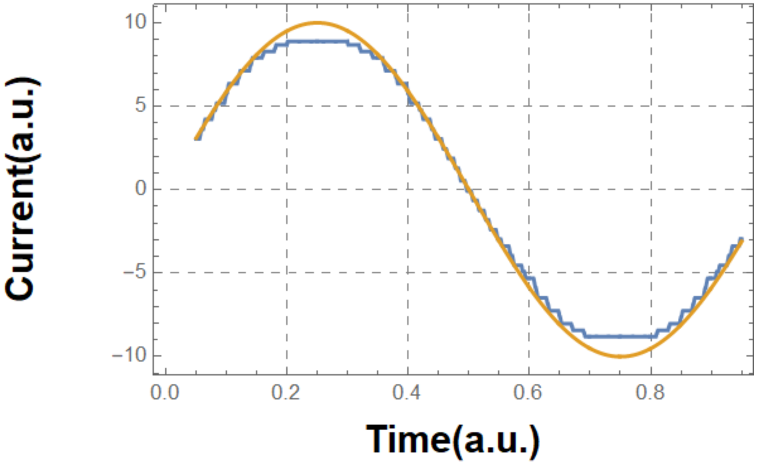

Single swing circuit

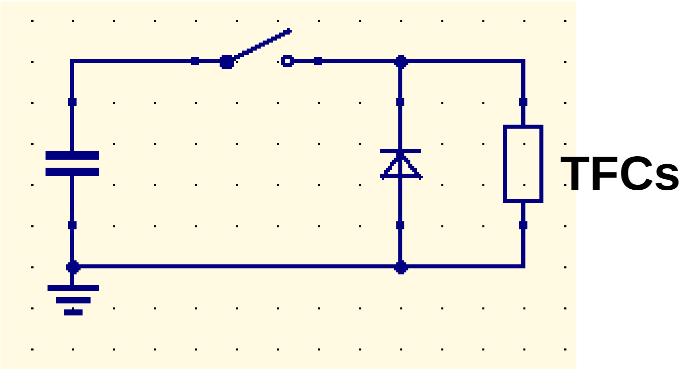

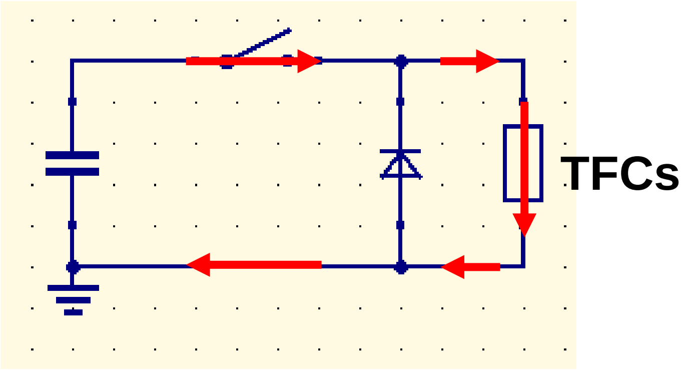

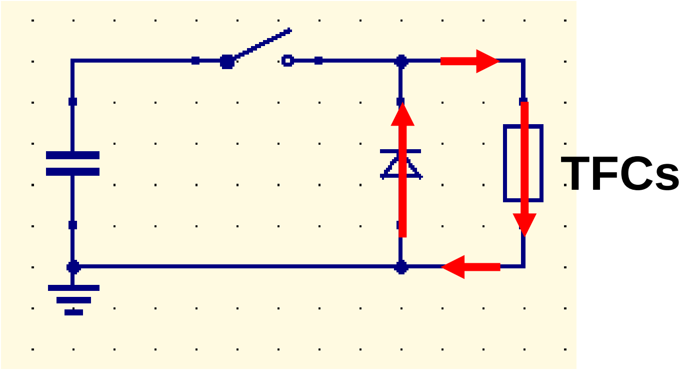

Outlines

- **Power and voltage adding**
  - **Marx generator**
  - **LC generator**
  - **Line pulse transformers**
  - **Induction voltage adder (IVA)**
  - **Linear induction accelerator (LIA)**
  - **Linear transformer driver (LTD)**
- **Diagnostics**
  - **Voltage measurement**
  - **Current measurement**
- **Applications of pulsed-power system**

Power and voltage adding

- For pulsed-power levels become very high (≧15 TW), the generator must be divided into separately units, which can be constructed much more compactly and thus use the available volume much more efficiently.
- Synchronizing independent lines requires special measures, e.g., laser-triggered switches with very low jitter.
- Match load needed:

$$R_L = \frac{R_g}{n}$$

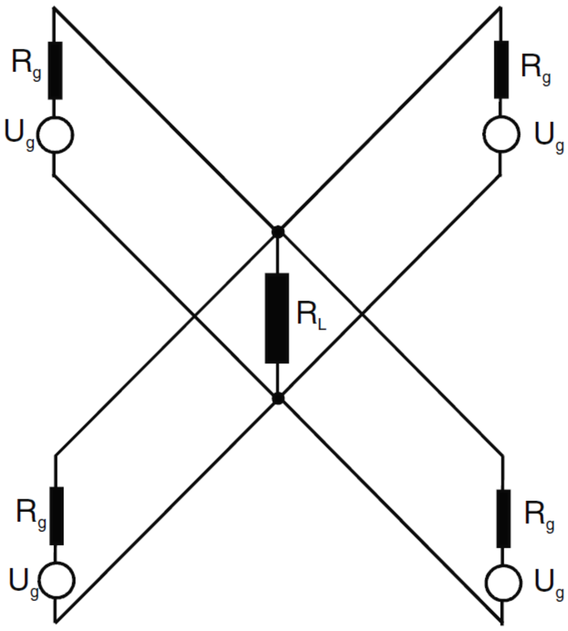

Marx generator

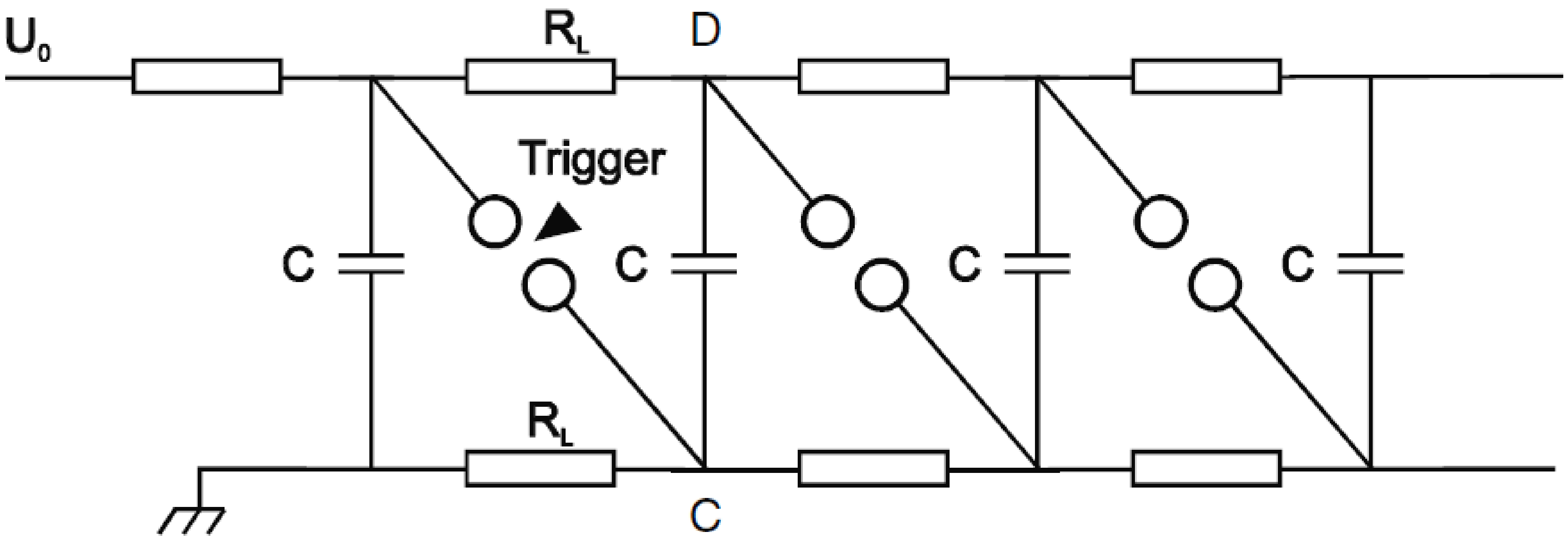

PFN-Marx

- **PFN:**

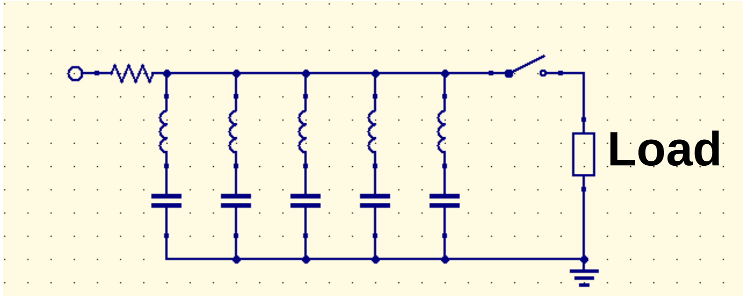

- **2-stage PFN:**

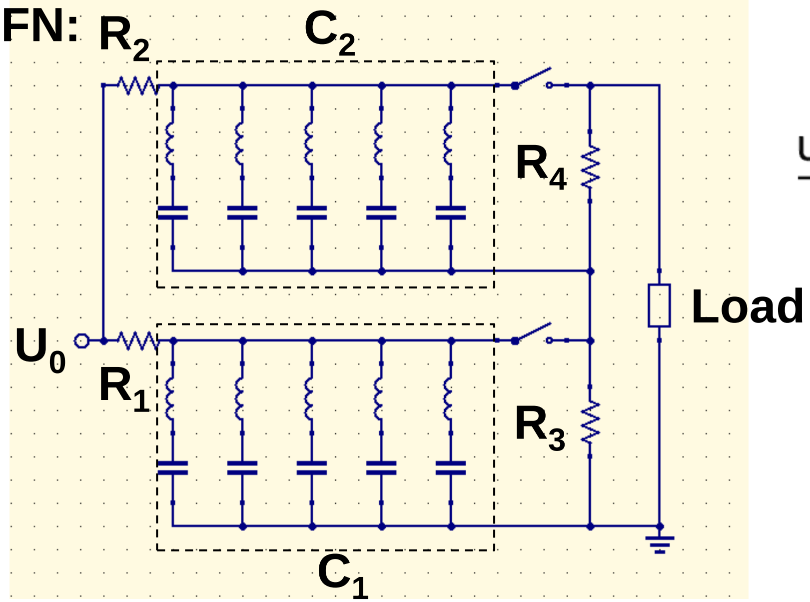

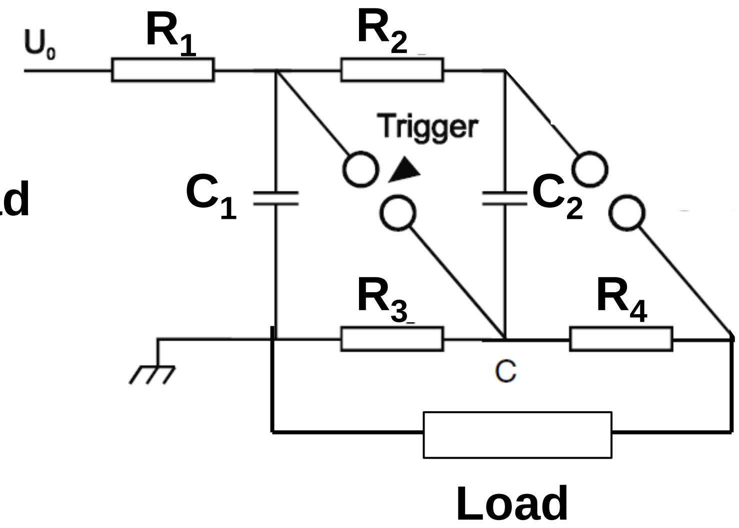

LC generator

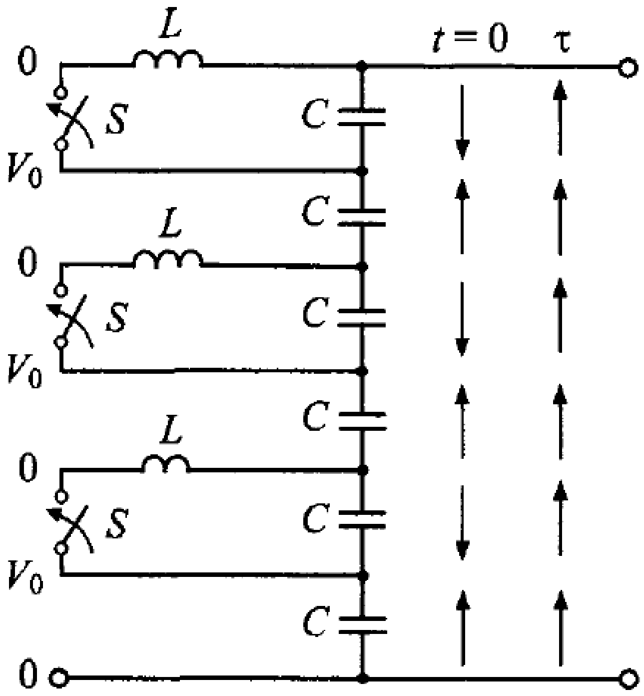

$$t = \tau = \pi\sqrt{LC} \quad V_{out} = NV_0$$

$$V_{out}(t) = NV_0[1 - e^{\alpha t}\cos(\omega t)]$$

- **Advantages:**
  - **the number of switches is halved.**
  - **The resistances and inductances of the switches have no effect on the circuit output impedance if the LC generator picks up the load through an additional fast switch.**
- **Disadvantage: switches must be operated as simultaneously as possible.**

Adding of voltage pulses by transit-time isolation

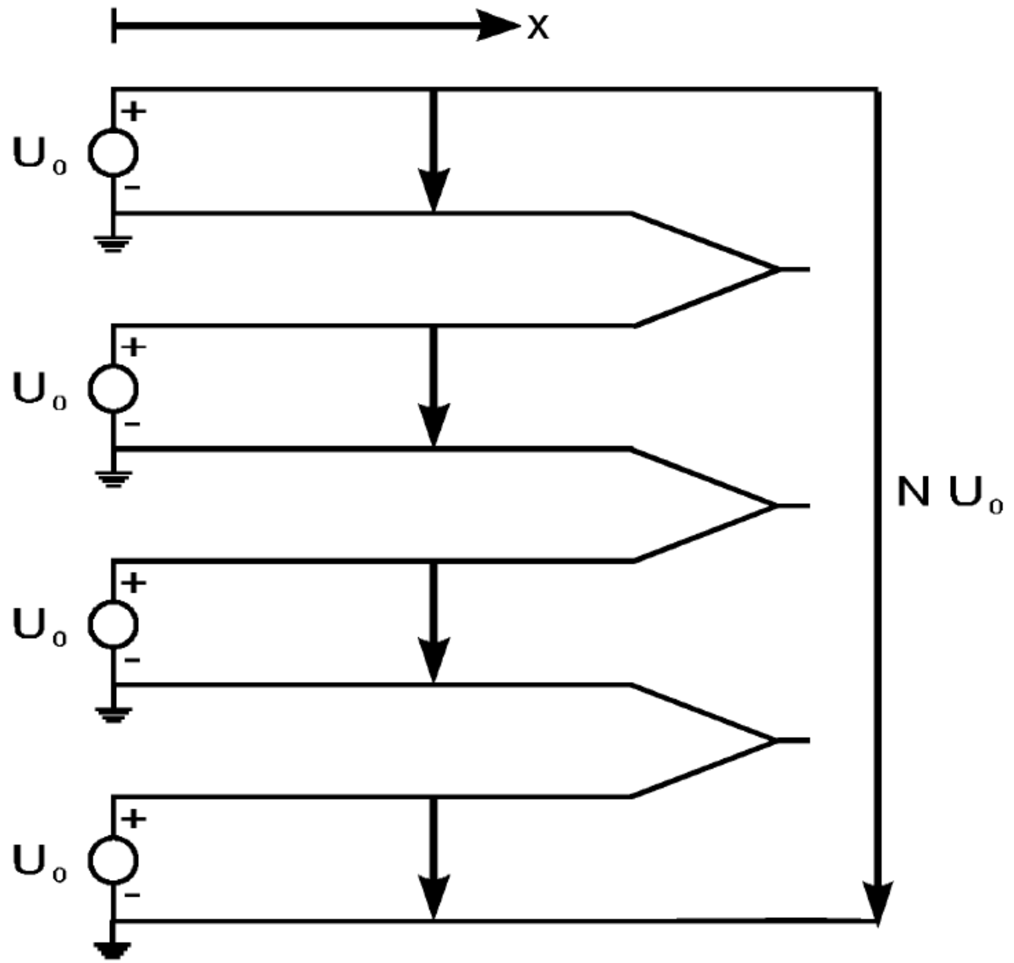

Transmission transformer

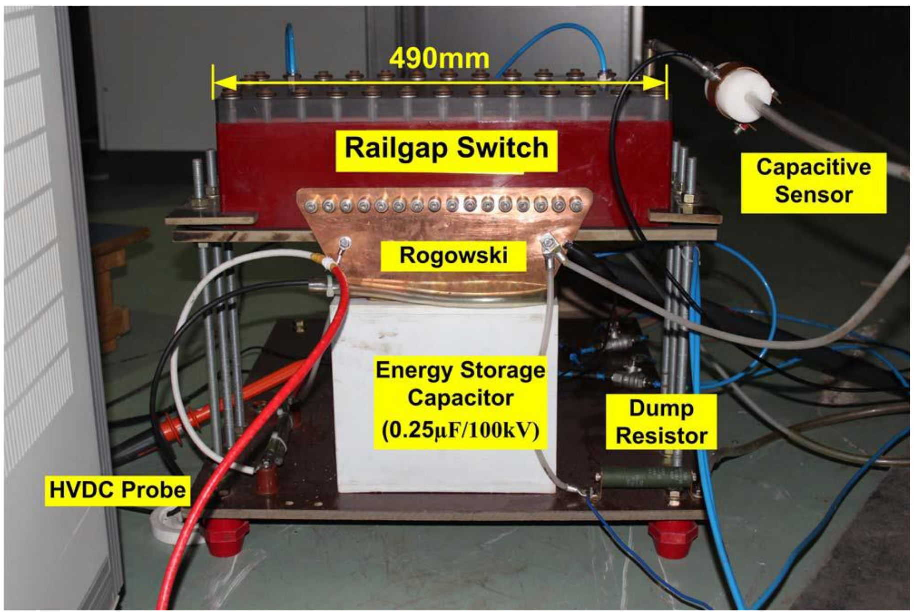

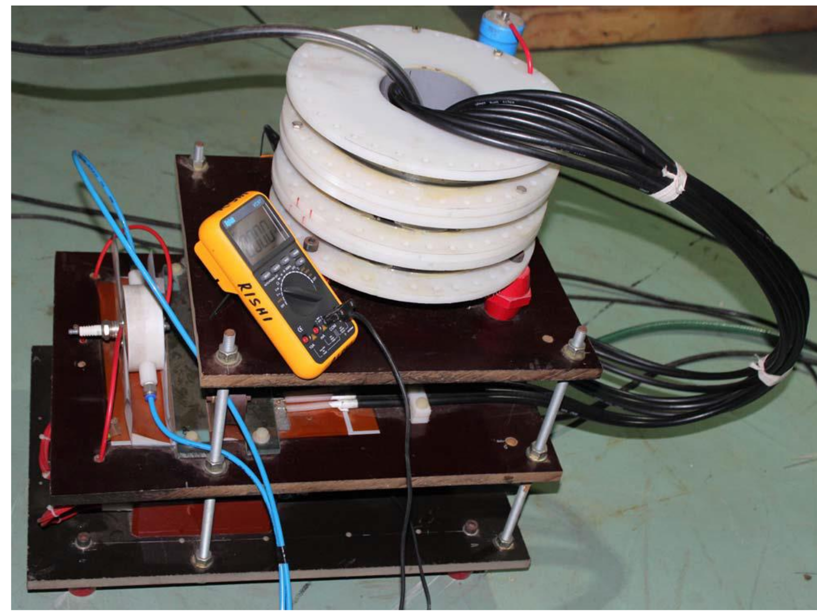

- **Multi-channel discharges between two rail-like electrodes will be triggered by a fast trigger pulse generator (rising speed > 5kV/ns).**

P.-Y. Chang etc. Rev. Sci. Instrum. 91, 114703 (2020)
R.Verma etc., Rev. Sci. Instrum. 85, 095117 (2014)

Transmission transformer

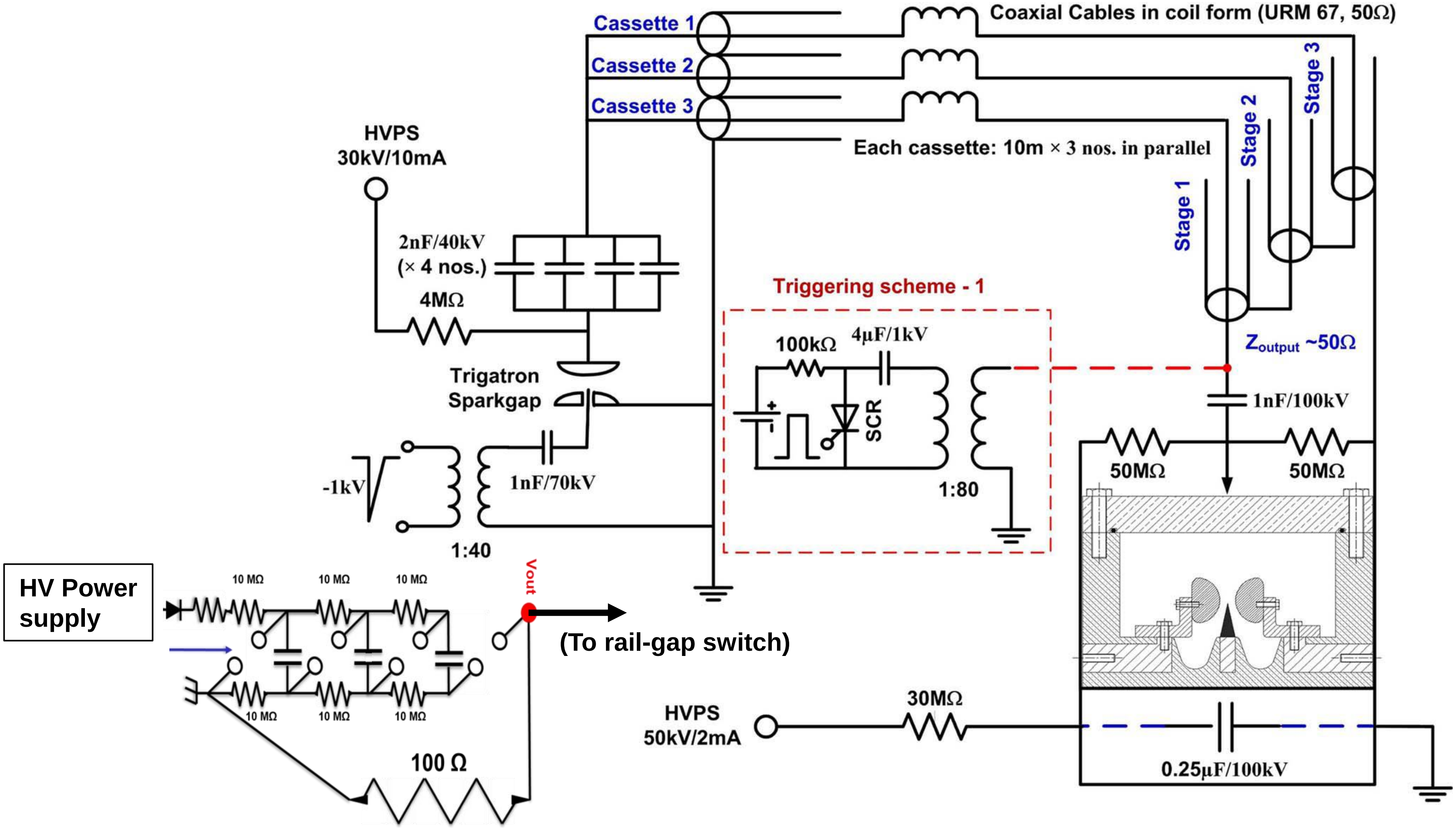

R. Verma, etc., Rev. Sci. Instrum. 85, 095117 (2014)

Line pulse transformers (LTP)

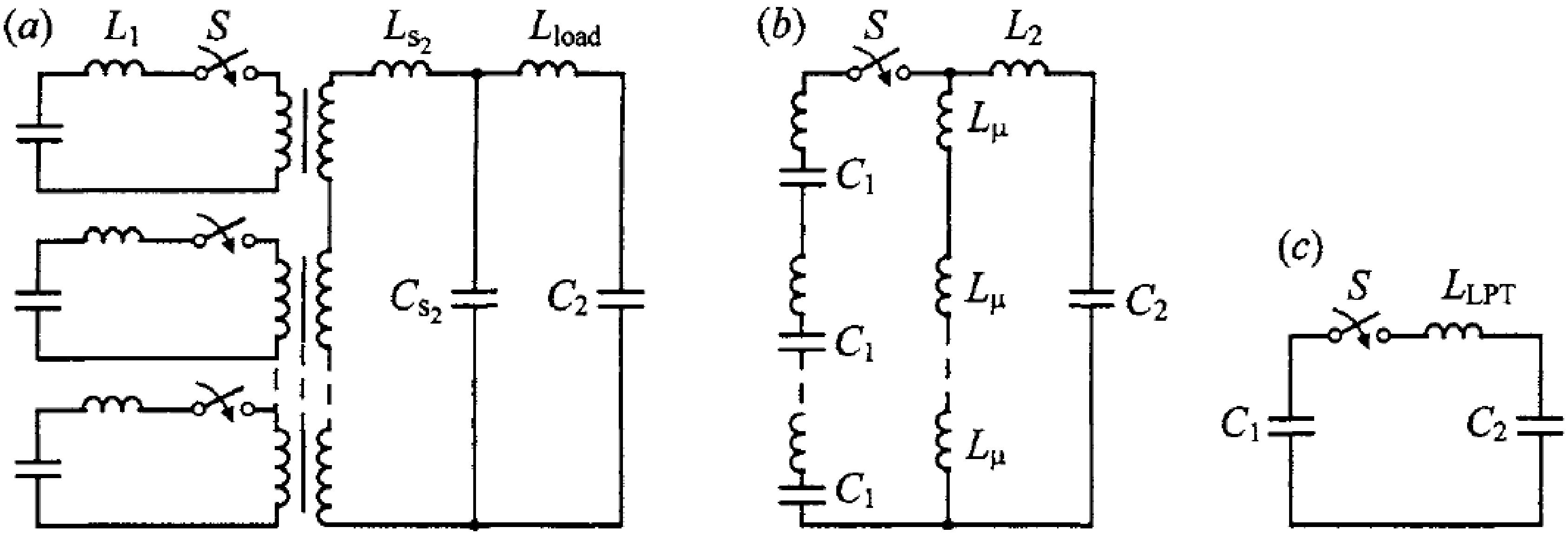

Figure 1.6. The equivalent (*a*), reduced (*b*), and simplified circuit (*c*) of a line transformer

Induction voltage adder (IVA)

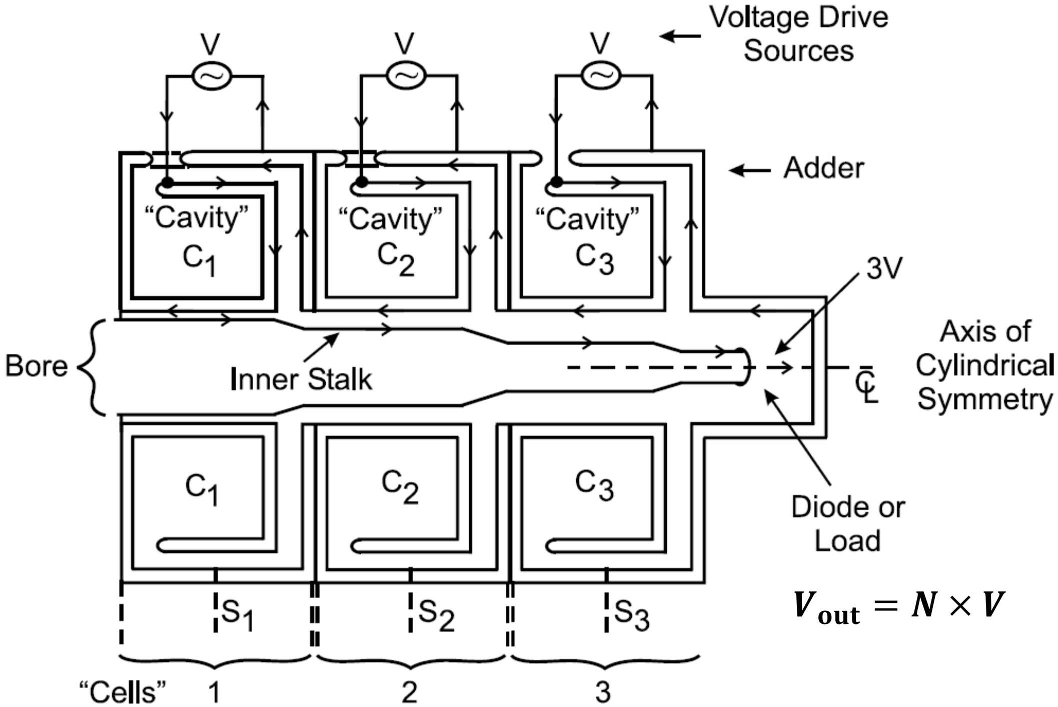

$$V_{\mathbf{out}} = N \times V$$

Example of IVA of KALIF-HELIA (High Energy Linear Induction Accelerator)

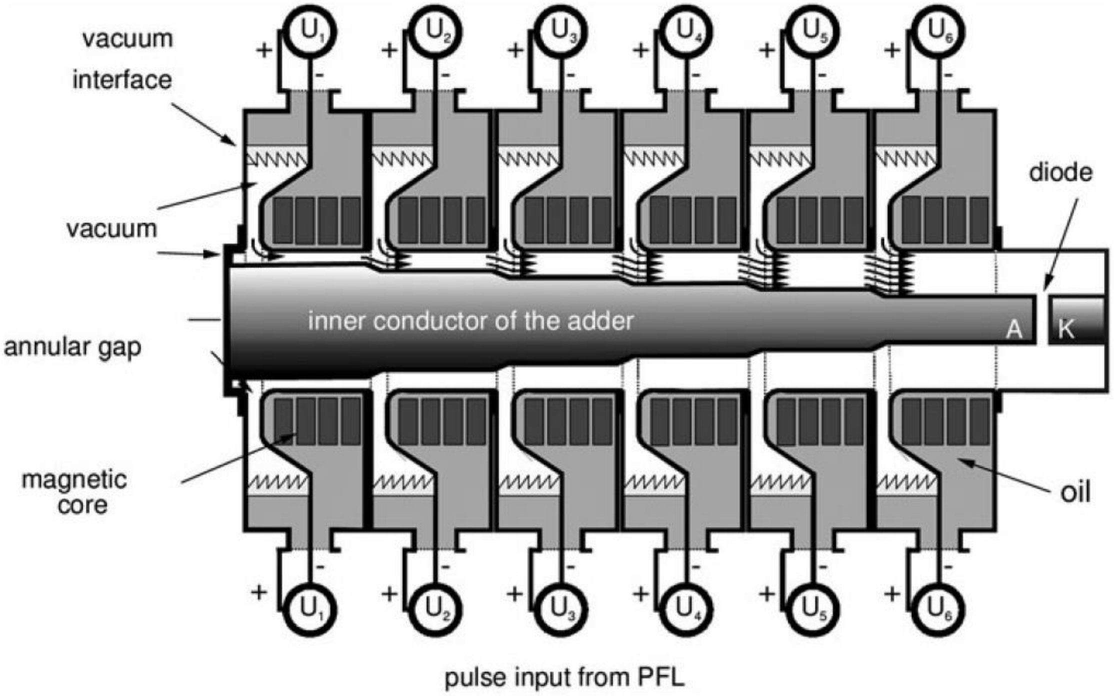

Linear Induction Accelerator (LIA)

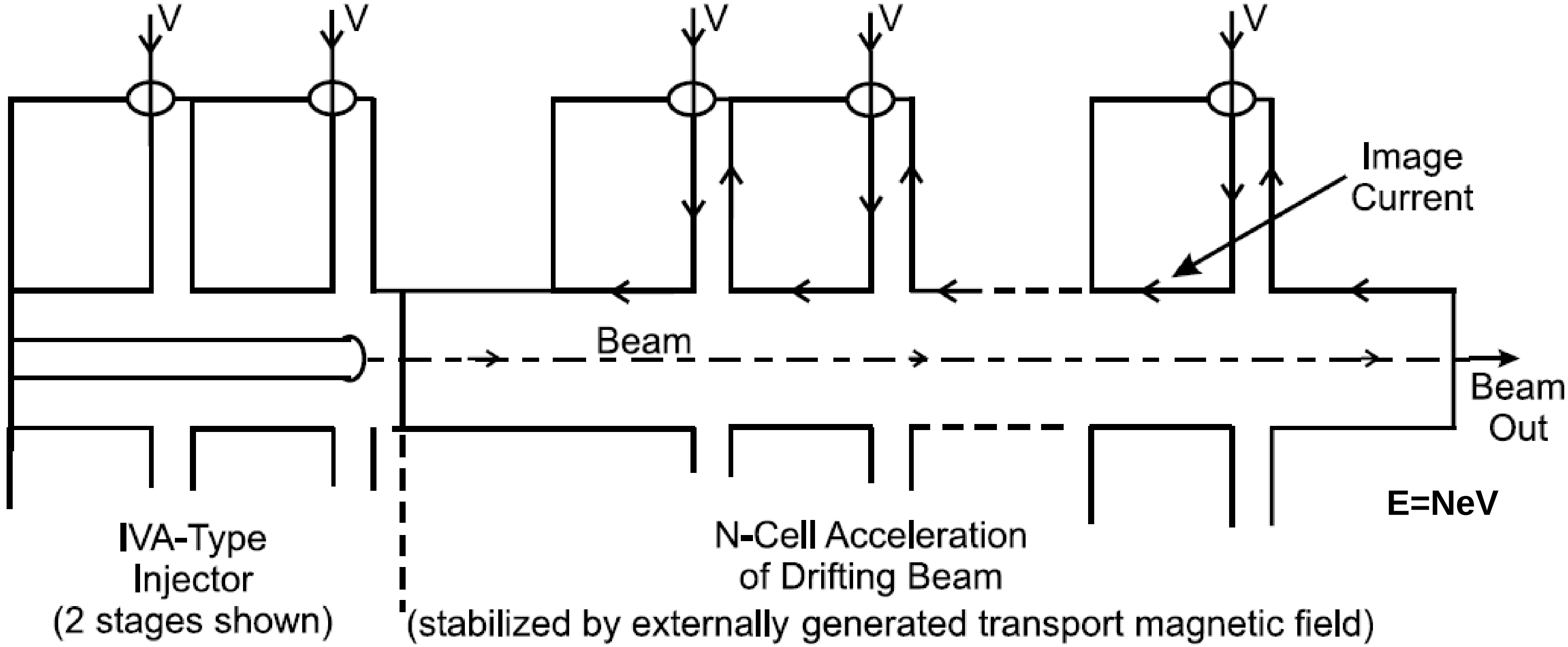

Linear Transformer Driver (LTD)

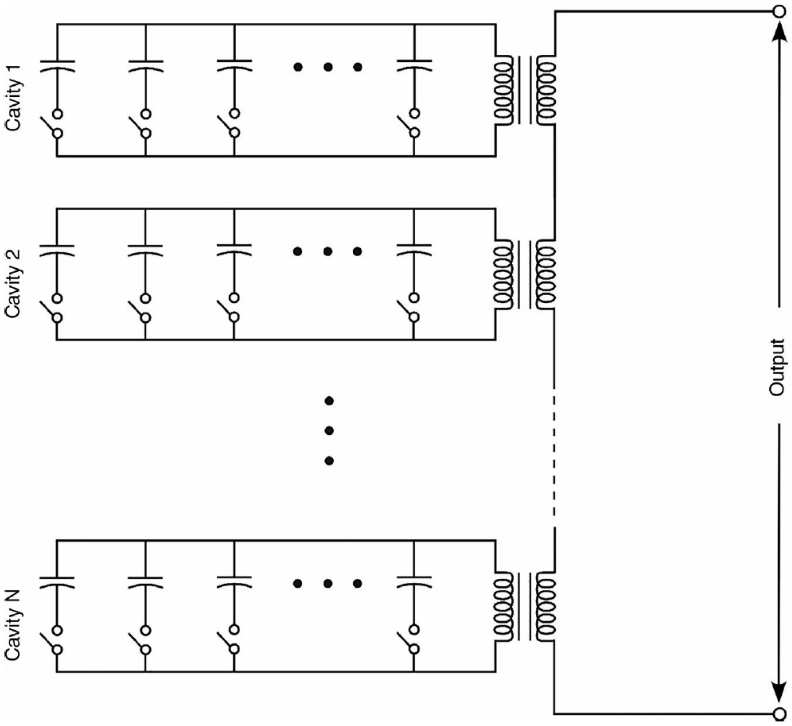

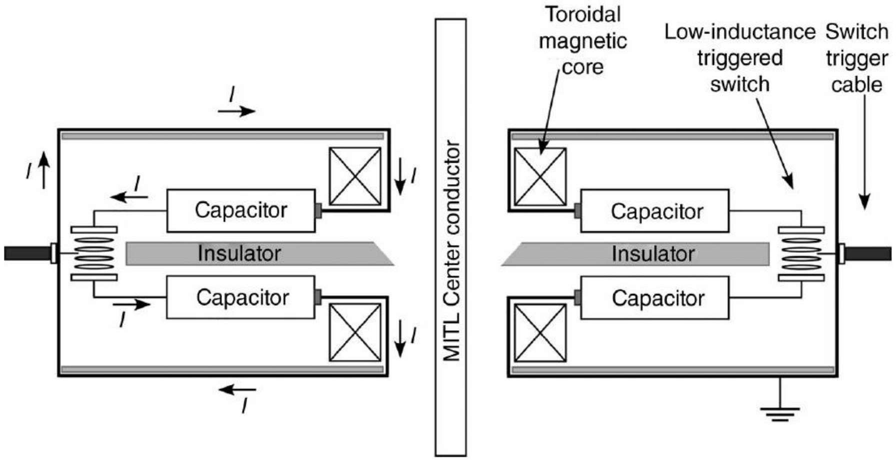

Linear Transformer Driver (LTD)

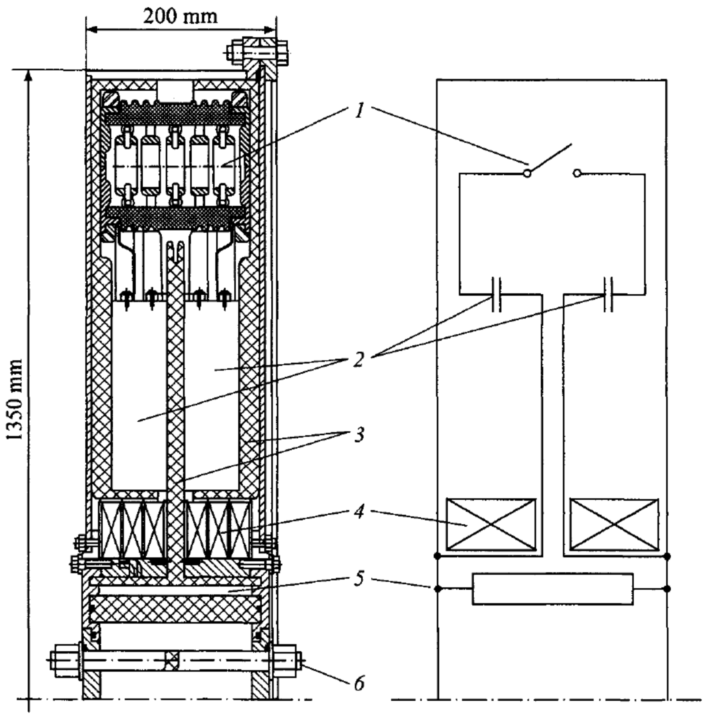

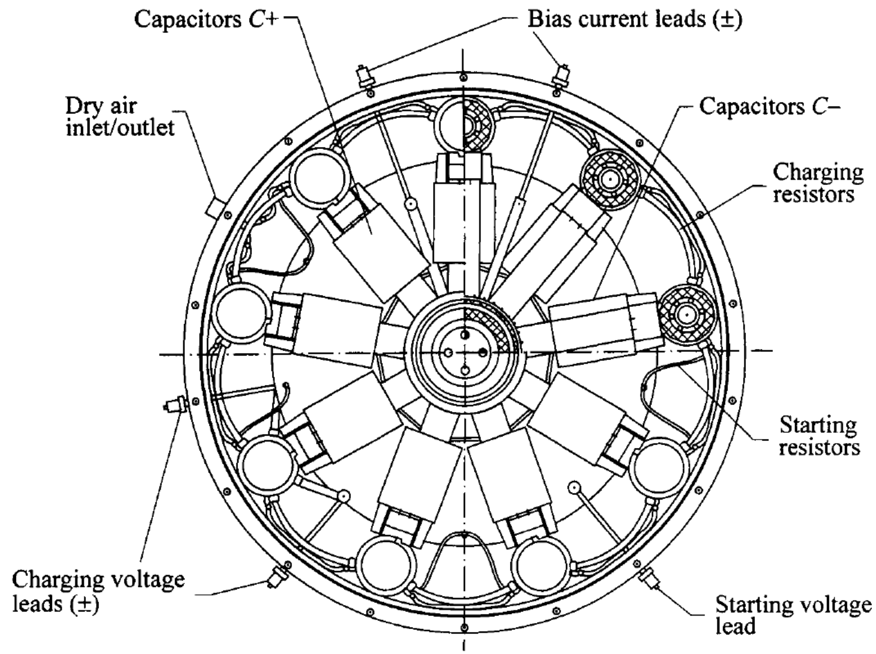

Linear transformer driver

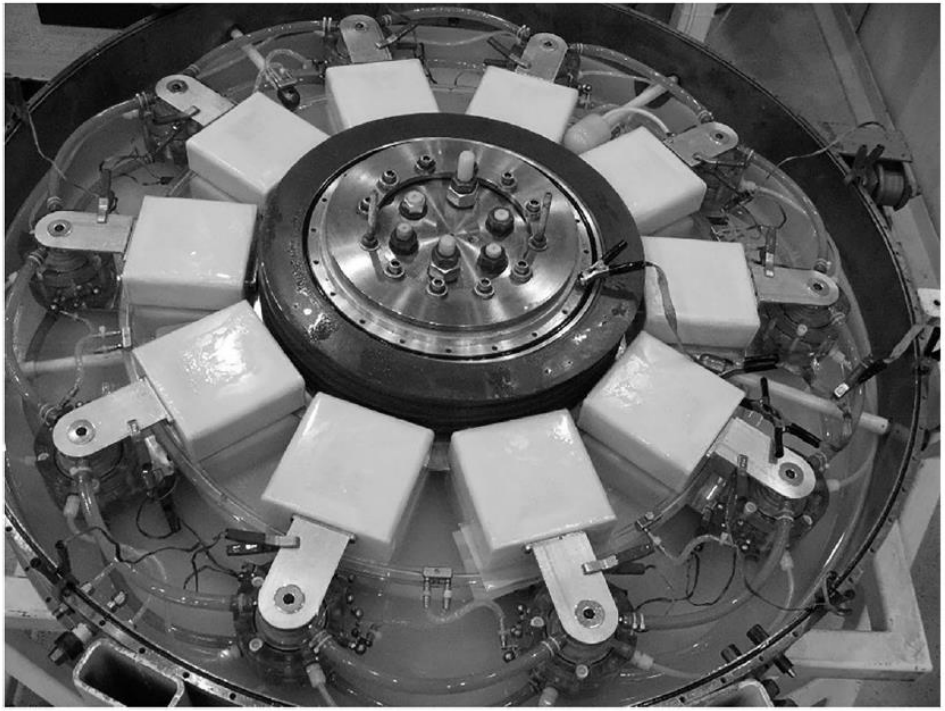

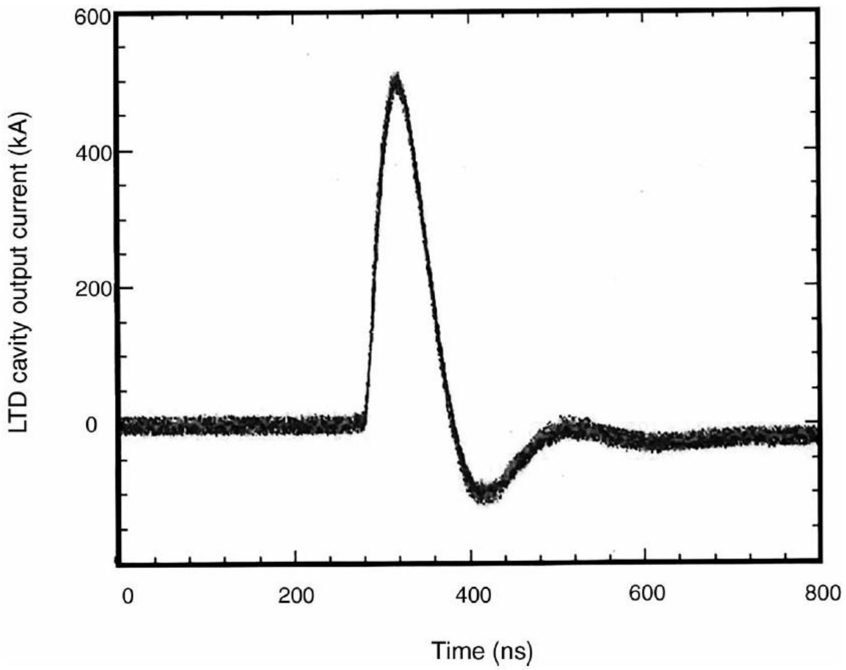

Linear Transformer Driver (LTD)

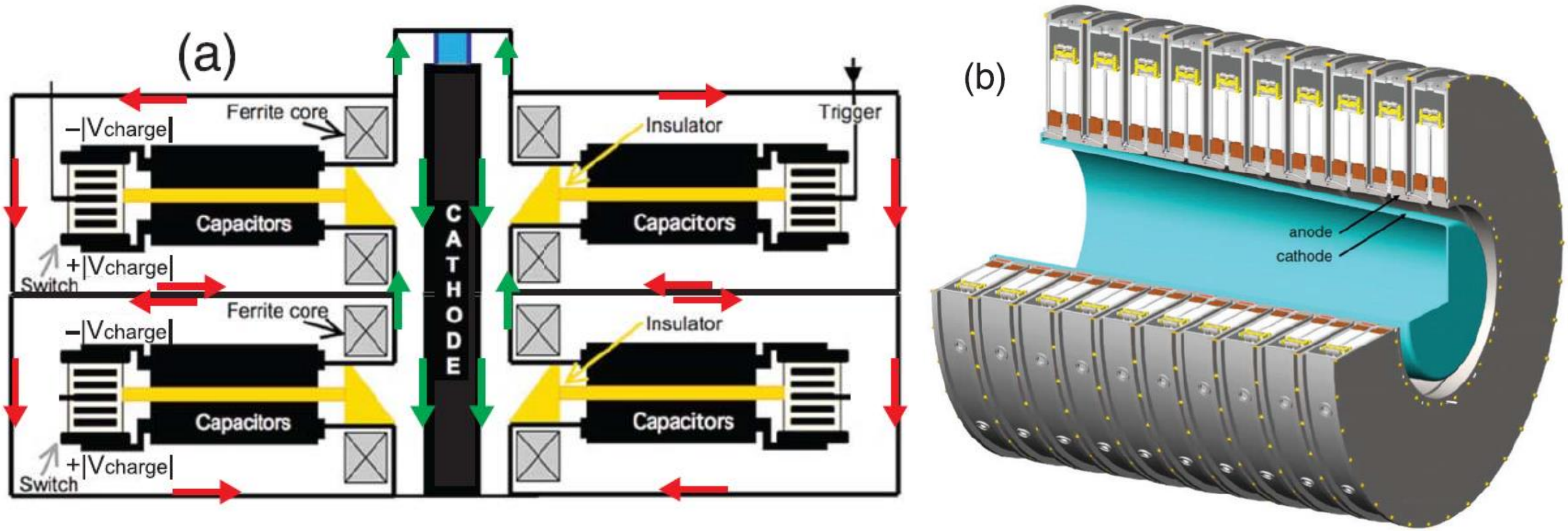

Characteristics of LTD

- **Advantages:**
  - **LTD stages enclose the primary storage. The LTD driver is more compact compared to other generators having similar output parameters.**
  - **LTD driver is simple.**
  - **It is practical and convenient to be built with relatively small size capacitors, which necessarily have less capacitance C. => short pulse**
  - **It can be operated in both LPT and IVA modes.**
- **Small capacitor, and reduced inductance (because of connected in parallel) lead to short pulse width.**
- **To increase energy storage, high voltage is used.**

Our design

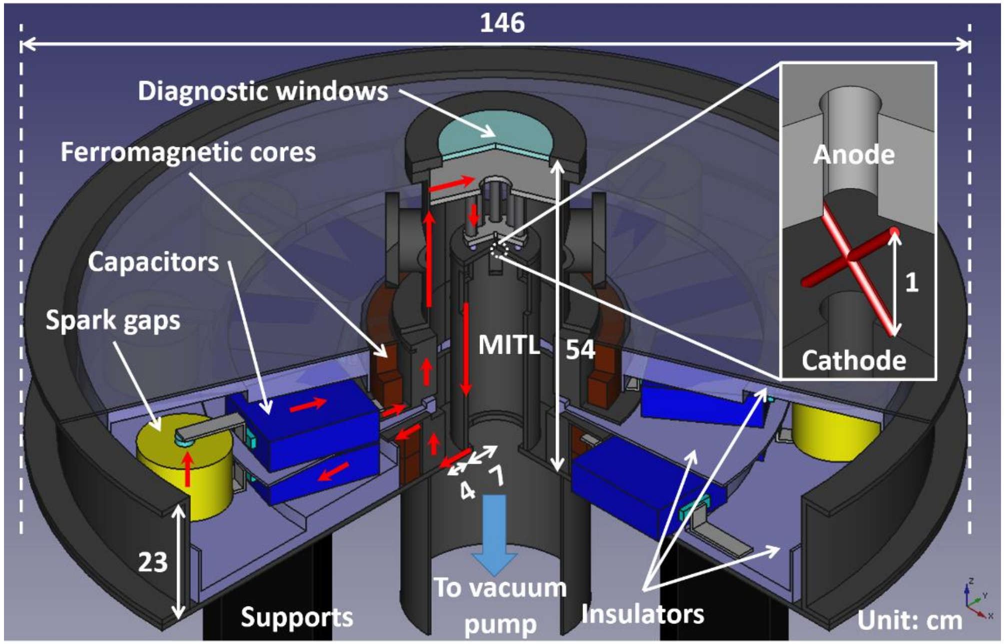
146
Diagnostic windows
Ferromagnetic cores
Capacitors
Spark gaps
Anode
Cathode
1
MITL
54
23
4
7
To vacuum pump
Insulators
Supports
Unit: cm

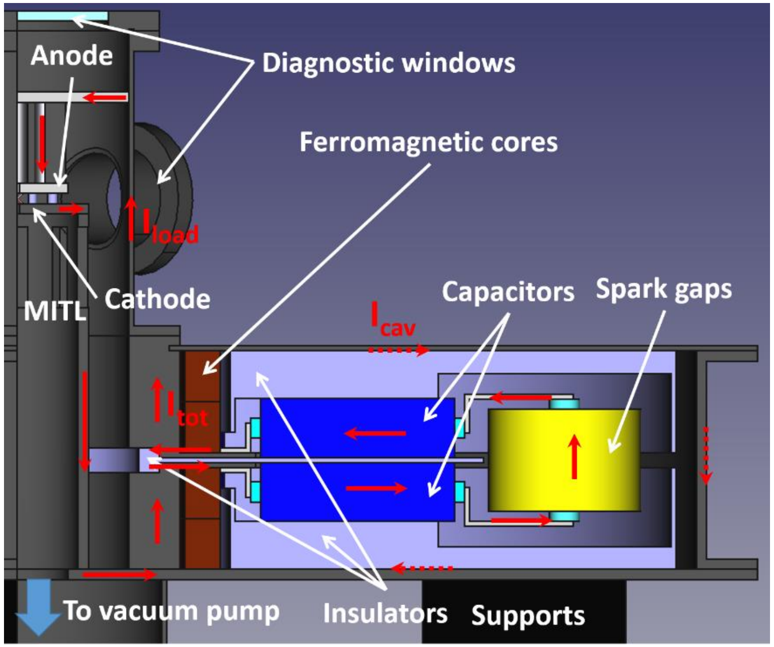
Anode
Diagnostic windows
Ferromagnetic cores
I_{load}
MITL
Cathode
Capacitors
Spark gaps
I_{cav}
I_{tot}
To vacuum pump
Insulators
Supports

Outlines

- Power and voltage adding
  - Marx generator
  - LC generator
  - Line pulse transformers
  - Induction voltage adder (IVA)
  - Linear induction accelerator (LIA)
  - Linear transformer driver (LTD)
- **Diagnostics**
  - **Voltage measurement**
  - **Current measurement**
- Applications of pulsed-power system

Diagnostics

- The basic electrical quantities are always the electromagnetic fields E and B from which pulse current and voltage must be derived.
- A suitable sensor does not perturb the fields to be measured is achieved with
  - capacitive sensors;
  - inductive sensors;
  - electro-optical methods;
  - resistive voltage dividers. It may create weak points in the high-voltage insulation.

Electromagnetic field sensors

- Rapidly changing electromagnetic fields, i.e., $\frac{d\vec{B}}{\mathrm{dt}}$ or $\frac{d\vec{E}}{\mathrm{dt}}$

 → induced currents / voltages in the conductors of a sensor.

 → only consider electrically short sensors:

 size < λ of the field where λ is the scale length or wavelength.

 or d << cτ_r, the distance of the wave that propagates where τ_r is the pulse rise time

 → conduction current density: $\vec{j}_c = \sigma\vec{E}$

 displacement current density: $\vec{j}_d = \frac{\partial\vec{D}}{\partial t}$

 Maxwell's eq:

$$\nabla\times\vec{E} = -\frac{\partial\vec{B}}{\partial t}$$

$$\nabla\times\vec{H} = -\frac{\partial\vec{D}}{\partial t} + \vec{j}$$

Electromagnetic field sensors

- **Ideal conducting sensor of area *A*:**

$$i(t) = [j_c(t) + \dot{D}(t)]A = [\sigma E(t) + \epsilon\epsilon_o \dot{E}(t)]A$$

The sensitivity depends on σ, ϵ, *A*, $E(t)$, $\dot{E}(t)$, and ω.

- **Alternating magnetic fields => induce currents in conducting loops.**

$$u(t) = -\oint \dot{\vec{B}}(t)d\vec{A} \approx -\dot{\vec{B}}(t)\vec{A}$$ **<= if field is homogeneous.**

The sensitivity depends on *A*, $\dot{B}(t)$, and ω.

Quasistationary Fields

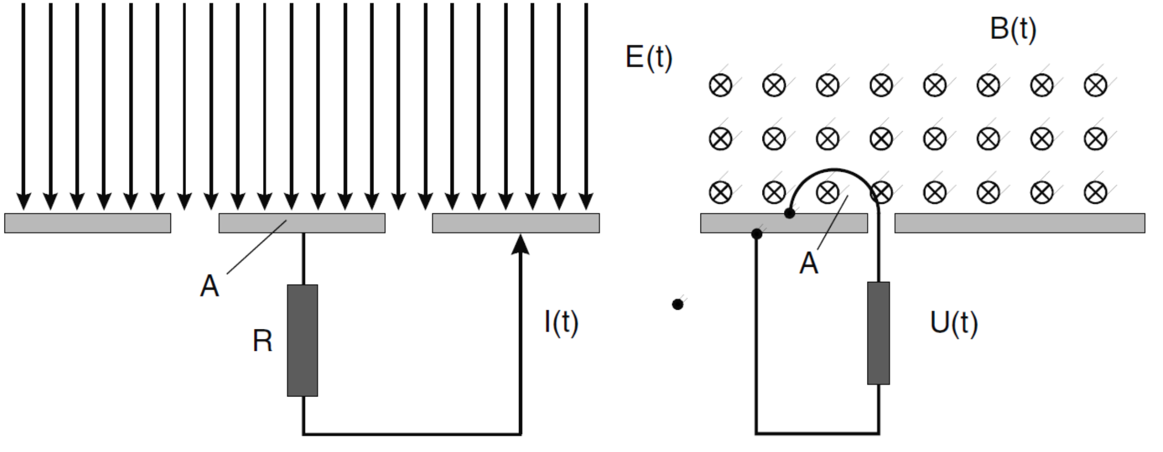

- **The coupling may also couple the undesired noise.**

Capacitive/Inductive sensors

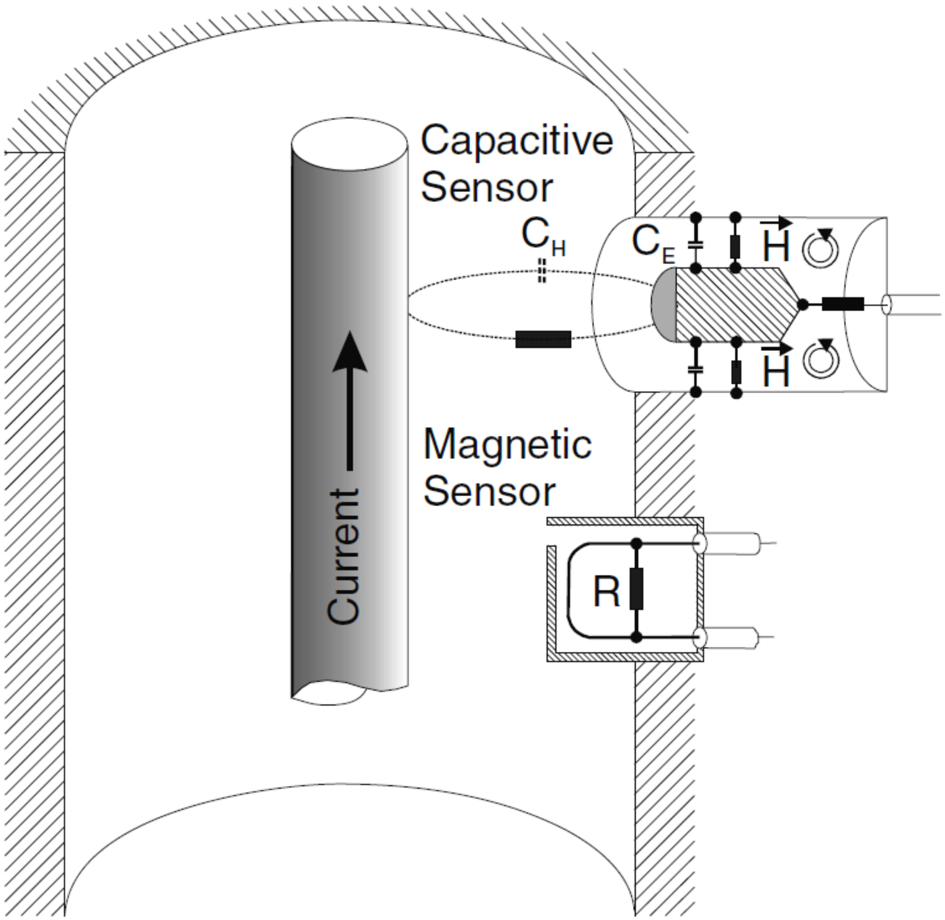

$$u(t) = \frac{C_H}{C_H + C_E} U(t)$$

$$u(t) = -\oint \dot{\vec{B}}(t) d\vec{A} = -\frac{d\phi}{dt}$$

Capacitive sensor for voltage measurement

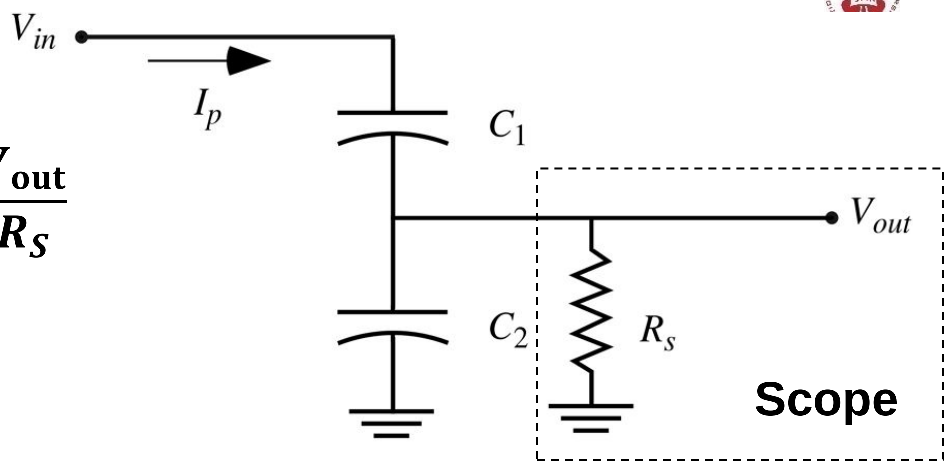

$$V_{\text{in}} = V_{C_1} + V_{\text{out}} \qquad I_p = I_{C_2} + I_{R_s}$$

$$I_p = C_1 \frac{\mathrm{dV}_{C_1}}{\mathrm{dt}} \qquad I_{C_2} = C_2 \frac{\mathrm{dV}_{\text{out}}}{\mathrm{dt}} \qquad I_{R_S} = \frac{V_{\text{out}}}{R_S}$$

$$C_1 \frac{\mathrm{dV}_{C_1}}{\mathrm{dt}} = C_2 \frac{\mathrm{dV}_{\text{out}}}{\mathrm{dt}} + \frac{V_{\text{out}}}{R_S}$$

$$\frac{dV_{C_1}}{\mathrm{dt}} = \frac{C_2}{C_1} \frac{\mathrm{dV}_{\text{out}}}{\mathrm{dt}} + \frac{V_{\text{out}}}{R_S C_1}$$

$$\frac{dV_{\text{in}}}{\mathrm{dt}} = \frac{\mathrm{dV}_{C_1}}{\mathrm{dt}} + \frac{\mathrm{dV}_{\text{out}}}{\mathrm{dt}}$$

$$\frac{dV_{\text{in}}}{\mathrm{dt}} = \left(\frac{C_1 + C_2}{C_1}\right) \frac{\mathrm{dV}_{\text{out}}}{\mathrm{dt}} + \frac{V_{\text{out}}}{R_S C_1}$$

$$\frac{V_{\text{in}}}{V_{\text{out}}} = \left(\frac{C_1 + C_2}{C_1}\right) + \frac{1}{\mathrm{sR}_S C_1}$$

$$= \left(\frac{C_1 + C_2}{C_1}\right)\left[1 + \frac{1}{\mathrm{sR}_S (C_1 + C_2)}\right]$$

$$\omega_{3\text{dB}} = \frac{1}{R_S (C_1 + C_2)}$$

- **Low frequency:**

$$V_{\text{out}} = \frac{C_1}{C_1 + C_2} V_{\text{in}}$$

- **High frequency:**

$$V_{\text{out}} = R_S C_1 \frac{\mathrm{dV}_{\text{in}}}{\mathrm{dt}}$$

Inductive sensor with RC integrator for current measurement

$$|u(t)| = \frac{d\phi}{dt} = L\frac{di}{dt} + Ri + \frac{1}{C}\int_0^t i\,dt'$$

$$|u(t)| = \frac{d\phi}{dt} = k\frac{di}{dt}$$

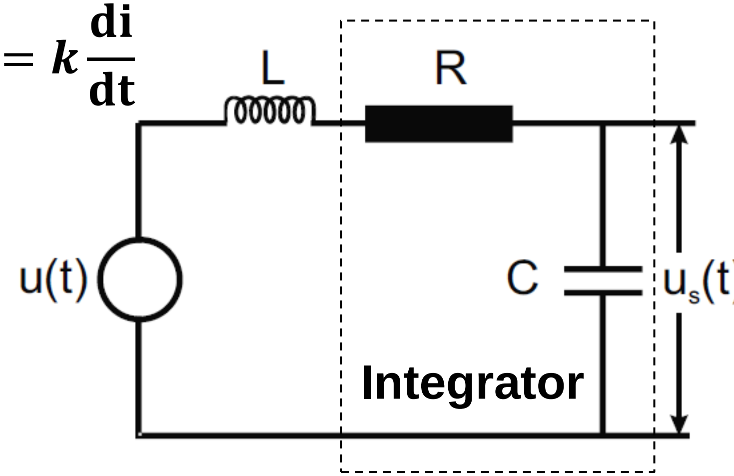

$$|u(t)| = \frac{d\phi}{dt} \approx Ri + \frac{1}{C}\int_0^t i\,dt'$$

$$u_s = \frac{1}{C}\int_0^t i\,dt' \Rightarrow C\dot{u}_S = i$$

$$u = RC\dot{u}_S + u_s$$

$$\dot{u}_S + \frac{1}{RC}u_s = \frac{1}{RC}u$$

$$\dot{u}_S e^{\frac{1}{RC}t} + \frac{1}{RC}u_s e^{\frac{1}{RC}t} = \frac{1}{RC}u e^{\frac{1}{RC}t}$$

$$\frac{d}{dt}\left(u_S e^{\frac{1}{RC}t}\right) = \frac{1}{RC}u e^{\frac{1}{RC}t}$$

$$\int d\left(u_S e^{\frac{1}{RC}t'}\right) = \frac{1}{RC}\int_0^t u e^{\frac{1}{RC}t'}dt'$$

$$u_S e^{\frac{1}{RC}t} - u_S(0) = \frac{1}{RC}\int_0^t u e^{\frac{1}{RC}t'}dt'$$

$$u_s = \frac{e^{-\frac{1}{RC}t}}{RC}\int_0^t u e^{\frac{1}{RC}t'}dt' \approx \frac{1}{RC}\int_0^t u\,dt'$$

$$= \frac{k}{RC}i(t)$$

- **Working regime:**

$$RC >> t \approx \frac{1}{\omega} \qquad \omega >> \frac{1}{RC}$$

Rogowski coil

- **In situ calibration is needed to obtain *k*.**

$$|u(t)| = \frac{d\phi}{dt} = k\frac{di}{dt}$$

- **If in situ calibration is not possible, Rogowski coil instead of a simple current loop is used.**
- **Rogowski coil is a coil consisting of many windings lined up in a toroidal configuration encircling the current path.**

$$\oint \vec{B} \cdot d\,\vec{l} = \mu_o I \qquad B = \frac{\mu_o}{2\pi r} I$$

$$\phi_1 = BA = \frac{\mu_o A}{2\pi r} I$$

$$|u| = \frac{d\phi}{dt} = N\frac{d\phi_1}{dt} = \frac{\mu_o AN}{2\pi r}\frac{dI}{dt}$$

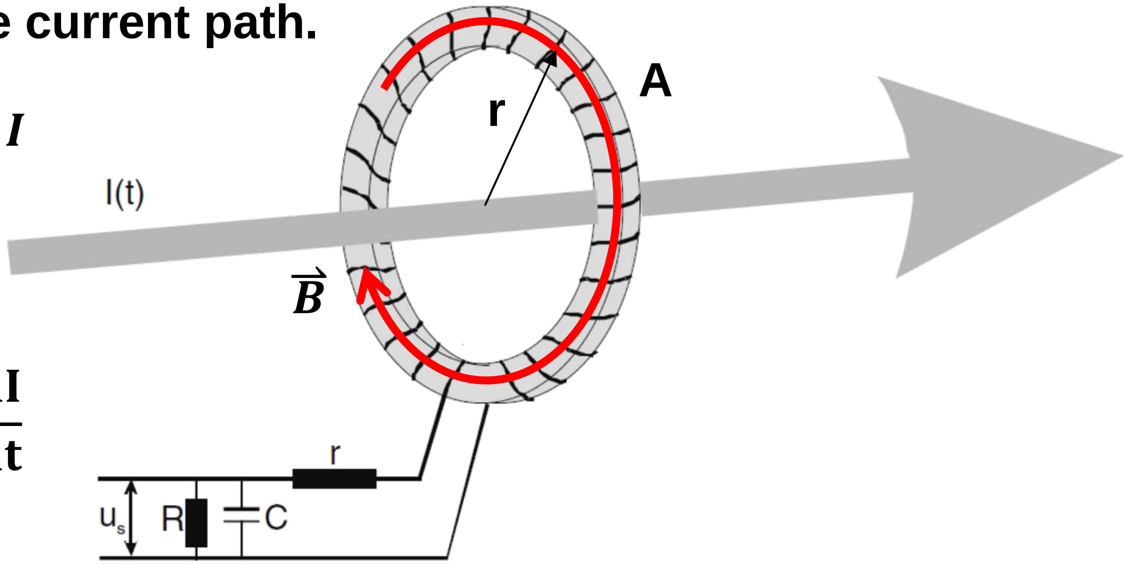

$$u_S(t) = \frac{1}{RC}\int u dt = \frac{1}{RC}\frac{\mu_o AN}{2\pi r}\int \frac{dI}{dt}dt = \frac{1}{RC}\frac{\mu_o AN}{2\pi r} I$$

Assumption for Rogowski coil

- Neglect the spatial dependence of the magnetic induction over the area A
- Cross section A are all the same.
- Number of turns per unit length is const.
- When #/ of turns increase,

  L may be large

  => $L\omega \ll R$ may not be met.

  => use the opposite regime

  where $L\omega \gg R$.

  It becomes "self-integrated."

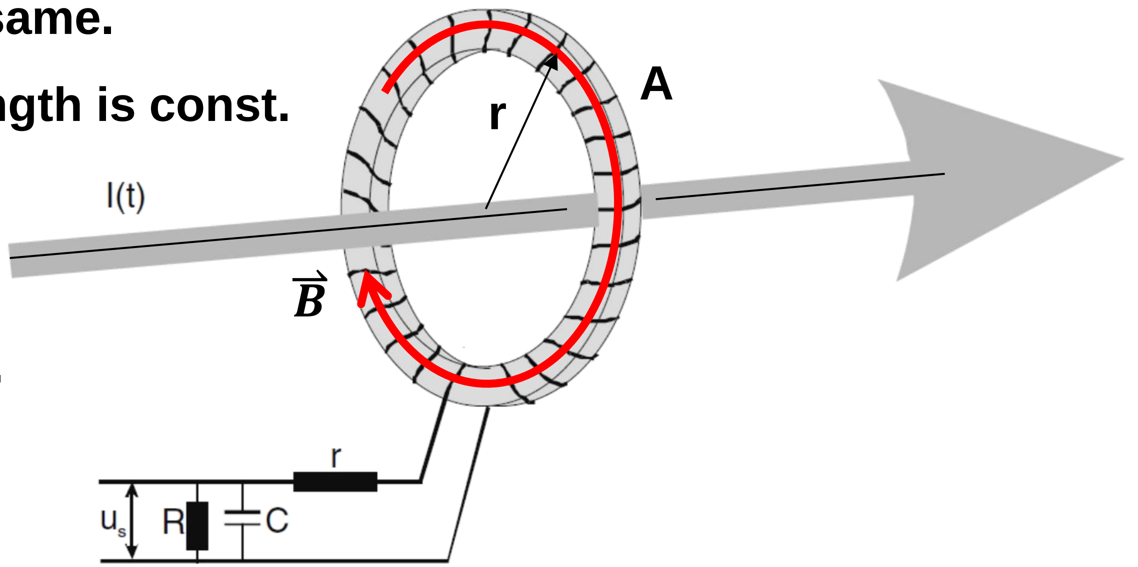

Self-integrated current monitor where Lω >> R

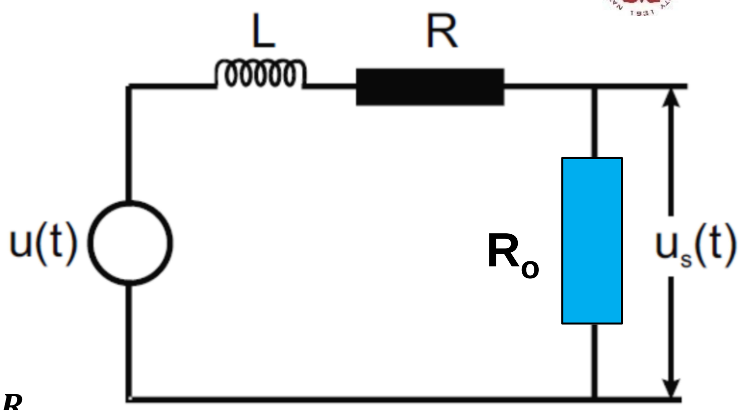

$$R_o >> R \qquad L\omega >> R_o + R$$

$$u - L\frac{\mathrm{dI}}{\mathrm{dt}} = u_S \qquad u_S = \mathrm{IR}_o$$

$$u - \frac{L}{R_o}\frac{\mathrm{du_s}}{\mathrm{dt}} = u_S \qquad \frac{du_S}{\mathrm{dt}} + \frac{R_o}{L}u_S = \frac{R_o}{L}u$$

$$e^{-\frac{R_o}{L}t}\frac{d}{\mathrm{dt}}\left(u_s e^{\frac{R_o}{L}t}\right) = \frac{R_o}{L}u \qquad \frac{d}{\mathrm{dt}}\left(u_s e^{\frac{R_o}{L}t}\right) = \frac{R_o}{L}\mathrm{ue}^{\frac{R_o}{L}t}$$

$$u_S e^{\frac{R_o}{L}t} - u_S(0) = \frac{R_o}{L}\int \mathrm{ue}^{\frac{R_o}{L}t'}\mathrm{dt}'$$

$$u_s = \frac{R_o}{L}e^{-\frac{R_o}{L}t}\int \mathrm{ue}^{\frac{R_o}{L}t'}\mathrm{dt}' \qquad \mathrm{L\omega} >> R_o \qquad t\frac{R_o}{L} \ll 1 \quad |u| = \frac{\mathrm{d\phi}}{\mathrm{dt}} = N\frac{\mathrm{d\phi_1}}{\mathrm{dt}} = \frac{\mu_o\mathrm{AN}}{2\pi\mathrm{r}}\frac{\mathrm{dI}}{\mathrm{dt}}$$

$$u_s = \frac{R_o}{L}\int \mathrm{udt}' = \frac{R_o}{L}\int \frac{\mu_o\mathrm{AN}}{2\pi\mathrm{r}}\frac{\mathrm{dI}}{\mathrm{dt}}\mathrm{dt}' = \frac{R_o}{L}\frac{\mu_o\mathrm{AN}}{2\pi\mathrm{r}}I$$ **<= self integrated!**

$u_S \propto R_o$

- **Ferromagnetic material in the torus may be used to increase inductance.**

Additional note for Rogowski coil

- **To reduce the capacitive coupling, wrap the Rogowski coil with a slotted metallic case. However, it need to let the flux goes into the winding. NO closed loop is allowed.**
- **A large flux penetrating the main opening of the torus may induce additional voltage. To compensate for this signal, feed one end of the wire back through the windings**

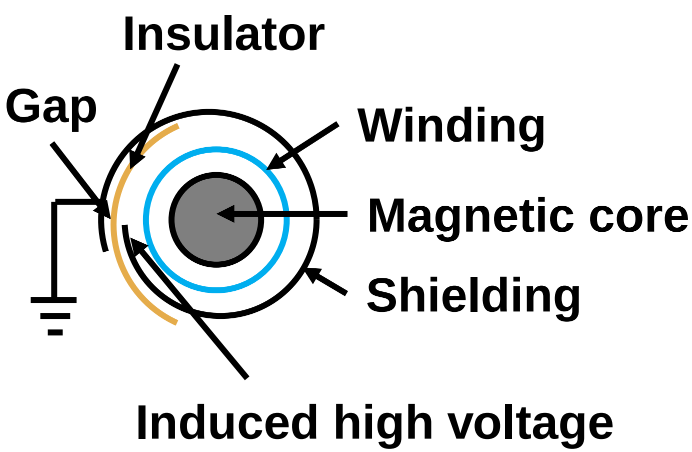

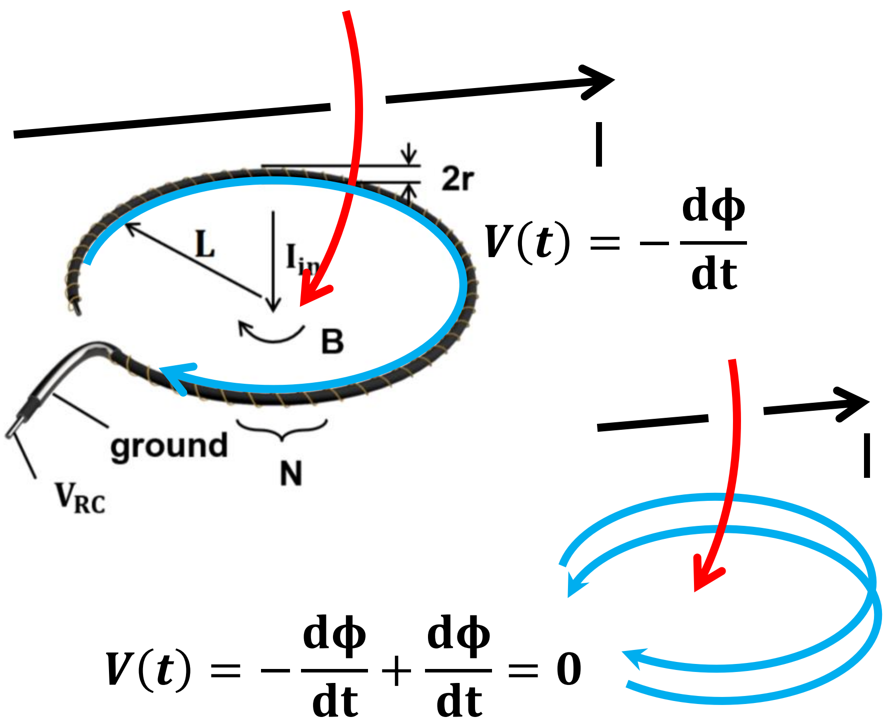

$$V(t) = -\frac{d\phi}{dt}$$

$$V(t) = -\frac{d\phi}{dt} + \frac{d\phi}{dt} = 0$$

Chih-Rui Hsieh, Master thesis (2020)

Fabrication of the Rogowski coil using a coaxial cable

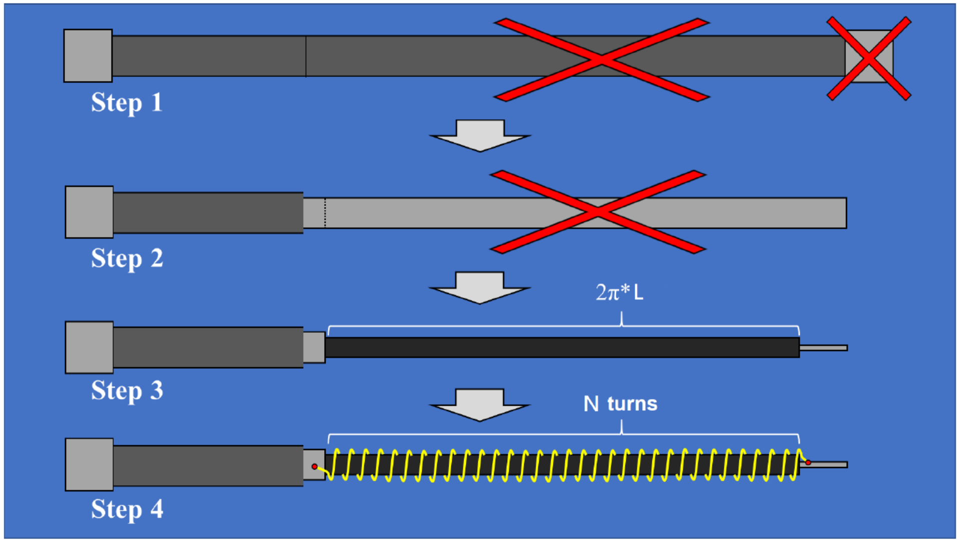

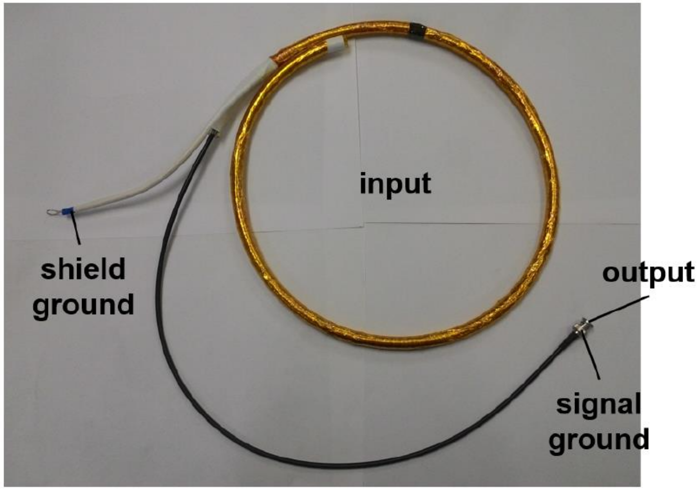

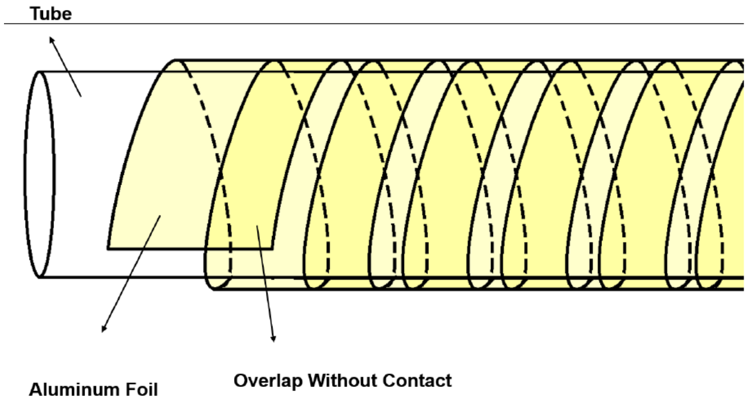

Chih-Rui Hsieh, Master thesis (2020)

Other ways of making compensated Rogowski coil

- **Bifiliar**
- **Inner compensating coil**
- **Outer compensating coil**

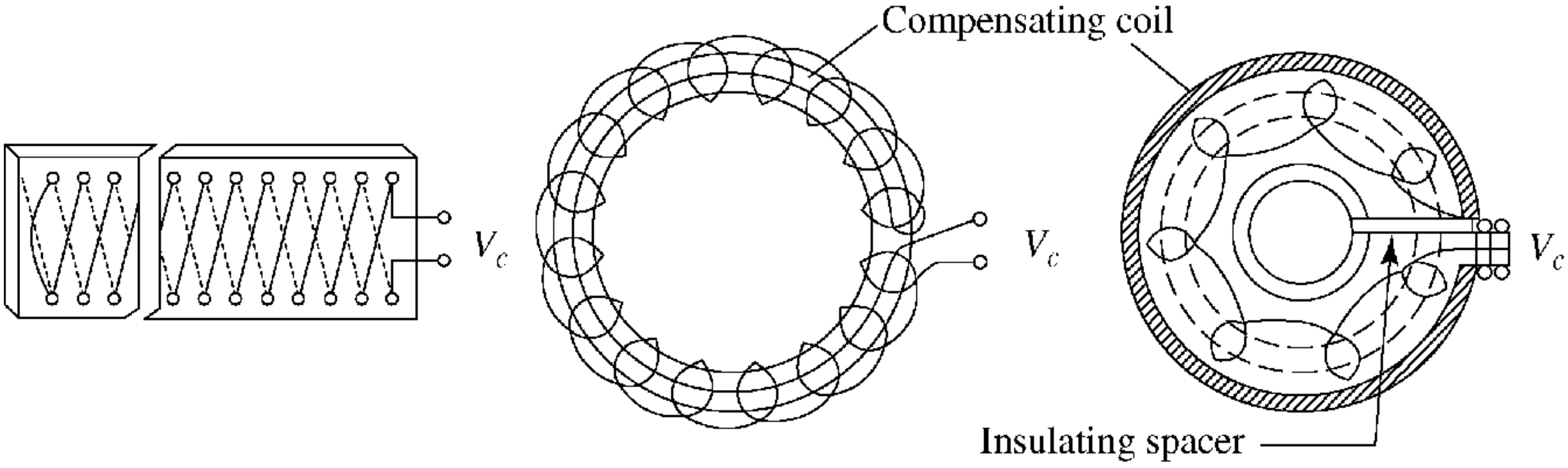

(a) (b) (c)

Current-viewing resistors (CVRs)

- **It is also called "shunts."**
- **Measurement of the voltage drop across a resistor of known value, incorporated into the circuit.**

$$I = \frac{V}{R}$$

- **The current path and the measuring circuit are coupled not only through the Ohmic resistor but also magnetically.**

=> preferable to place the metering contact in a field-free space or reduce the coupling efficiency.

- **Cylindrically symmetric shunt geometry provides an zero magnetic coupling.**

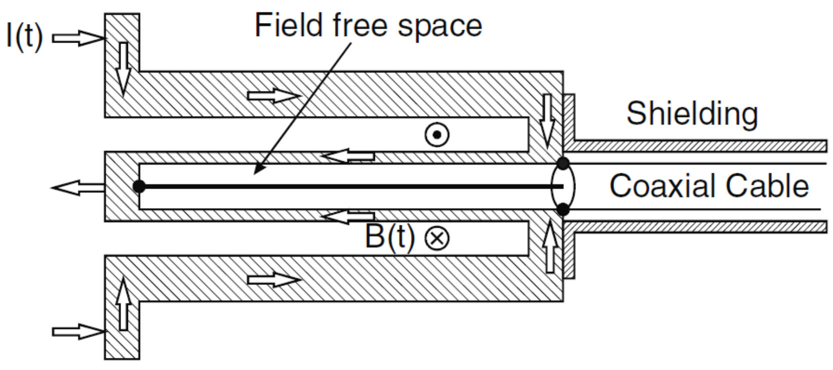

Shunts

- **Folded strip shunt**

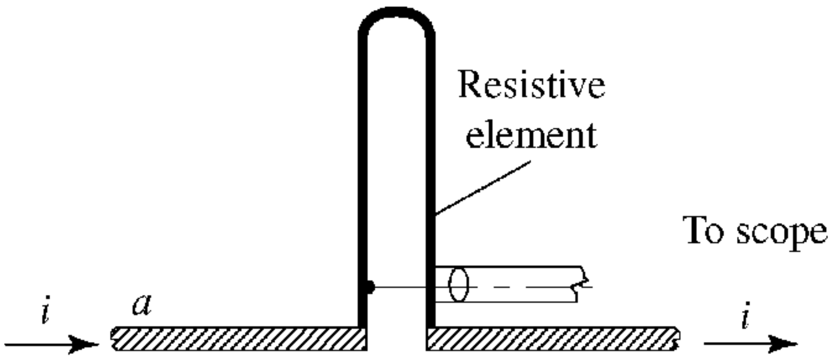

(a)

- **Parallel twisted shunt**

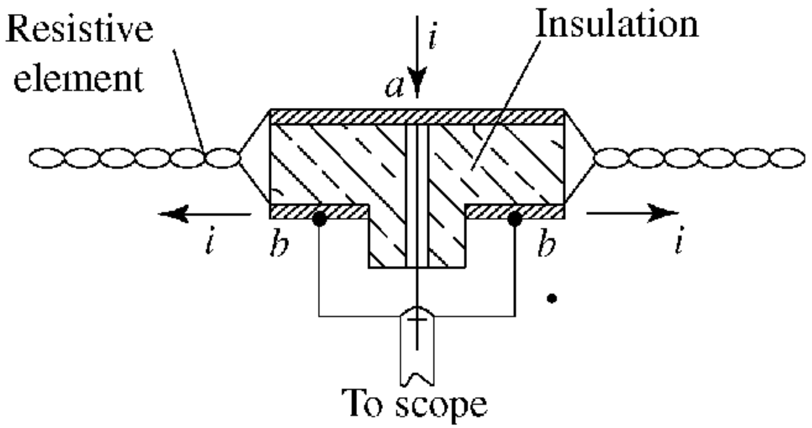

(b)

CVR integrated into the outer conductor of a coaxial transmission line

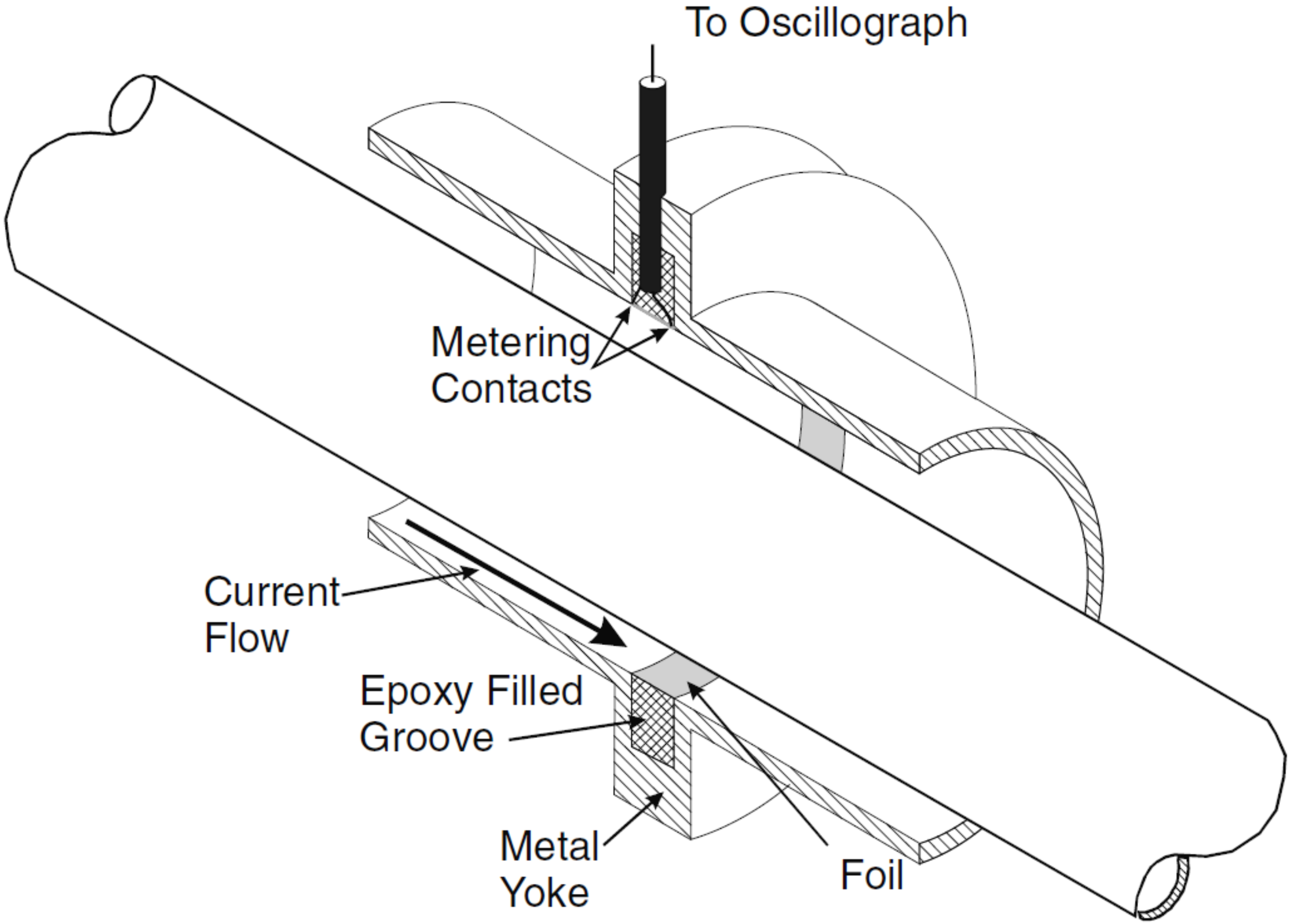

Example of current and voltage monitor using B-dot and D-dot monitors

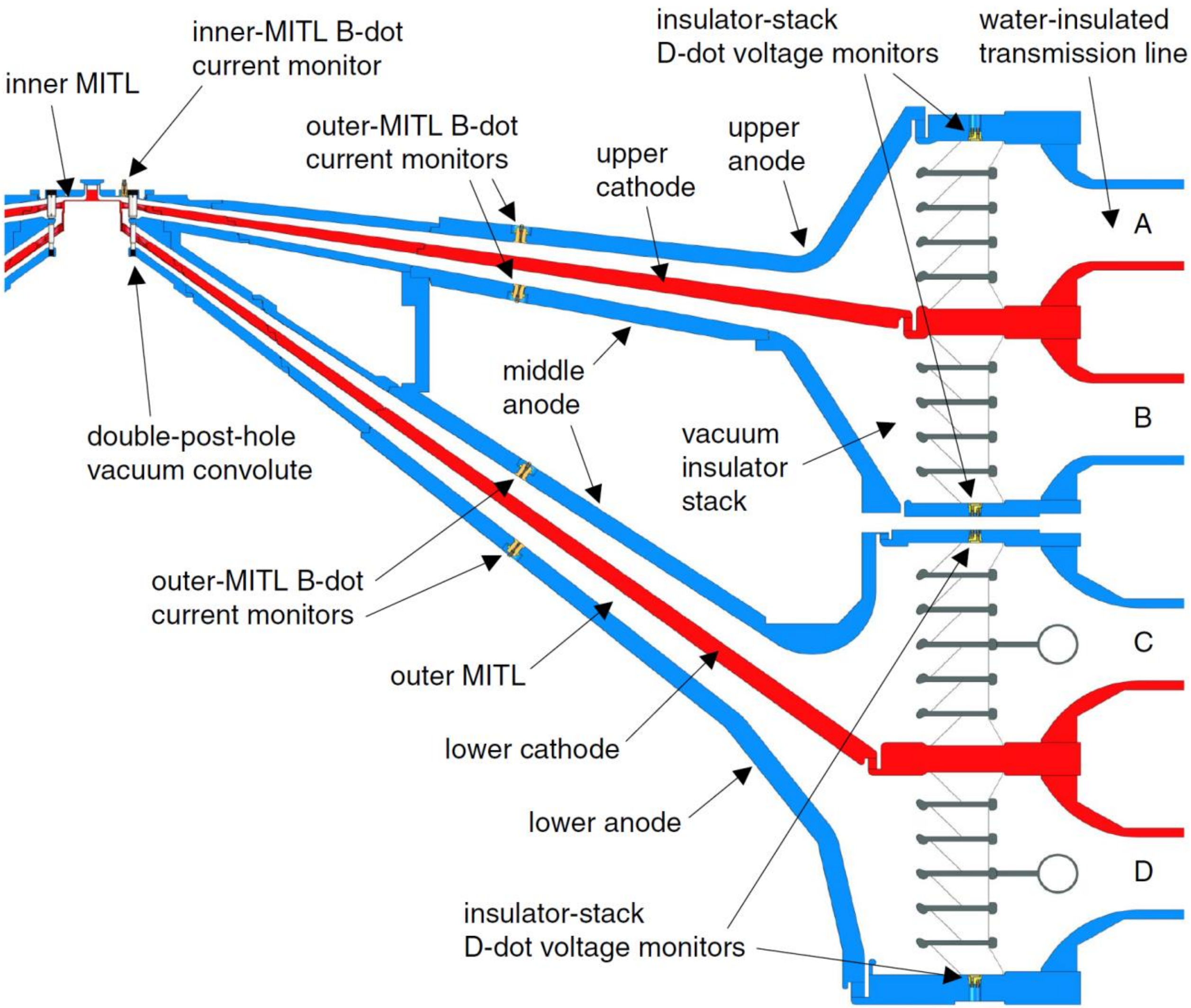

T. C. Wagoner, etc., Phys. Rev. ST Accel. Beams 11, 100401 (2008)

Differential current monitors

- **Outer MITL B-dot current monitors:**

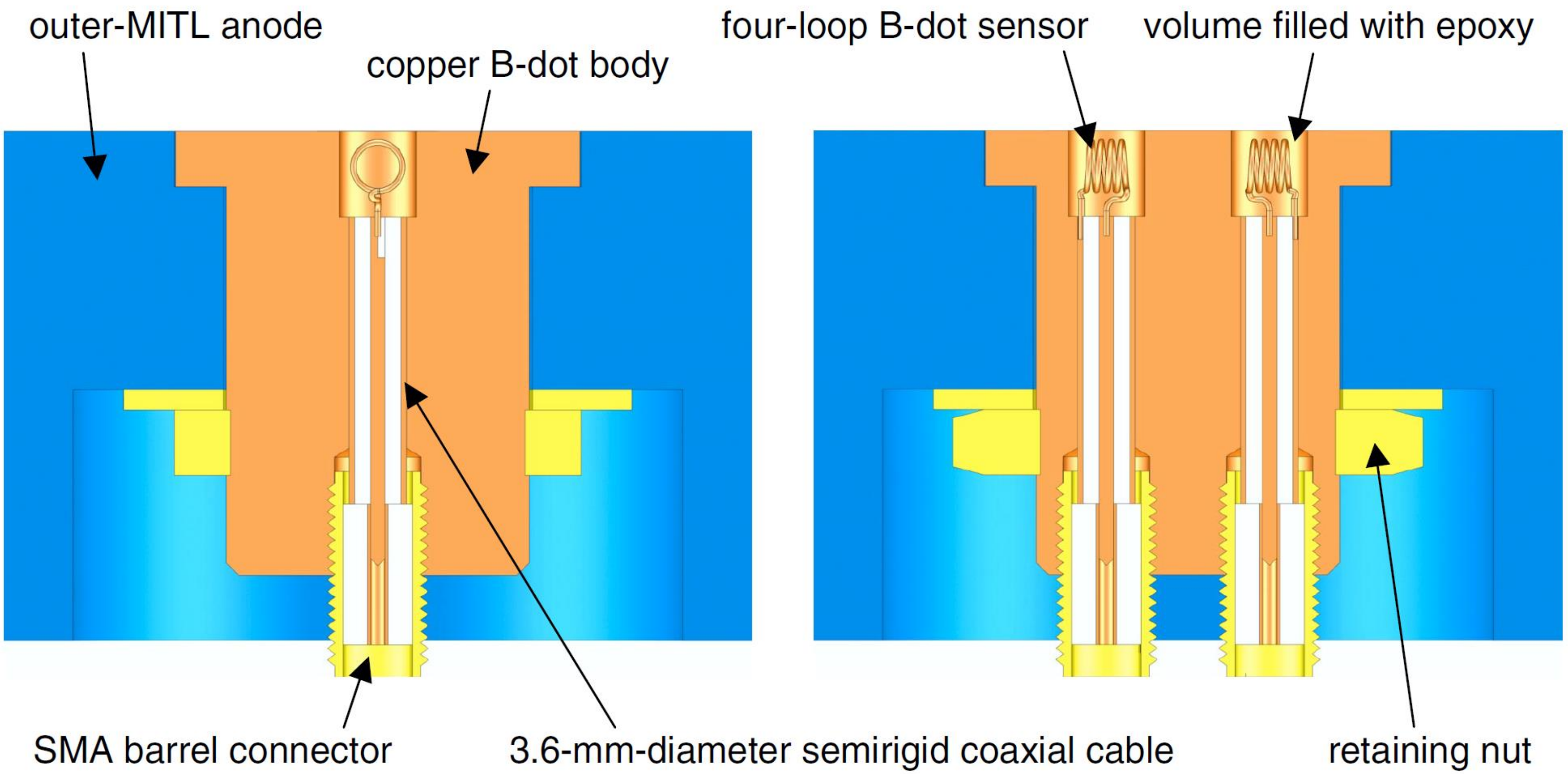

Differential current monitors

- The two B-dot sensors of each B-dot current monitor are designed to produce “opposite-polarity” signals for “common-mode-noise” rejection.

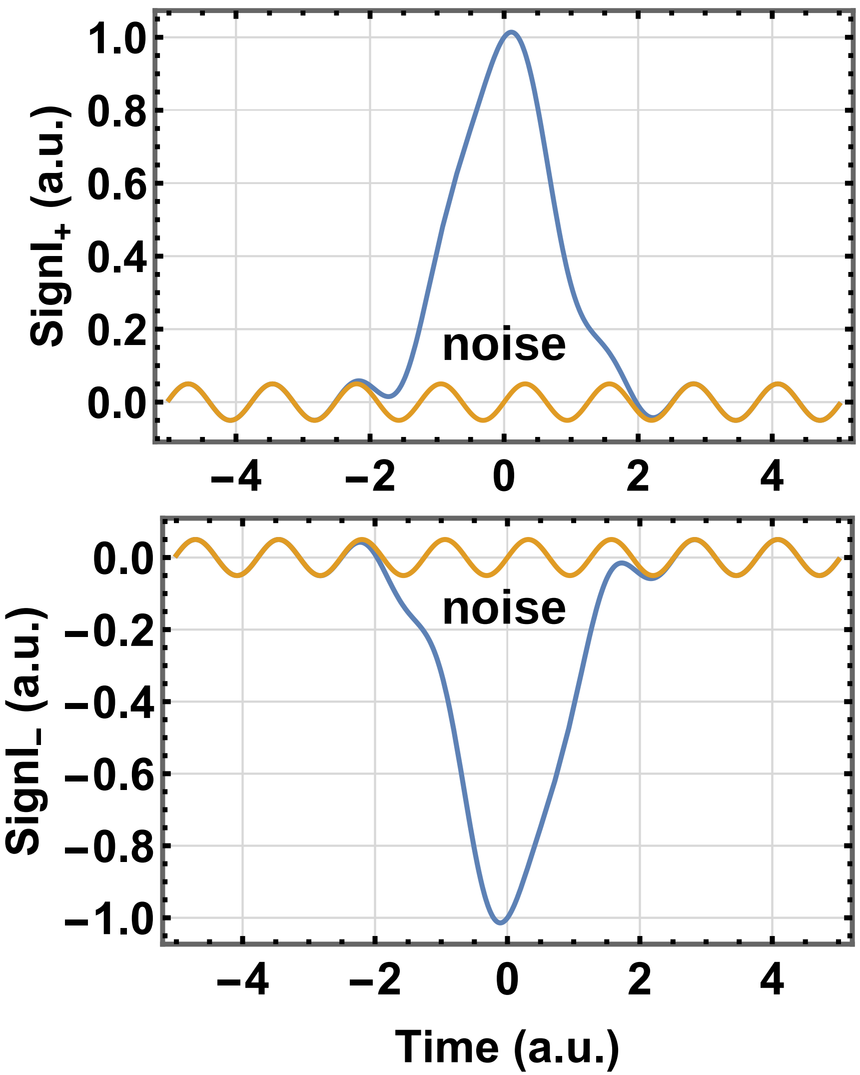

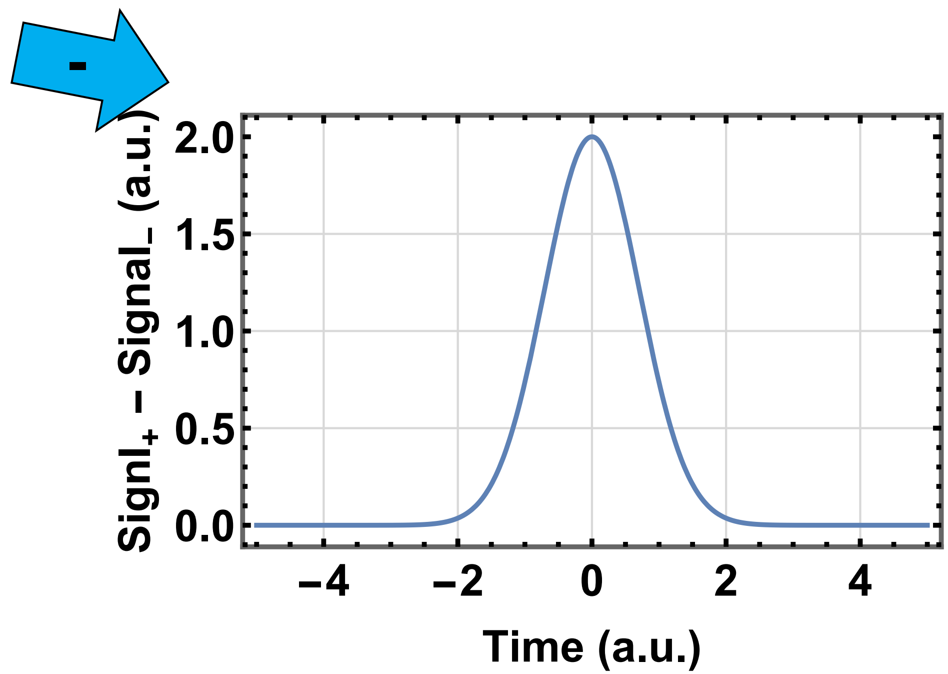

Differential voltage monitor

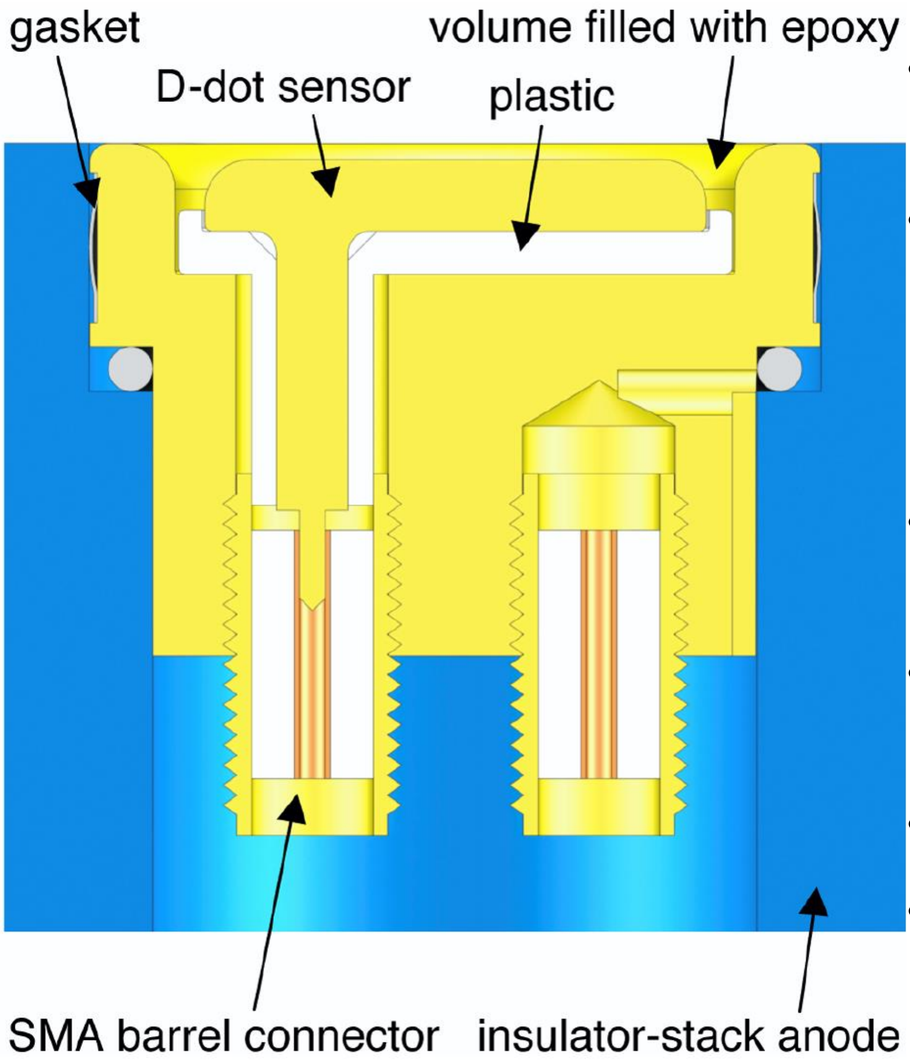

- **D-dot voltage monitor: the displacement-current monitor**
- **Opening-circuit termination for null measurements, i.e., common-mode noise reduction.**

- **Vacuum potted using stycast epoxy.**
- **Common-mode noise reduction is applied.**
- **Numerically cable compensated.**
- **Numerically integrated the signal.**

Voltage divider using resistors

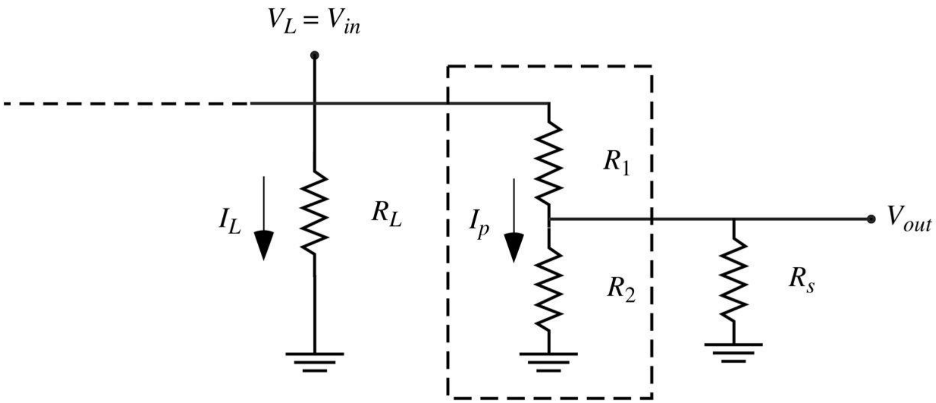

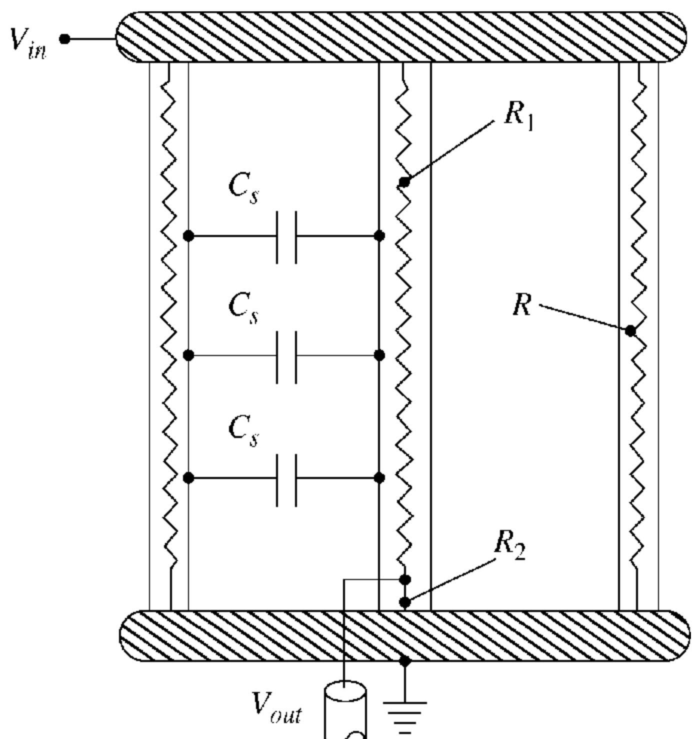

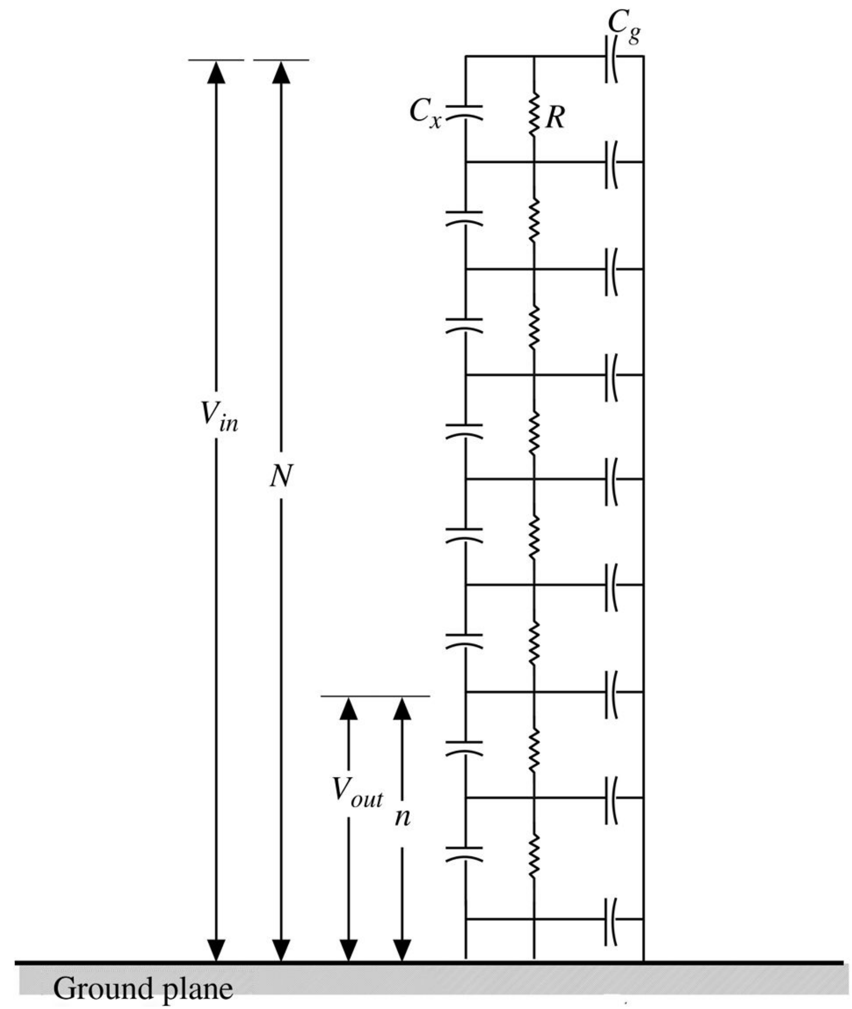

Voltage divider liquid resistors and grading electrodes

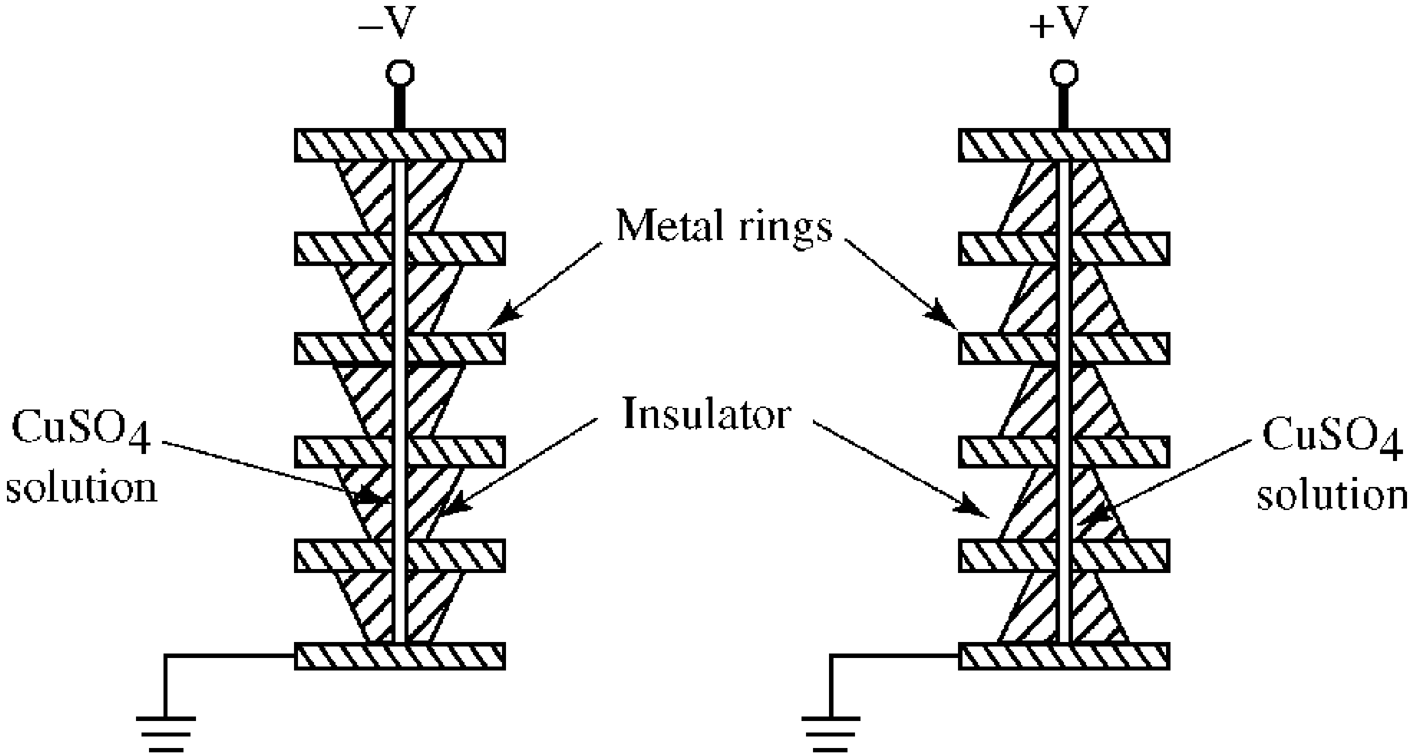

Voltage divider on Mega Ampere Generator for Plasma Implosion Experiments (MAGPIE) facility

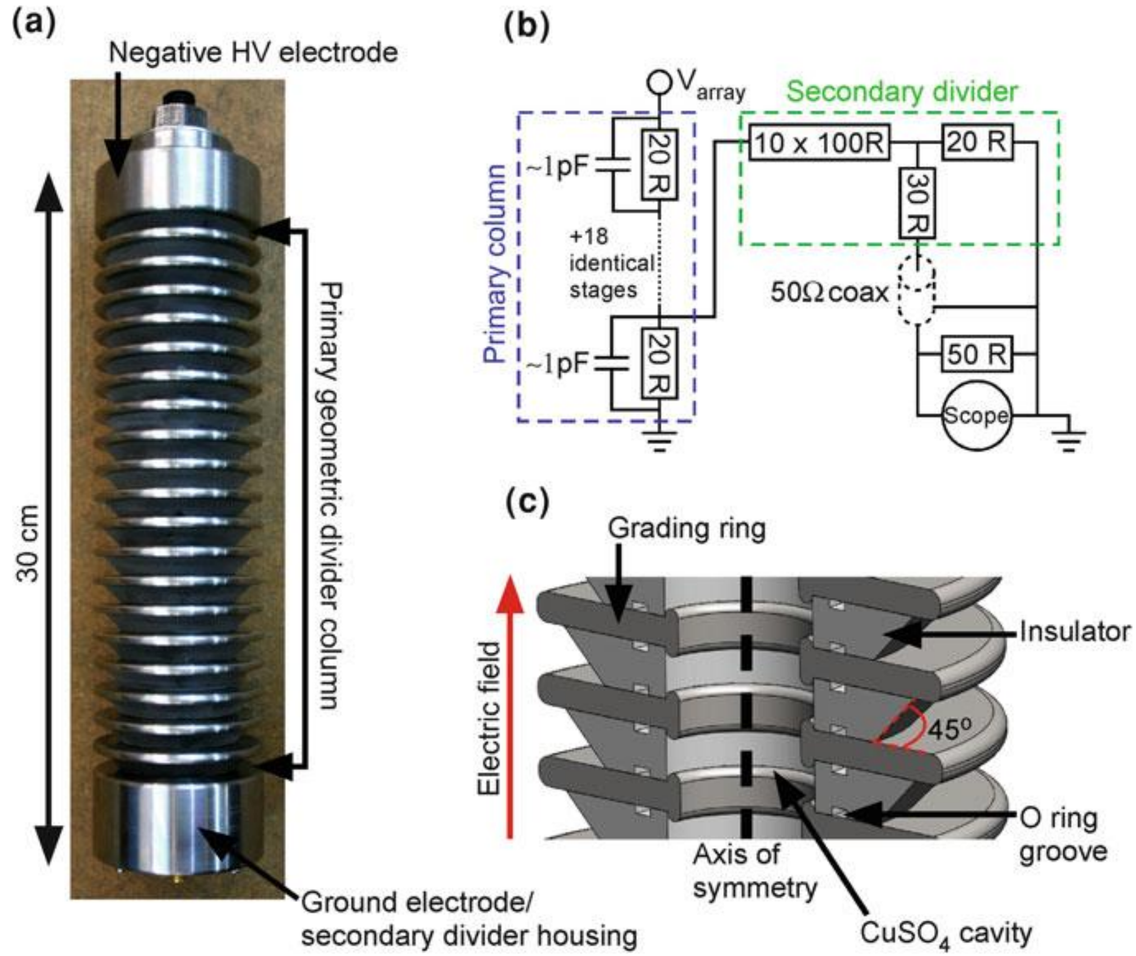

Guy C. Burdiak, Cylindrical Liner Z-pinches as Drivers for Converging Strong Shock Experiments

Voltage divider on Mega Ampere Generator for Plasma Implosion Experiments (MAGPIE) facility

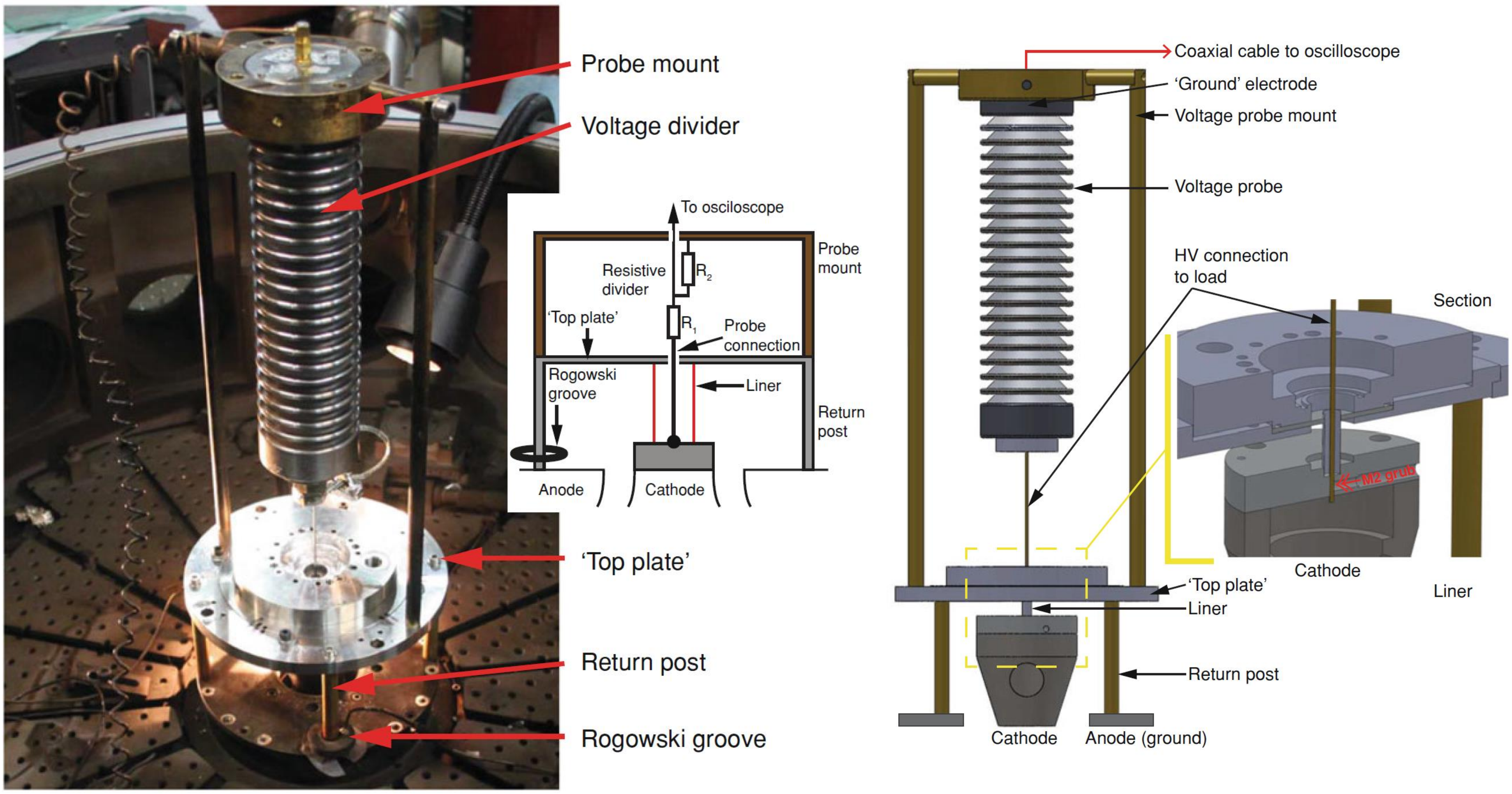

Guy C. Burdiak, Cylindrical Liner Z-pinches as Drivers for Converging Strong Shock Experiments

Voltage divider on Mega Ampere Generator for Plasma Implosion Experiments (MAGPIE) facility

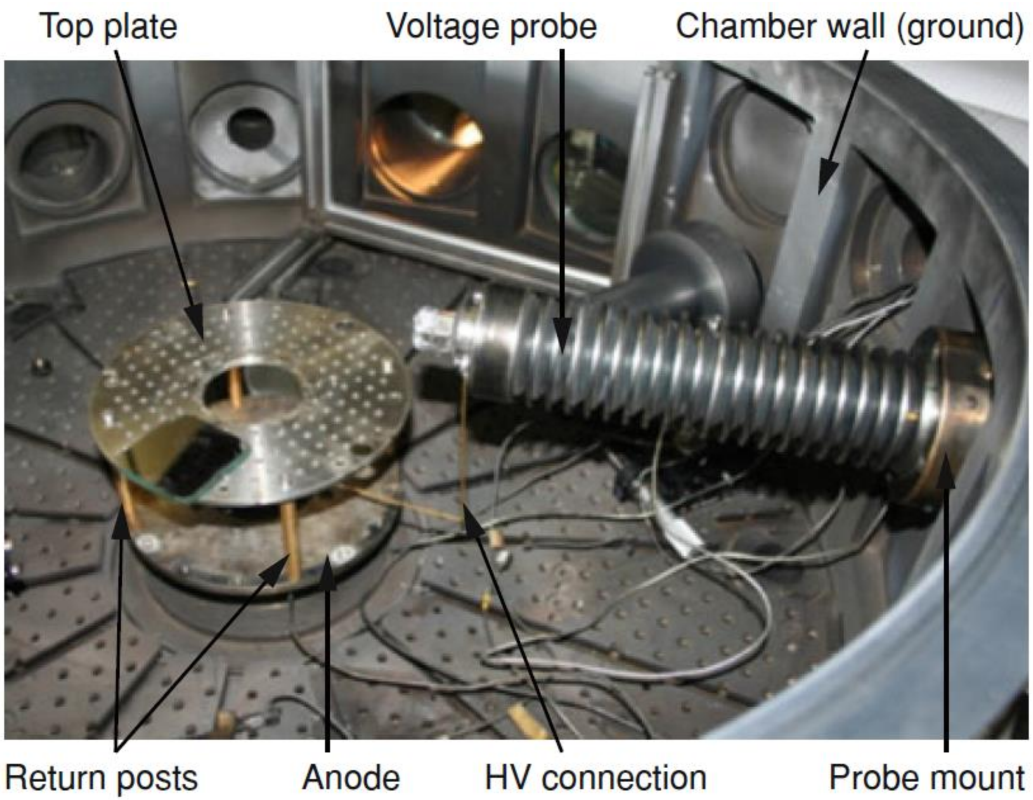

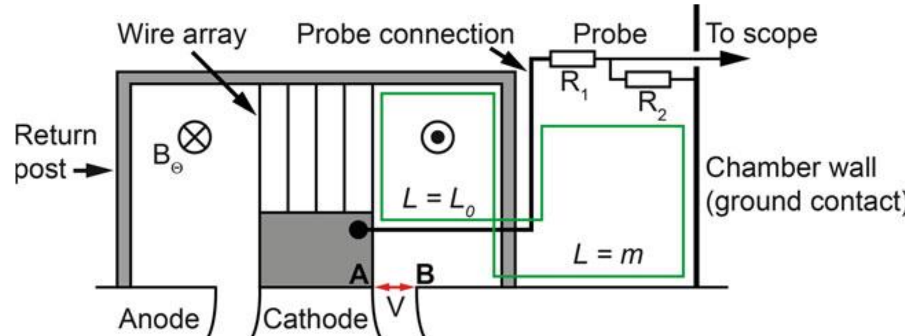

Guy C. Burdiak, Cylindrical Liner Z-pinches as Drivers for Converging Strong Shock Experiments

Voltage divider using both resistors and capacitors

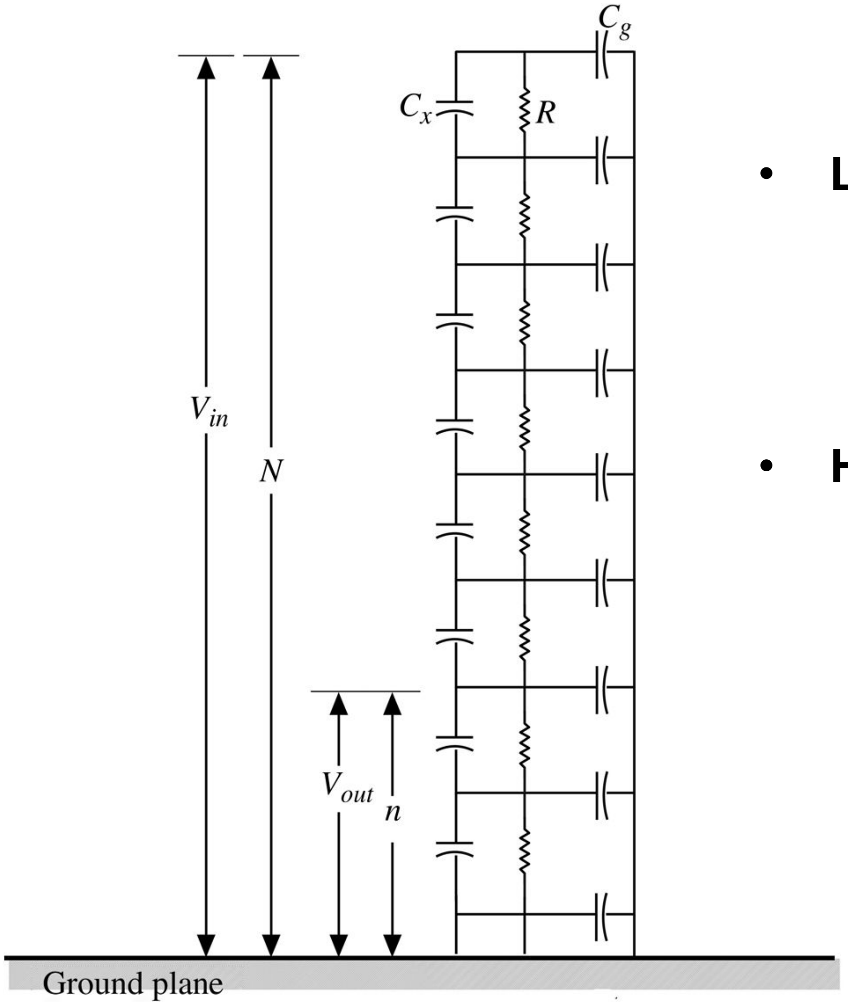

- **Low frequency:**

$$V_{\text{out}} = \frac{R_o}{\Sigma R_o} V_{\text{in}} = \frac{R_o}{N R_o} V_{\text{in}} = \frac{1}{N} V_{\text{in}}$$

- **High frequency:**

$$V_{\text{out}} = \frac{\frac{C_o}{N-1}}{\frac{C_o}{N-1} + C_o} V_{\text{in}} = \frac{\frac{1}{N-1}}{\frac{1}{N-1} + 1} V_{\text{in}}$$

$$= \frac{1}{1 + (N-1)} V_{\text{in}} = \frac{1}{N} V_{\text{in}}$$

or $$V_{\text{out}} = \frac{\frac{1}{j\omega C_o}}{\sum \frac{1}{j\omega C_o}} V_{\text{in}} = \frac{1}{N} V_{\text{in}}$$

Outlines

- Power and voltage adding
  - Marx generator
  - LC generator
  - Line pulse transformers
  - Induction voltage adder (IVA)
  - Linear induction accelerator (LIA)
  - Linear transformer driver (LTD)
- Diagnostics
  - Voltage measurement
  - Current measurement
- **Applications of pulsed-power system**

Karlsruche Light Ion Facility (KALIF)

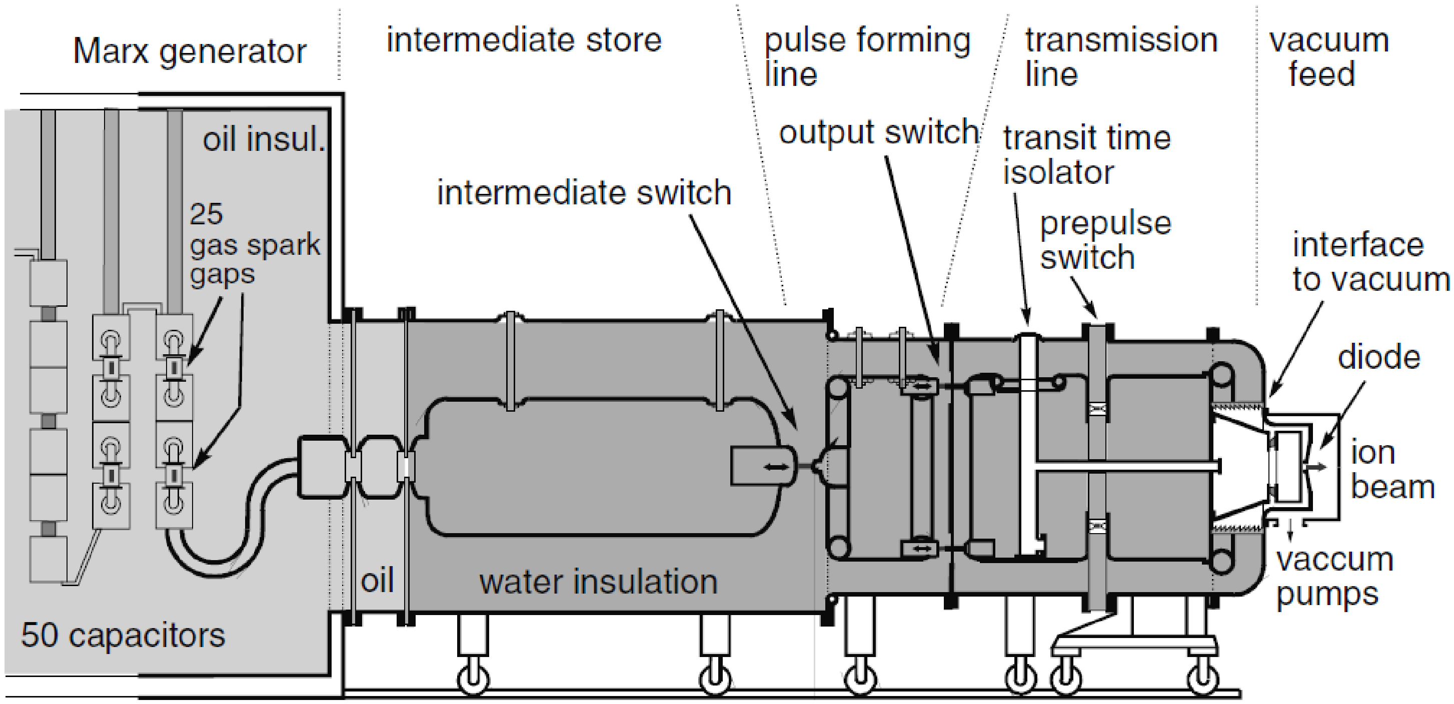

Fig. 8.1. Schematic illustration of the 1.5 TW pulse generator KALIF. The data for the pulse at the vacuum interface are: power = 1.5 TW, voltage = 1.7 MV, pulse duration = 50 ns, pulse energy = 75 kJ, electrical efficiency = 30%

Magpie at Imperial college

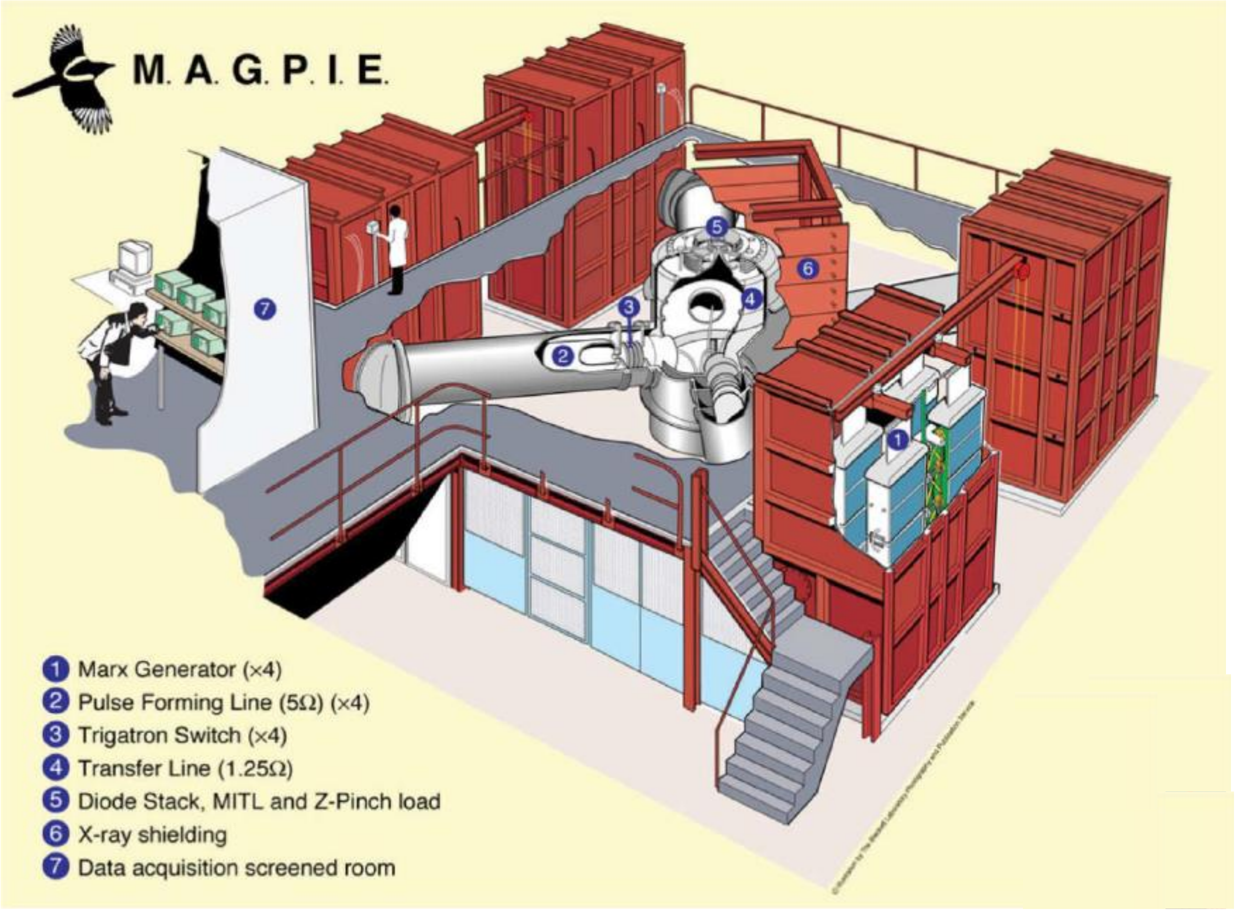

E = 86 kJ
I = 1 MA
T_{rise} = 250 ns

R. D. McBride, *et. cl.*, IEEE TRANS. PLAS. SCIE., 46, 3928 (2018)

Cobra at Cornell University

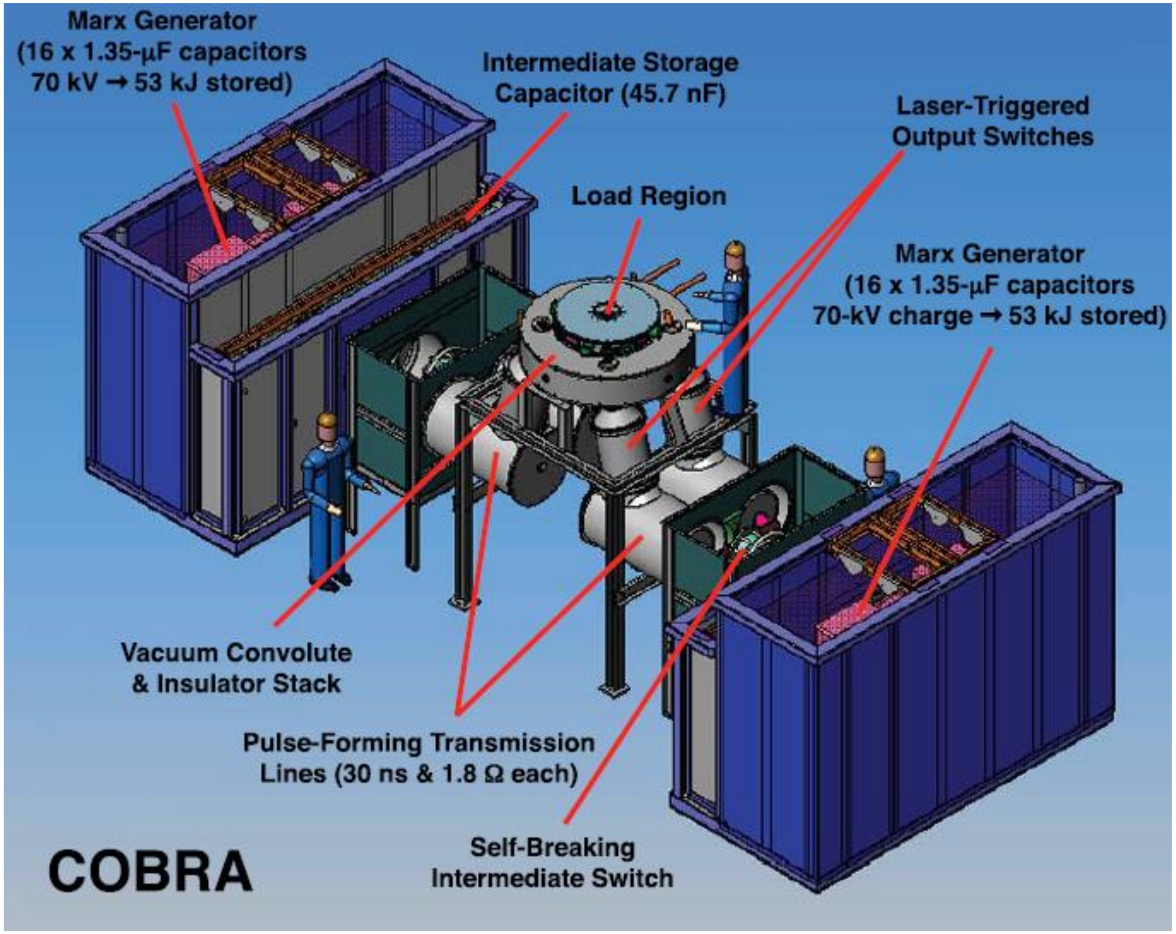

E = 105 kJ
I = 1 MA
T_{rise} = 100 ns

R. D. McBride, *et. cl.*, IEEE TRANS. PLAS. SCIE., 46, 3928 (2018)

Zebra at University of Nevada, Reno

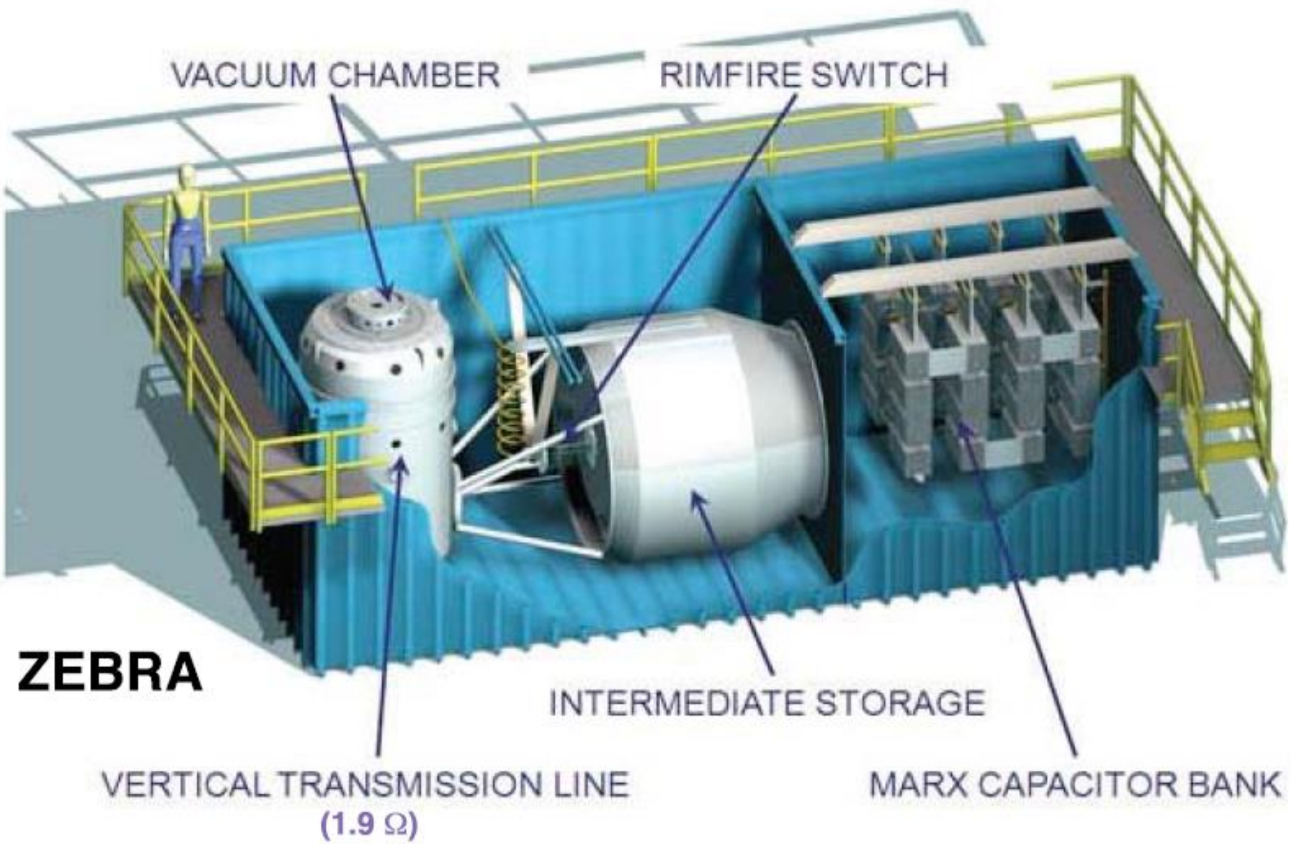

E = 200 kJ
I = 1 MA
T_{rise} = 100 ns

R. D. McBride, *et. cl.*, IEEE TRANS. PLAS. SCIE., 46, 3928 (2018)

Maize LTD at University of Michigan

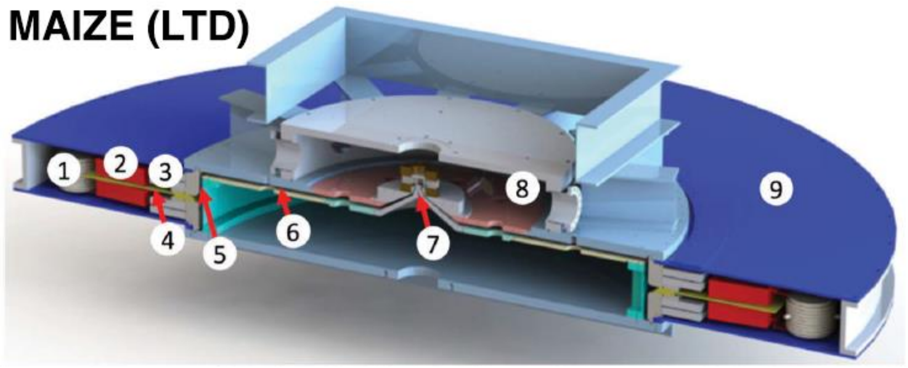

E = 16 kJ
I = 1 MA
T_{rise} = 100 ns

R. D. McBride, *et. cl.*, IEEE TRANS. PLAS. SCIE., 46, 3928 (2018)

Hades at University of Rochester

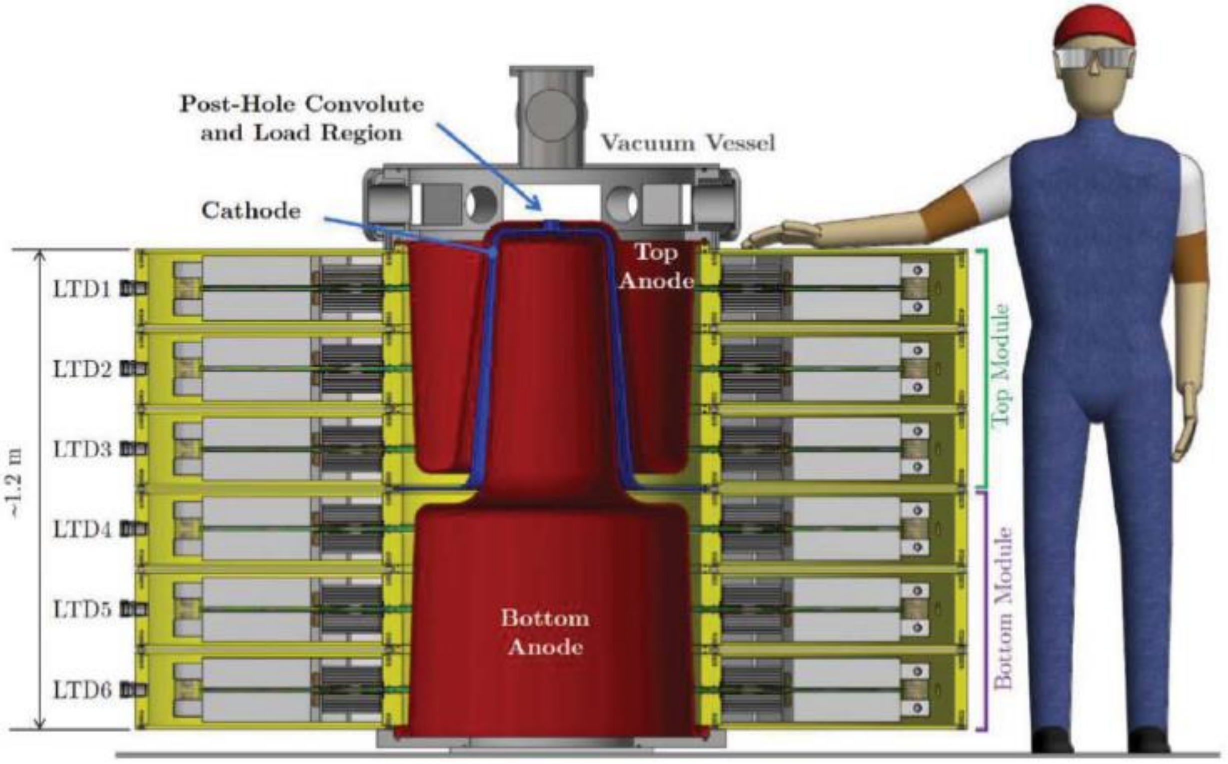

E = 75 kJ
I = 1 MA
T_{rise} = 125 ns

R. D. McBride, *et. cl.*, IEEE TRANS. PLAS. SCIE., 46, 3928 (2018)

Particle Beam Fusion Accelerator (PBFA 2) and the Z-Machine

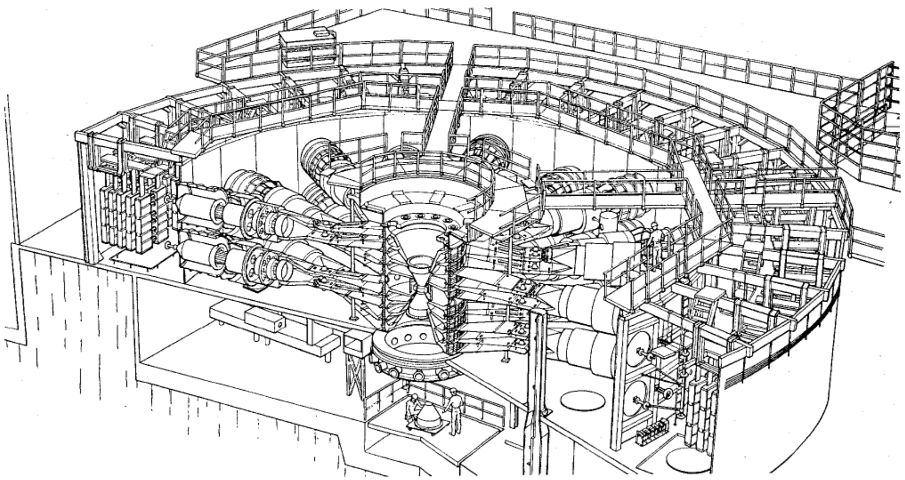

Fig. 8.2. Perspective drawing of the multimodular generator PBFA 2

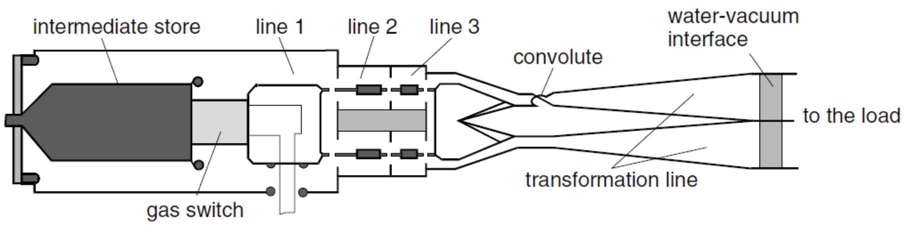

Fig. 8.3. Pulse-forming network of a single module of the PBFA 2 device

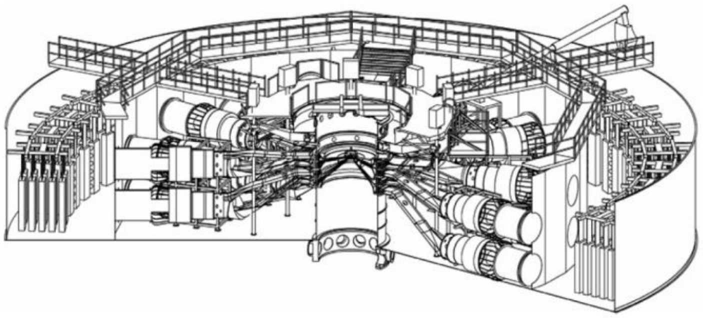

Fig. 8.4. Schematic illustration of the Z-Machine for driving Z-pinches, located at Sandia National Laboratory

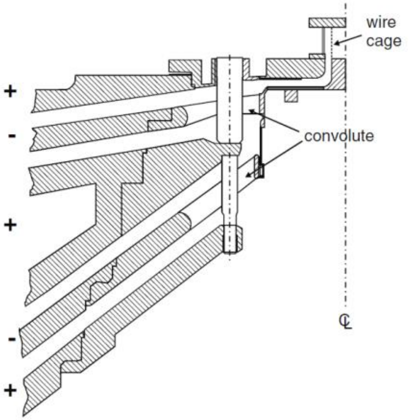

Fig. 8.5. Post-hole convolute in the Z-Machine

Sandia's Z machine is the world's most powerful and efficient laboratory radiation source

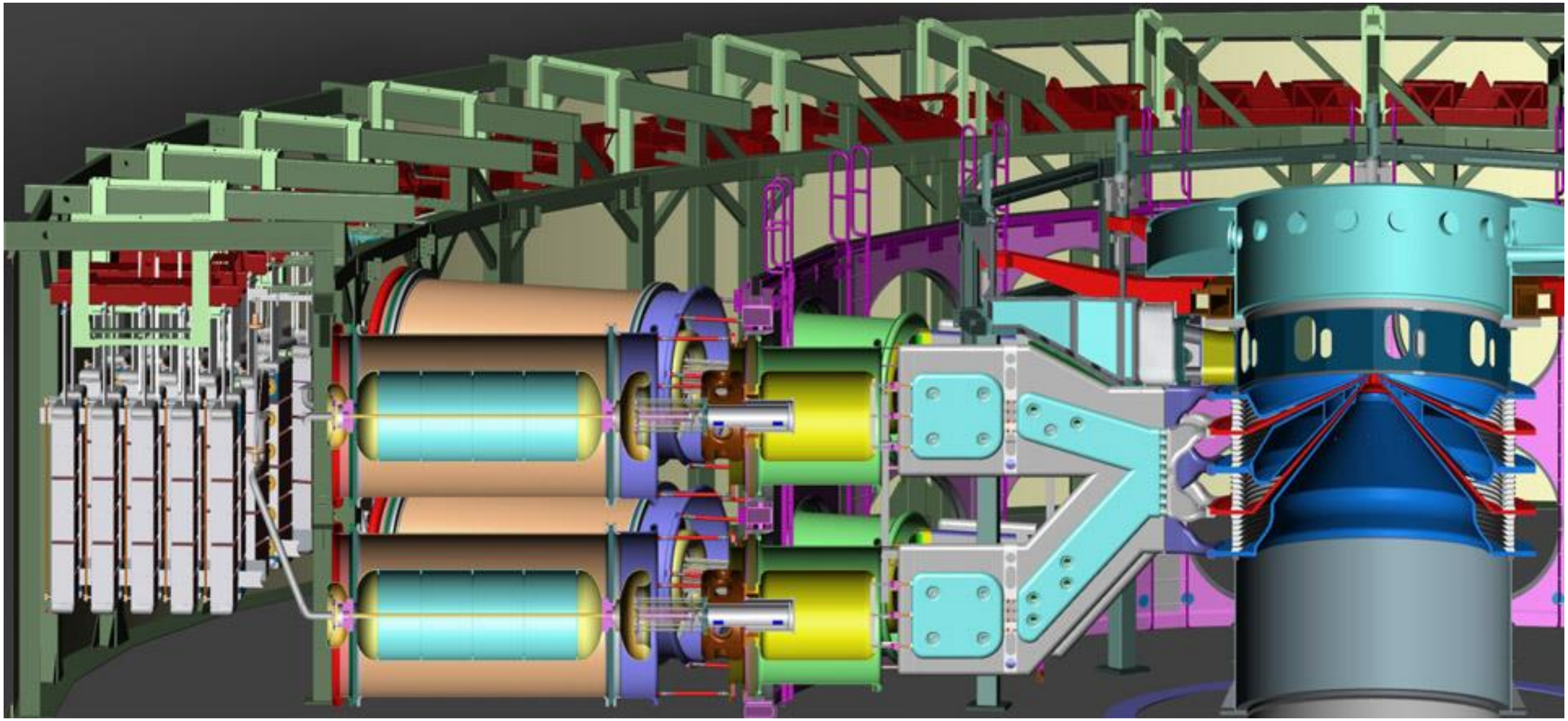

- Stored energy: 20 MJ
- Marx charge voltage: 85 kV
- Peak electrical power: 85 TW
- Peak current: 26 MA
- Rise time: 100 ns
- Peak X-ray emissions: 350 TW
- Peak X-ray output: 2.7 MJ

Z pulsed-power accelerator: 20 MA, 3MV, 55TW

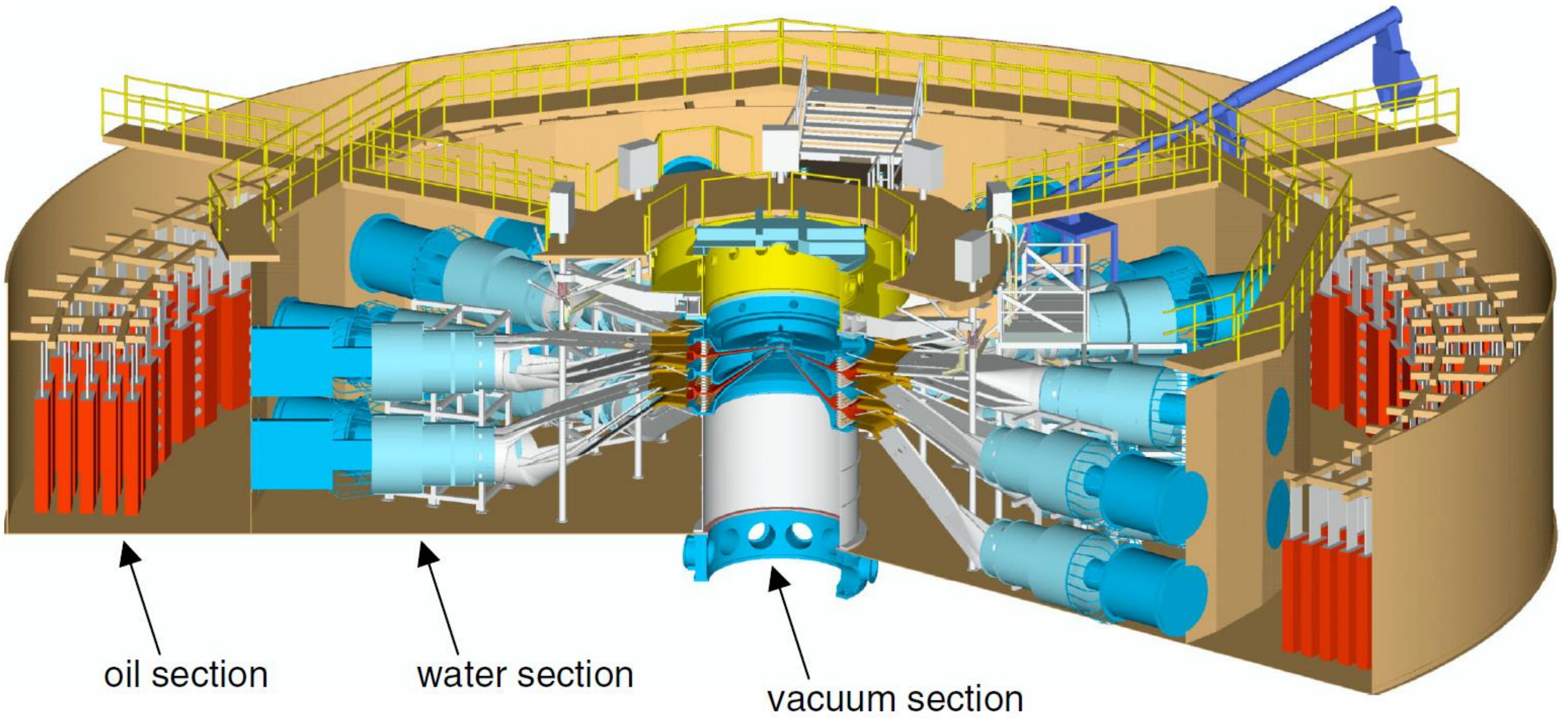

Self-magnetically insulated vacuum transmission lines (MITLs)

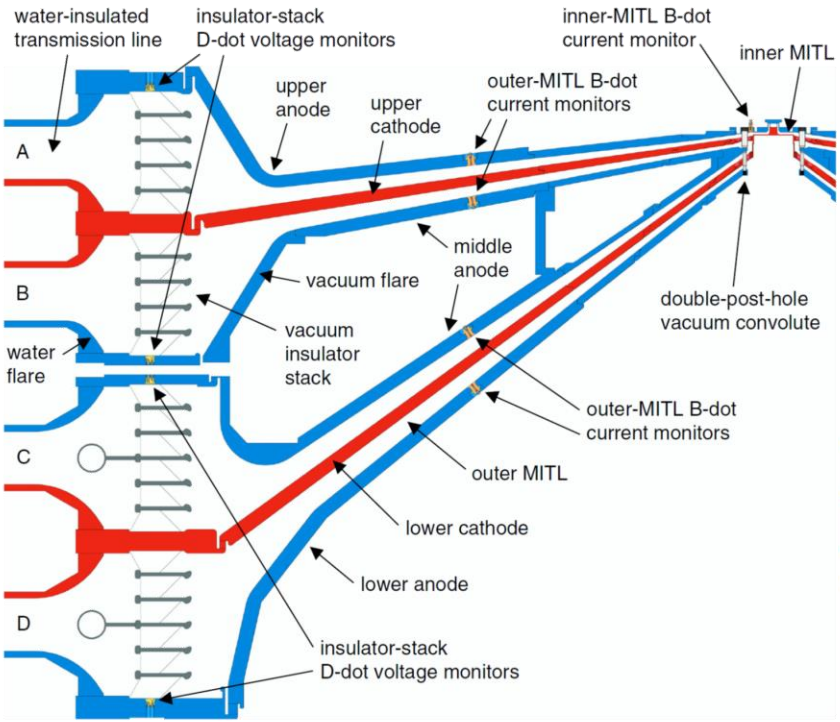

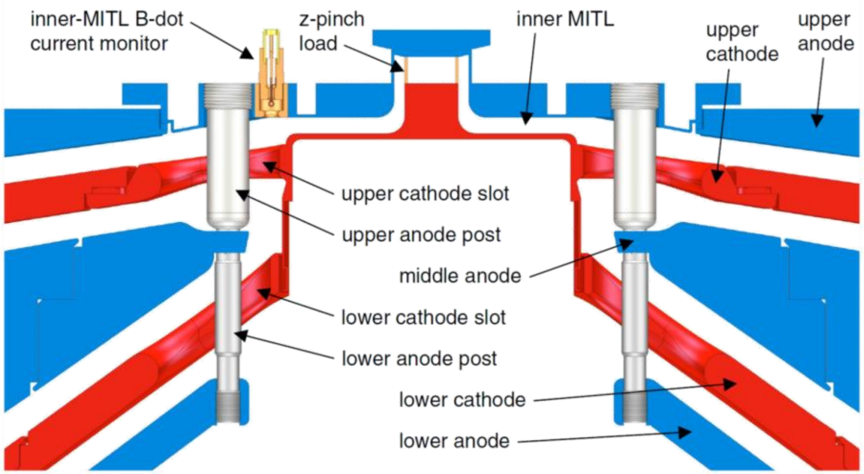

Z machine

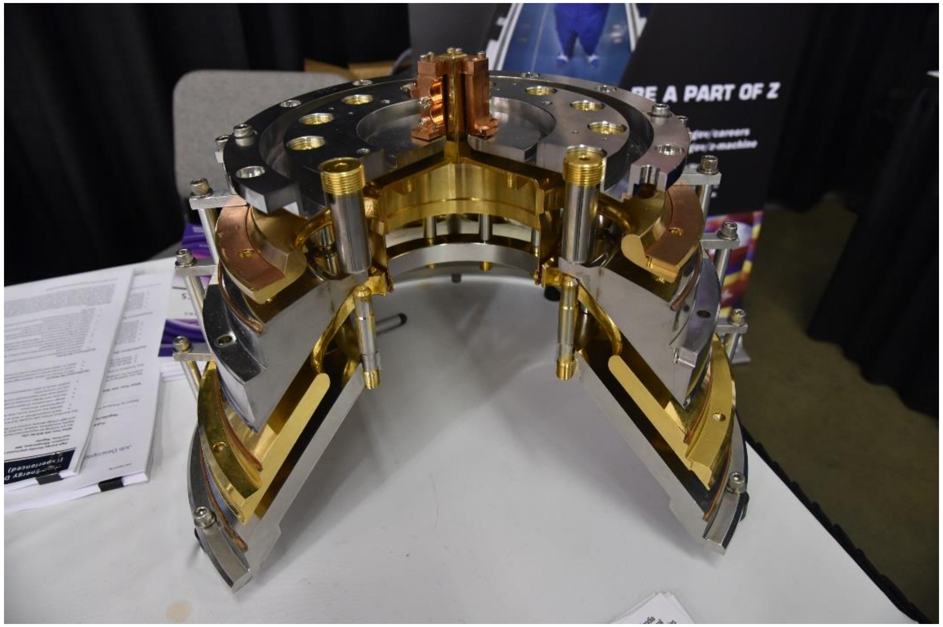

Z machine

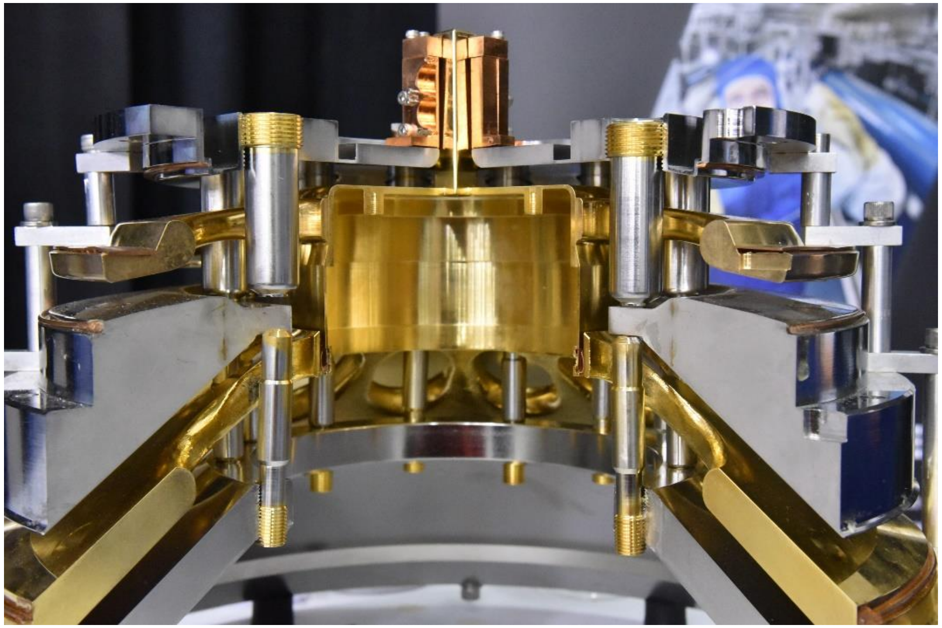

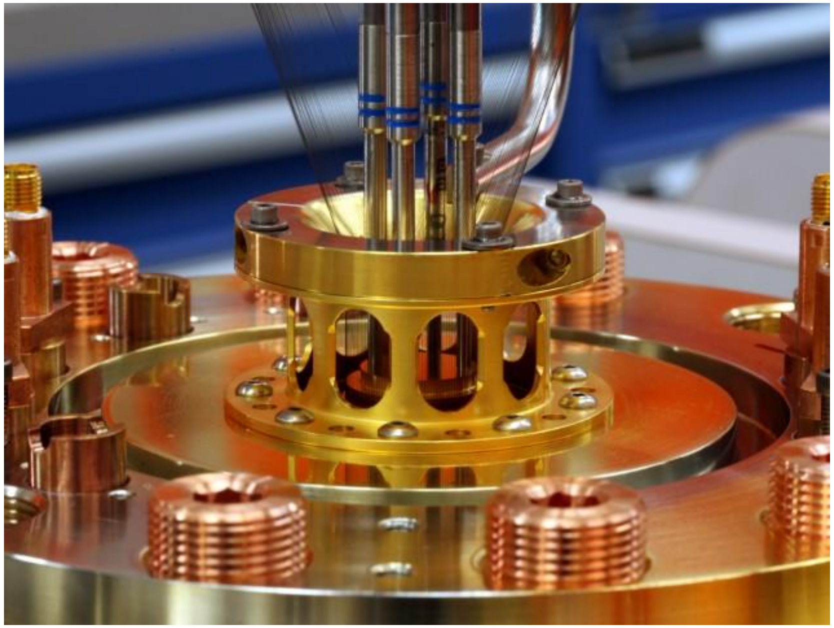

Z machine discharge

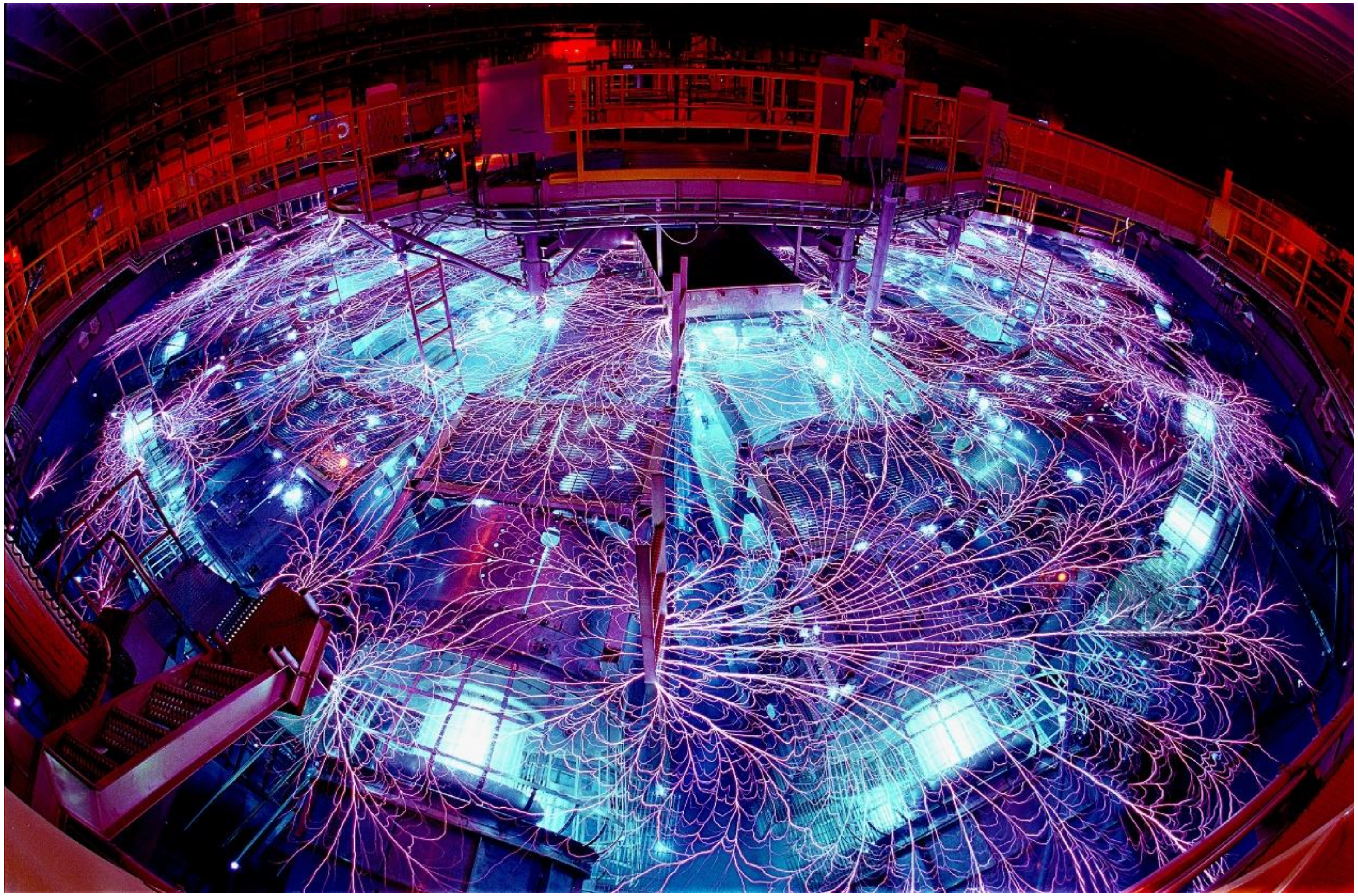

Before and after shots

- **Before shots**

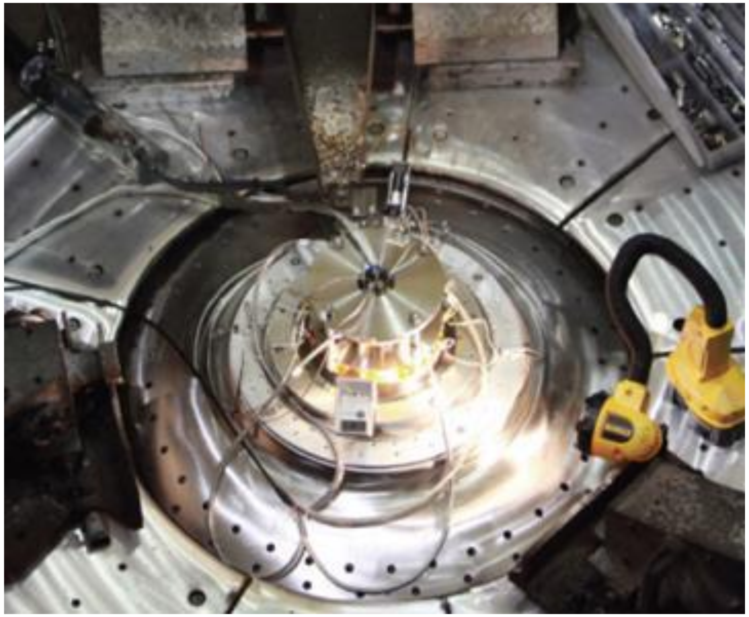

- **After shots**

SAND2017-0900PE_The sandia z machine - an overview of the world's most powerful pulsed power facility.pdf

The “iron group” of isotopes are the most tightly bound

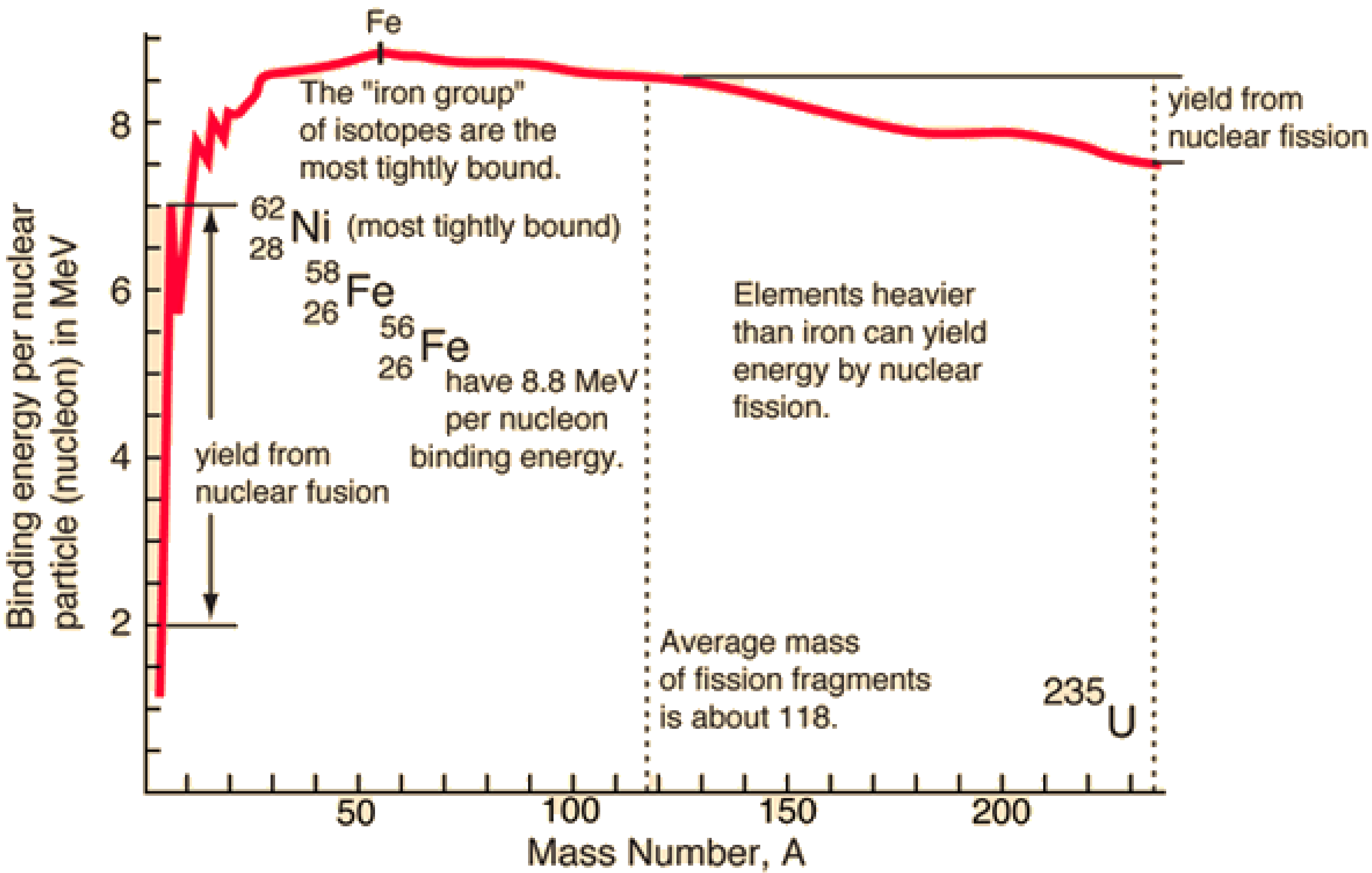

http://hyperphysics.phy-astr.gsu.edu/hbase/nucene/nucbin.html

Fusion is much harder than fission

- **Fission:** $n +^{235}_{92} U \rightarrow^{236}_{92} U \rightarrow^{144}_{56} Ba +^{89}_{36} Kr + 3n + 177\ \mathrm{MeV}$
- **Fusion:** $D + T \rightarrow He^4\,(3.5\ \mathrm{MeV}) + n\,(14.1\ \mathrm{MeV})$

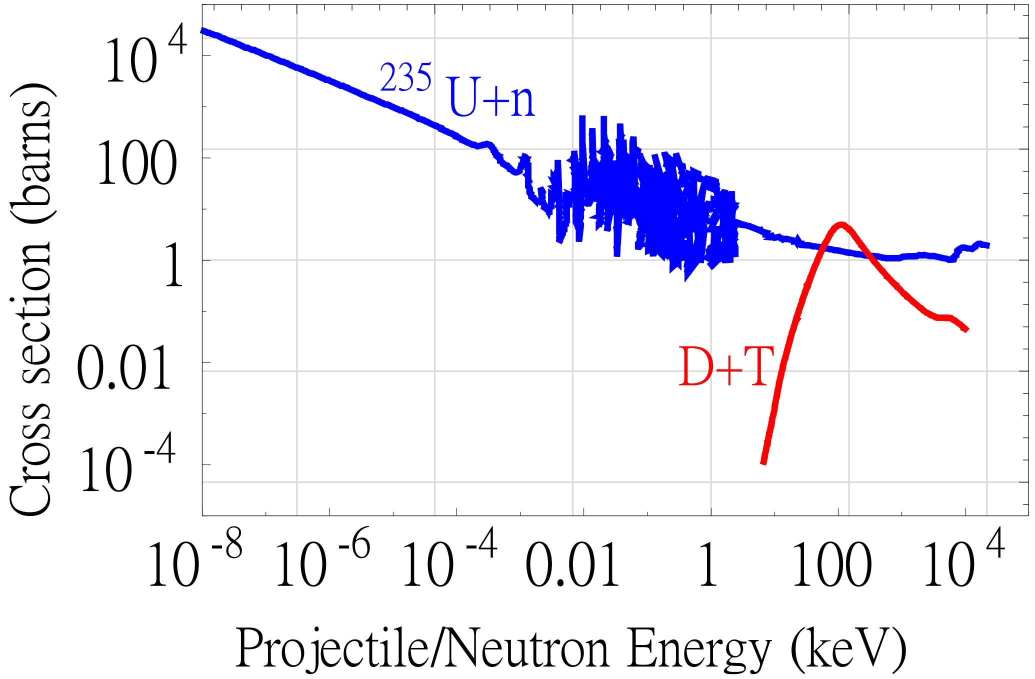

The fusion process

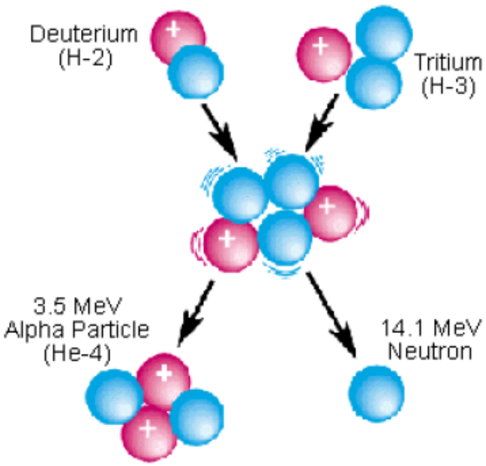

Deuterium-Tritium Fusion Reaction

$^2H + ^3H \Rightarrow ^4He + n + Q \equiv 17.6$ MeV

Energy release Q=17.6 MeV

In comparison

$^2H + ^2H \Rightarrow ^1H + ^3H + Q \equiv 4.0$ MeV

$^2H + ^2H \Rightarrow ^3He + n + Q \equiv 3.2$ MeV

$^3H + ^3H \Rightarrow ^4He + 2n + Q \equiv 11.3$ MeV

$^{235}U + n \Rightarrow X_A + X_B + 3n + Q \approx 200$ MeV

Fusionable Material, deuterium ^2H (D) and tritium ^3H (t):

Deuterium: natural occurrence (heavy water) (0.015%).

Tritium: natural occurrence in atmosphere through cosmic ray bombardment; radioactive with $T_{1/2}$=12.3 y.

https://isnap.nd.edu/Lectures/phys20061/pdf/10.pdf

Enormous fusion fuel can be produced from sea water

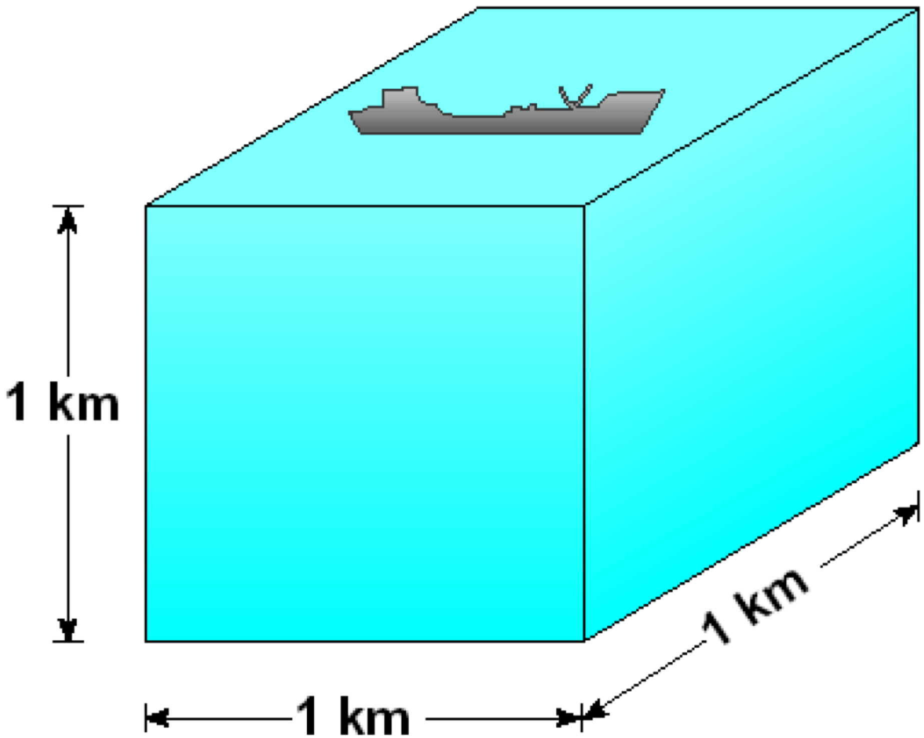

= Total energy of world oil reserve

“Advantages” of hydrogen bomb

Fusion of $^2H + ^3H$: $$\frac{Q}{A} = \frac{17.6\ MeV}{(3+2)\ amu} = 3.5\ \frac{MeV}{amu}$$

Fission of ^{235}U: $$\frac{Q}{A} = \frac{200\ MeV}{236\ amu} = 0.85\ \frac{MeV}{amu}$$

Fusion is 4 times more powerful than fission
and generates 24 times more neutrons!

https://isnap.nd.edu/Lectures/phys20061/pdf/10.pdf

Fusion doesn't come easily

$$\text{averaged reaction rate :} \quad \langle \sigma v \rangle = \int\int d\vec{v}_1 d\vec{v}_2 \sigma_{1,2}(v)\, v f_1(v_1)$$

$$f_j(v_j) = \left(\frac{m_j}{2\pi k_B T}\right)^{3/2} \exp\left(-\frac{m_j v_j^2}{2 k_B T}\right)$$

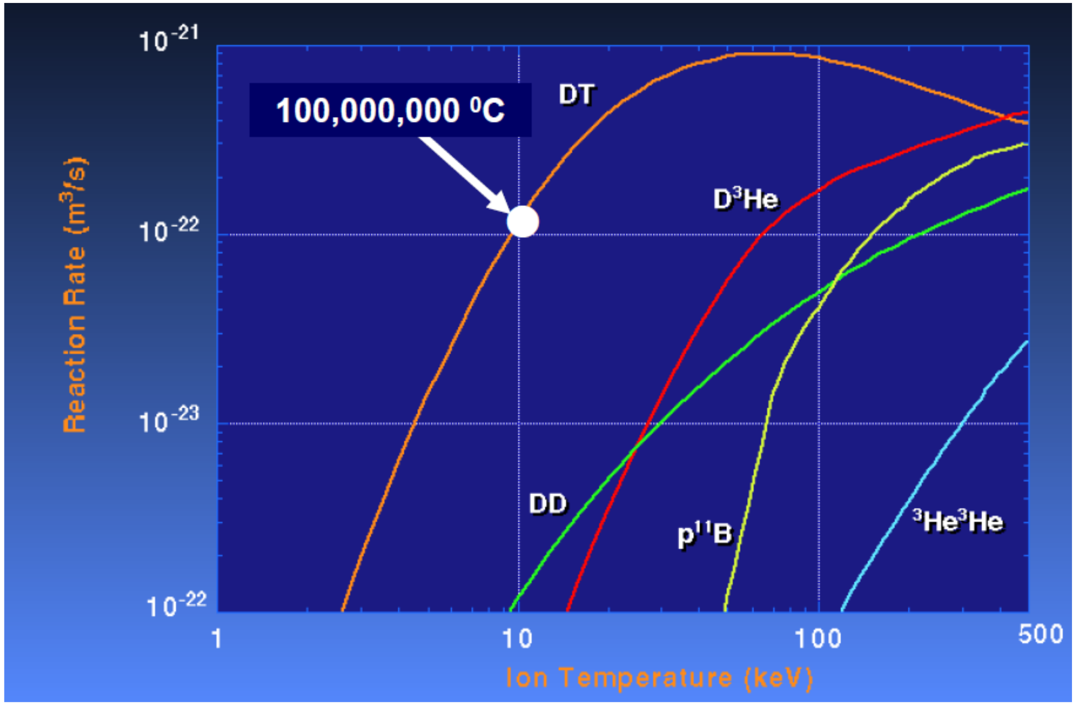

- **Use α particles to heat the plasma** $D + T \rightarrow He^4\,(3.5\ \mathrm{MeV}) + n\,(14.1\ \mathrm{MeV})$

Magnetic confinement fusion (MCF) vs Inertial confinement fusion (ICF)

Tokamak

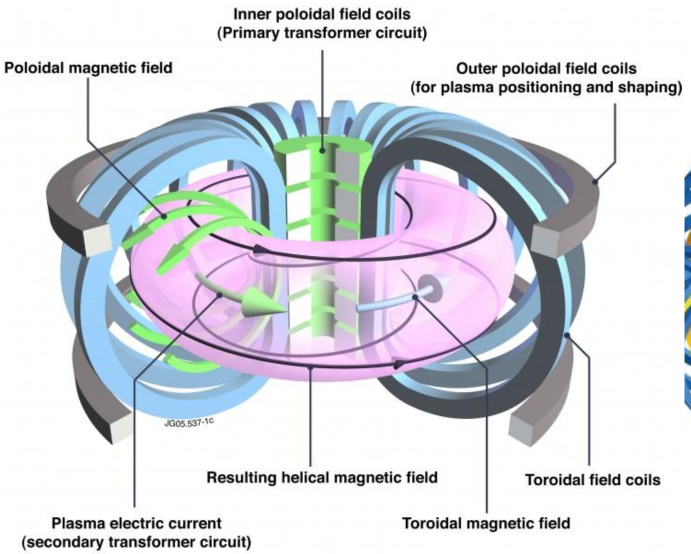

Stellarator

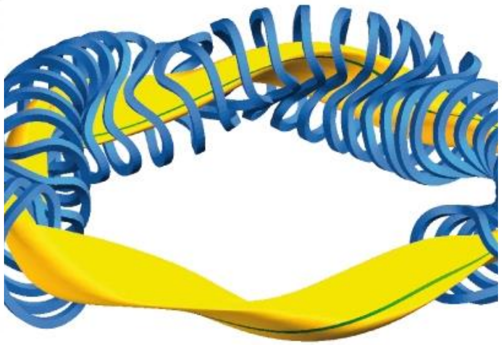

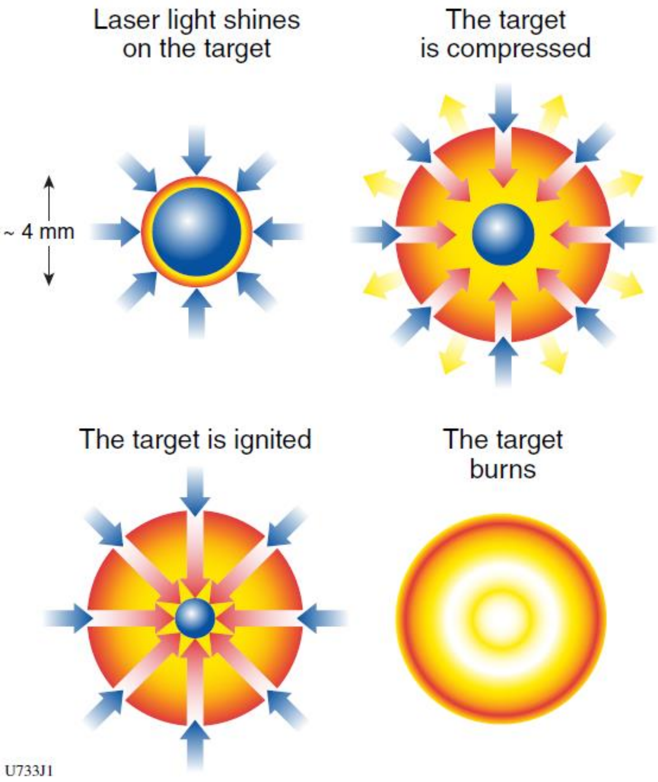

P~atm, τ~sec, T~10 keV

P~Gigabar, τ~nsec, T~10 keV

https://www.euro-fusion.org/2011/09/tokamak-principle-2/
https://en.wikipedia.org/wiki/Stellarator

Inertial confinement fusion

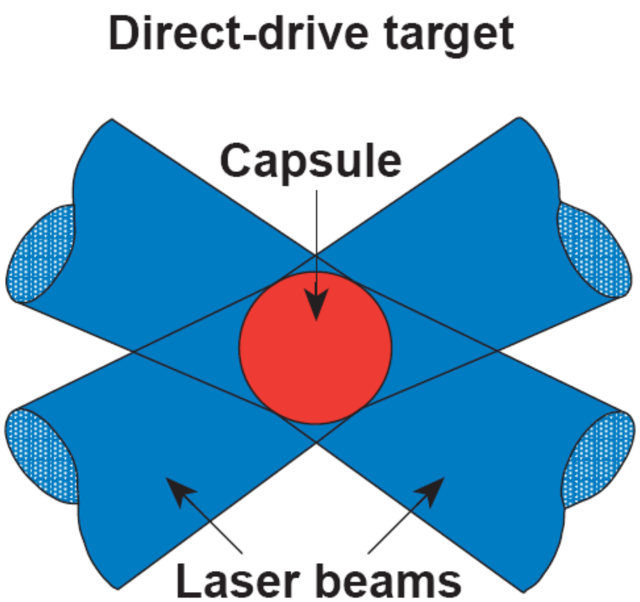

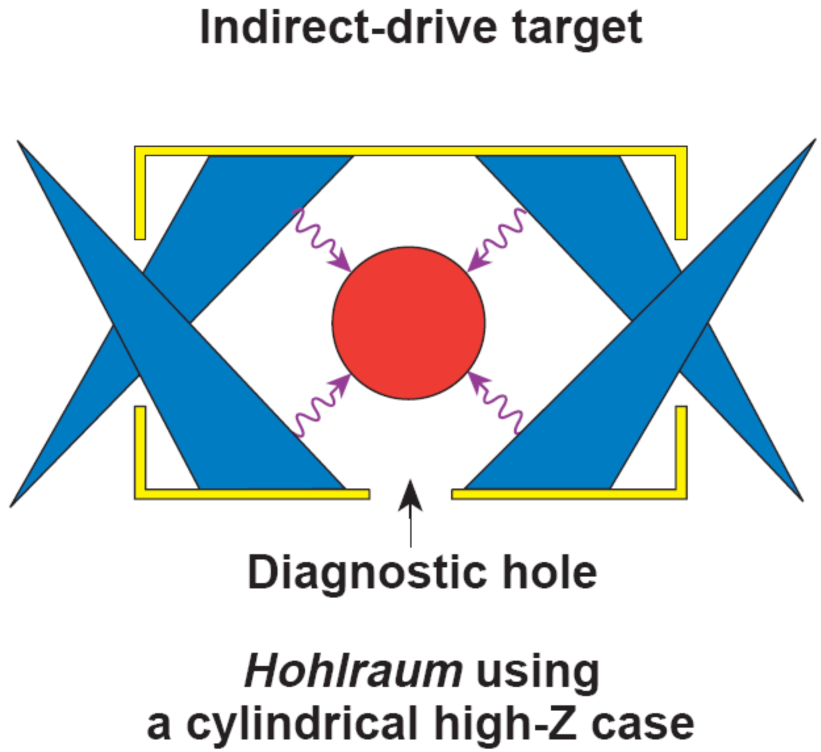

Reference:
Riccardo Betti,
University of Rochester,
HEDSA HEDP summer school,
San Diego, CA, August 16-21, 2015

Hohlraum at National Ignition Facility (NIF)

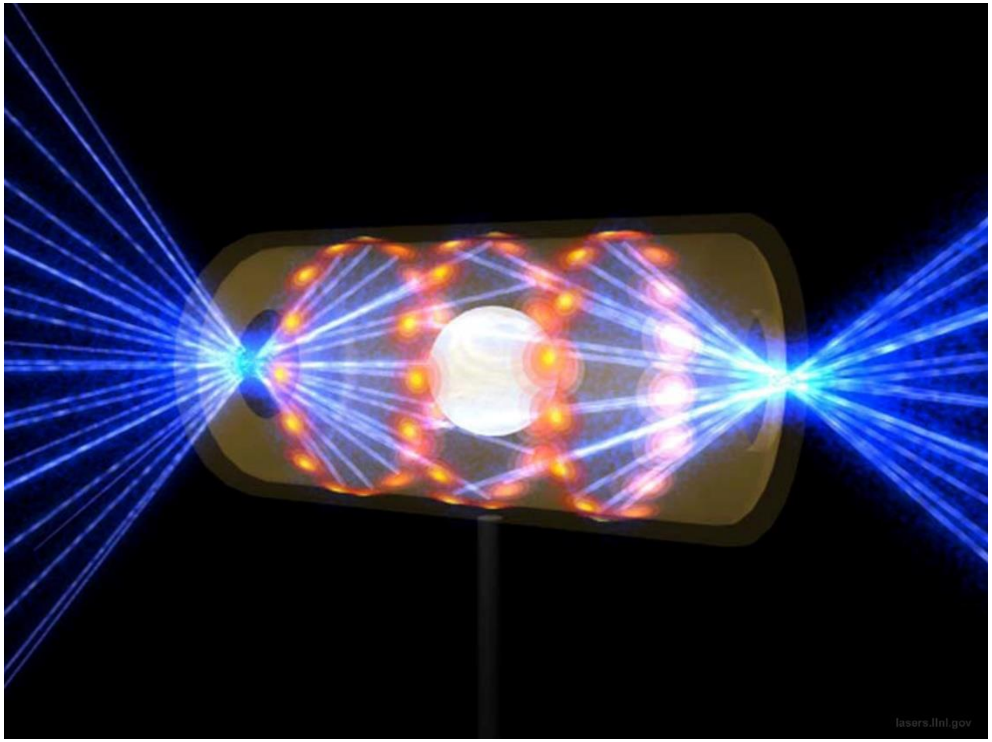

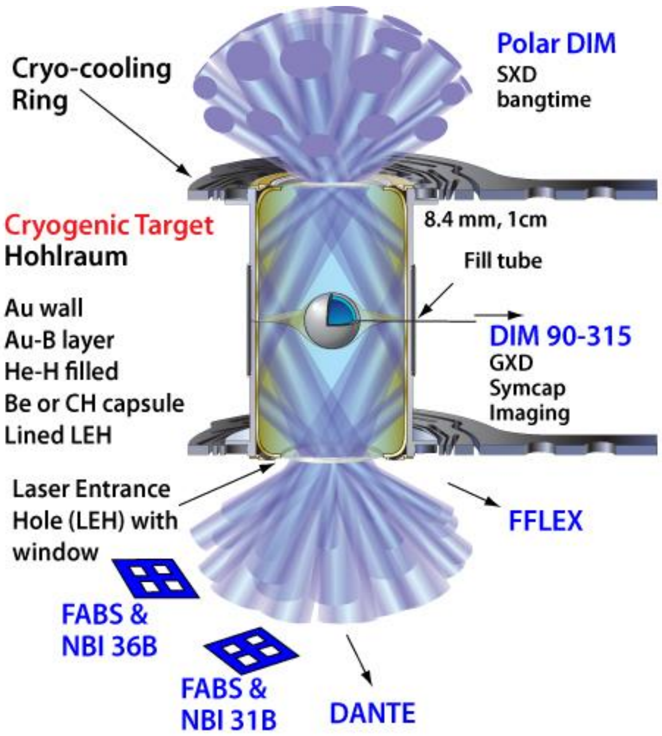

NIF target

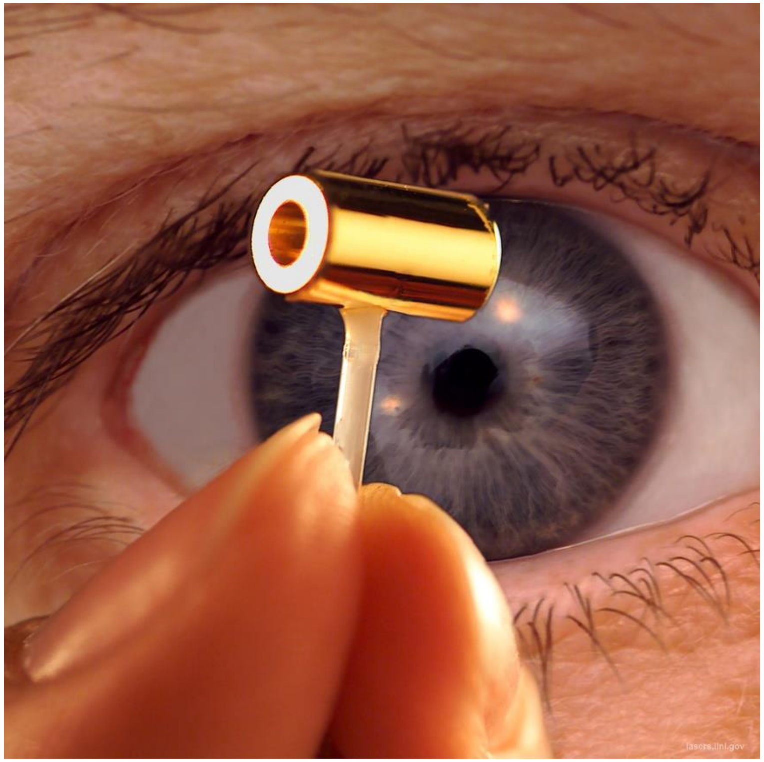

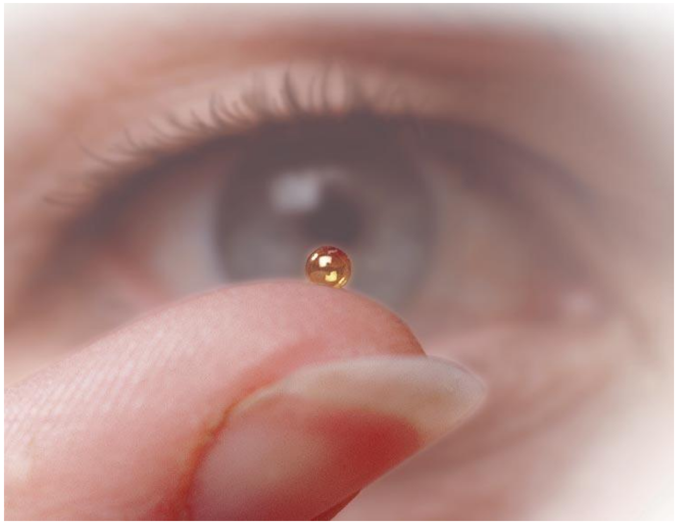

Targets used in ICF

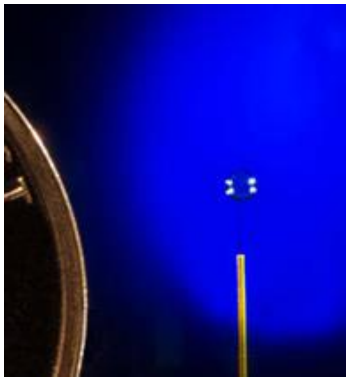

a

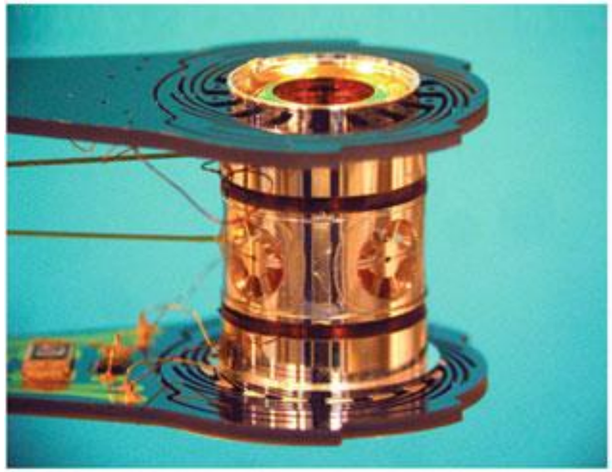

b

c Rugby hohlraum

d Tent holder

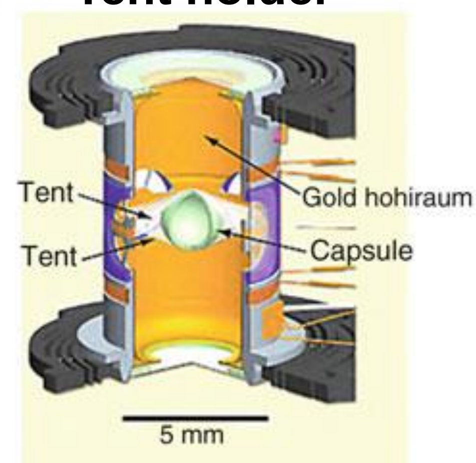

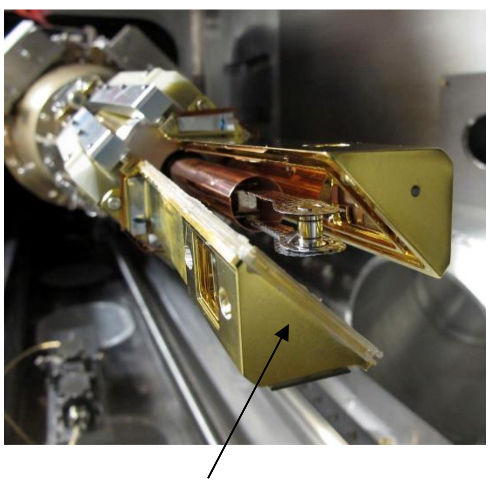

Cryogenic shroud

https://www.lle.rochester.edu
https://upload.wikimedia.org/wikipedia/commons/7/7b/Nif-shot_target-arm-before_big.jpg
https://www.lle.rochester.edu/index.php/2014/11/10/next-generation-cryo-target/

NIF achieved ignition (Q=1.5) on Dec. 5, 2022

- **Input Laser energy: 2.05 MJ**
- **Output energy: 3.15 MJ**

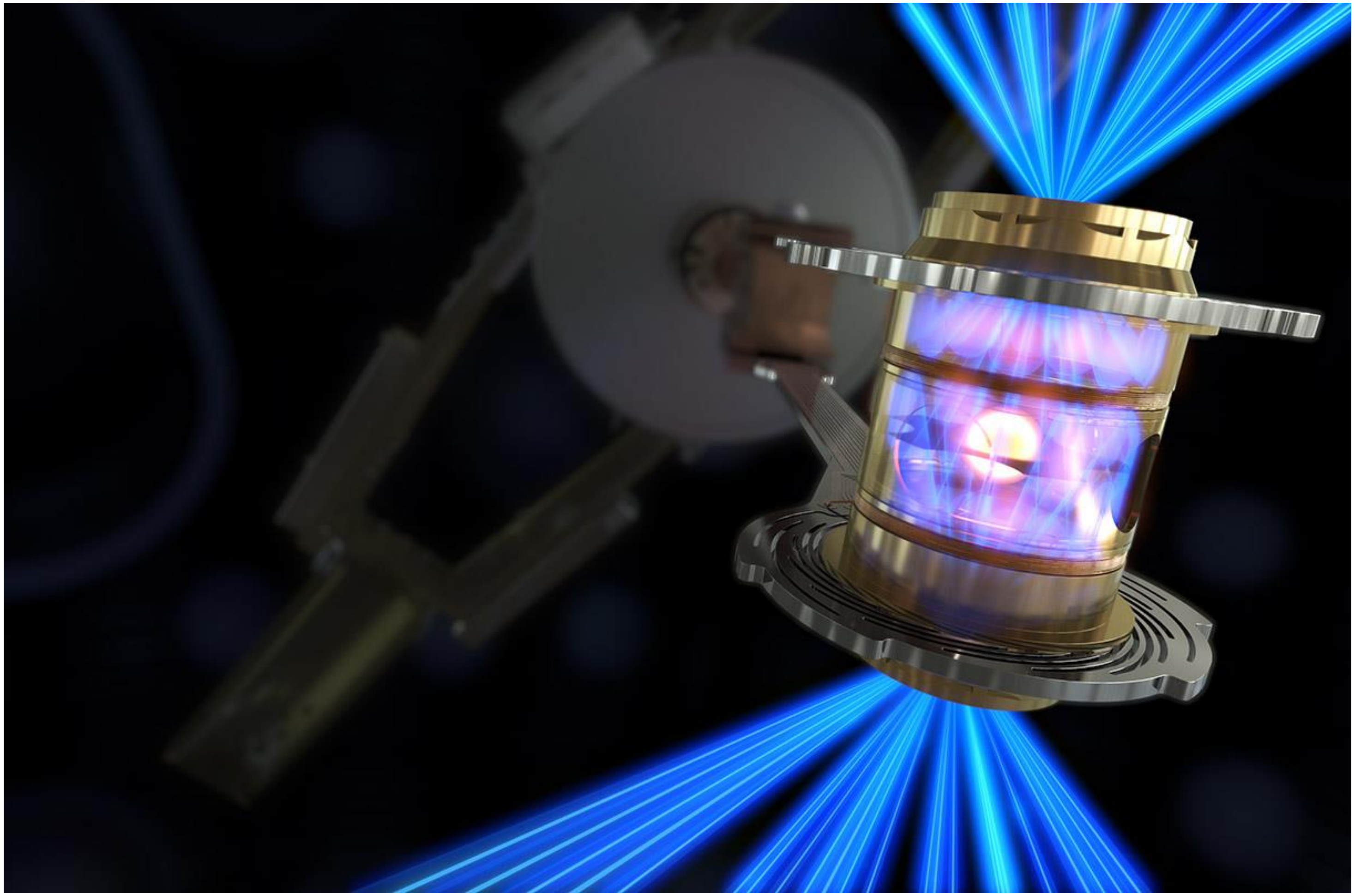

https://www.science.org/content/article/historic-explosion-long-sought-fusion-breakthrough

National Ignition Facility (NIF) achieved a yield of more than 1.3 MJ from ~1.9 MJ of laser energy in 2021 (Q~0.7)

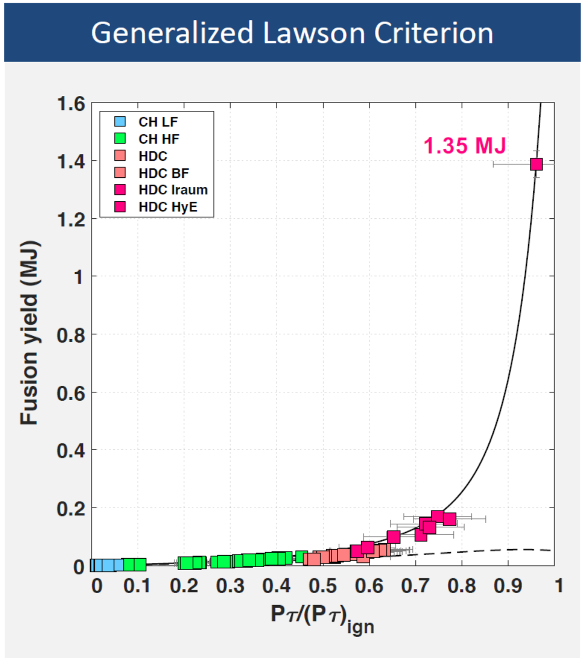

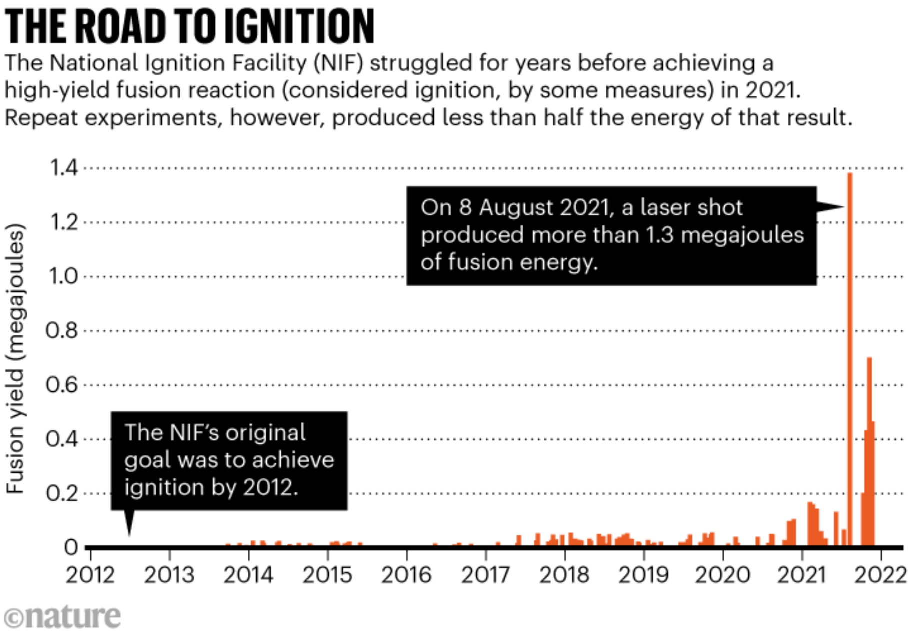

- National Ignition Facility (NIF) achieved a yield of more than 1.3 MJ (Q~0.7). This advancement puts researchers at the threshold of fusion ignition.
- Laser-fusion facility heads back to the drawing board.

T. Ma, ARPA-E workshop, April 26, 2022
J. Tollefson, Nature (News) 608, 20 (2022)

“Ignition” (target yield larger than one) was achieved in NIF on 2022/12/5

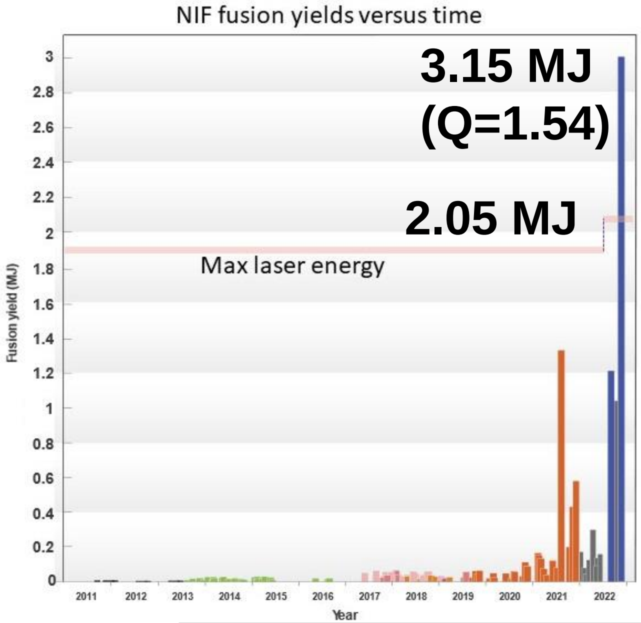

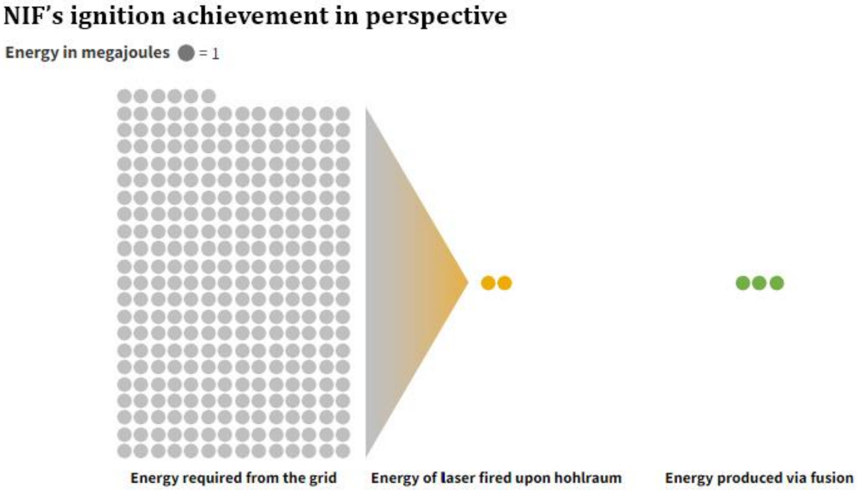

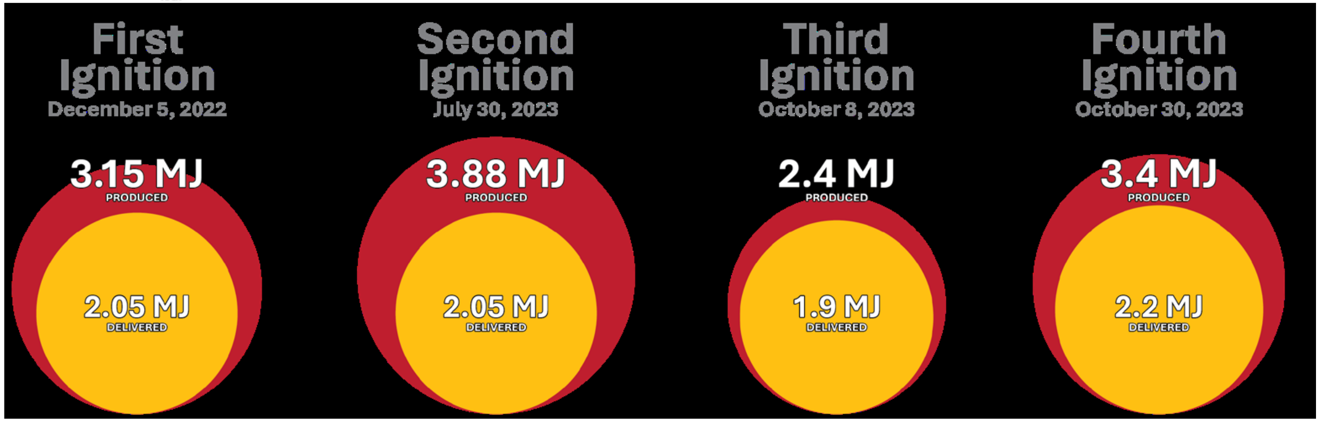

https://physicstoday.scitation.org/do/10.1063/PT.6.2.20221213a/full/
The age of ignition: anniversary edition, LLNL-BR-857901

ICF via z pinch or z-pinch driven dynamic-hohlraums

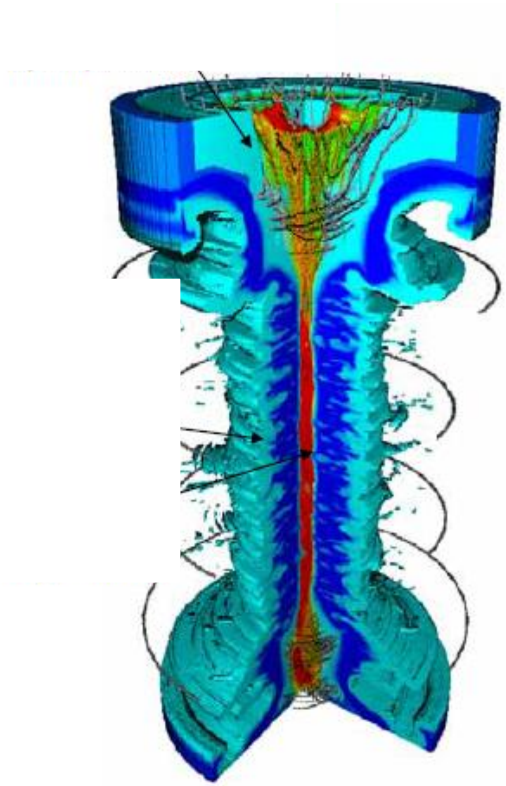

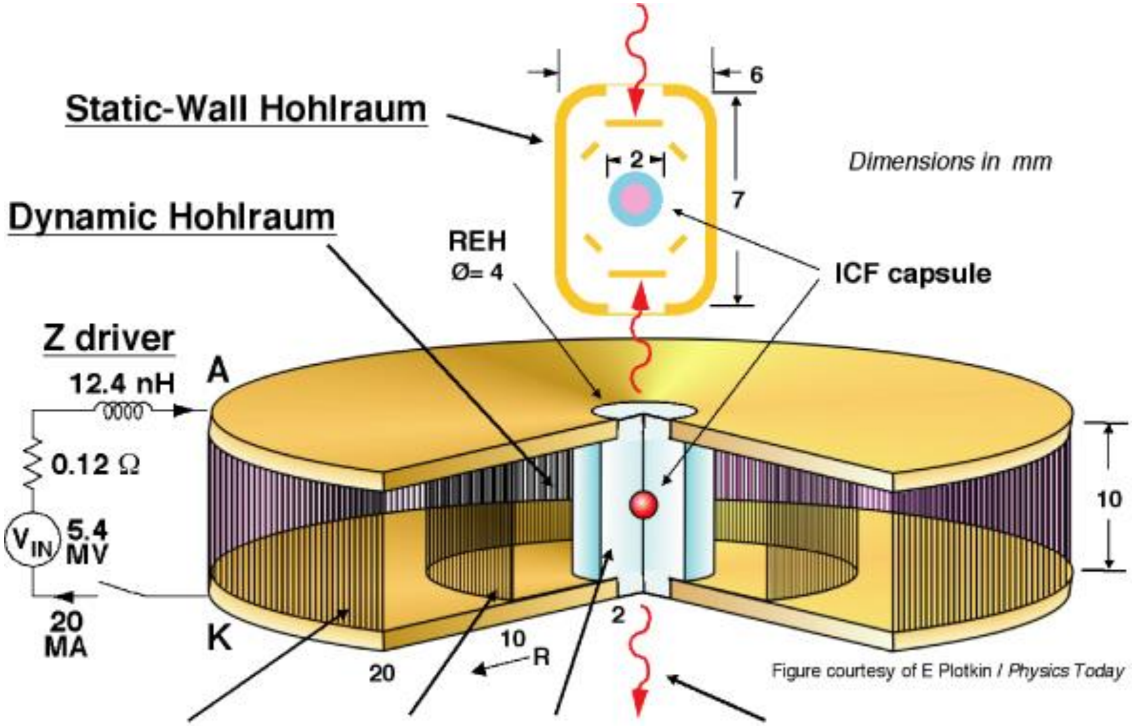

Figure courtesy of E Plotkin / *Physics Today*

magnetized liner inertial fusion (MagLIF)

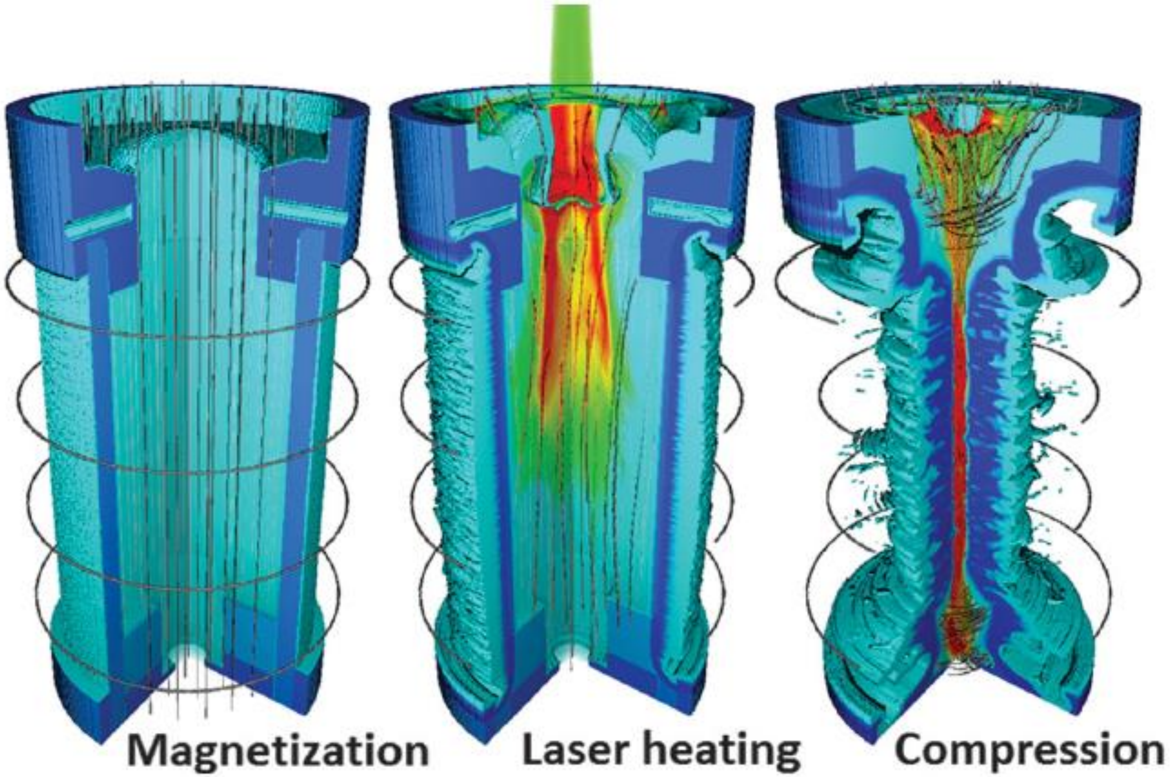

M. R. Gomez, *et. cl.*, Phys. Rev. Let., 113, 155003 (2014)

MagLIF target

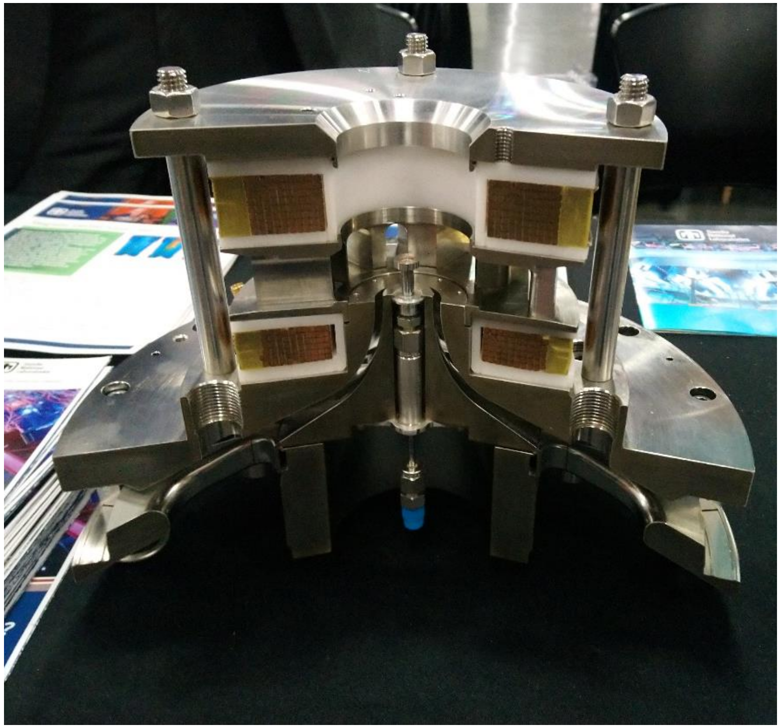

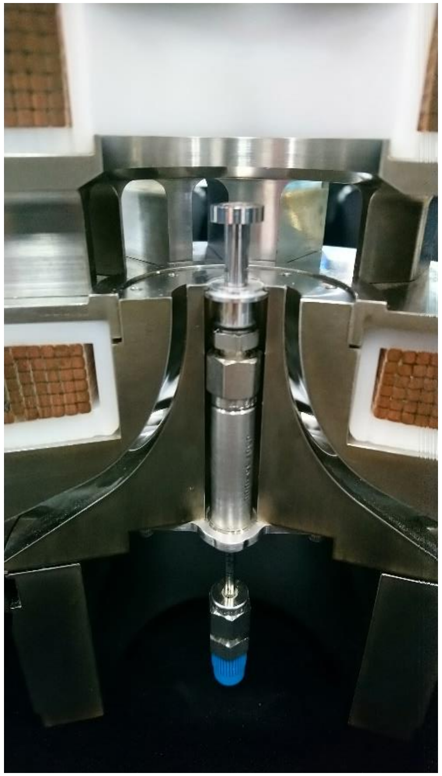

Neutron yield increased by 100x with preheat and external magnetic field.

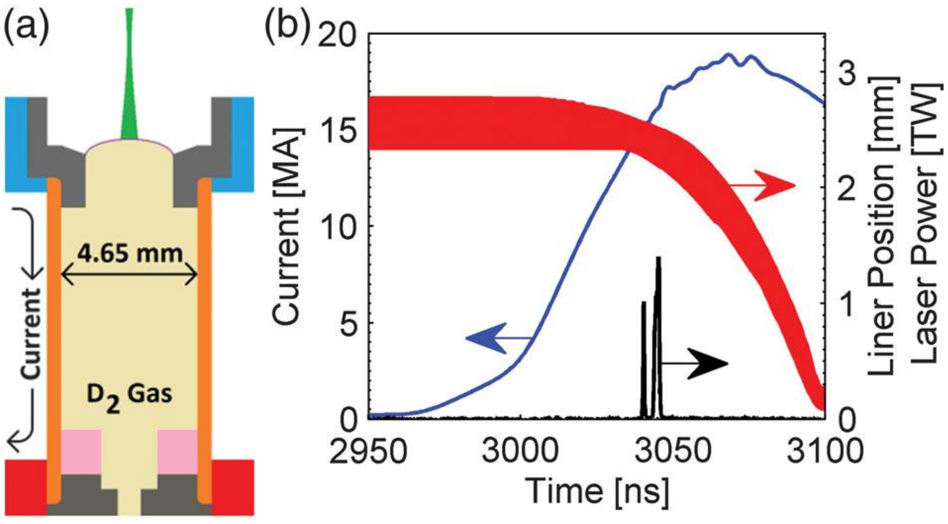

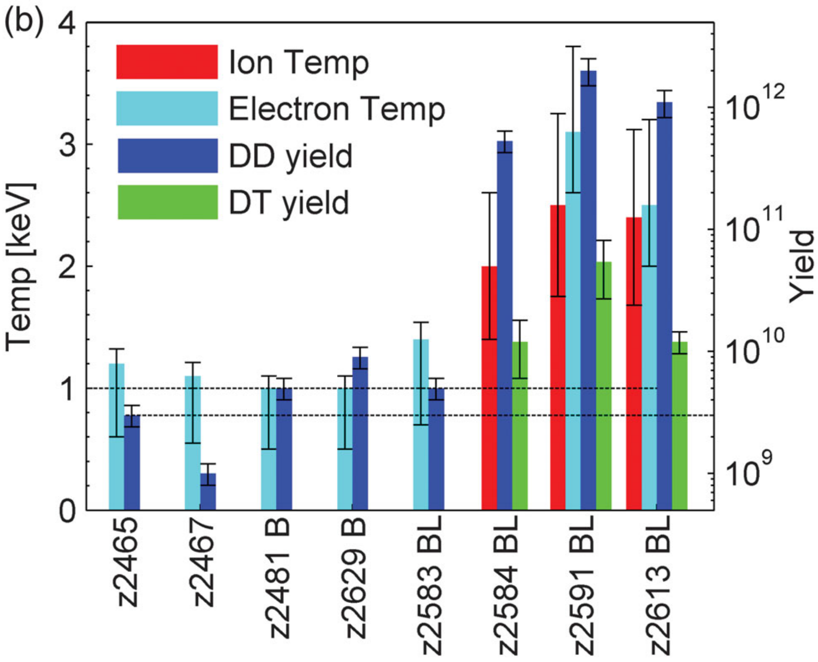

M. R. Gomez *et al* Phys. Rev. Lett. 113 155003 (2014)

Sheared flow stabilizes MHD instabilities

m = 0 (sausage)

Perturbation $\propto e^{(im\theta + ikz + \gamma t)}$

m = 1 (kink)

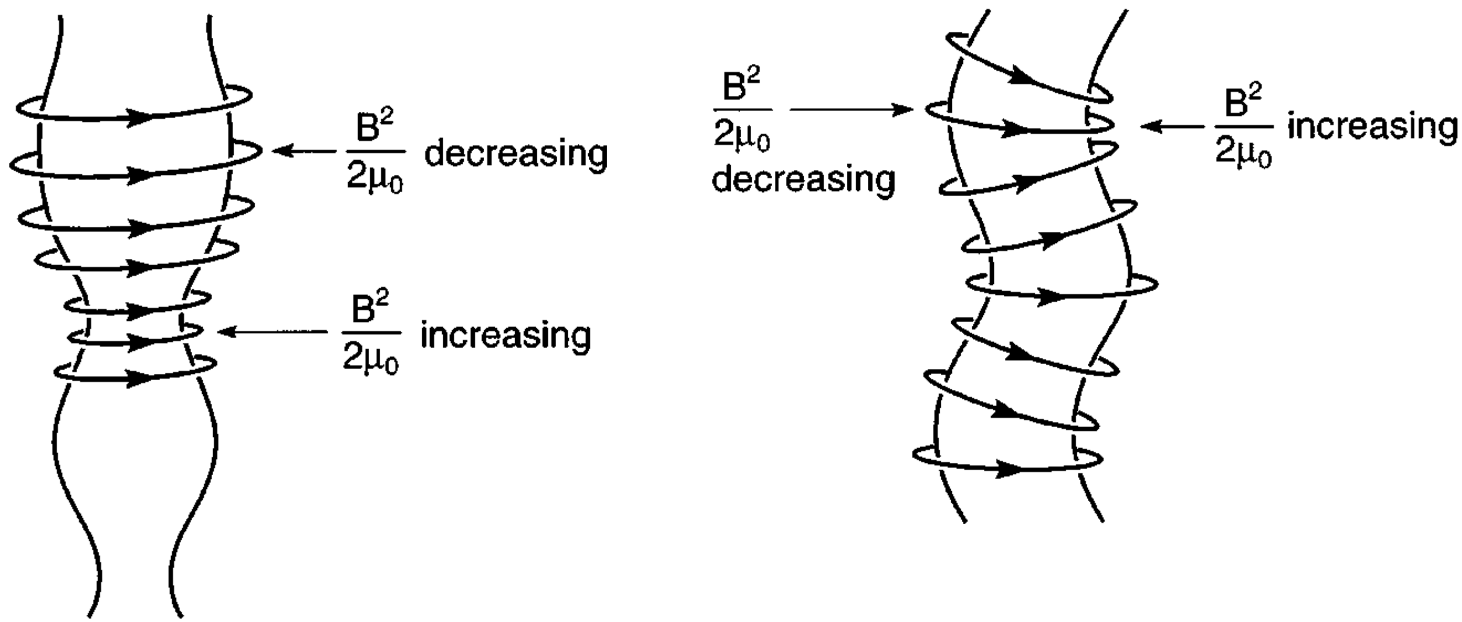

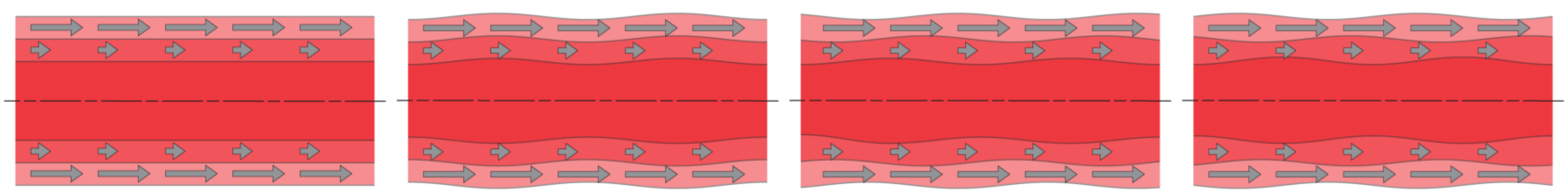

$$\frac{dV_Z}{dr} \neq 0$$

M. G. Haines, etc., Phys. Plasmas 7, 1672 (2000)
U. Shumlak, etc., Physical Rev. Lett. 75, 3285 (1995)
U. Shumlak, etc., ALPHA Annual Review Meeting 2017

A z-pinch plasma can be stabilized by sheared flows

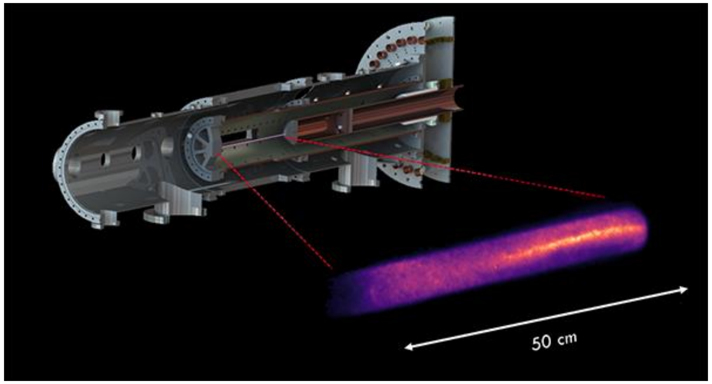

ZAP ENERGY™

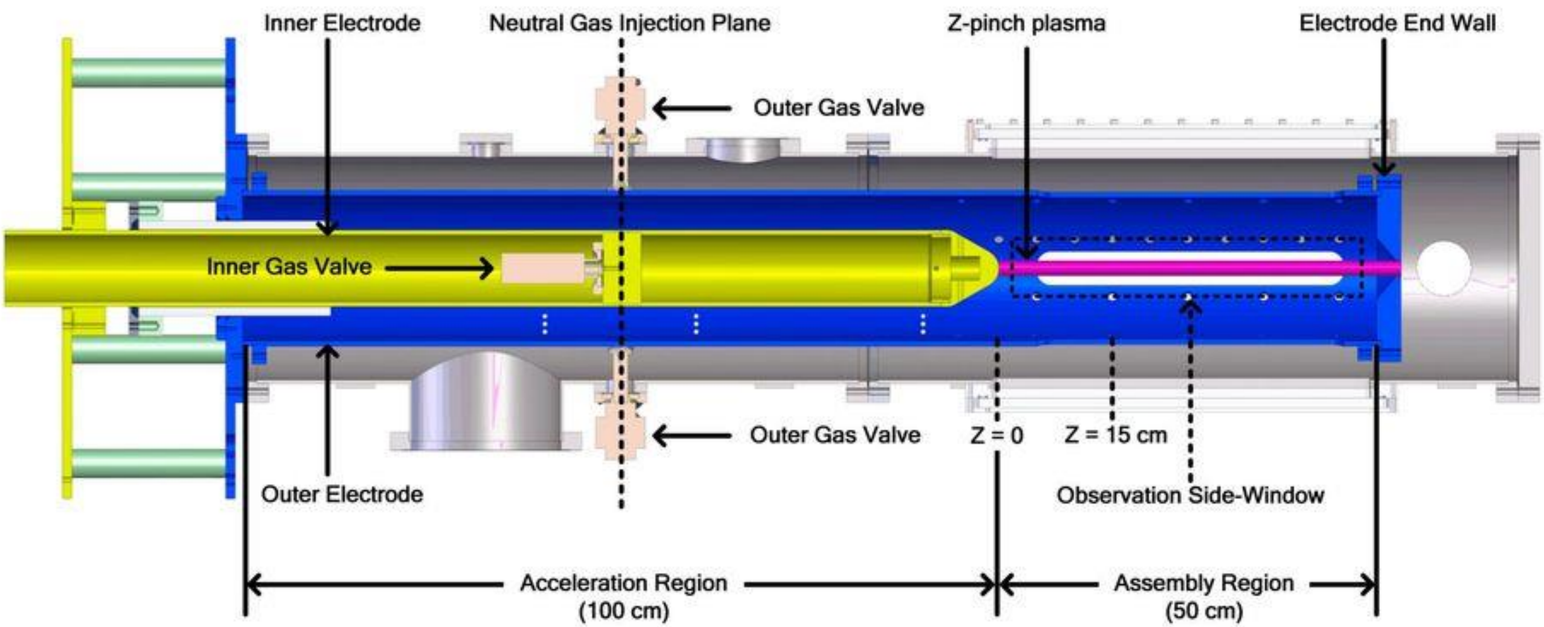

https://www.zapenergyinc.com/about
A. D. Stepanov, etc., Phys. Plasmas 27, 112503 (2020)

Fusion reactor concept by ZAP energy

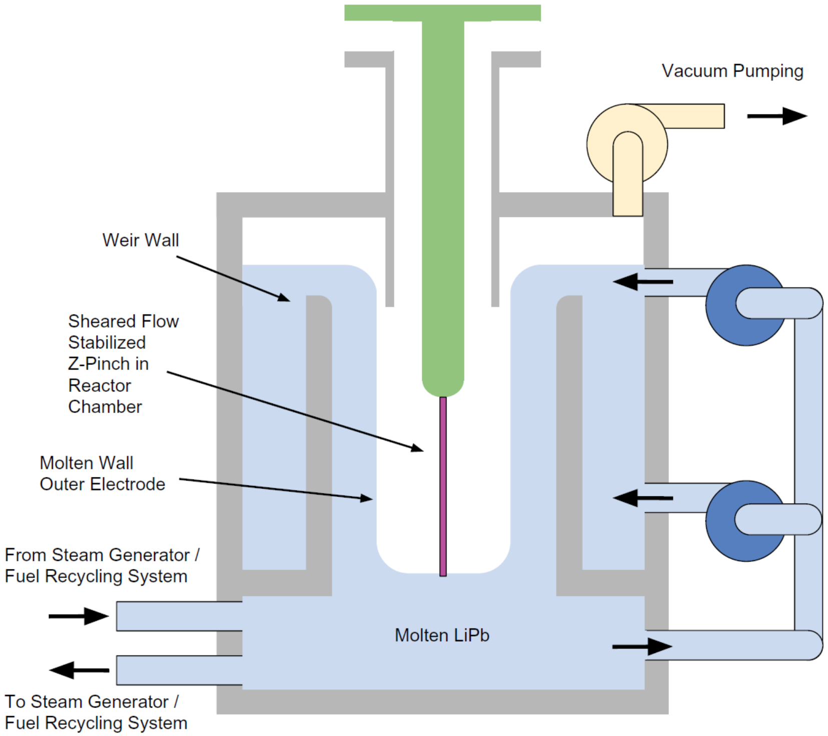

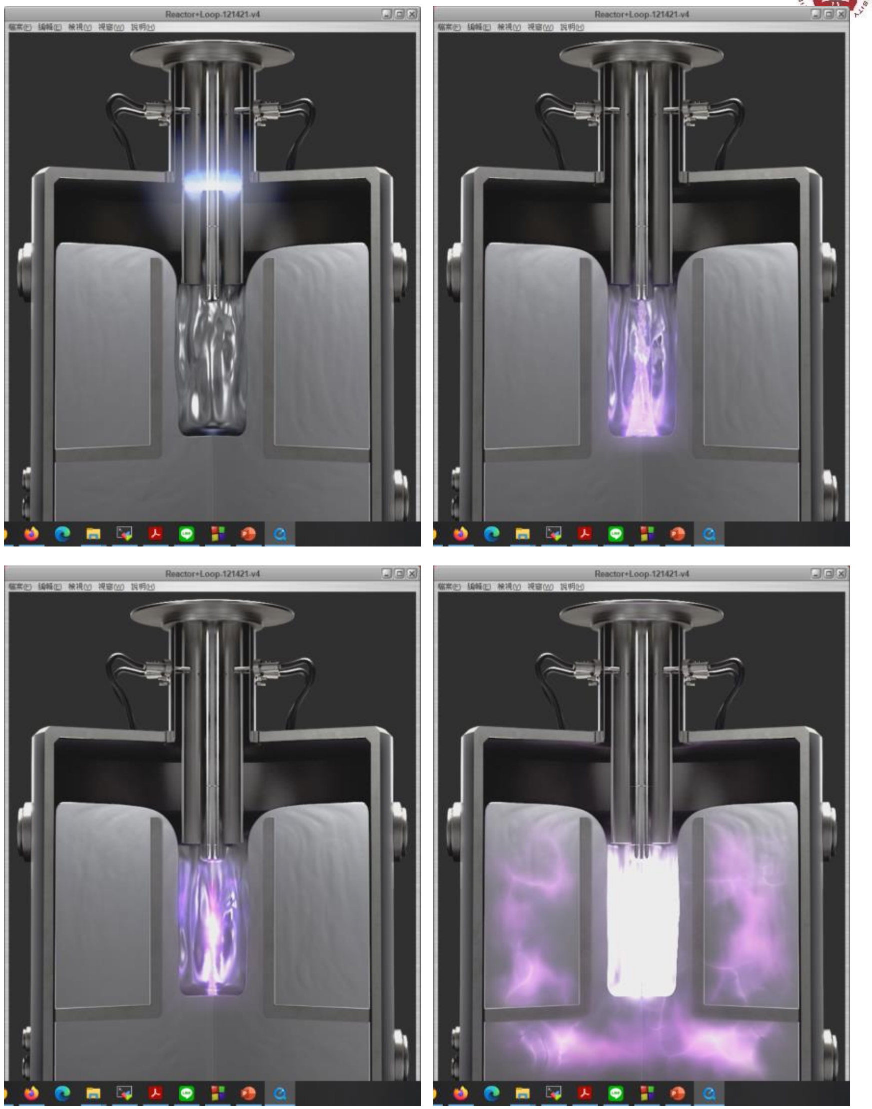

https://www.zapenergyinc.com/about

E. G. Forbes, etc., Fusion Sci. Tech. 75, 599 (2019)

First light fusion, UK

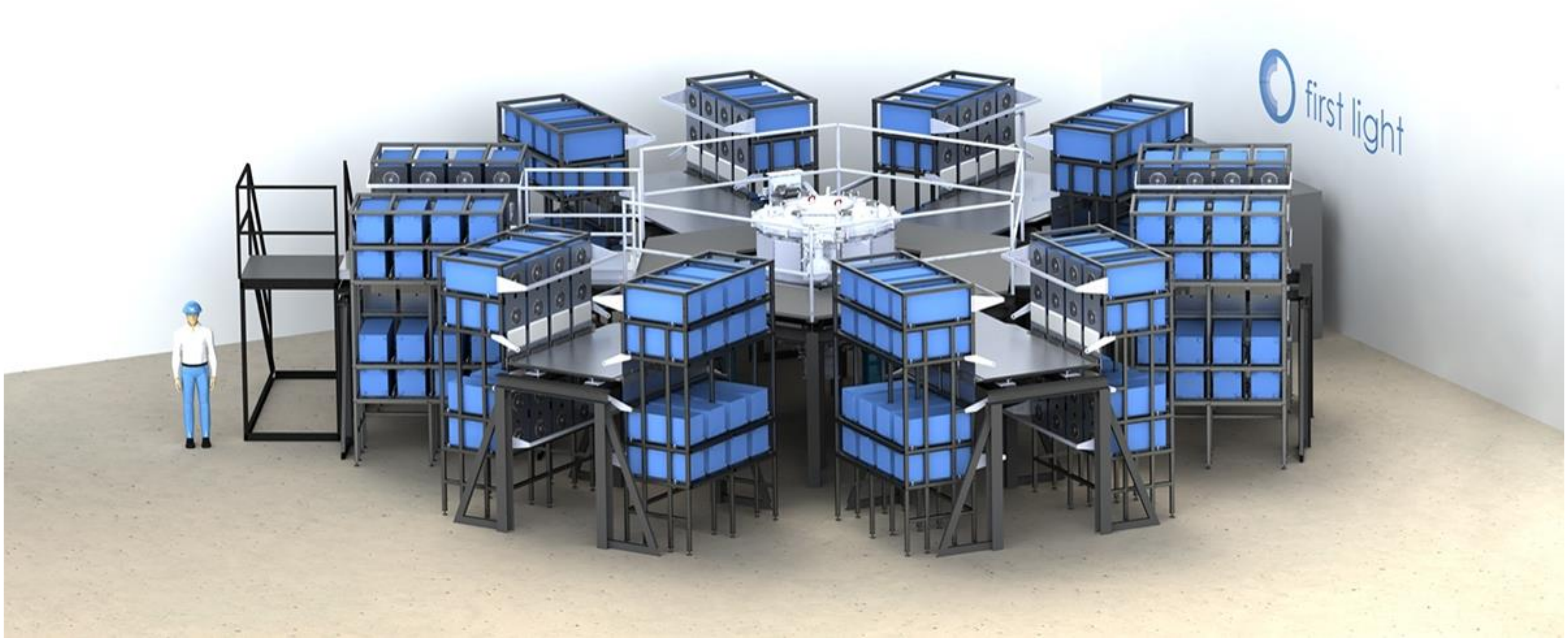

- **2.5 MJ @ 200 kV**
- **14 MA with t_{rise}~2 us**

https://images.app.goo.gl/vcsJTuwVrbY29QELA

First light fusion, UK

https://www.all-electronics.de/wp-content/uploads/2019/08/1_Pic_192-capacitors-around-vaccum-chamber_lowres-1024x768.jpg

Projectile Fusion is being established at First Light Fusion Ltd, UK

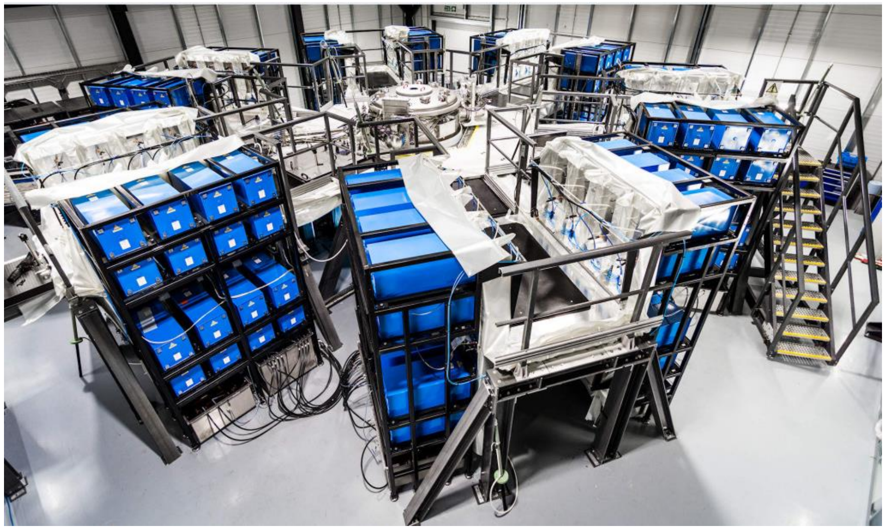

- **Stored energy: 2.5 MJ @ 200 kV (C_{tot}=125 uF)**
- **I_{peak}=14 MA w/ T_{rise}~2us.**

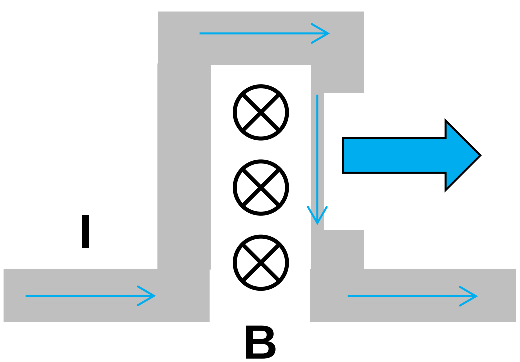

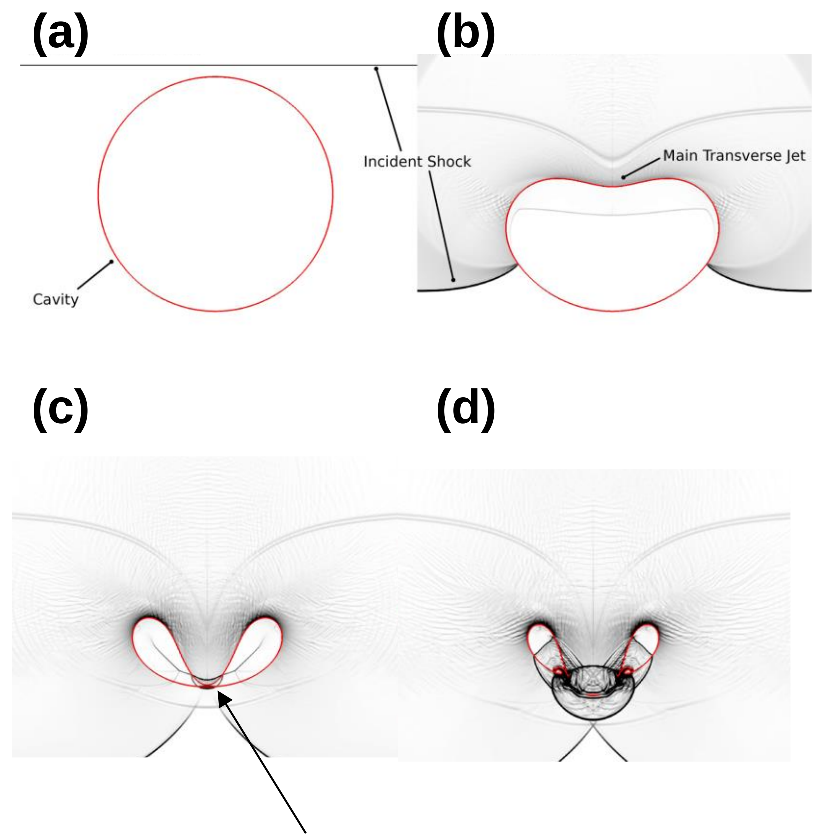

- **High pressure is generated by the colliding shock.**

https://firstlightfusion.com/
B. Tully and N. Hawker, Phys. Rev. **E93**, 053105 (2016)

First light fusion, UK – achieving ignition using shock wave

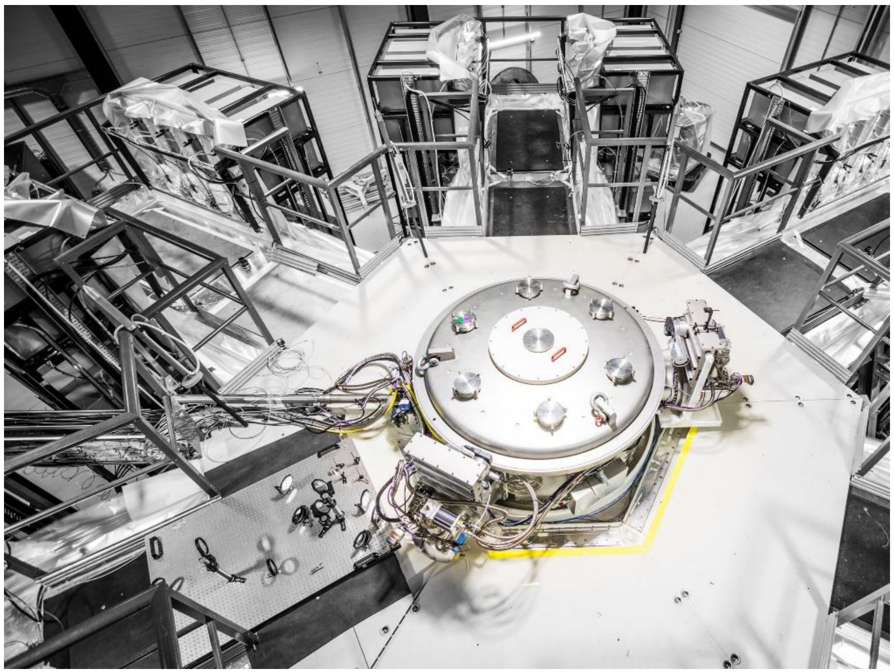

First Light Fusion

First Light Fusion is a spin-off from Oxford University department of mechanical engineering and claims to be able to harness instabilities by using asymmetrical implosion.

See http://firstlightfusion.com/

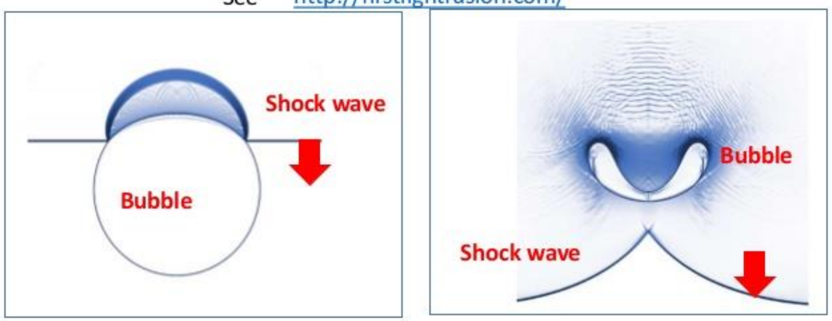

https://fsmedia.imgix.net/27/26/b2/01/8b3f/4aee/810c/8da397223c59/machine-3-23jpg.jpeg?crop=edges&fit=crop&auto=format%2Ccompress&dpr=2&h=900&w=1200
http://laurencehunt.blogspot.com/2019/

A gas gun is used to eject the projectile

https://www.youtube.com/watch?v=JN7IyxC11n0
https://www.youtube.com/watch?v=aW4eufacf-8

The pulsed-power system was built by only students

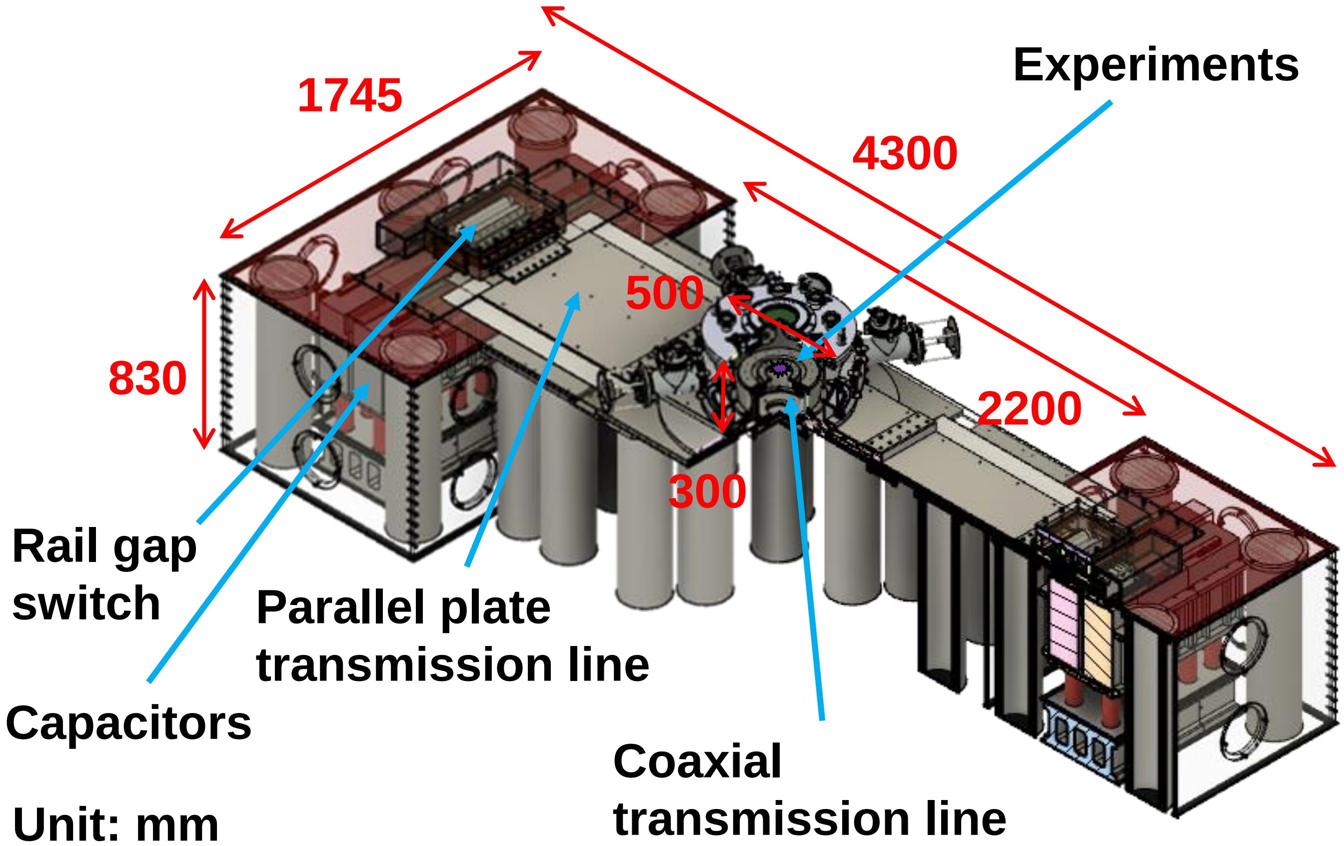

- A 1 kJ pulsed-power system at ISAPS, NCKU started being operated since September, 2019.

The 1-kJ pulsed-power system

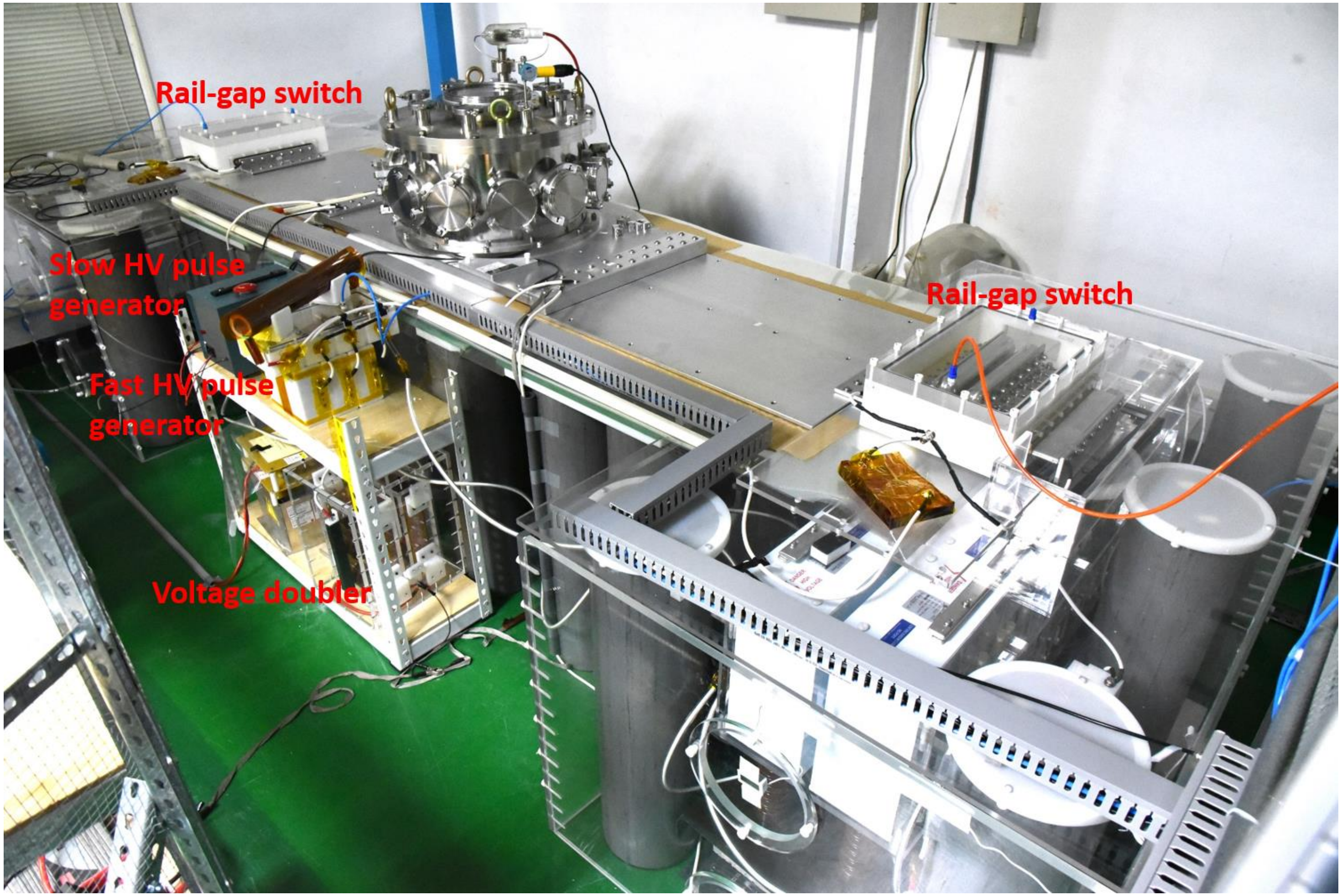

A peak current of ~135 kA with a rise time of ~1.6 us is provided by the pulsed-power system

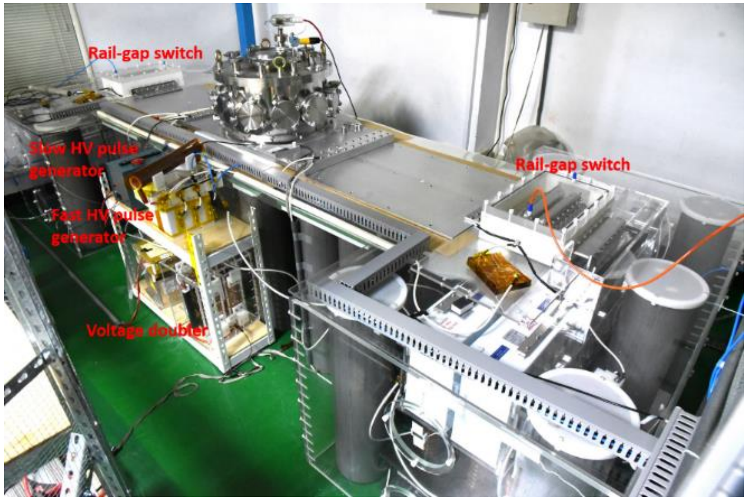

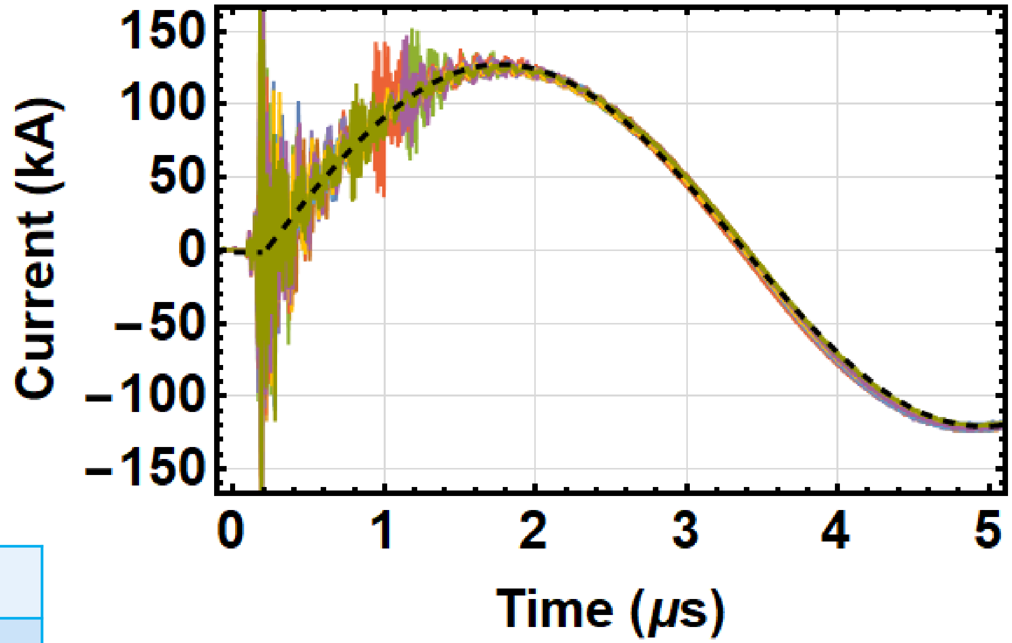

Capacitance (μF)	5
V_{charge} (kV)	20
Energy (kJ)	1
Inductance (nH)	204 ± 4
Rise time (quarter period, ns)	1592 ± 3
I_{peak} (kA)	135 ± 1

First shot with two synchronized rail-gap switches

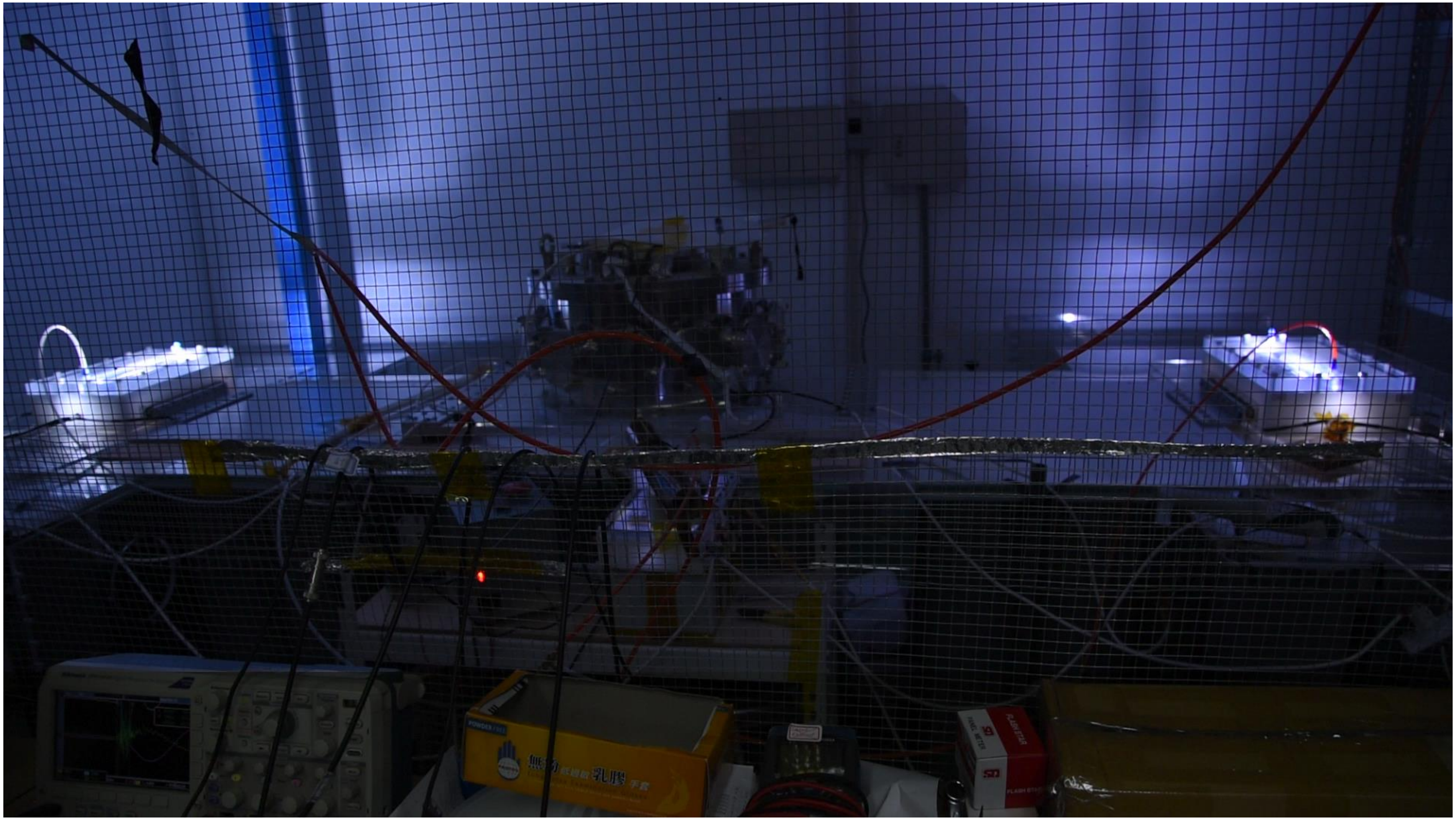

Time-resolved imaging system with temporal resolution in the order of nanoseconds was implemented

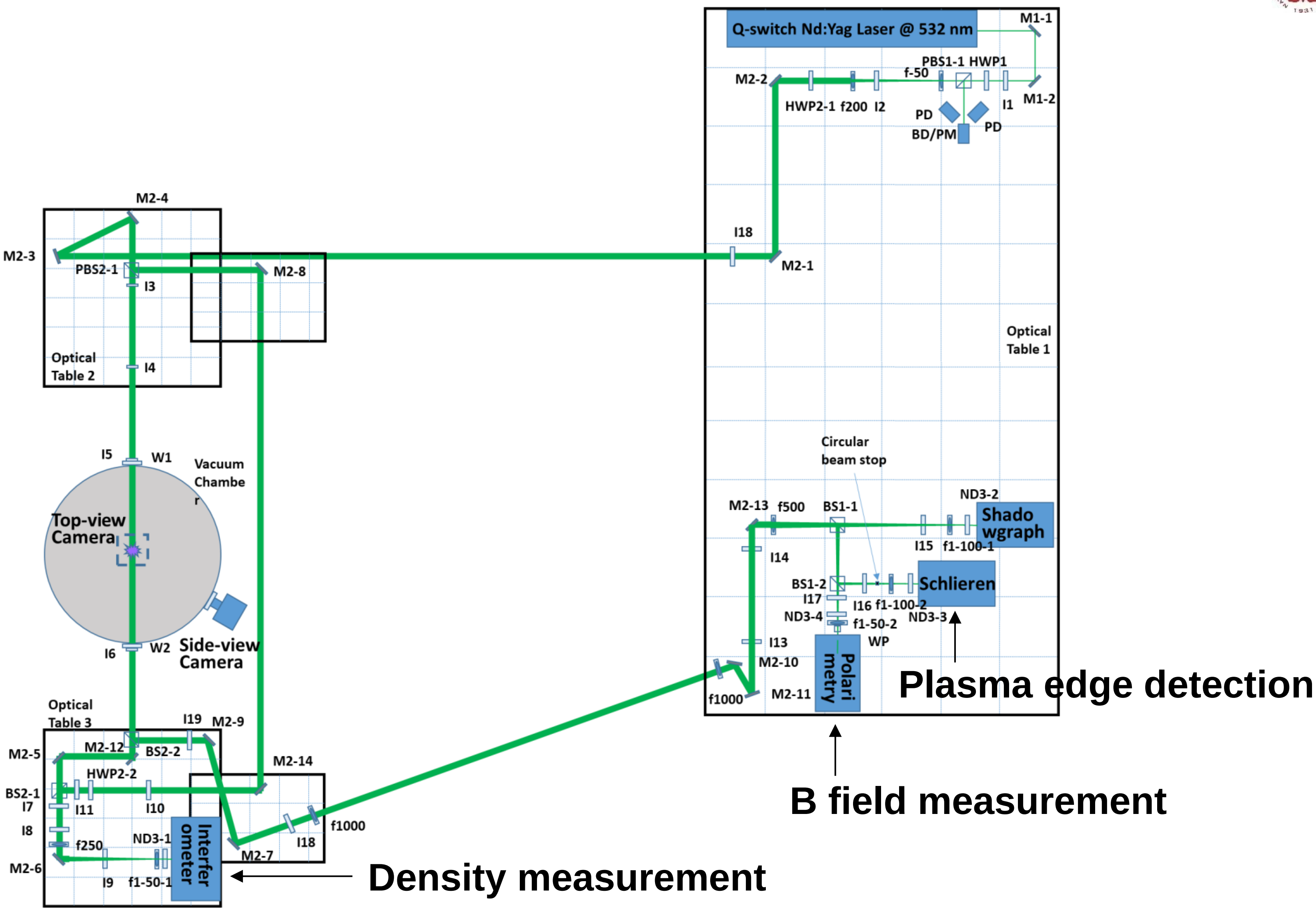

Varies diagnostics were integrated to the system

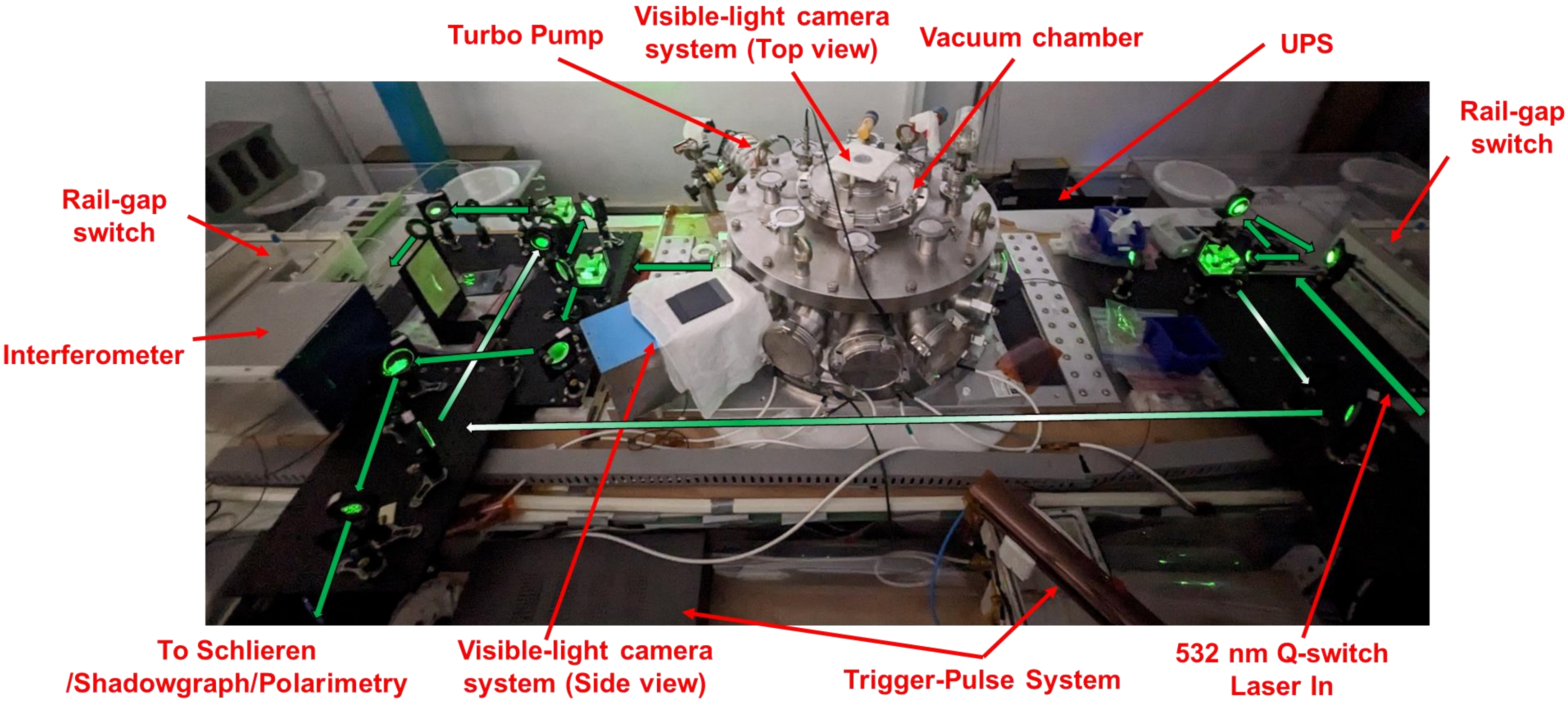

Beam path

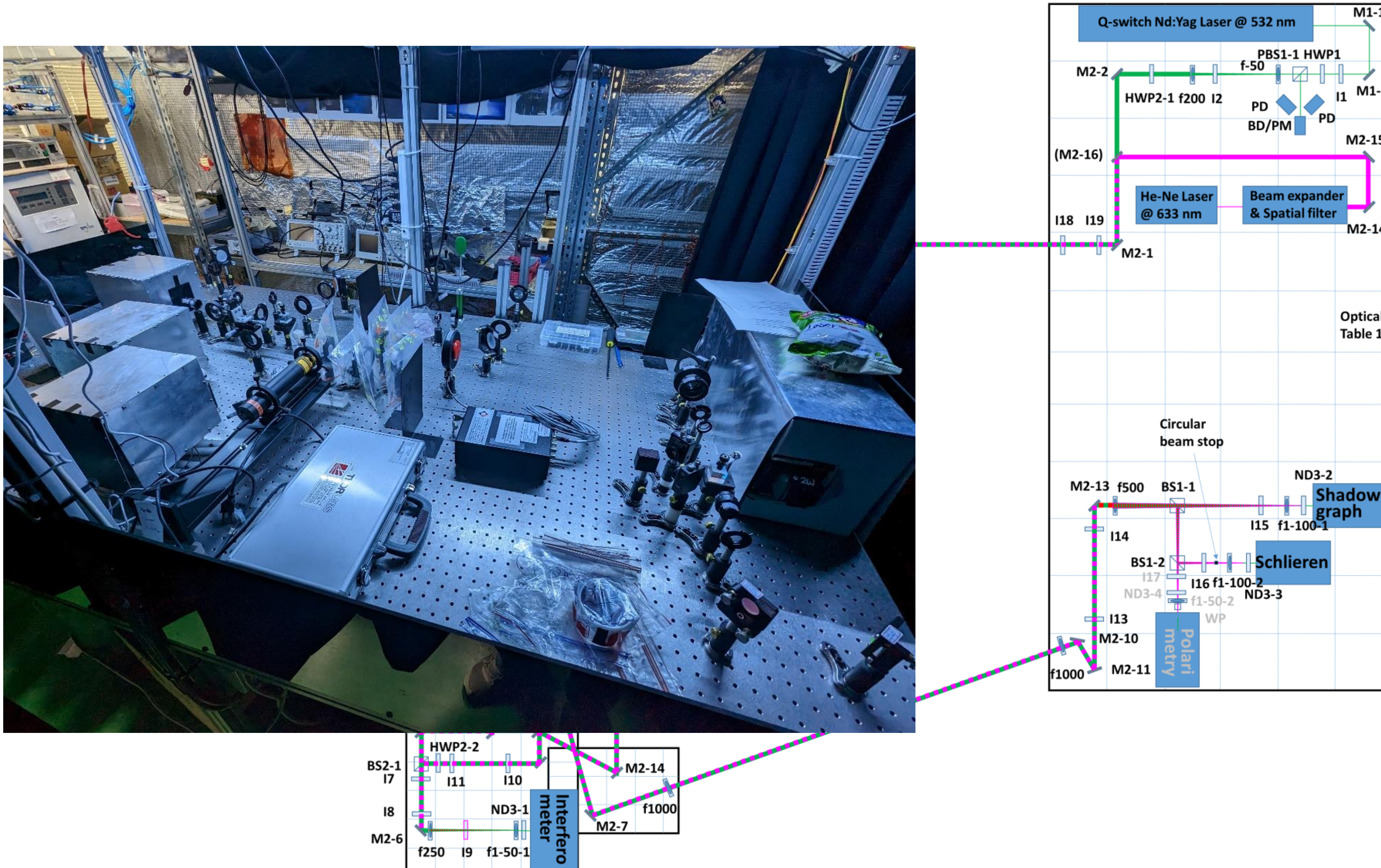
Q-switch Nd:Yag Laser @ 532 nm
M1-1
PBS1-1 HWP1
f-50
M2-2
HWP2-1 f200 I2
I1
M1-2
PD
PD
BD/PM
M2-15
(M2-16)
He-Ne Laser @ 633 nm
Beam expander & Spatial filter
I18 I19
M2-14
M2-1
Optical Table 1
Circular beam stop
ND3-2
M2-13 f500 BS1-1
Shadow graph
I15 f1-100-1
I14
BS1-2
Schlieren
I17
I16 f1-100-2
ND3-4
f1-50-2
ND3-3
WP
I13
M2-10
Polari metry
f1000
M2-11
HWP2-2
BS2-1
I7
I11
I10
M2-14
I8
ND3-1
Interfero meter
f1000
M2-6
M2-7
f250
I9
f1-50-1

Beam path

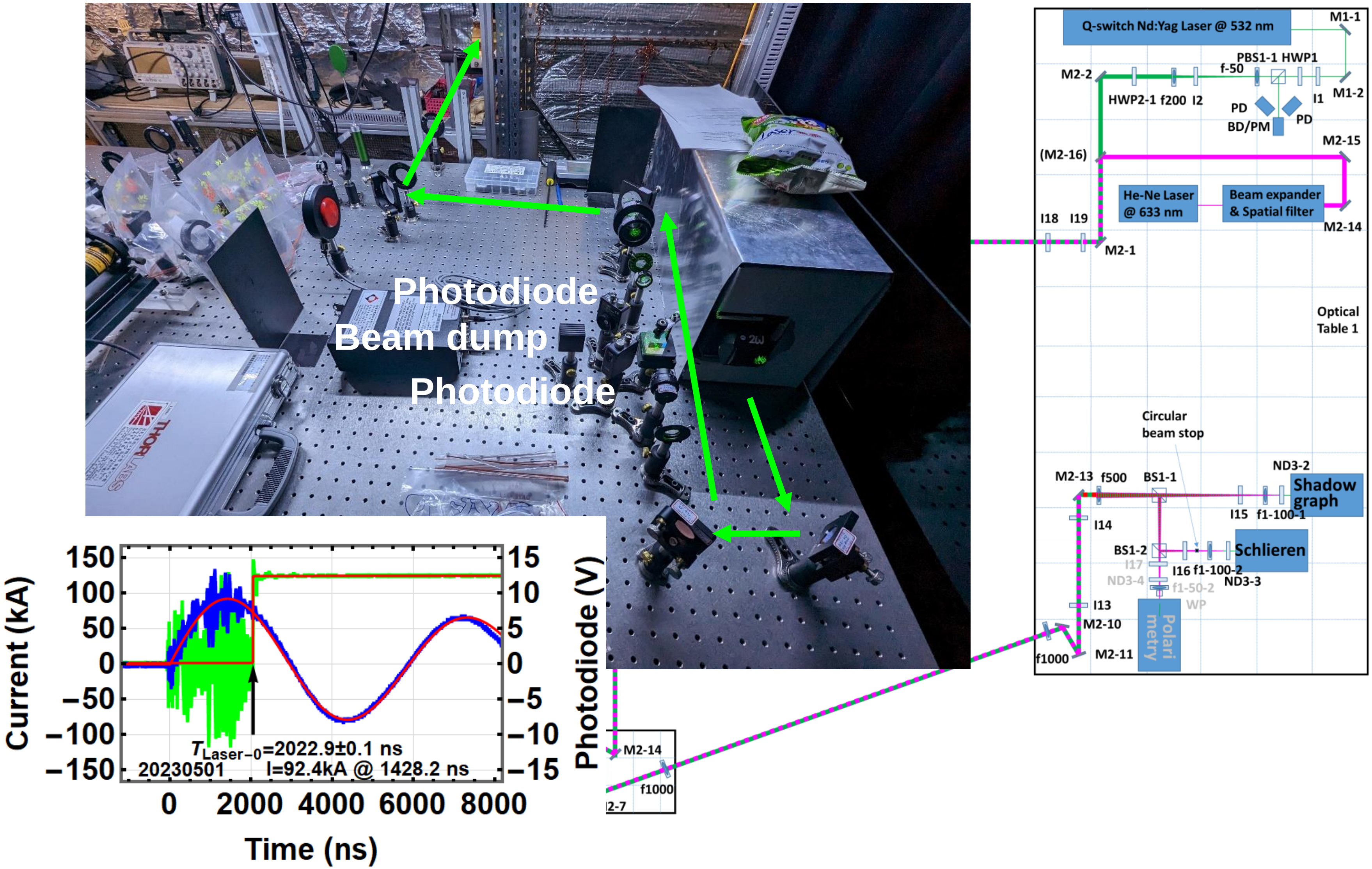

Photodiode
Beam dump
Photodiode
Current (kA)
Photodiode (V)
Time (ns)
T_Laser-0=2022.9±0.1 ns
20230501
I=92.4kA @ 1428.2 ns
Q-switch Nd:Yag Laser @ 532 nm
M1-1
M2-2
PBS1-1 HWP1
f-50
HWP2-1 f200 I2
I1
M1-2
PD
PD
BD/PM
M2-15
(M2-16)
He-Ne Laser @ 633 nm
Beam expander & Spatial filter
M2-14
I18 I19
M2-1
Optical Table 1
Circular beam stop
ND3-2
M2-13 f500
BS1-1
Shadow graph
I15 f1-100-1
I14
BS1-2
Schlieren
I17
I16 f1-100-2
ND3-4
f1-50-2
ND3-3
WP
I13
M2-10
Polari metry
f1000
M2-11
M2-14
f1000

Beam path

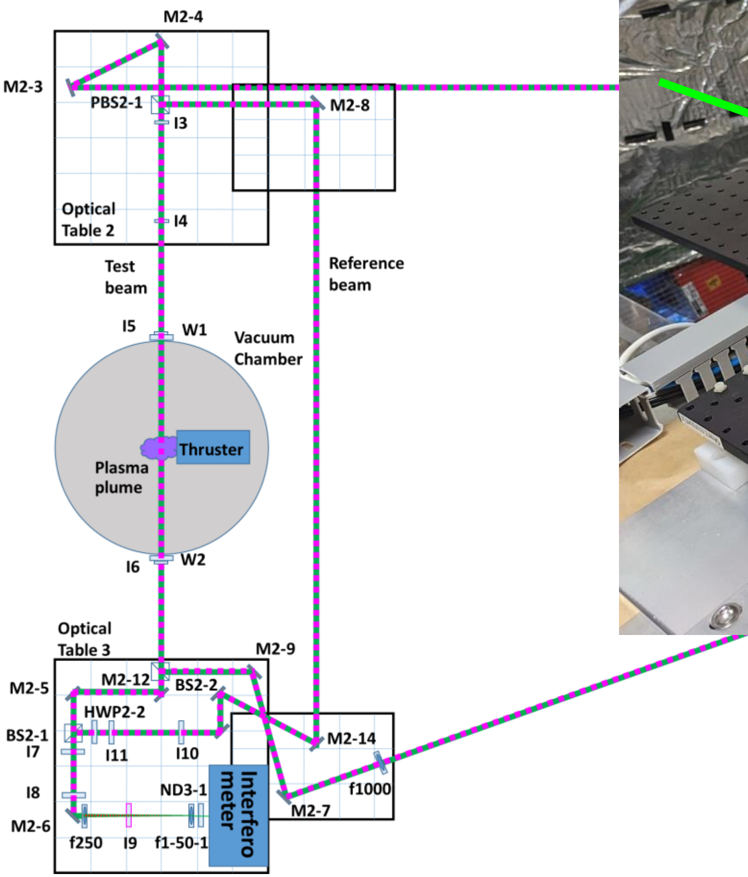
M2-4
M2-3
PBS2-1
I3
M2-8
Optical Table 2
I4
Test beam
Reference beam
I5
W1
Vacuum Chamber
Thruster
Plasma plume
I6
W2
Optical Table 3
M2-9
M2-5
M2-12
BS2-2
HWP2-2
BS2-1
I7
I11
I10
M2-14
I8
ND3-1
Interfero meter
f1000
M2-7
M2-6
f250
I9
f1-50-1

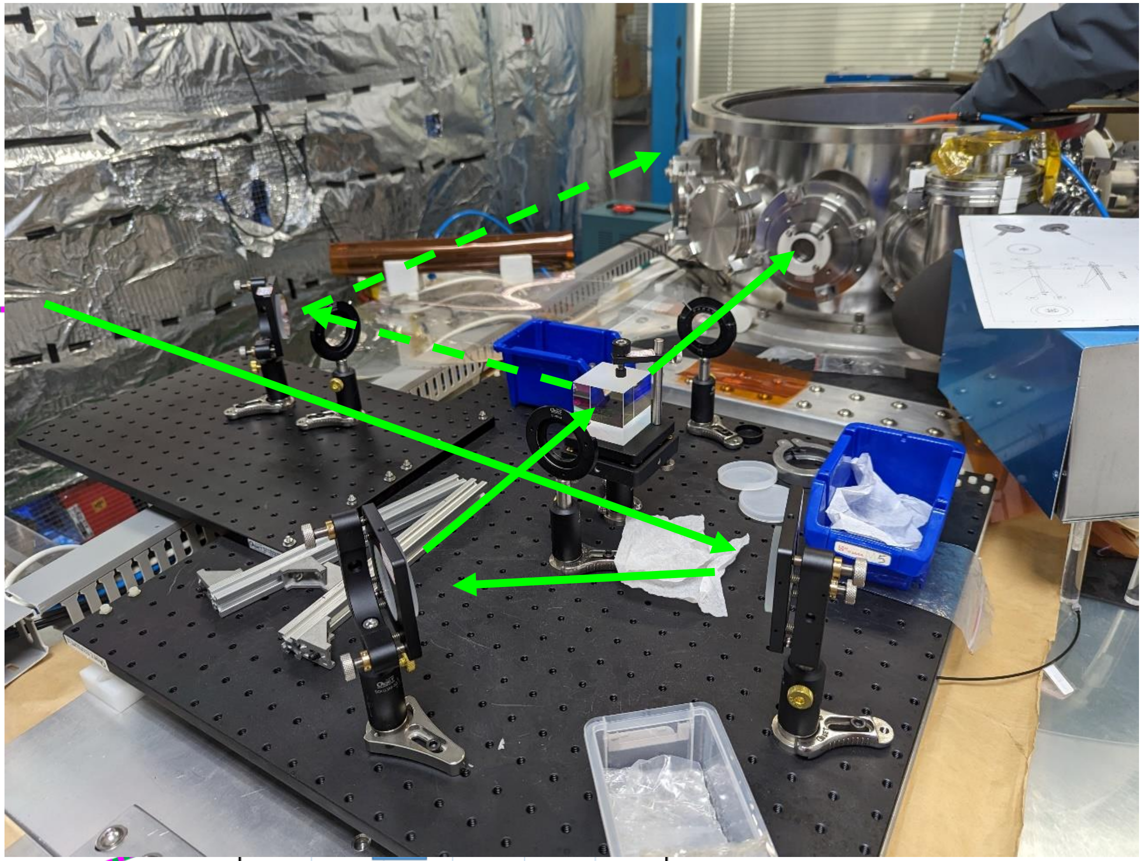

Beam path

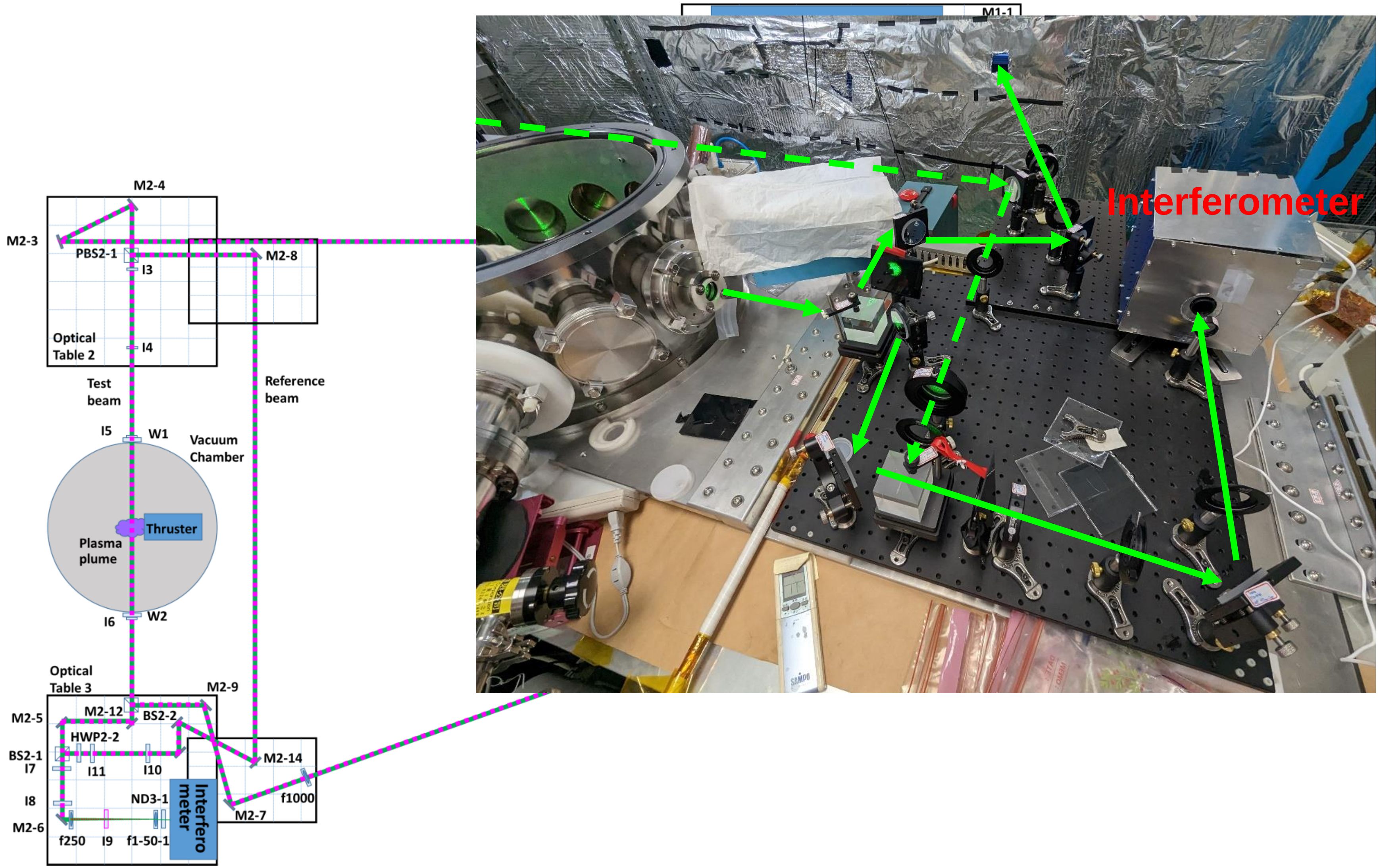
M1-1
M2-4
M2-3
PBS2-1
I3
M2-8
Optical Table 2
I4
Test beam
Reference beam
I5
W1
Vacuum Chamber
Thruster
Plasma plume
I6
W2
Optical Table 3
M2-9
M2-5
M2-12
BS2-2
HWP2-2
BS2-1
I7
I11
I10
M2-14
I8
ND3-1
Interfero meter
f1000
M2-7
M2-6
f250
I9
f1-50-1
Interferometer

Beam path

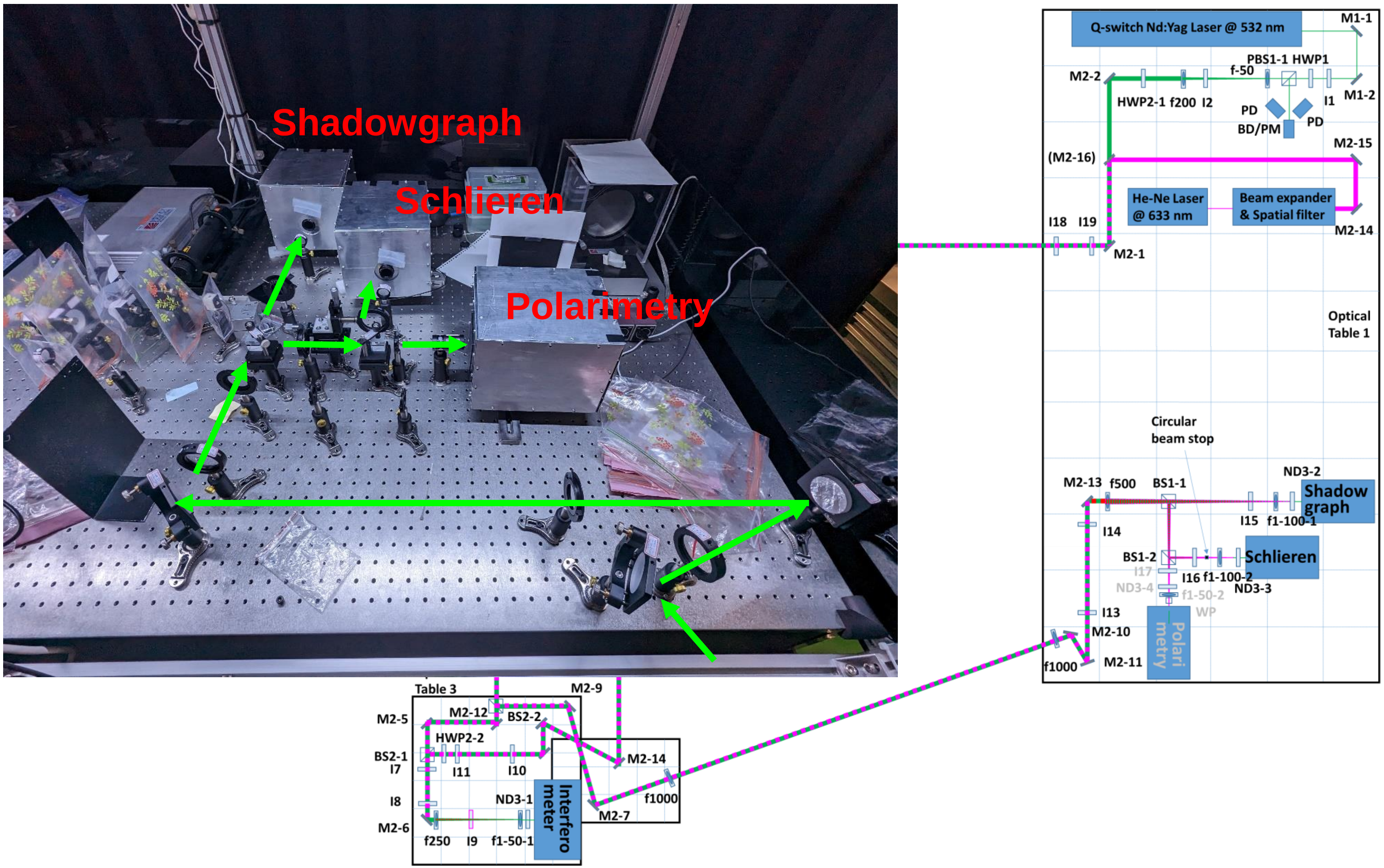

Shadowgraph
Schlieren
Polarimetry
Q-switch Nd:Yag Laser @ 532 nm
M1-1
PBS1-1 HWP1
f-50
M2-2
HWP2-1 f200 I2
I1
M1-2
PD
PD
BD/PM
M2-15
(M2-16)
He-Ne Laser @ 633 nm
Beam expander & Spatial filter
I18 I19
M2-14
M2-1
Optical Table 1
Circular beam stop
ND3-2
M2-13 f500
BS1-1
Shadow graph
I15 f1-100-1
I14
BS1-2
Schlieren
I17
I16 f1-100-2
ND3-4
f1-50-2
ND3-3
WP
I13
M2-10
Polari metry
f1000
M2-11
Table 3
M2-9
M2-5
M2-12
BS2-2
HWP2-2
BS2-1
I7
I11
I10
M2-14
I8
ND3-1
Interfero meter
f1000
M2-6
M2-7
f250
I9
f1-50-1

Laboratory astrophysics: plasma jet can be generated by a conical-wire array driven by the PGS machine

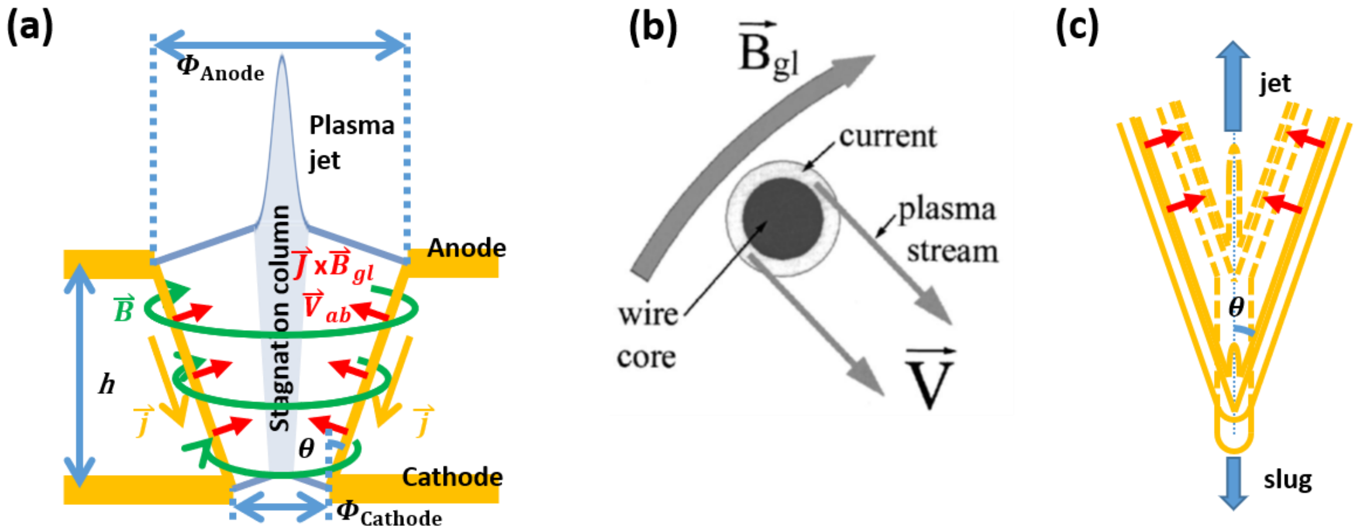

- **Herbig-Haro (HH) 111 is a plasma jet driven by a compact molecular core in the L1617 cloud complex where a young star locates*. The plasma jet in HH 111 is well collimated with the velocity of 220−330 km/s**.**

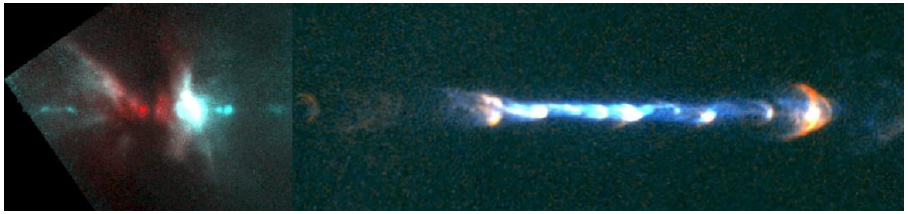

*Bo Reipurth and Steve Heathcote. 50 Years of Herbig-Haro Research, pages 3–18. Springer Netherlands, Dordrecht, 1997.
**Patrick Hartigan, Jon A. Morse, Bo Reipurth, Steve Heathcote, and John Bally. The Astrophysical Journal, 559(2):L157–L161, oct 2001.
*** Bo Reipurth and John Bally. Annual Review of Astronomy and Astrophysics, 39(1):403–455, sep 2001.

Our conical-wire array consists of 4 tungsten wires with an inclination angle of 30° with respect to the axis

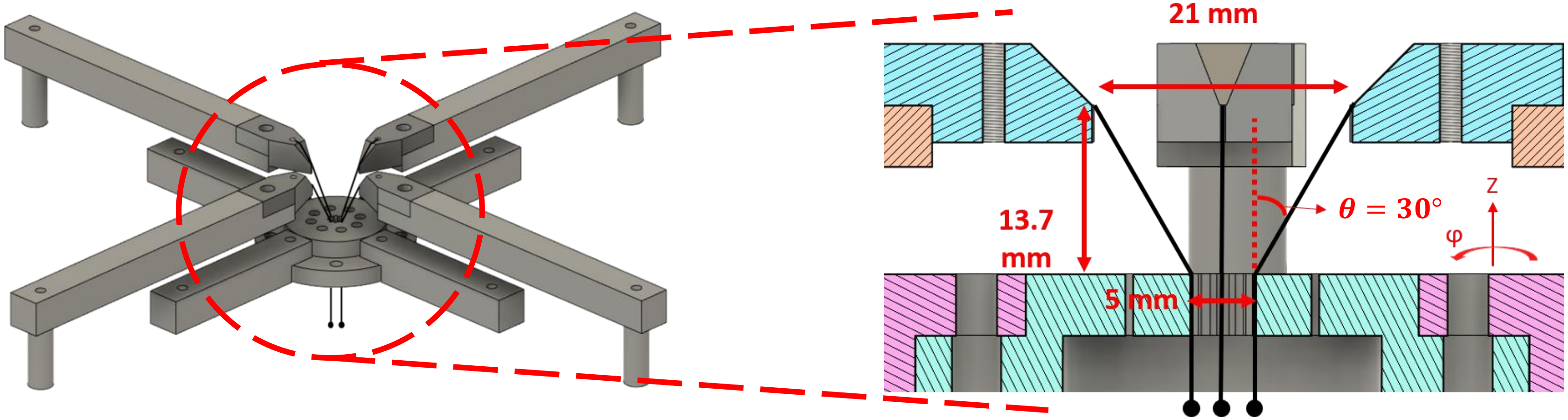

- **Conical-wire array**

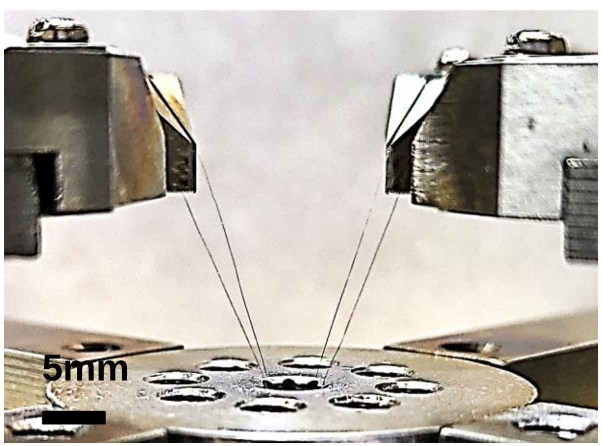

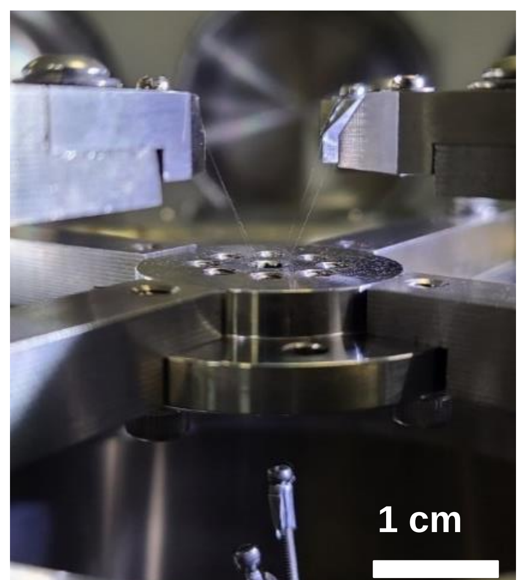

- **Material : Tungsten.**
- **Number of wires : 4.**
- **Diameter : 20 μm.**

Y.-C. Lin, NCKU Master Thesis 2021

Self-emission of the plasma jet in the UV to soft x-ray regions was captured by the pinhole camera

- **Image in UV/soft x ray**

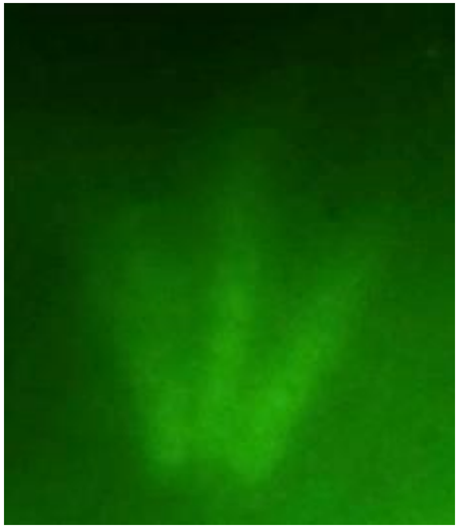

(Brightness is increased by 40 %.)

- **Pinhole diameter: 0.5 mm, i.e., spatial resolution: 1 mm.**

- **Image in visible light**

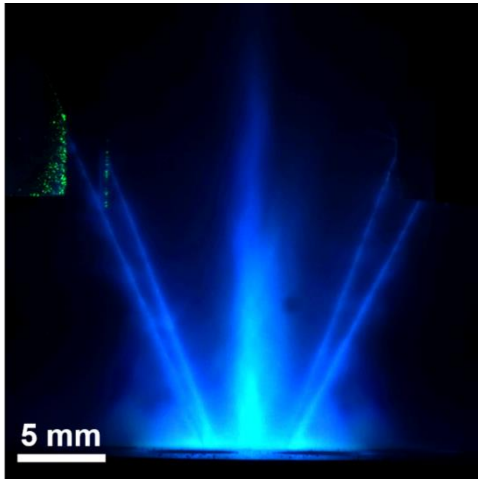

(Enhanced by scaling the intensity range linearly from 0 − 64 to 0 − 255.)

Y.-C. Lin, NCKU Master Thesis 2021
P.-Y. Chang, etc, Rev. Sci. Instrum., 93, 043505 (2022)

The MCP was burned due to the higher DC voltage supply

- **Image in UV/soft x ray**

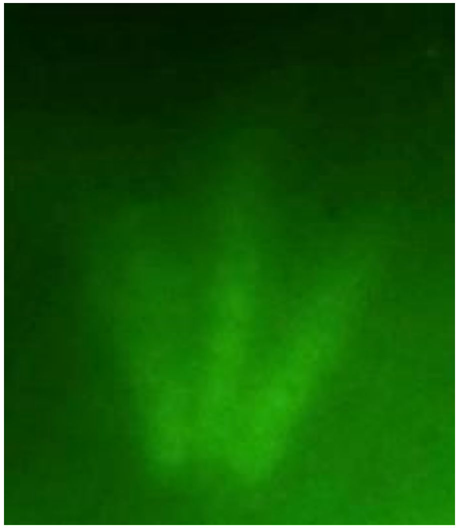

(Brightness is increased by 40 %.)

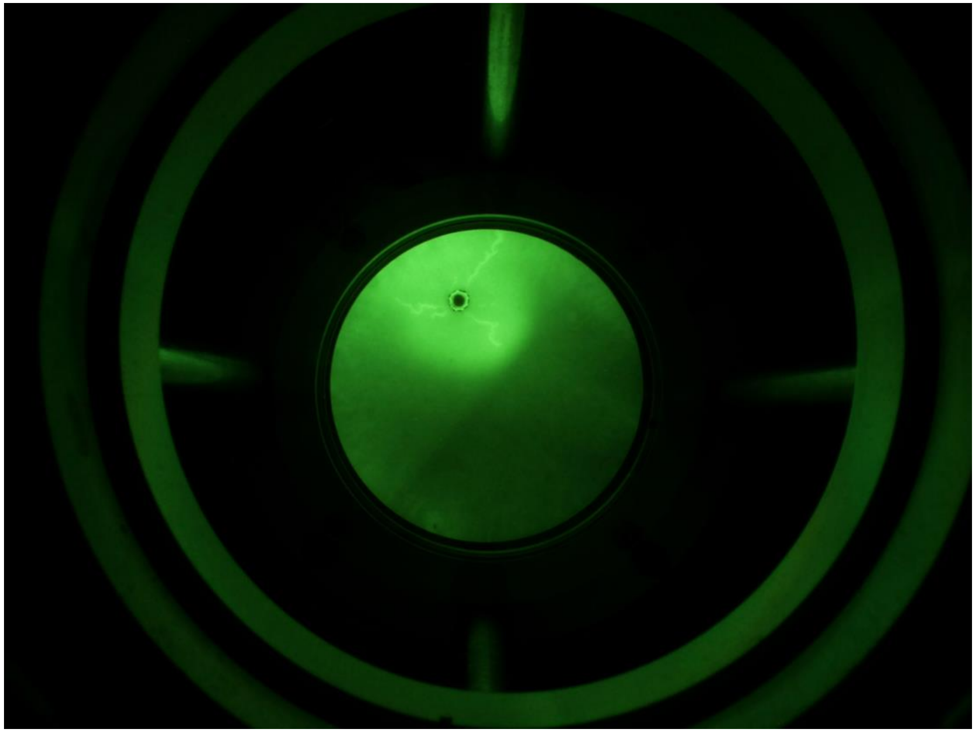

- **Pinhole diameter: 0.5 mm, i.e., spatial resolution: 1 mm.**

Y.-C. Lin, 2021/8/31 Final report
P.-Y. Chang, etc, Rev. Sci. Instrum., 93, 043505 (2022)

Plasma jet propagation was observed using laser diagnostics

- **Shadowgraph images:**

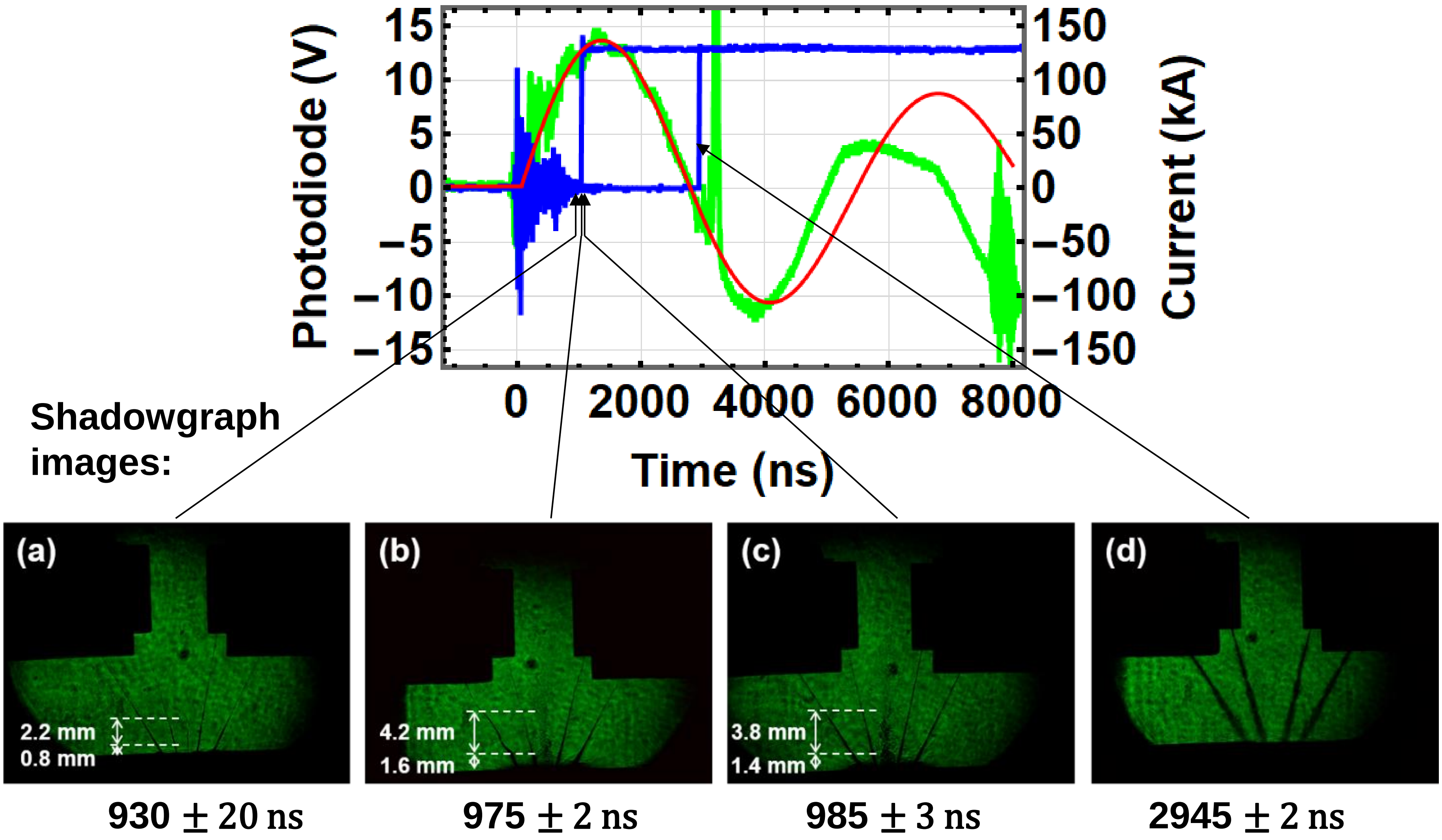

P.-Y. Chang, etc, Rev. Sci. Instrum., 93, 043505 (2022)

Length of the plasma jet at different time was obtained by the Schlieren images at different times

- **Shadowgraph images:**

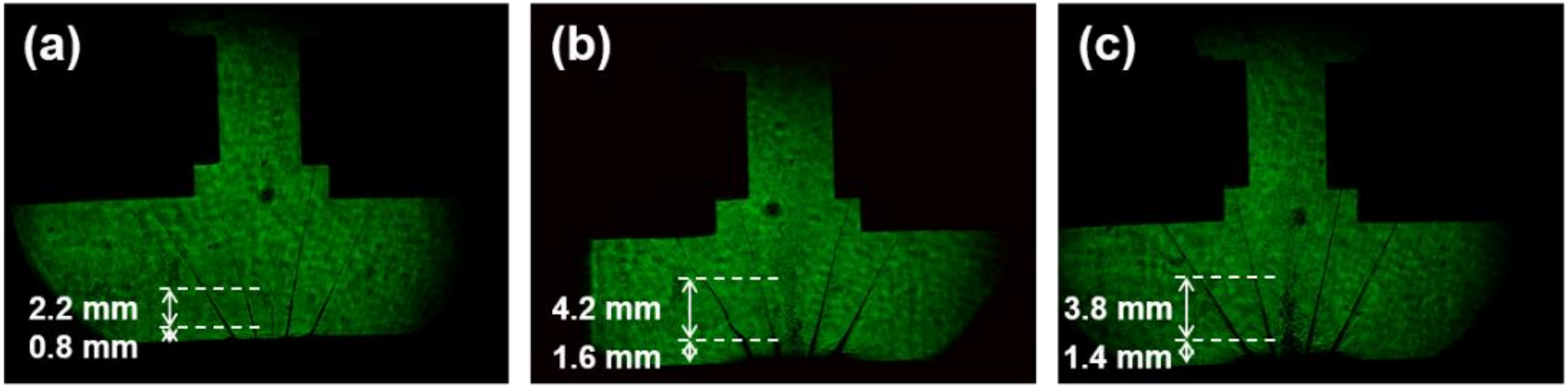

- **Schlieren images:**

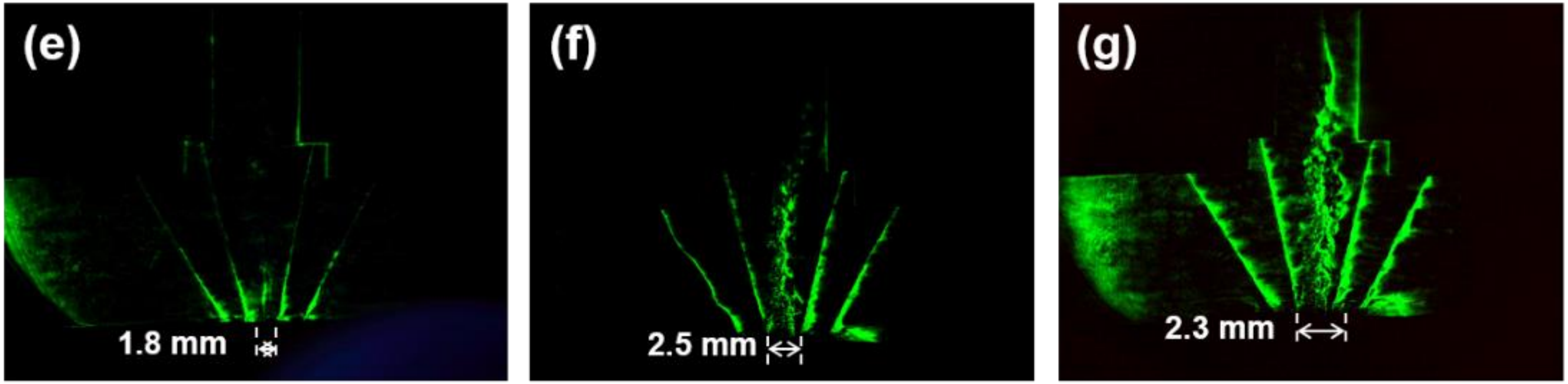

930 ± 20 ns | 975 ± 2 ns | 985 ± 3 ns

P.-Y. Chang, etc, Rev. Sci. Instrum., 93, 043505 (2022)

The measured plasma jet speed is 170 ± 70 km/s with the corresponding Mach number greater than 5

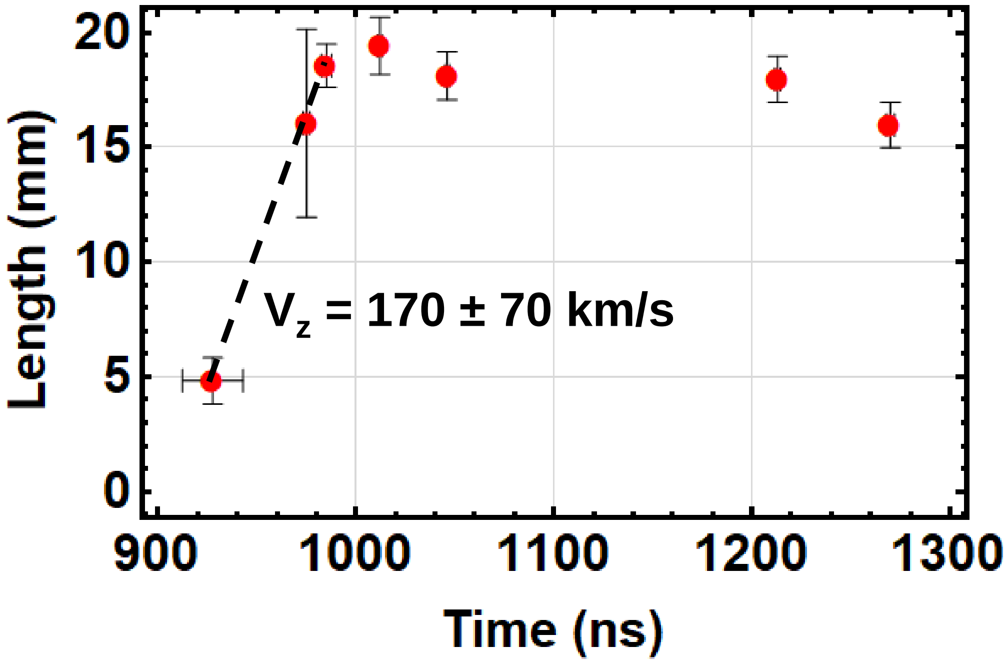

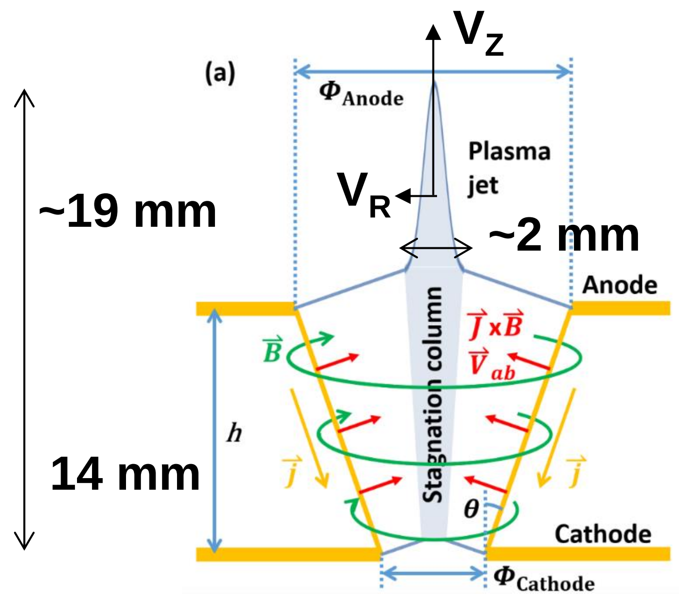

$$M = \frac{V_Z}{V_R} \geq \frac{Z}{r} \approx \frac{(19-14)\ \mathrm{mm}}{\frac{2\ \mathrm{mm}}{2}} = 5$$

$$V_{\mathrm{ab}} = V_{\mathrm{j}} \frac{\sin\theta}{1+\cos\theta} = 50\ \pm 20\ \mathrm{km/s}$$

P.-Y. Chang, etc, Rev. Sci. Instrum., 93, 043505 (2022)

Can a rotating plasma disk be formed?
To be continue…

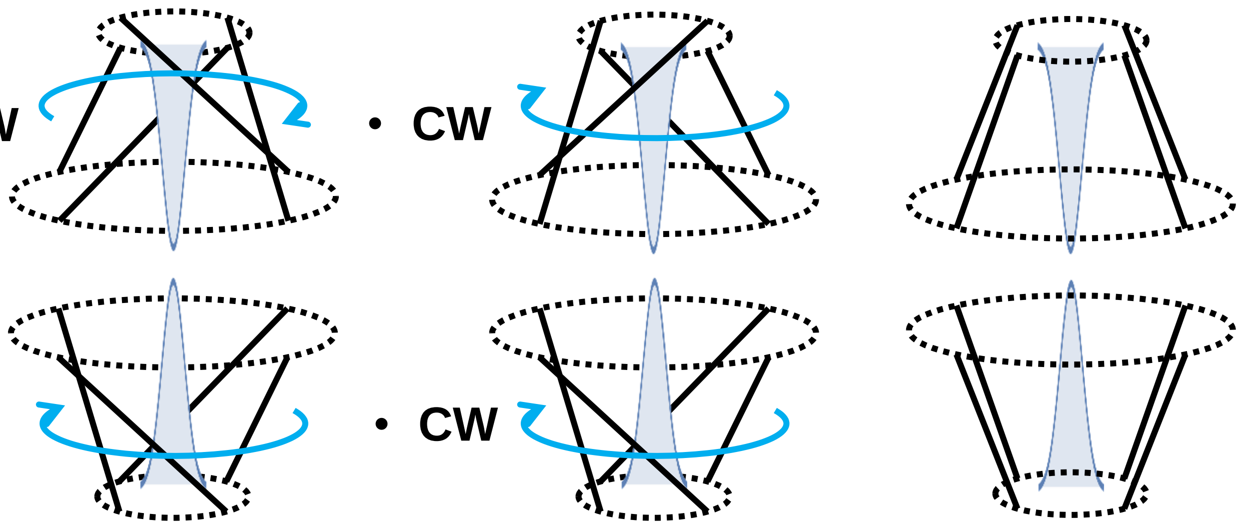

- CCW
- CW
- CW
- CW
- No rotation

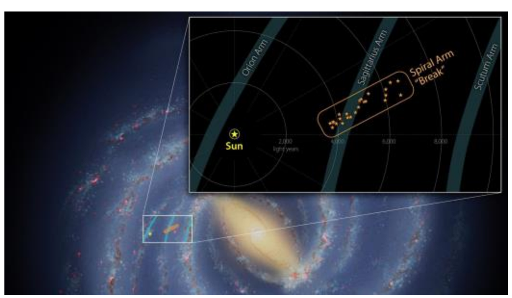

- **Astronomers Find a 'Break' in One of the Milky Way's Spiral Arms.**

https://www.nasa.gov/feature/jpl/astronomers-find-a-break-in-one-of-the-milky-way-s-spiral-arms

Plasma disk can be formed when two head-on plasma jets collide with each other

- **Astronomers Find a 'Break' in One of the Milky Way's Spiral Arms.**

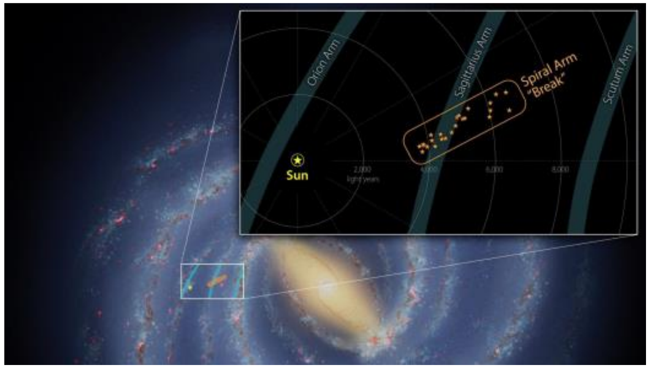

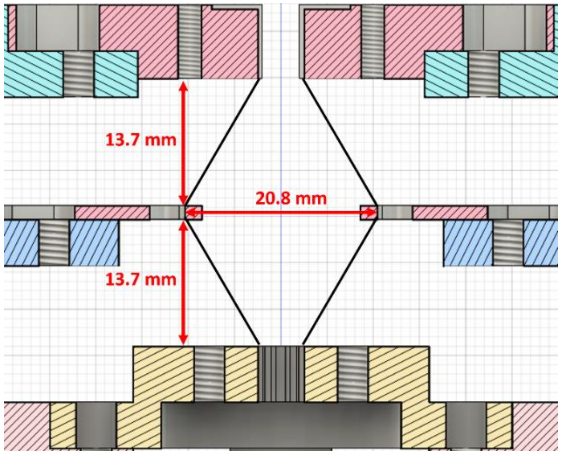

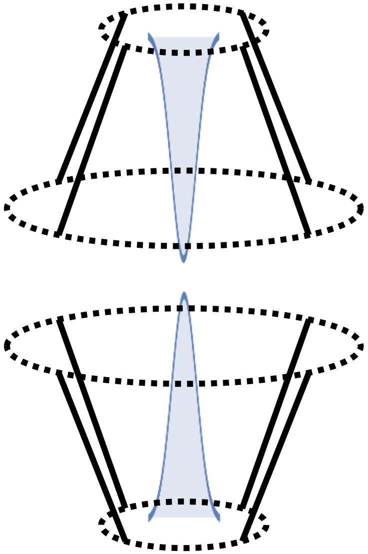

Jet Propulsion Laboratory [NASA/JPL] Astronomers Find a 'Break' in One of the Milky Way's Spiral Arms (Aug 17, 2021)

A plasma disk with a height of ~0.68 mm and a width of ~7.51 mm was generated ~0.15 mm above the middle plane

- **Schlieren image:**

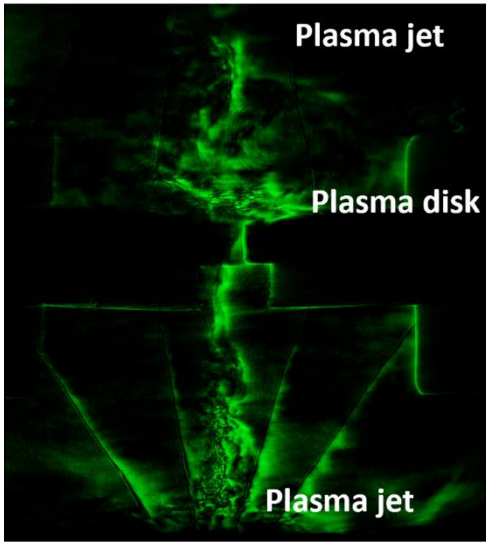

- **Time-integrated image:**

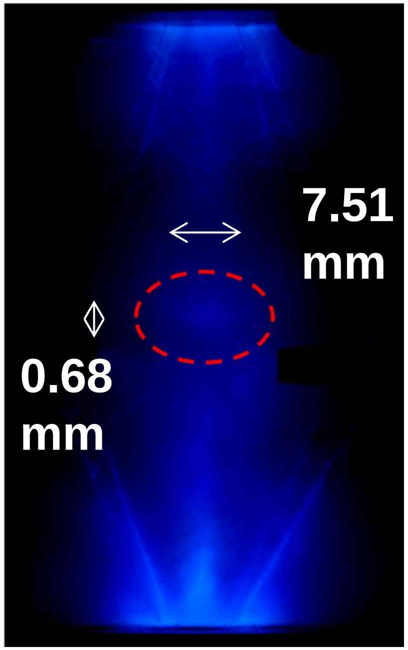

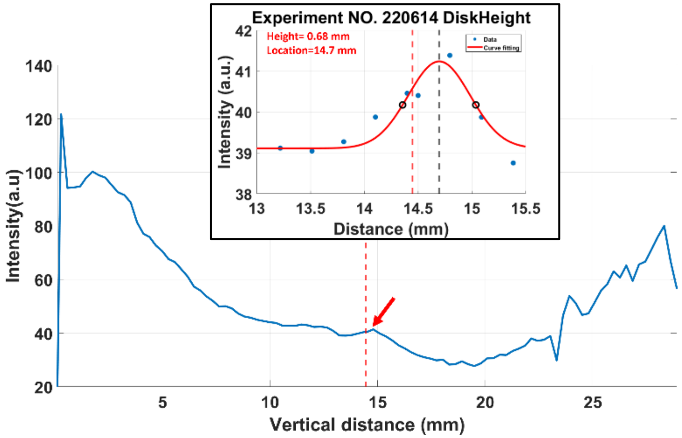

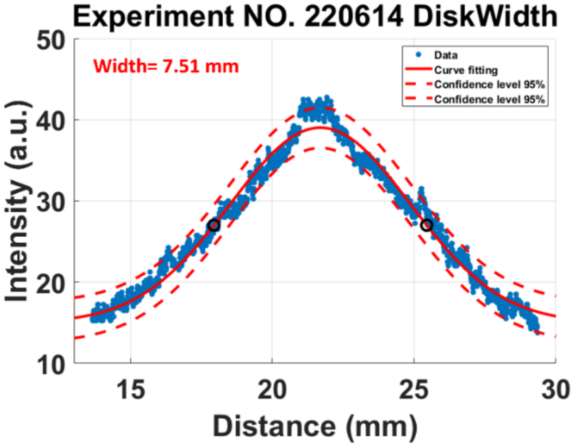

M.-S. Kuo, NCKU Master Thesis 2022

Plasma disk can be formed when two head-on plasma jets collide with each other

Schlieren

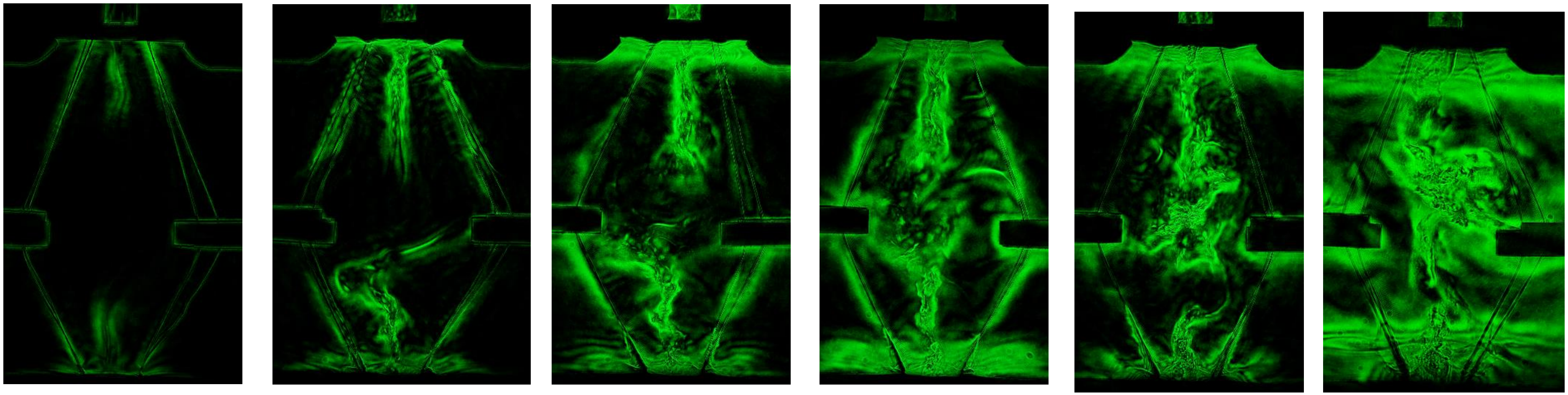

Interferometer

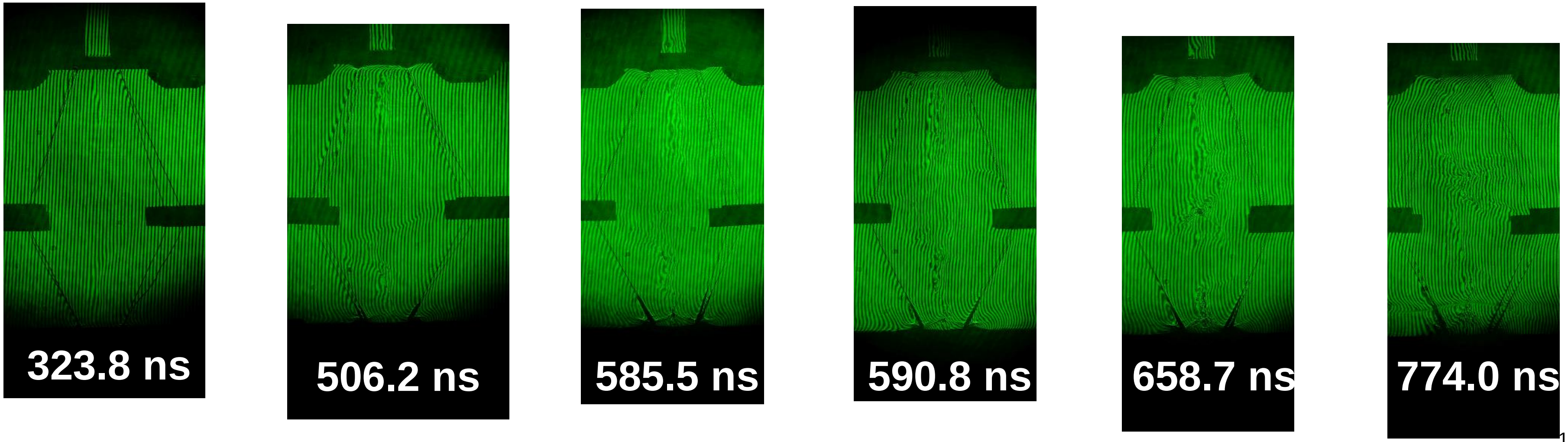

The plasma disk with a number density of ~ 10^{18} cm^{-3} was generated

Schlieren

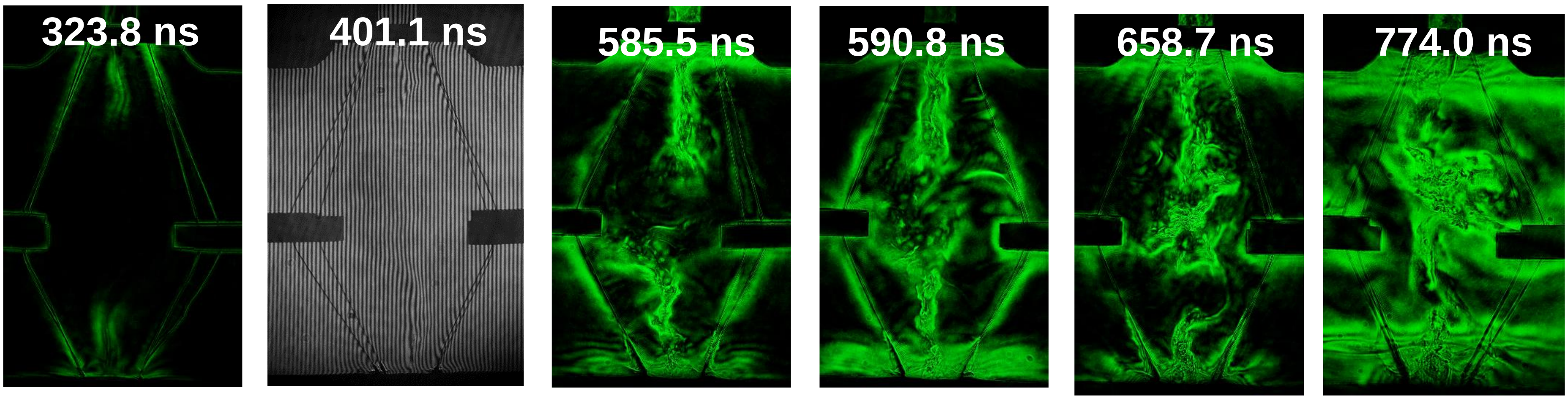

Interferometer

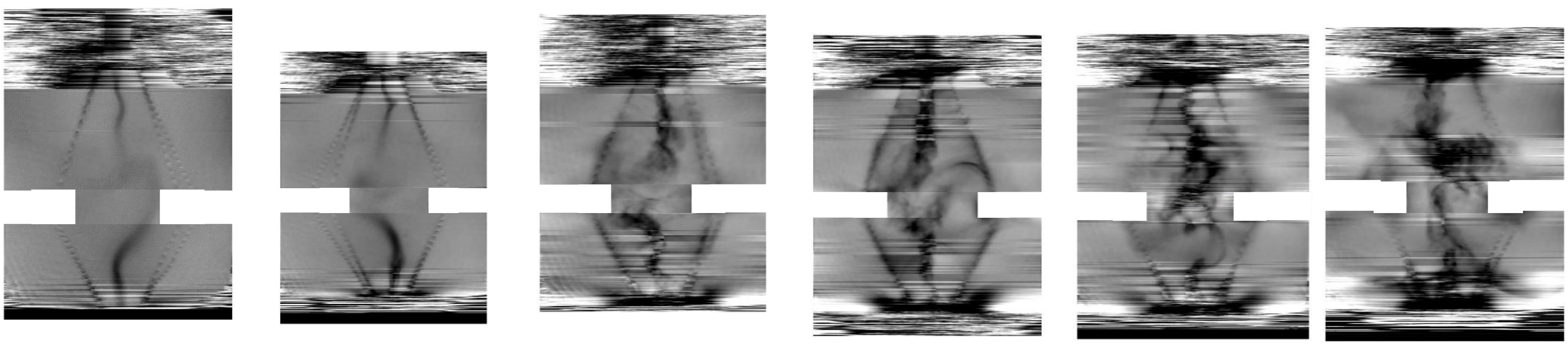

$-2\pi \sim 2\pi \Rightarrow 0 \sim 4.2 \times 10^{17}$ cm^{-2}

$\Rightarrow 8.4 \times 10^{17}$ cm^{-3} for L= 5mm

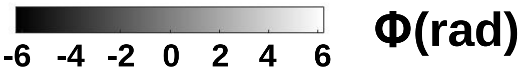

What if we twist the conical-wire array?

- **Non-rotation**

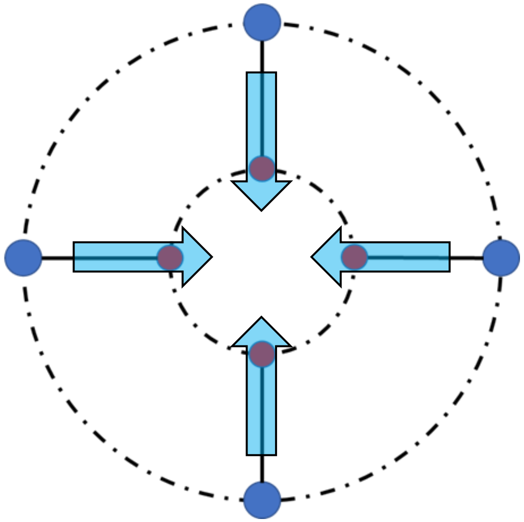

- **Clockwise 45°**

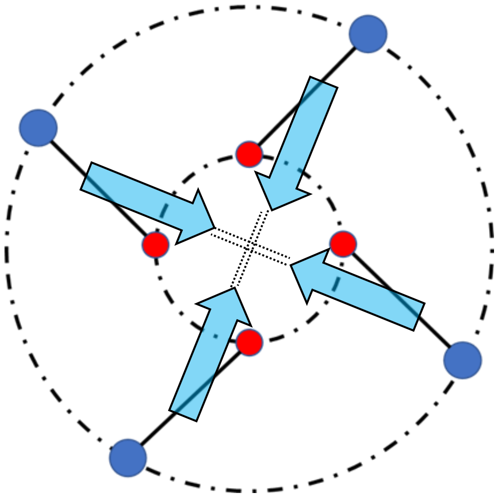

- **CCW 45°**

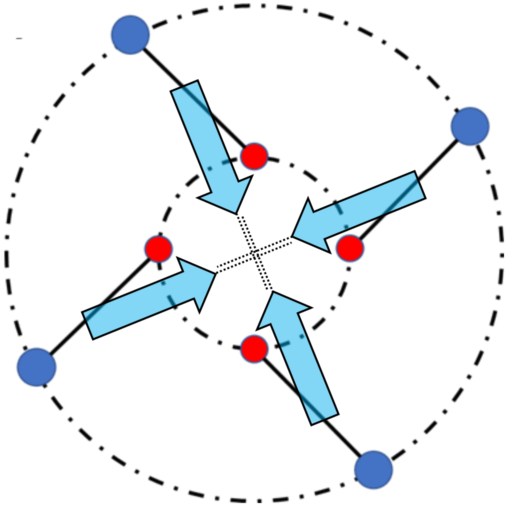

Y.-C. Lin, NCKU Master Thesis 2021

The plasma jet is a bright spot from the top view

- **Non-rotation**

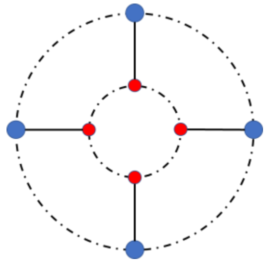

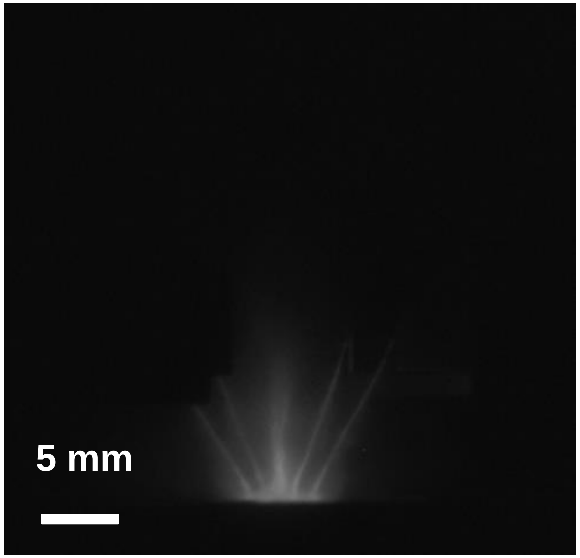

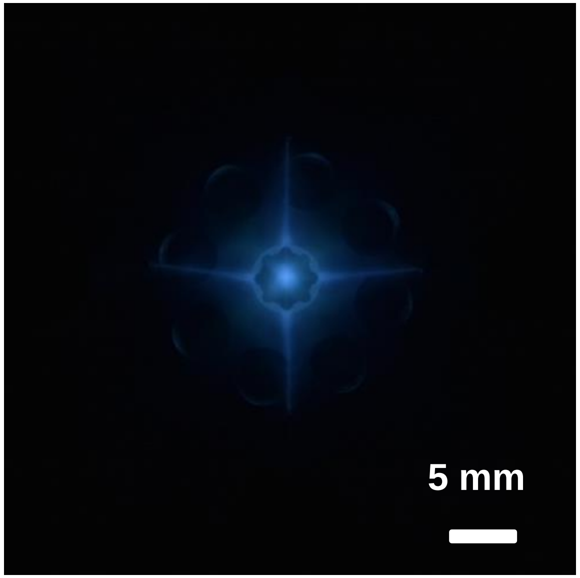

Y.-C. Lin, NCKU Master Thesis 2021

Hollow plasma jets were generated when the conical-wire arrays were twisted

- **Clockwise 30 °**

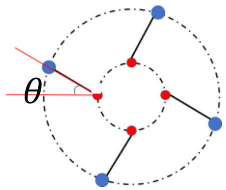

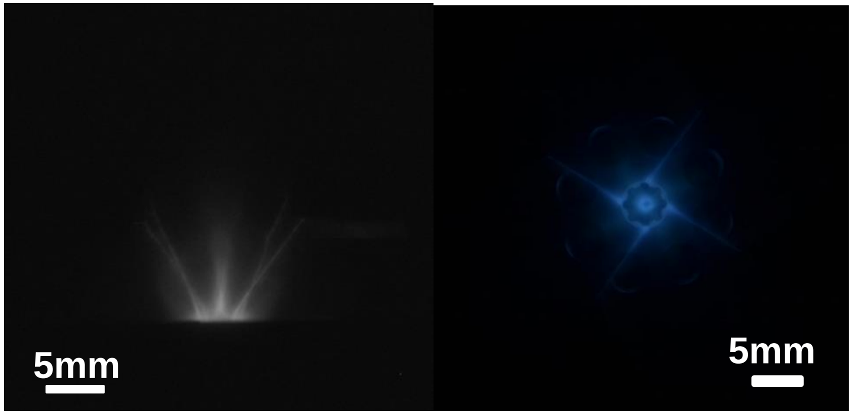

- **Counter clockwise 30 °**

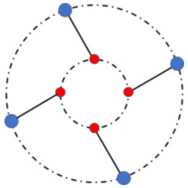

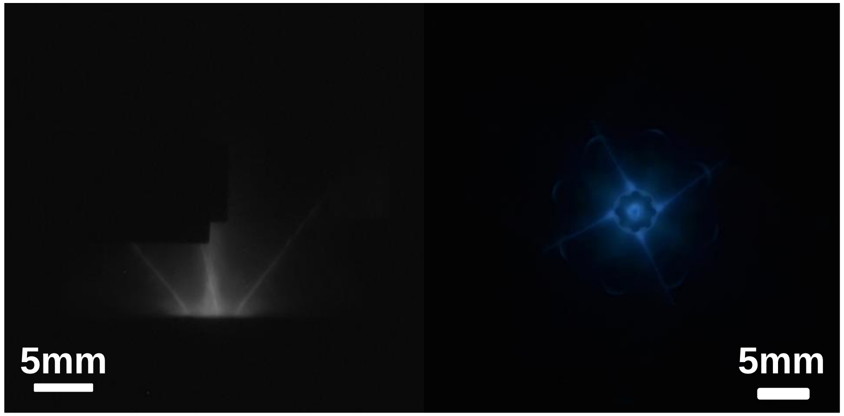

Y.-C. Lin, NCKU Master Thesis 2021

The hollow region at the center was due to angular momentum conservation of the in-coming plasma flow

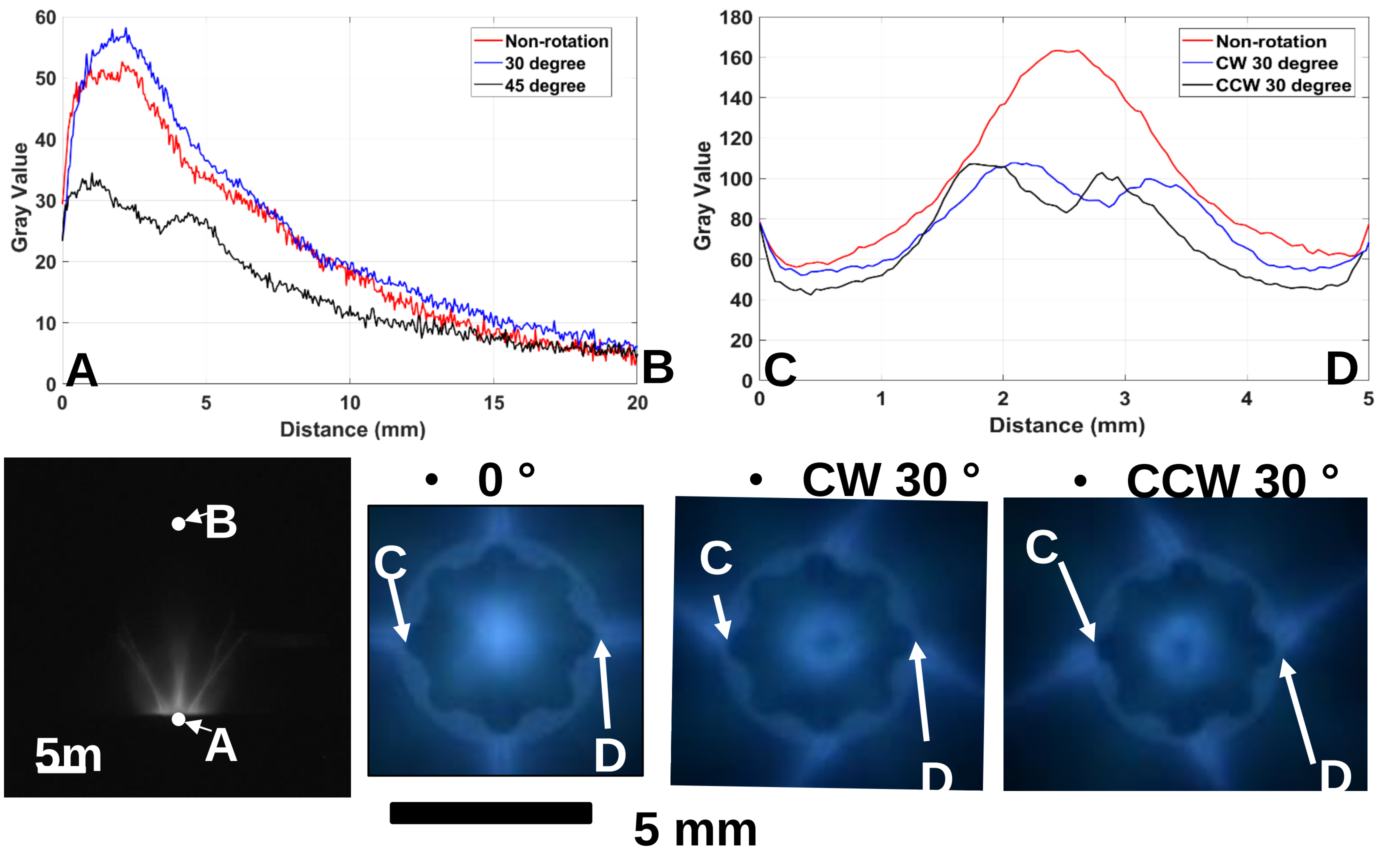

D. J. Ampleforda, et al., PRL 100, 035001 (2008)
Y.-C. Lin, NCKU Master Thesis 2021

A “tornado” is generated by the twisted conical-wire array

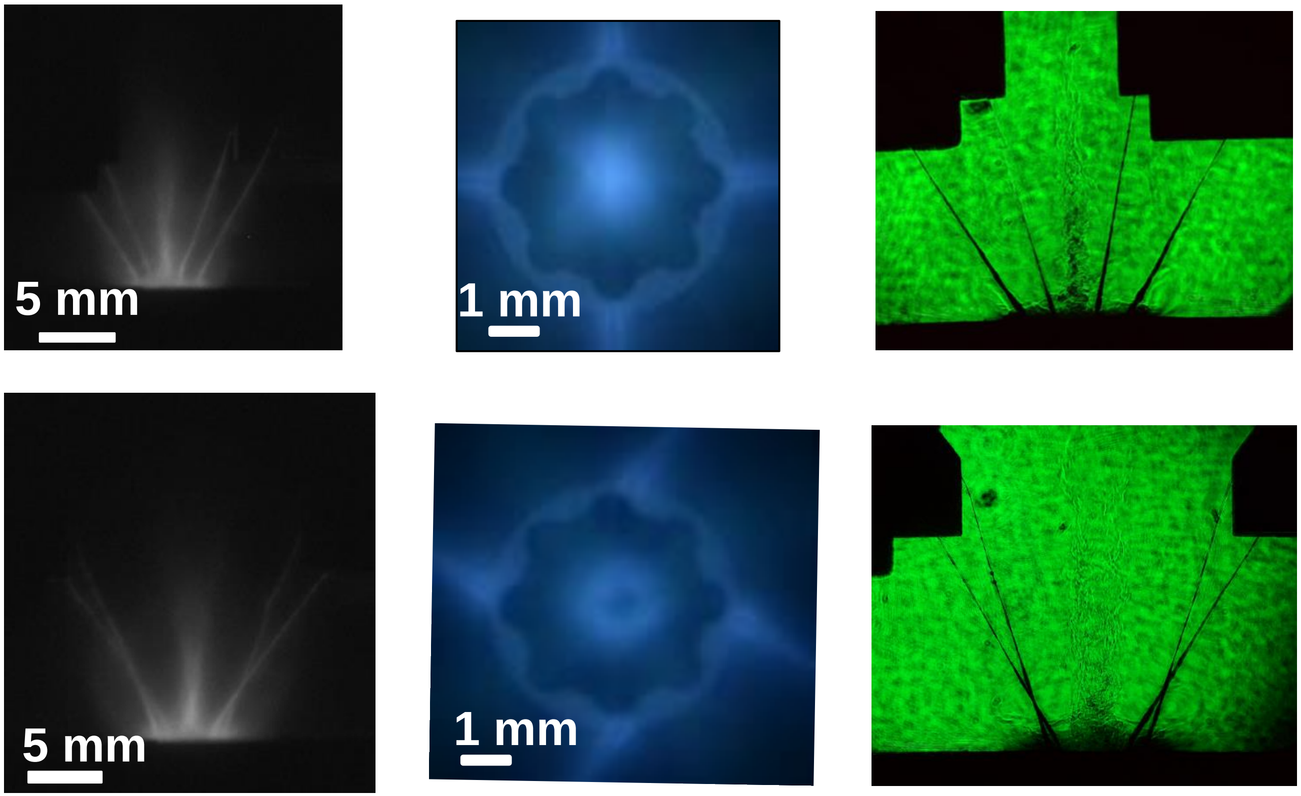

A “tornado” is generated by the twisted conical-wire array

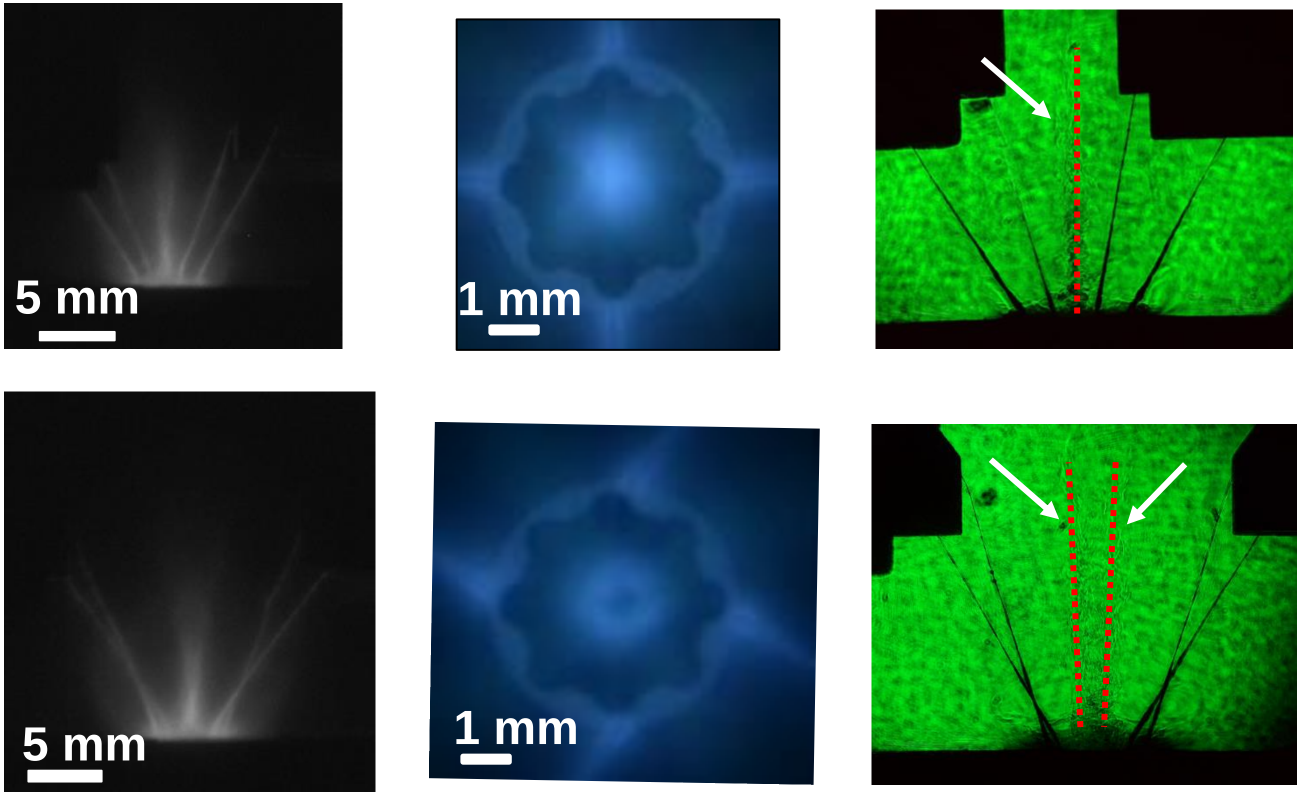

High energy density plasma (HEDP) is the regime where the pressure is greater than 0.1 T Pa (1 Mbar)

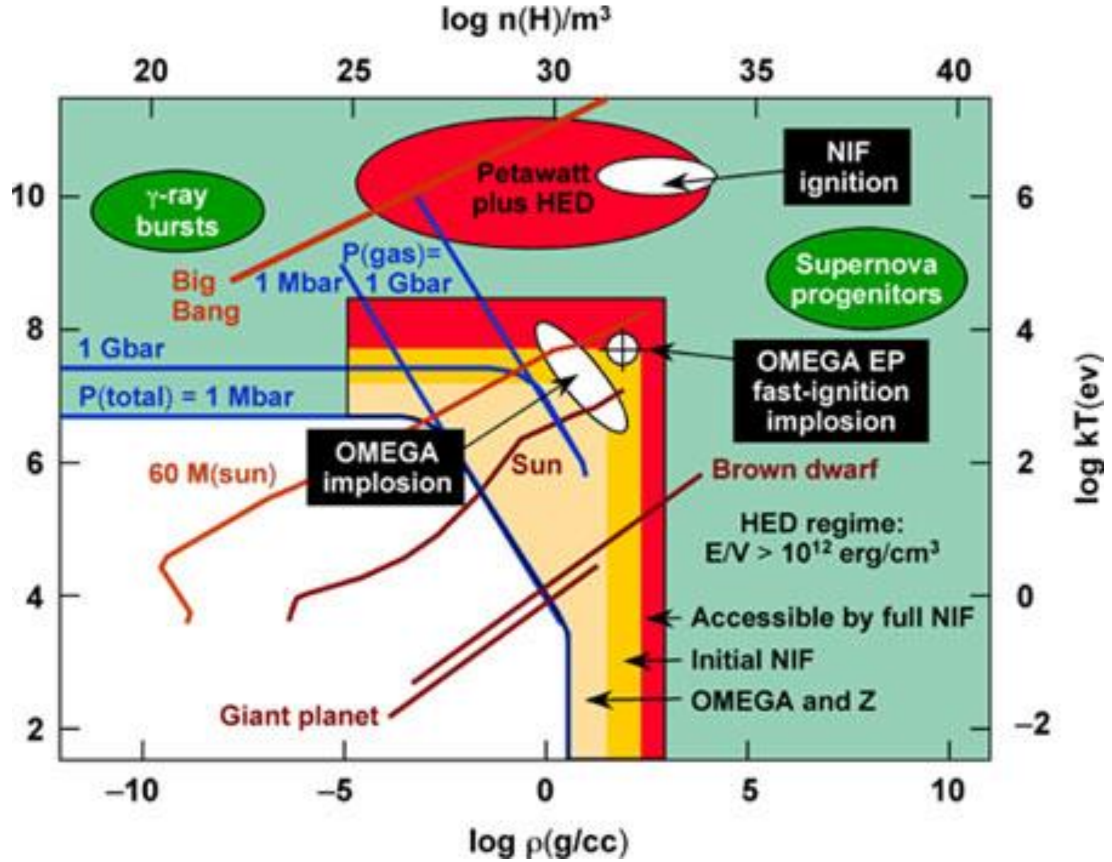

- **The energy density of HEDP regime is higher than 1 kJ of energy per 10 mm^3.**

Frontiers in High Energy Density Physics: The X-Games of Contemporary Science © (2003) by the National Academy of Sciences, courtesy of the National Academies Press, Washington, D.C.

Softer material can be compressed to higher density

- **Compression of a baseball**

- **Compression of a tennis ball**

https://www.youtube.com/watch?v=uxlIdMoAwbY
https://newsghana.com.gh/wimbledon-slow-motion-video-of-how-a-tennis-ball-turns-to-goo-after-serve/

A shock is formed due to the increasing sound speed of a compressed gas/plasma

- **Wave in the ocean:**

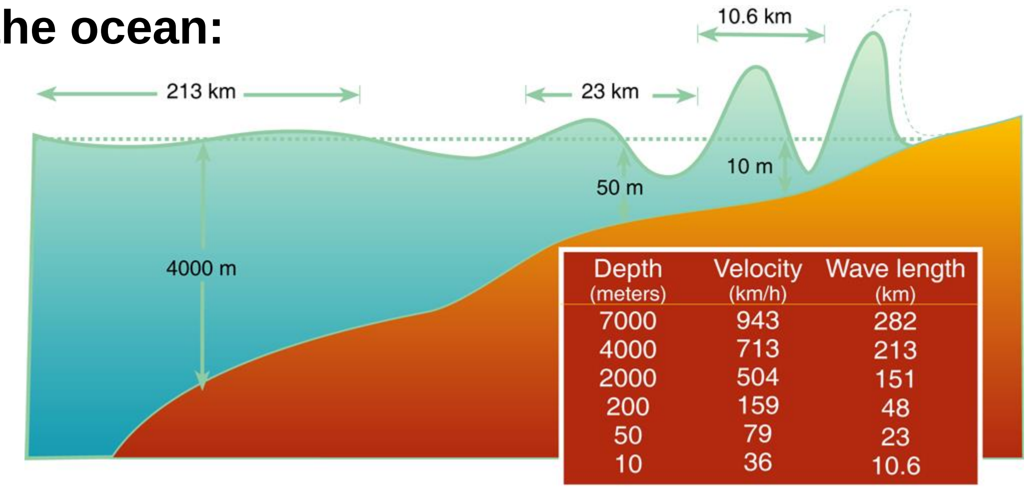

Depth (meters)	Velocity (km/h)	Wave length (km)
7000	943	282
4000	713	213
2000	504	151
200	159	48
50	79	23
10	36	10.6

- **Acoustic/compression wave driven by a piston:**

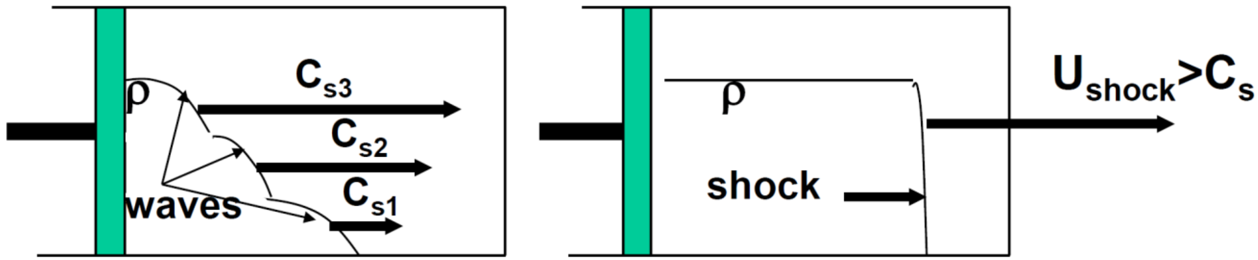

$$c_S \sim \sqrt{\gamma \frac{p}{\rho}} \sim \sqrt{\frac{\alpha\rho^{5/3}}{\rho}} \sim \sqrt{\alpha}\rho^{1/3}$$

http://neamtic.ioc-unesco.org/tsunami-info/the-cause-of-tsunamis
*R. Betti, HEDSA HEDP Summer School, 2015

A wave with small amplitude (perturbation) travels with the sound speed

$$\frac{\partial \rho}{\partial t} + \nabla \cdot (\rho \vec{u}) = 0$$

$$\rho \left(\frac{\partial \vec{u}}{\partial t} + \vec{u} \cdot \nabla \vec{u} \right) = -\nabla p + \rho \vec{f}$$

$$\frac{\partial}{\partial t} \left(\frac{\rho u^2}{2} + \rho \varepsilon \right) + \nabla \cdot \vec{u} \left[\left(\frac{\rho u^2}{2} + \rho \varepsilon \right) + p \right] = \rho \vec{f} \cdot \vec{u} - \nabla \cdot \vec{q}$$

$$\rho = \rho_o + \Delta\rho \qquad p = p_o + \Delta p \qquad \vec{u} = \vec{u}_o + \Delta \vec{u} \equiv (u_o + \Delta u)\hat{x} \equiv \Delta u \, \hat{x}$$

$$\frac{\partial \Delta\rho}{\partial t} = -\rho_o \frac{\partial \Delta u}{\partial x} \qquad \rho_o \frac{\partial \Delta u}{\partial t} = -\frac{\partial p}{\partial x} = -\left(\frac{\partial p}{\partial \rho} \right)_S \frac{\partial \Delta\rho}{\partial x} \equiv -{c_s}^2 \frac{\partial \Delta\rho}{\partial x}$$

$$\frac{\partial^2 \Delta\rho}{\partial t^2} = {c_s}^2 \frac{\partial^2 \Delta\rho}{\partial x^2}$$

$$\Delta\rho = \Delta\rho(x \pm c_S t)$$

$$\Delta p = \Delta p(x \pm c_S t)$$

$$\Delta u = \Delta u(x \pm c_S t)$$

$$c_S \sim \sqrt{\gamma \frac{p}{\rho}} \sim \sqrt{\frac{\alpha \rho^{5/3}}{\rho}} \sim \sqrt{\alpha} \rho^{1/3}$$

Y. B. Zel'dovich & Y. P. Raizer, Physics of shock waves and high-temperature hydrodynamic phenomena
Maria Alejandra Barrios Garcia, PhD Thesis, U of Rochester, 2010

A wave is distorted when the sound speed is not a constant

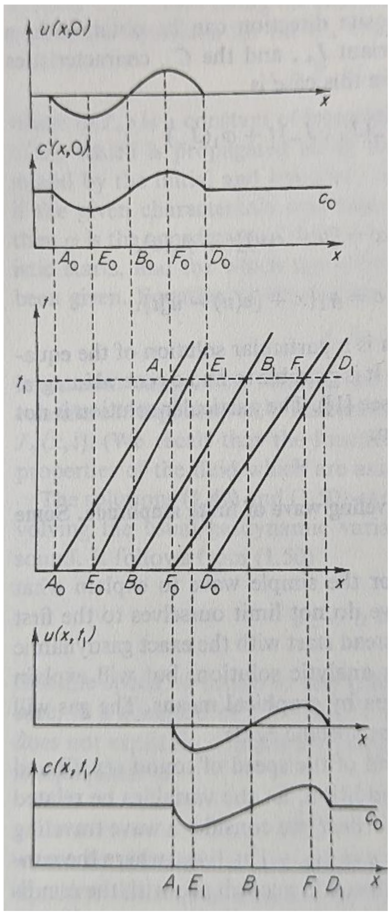

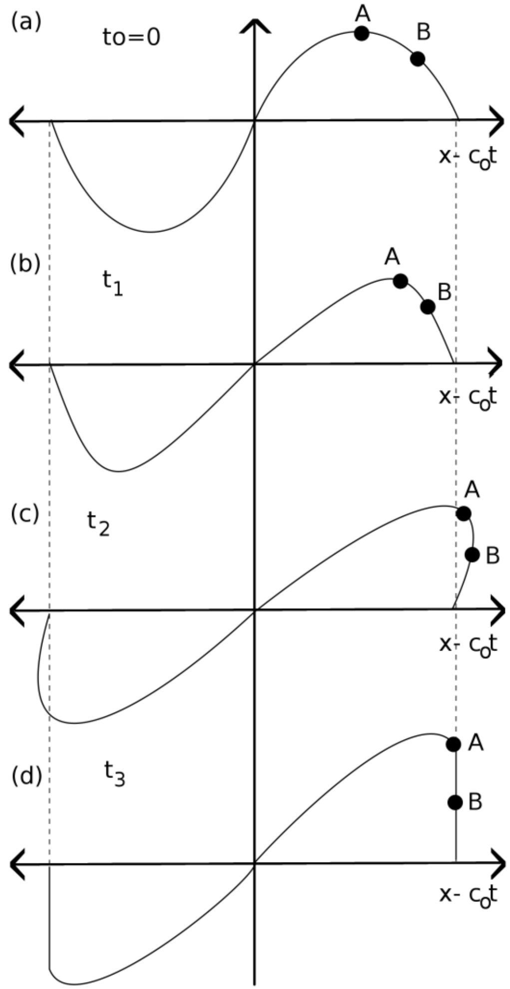

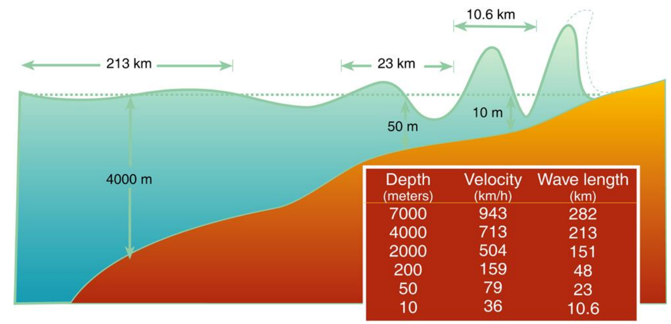

Depth (meters)	Velocity (km/h)	Wave length (km)
7000	943	282
4000	713	213
2000	504	151
200	159	48
50	79	23
10	36	10.6

- **A shock wave is formed when a discontinuity is formed.**

$$c_S \sim \sqrt{\alpha}\rho^{1/3}$$

Y. B. Zel'dovich & Y. P. Raizer, Physics of shock waves and high-temperature hydrodynamic phenomena
Maria Alejandra Barrios Garcia, PhD Thesis, U of Rochester, 2010
http://neamtic.ioc-unesco.org/tsunami-info/the-cause-of-tsunamis

A shock is formed when characteristics merge while a rarefaction wave is formed when characteristics spread out

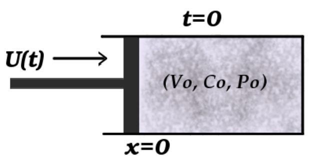

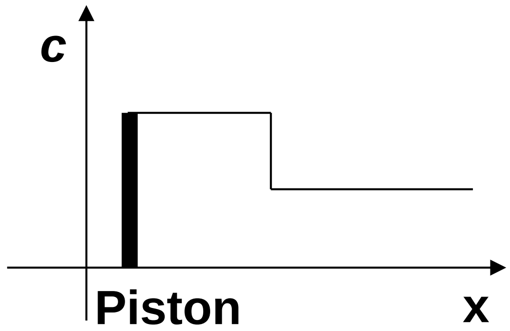

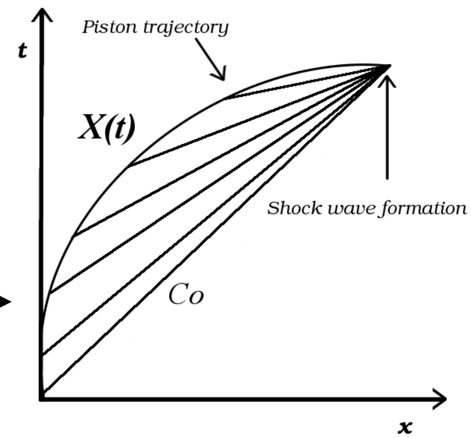

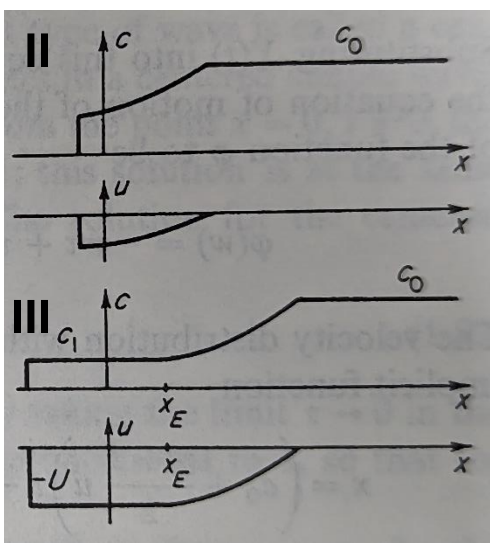

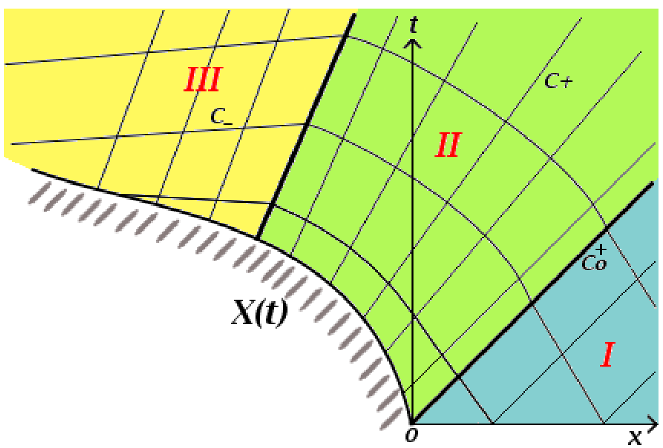

Y. B. Zel'dovich & Y. P. Raizer, Physics of shock waves and high-temperature hydrodynamic phenomena
Maria Alejandra Barrios Garcia, PhD Thesis, U of Rochester, 2010

A shock or a rarefaction wave may be formed depending on the driving force from the piston

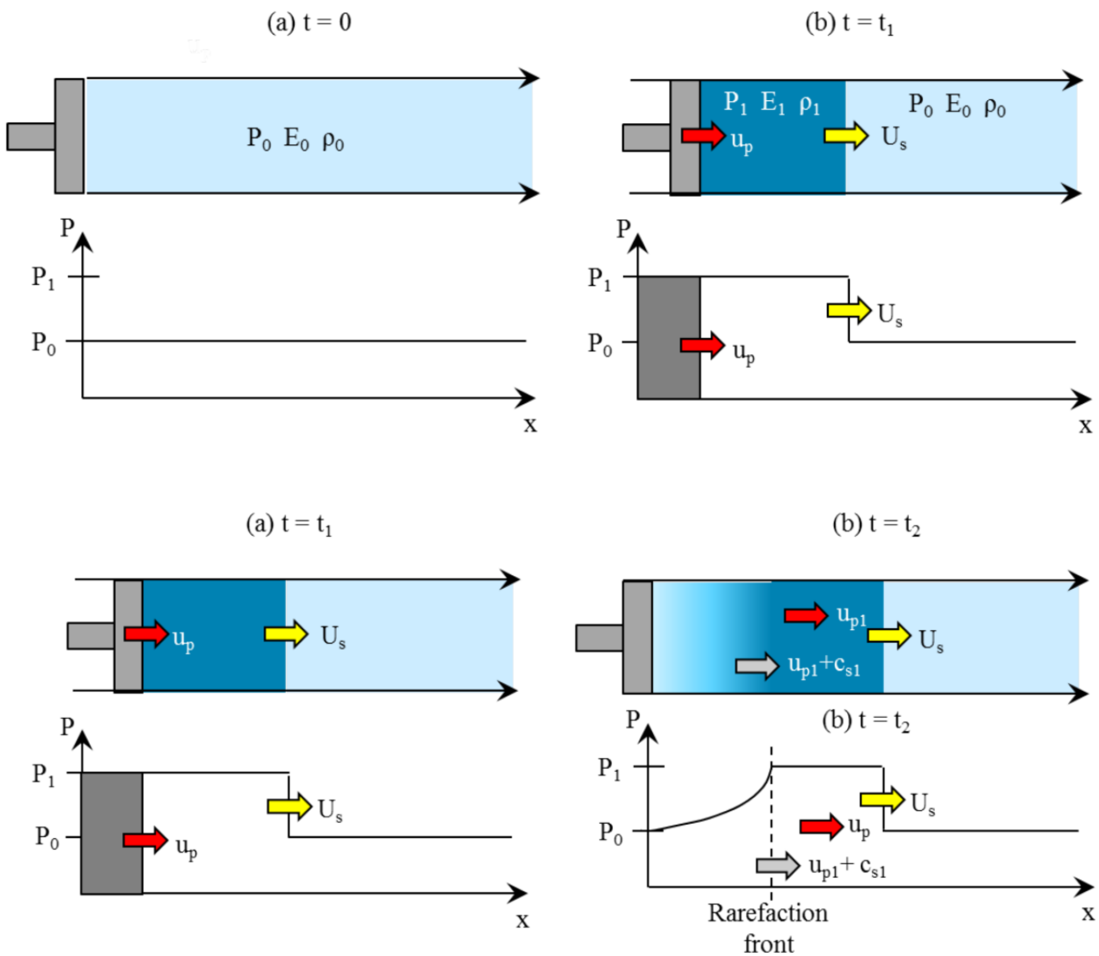

- **Show simulations.**

Michelle Colleen Gregor, PhD Thesis, U of Rochester, 2017

Mass, momentum, and energy is conserved across the shock front

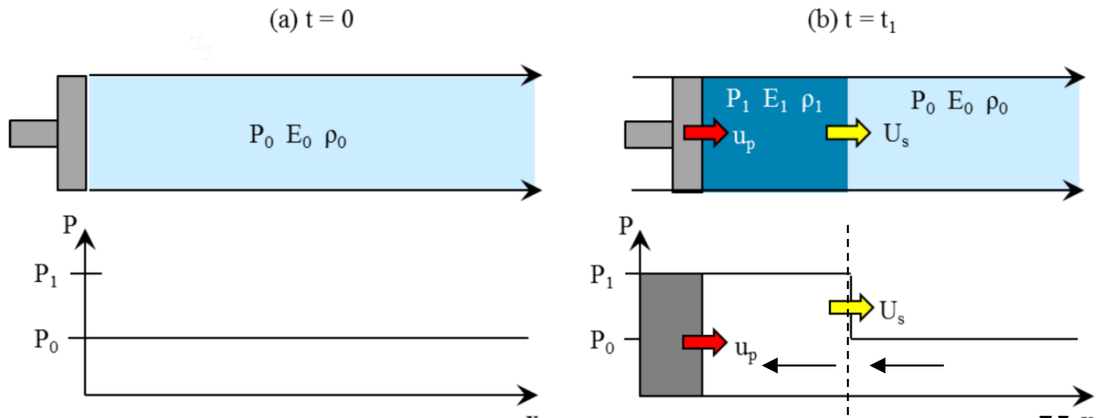

$$u_1 = U_S - U_P \qquad u_0 = -U_S$$

$$\frac{\partial \rho}{\partial t} + \nabla \cdot (\rho\, \vec{u}) = 0$$

$$\rho\left(\frac{\partial\, \vec{u}}{\partial t} + \vec{u} \cdot \nabla\, \vec{u}\right) = -\nabla p + \rho\, \vec{f}$$

$$\frac{\partial}{\partial t}\left(\frac{\rho u^2}{2} + \rho \varepsilon\right) + \nabla \cdot \vec{u}\left[\left(\frac{\rho u^2}{2} + \rho\varepsilon\right) + p\right] = \rho\, \vec{f} \cdot \vec{u} - \nabla \cdot \vec{q}$$

$$\rho_1 u_1 = \rho_0 u_0$$

$$p_1 + \rho_1 {u_1}^2 = p_0 + \rho_0 {u_0}^2$$

$$\epsilon_1 + \frac{p_1}{\rho_1} + \frac{{u_1}^2}{2} = \epsilon_0 + \frac{p_0}{\rho_0} + \frac{{u_0}^2}{2}$$

Michelle Colleen Gregor, PhD Thesis, U of Rochester, 2017

The Hugoniot equations relate the pre- and post-shock conditions via the particle velocity(U_p) and shock velocity (U_s)

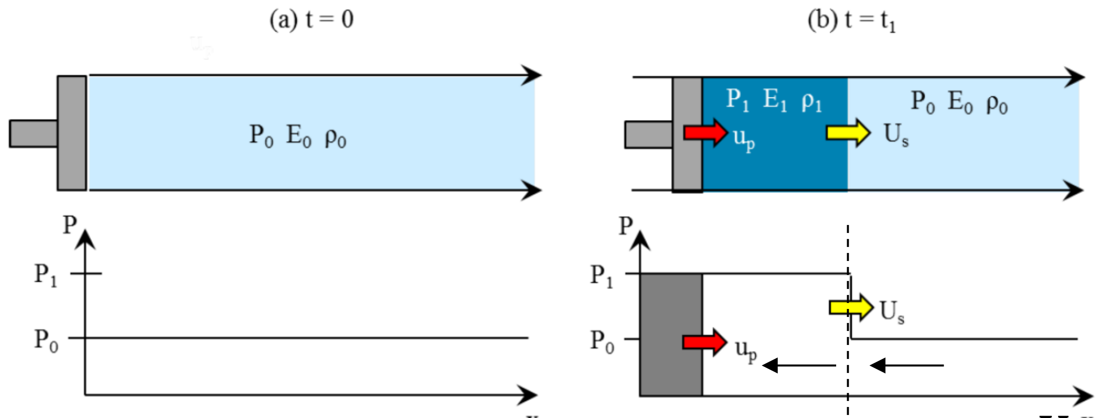

$u_1 = U_S - U_P$ $u_0 = -U_S$

$$\rho_1 u_1 = \rho_0 u_0$$

$$p_1 + \rho_1 {u_1}^2 = p_0 + \rho_0 {u_0}^2$$

$$\epsilon_1 + \frac{p_1}{\rho_1} + \frac{{u_1}^2}{2} = \epsilon_0 + \frac{p_0}{\rho_0} + \frac{{u_0}^2}{2}$$

$$\rho_0 U_S = \rho_1 (U_S - U_p)$$

$$p_1 - p_0 = \rho_o U_S U_p$$

$$u_0 \left[\frac{\rho_0 {u_0}^2}{2} + \rho_0 \epsilon_0 + p_0\right] = u_1 \left[\frac{\rho_1 {u_1}^2}{2} + \rho_1 \epsilon_1 + p_1\right]$$

$$p_0 u_0 - p_1 u_1 = \rho_1 u_1 \left(\epsilon_1 + \frac{{u_1}^2}{2}\right) - \rho_0 u_0 \left(\epsilon_0 + \frac{{u_0}^2}{2}\right) = \rho_0 u_0 \left[\left(\epsilon_1 + \frac{{u_1}^2}{2}\right) - \left(\epsilon_0 + \frac{{u_0}^2}{2}\right)\right]$$

Michelle Colleen Gregor, PhD Thesis, U of Rochester, 2017

The Hugoniot equations relate the pre- and post-shock conditions via the particle velocity(U_p) and shock velocity (U_s) – cont.

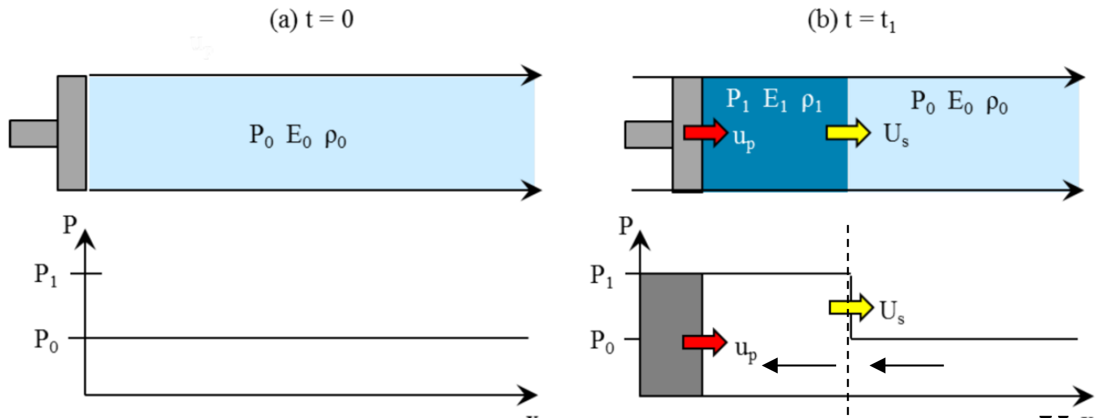

$$u_1 = U_S - U_P \qquad u_0 = -U_S$$

$$\rho_0 U_S = \rho_1 (U_S - U_p)$$

$$p_1 - p_0 = \rho_o U_S U_p$$

$$u_0\left[\frac{\rho_0 u_0^2}{2} + \rho_0\epsilon_0 + p_0\right] = u_1\left[\frac{\rho_1 u_1^2}{2} + \rho_1\epsilon_1 + p_1\right]$$

$$p_0 u_0 - p_1 u_1 = \rho_1 u_1\left(\epsilon_1 + \frac{u_1^2}{2}\right) - \rho_0 u_0\left(\epsilon_0 + \frac{u_0^2}{2}\right) = \rho_0 u_0\left[\left(\epsilon_1 + \frac{u_1^2}{2}\right) - \left(\epsilon_0 + \frac{u_0^2}{2}\right)\right]$$

Let $V_{1,2} \equiv \dfrac{1}{\rho_{1,2}}$

$$u_0^2 = V_0^2 \frac{p_1 - p_0}{V_0 - V_1} \qquad u_1^2 = V_1^2 \frac{p_1 - p_0}{V_0 - V_1}$$

$$\epsilon_1 - \epsilon_0 = \frac{1}{2}(p_0 + p_1)(V_0 - V_1)$$

Michelle Colleen Gregor, PhD Thesis, U of Rochester, 2017

The density is only compressed by a limited amount even in a strong shock

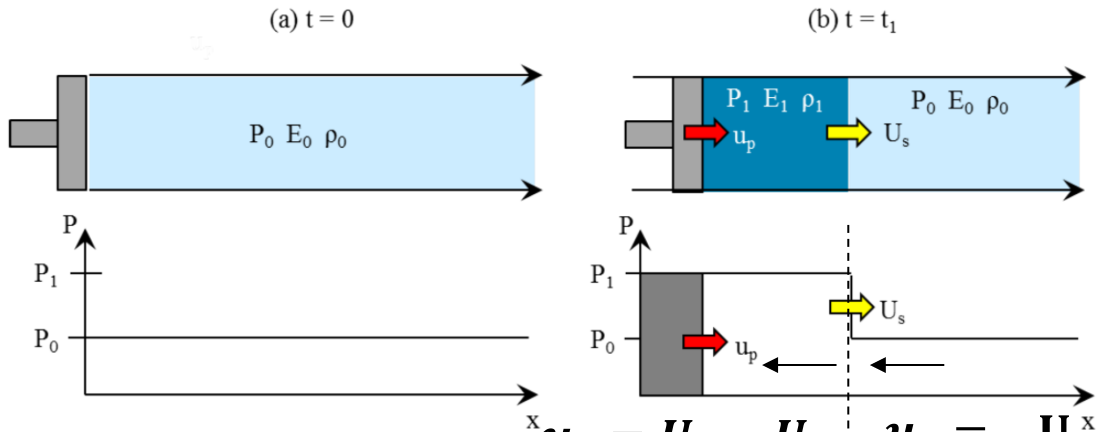

$u_1 = U_S - U_P$ $\quad u_0 = -U_S$

$$V_{0,1} \equiv \frac{1}{\rho_{0,1}} \quad u_0{}^2 = V_0{}^2 \frac{p_1 - p_0}{V_0 - V_1} \quad u_1{}^2 = V_1{}^2 \frac{p_1 - p_0}{V_0 - V_1} \quad \epsilon_1 - \epsilon_0 = \frac{1}{2}(p_0 + p_1)(V_0 - V_1)$$

$$\frac{\rho_1}{\rho_0} = \frac{V_0}{V_1} = \frac{p_1(\gamma+1) + p_0(\gamma-1)}{p_1(\gamma-1) + p_0(\gamma+1)} \sim \frac{\gamma+1}{\gamma-1}\left(\text{for } \frac{p_1}{p_0} \gg 1\right) \sim 4\left(\text{for } \gamma = \frac{5}{3}\right)$$

$$u_0{}^2 = \frac{V_0}{2}[(\gamma-1)p_0 + (\gamma+1)p_1] = \frac{p_0}{\rho_0}\frac{(\gamma+1)\,p_1/p_0 + (\gamma-1)}{2}$$

$$u_1{}^2 = \frac{V_0}{2}\frac{[(\gamma+1)p_0 + (\gamma-1)p_1]^2}{(\gamma-1)p_0 + (\gamma+1)p_1}$$

Michelle Colleen Gregor, PhD Thesis, U of Rochester, 2017

The Hugoniot curve is a curve on the *p*, *V* diagram passing through the initial state p_0, V_0

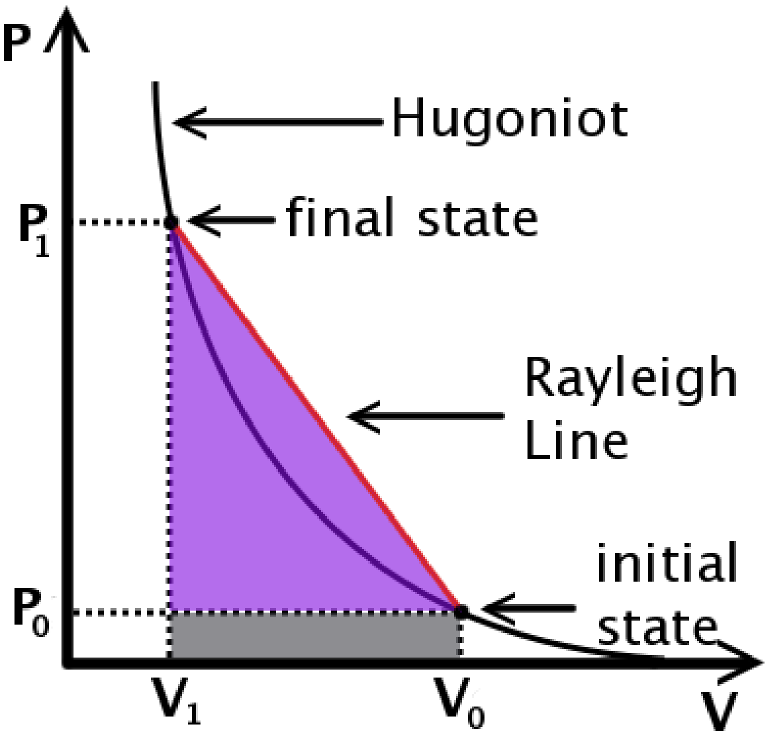

$$\frac{V_0}{V_1} = \frac{p_1(\gamma+1) + p_0(\gamma-1)}{p_1(\gamma-1) + p_0(\gamma+1)}$$

$$V_{0,1} \equiv \frac{1}{\rho_{0,1}}$$

Maria Alejandra Barrios Garcia, PhD Thesis, U of Rochester, 2010

Pressure can be referred by measuring the shock speed with a sample with known Hugoniot curve

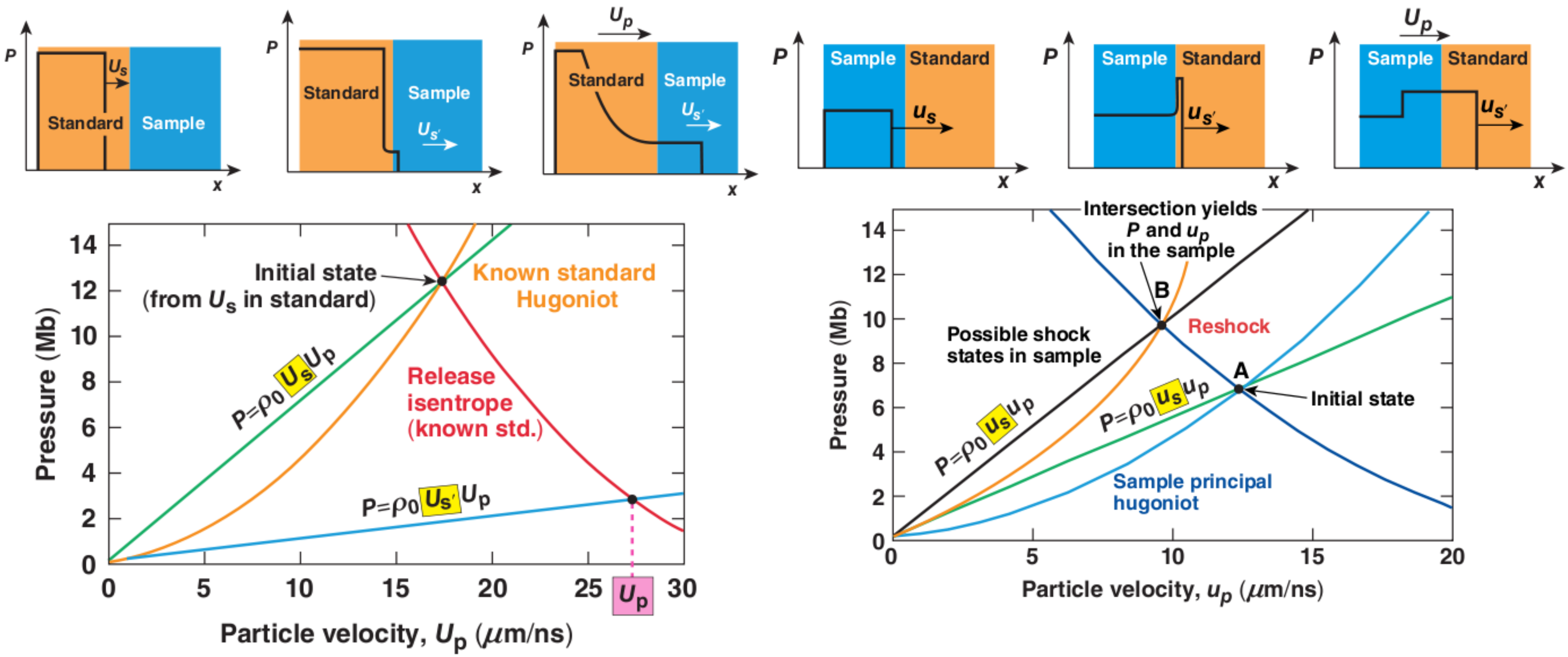

$$p_1 - p_0 = \rho_o U_S U_p$$

Isentrope: adiabatic flow with no change in entropy

Maria Alejandra Barrios Garcia, PhD Thesis, U of Rochester, 2010

Shock velocities are measured using time-resolved Velocity Interferometer System for Any Reflector (VISAR)

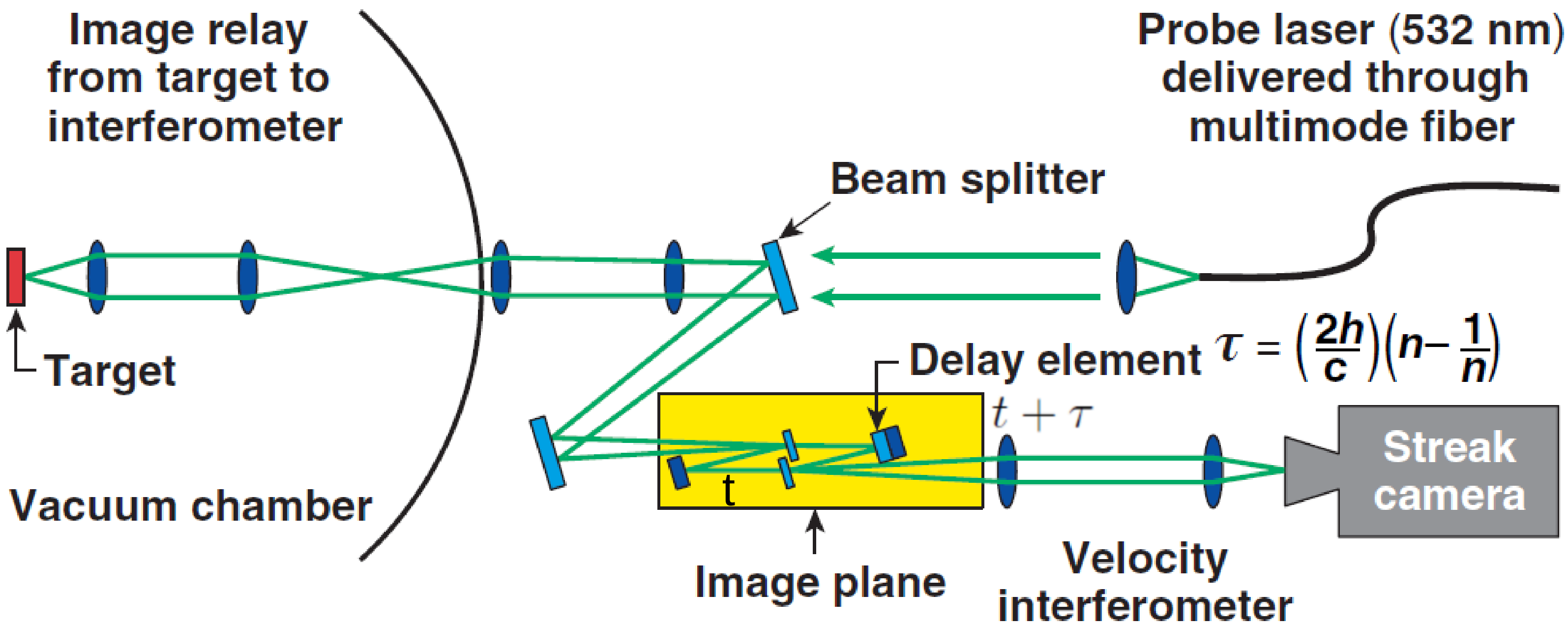

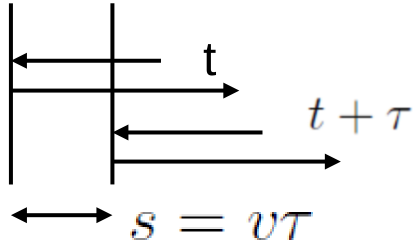

$$\Delta\phi = \frac{v\tau}{\lambda} \propto v$$

Shock velocities are measured using time-resolved Velocity Interferometer System for Any Reflector (VISAR)

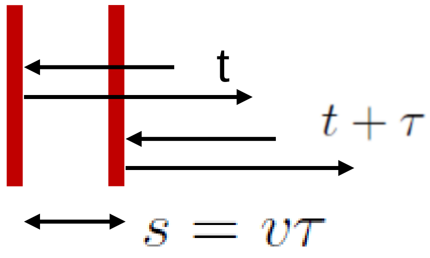

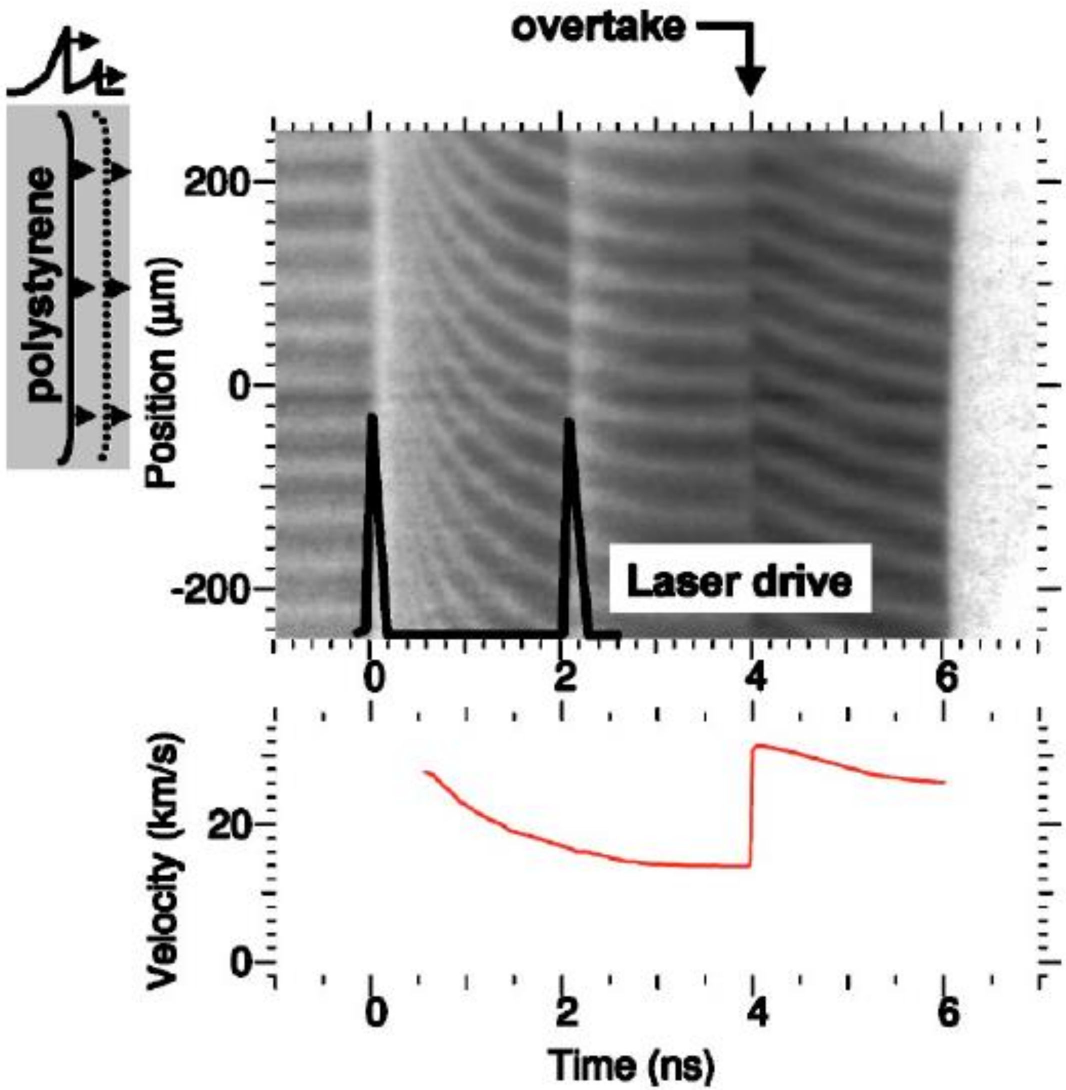

P. M. Celliers *et al.*, Rev. Sci. Insytum. **75**, 4916 (2004)

A piston can be driven by a gas gun

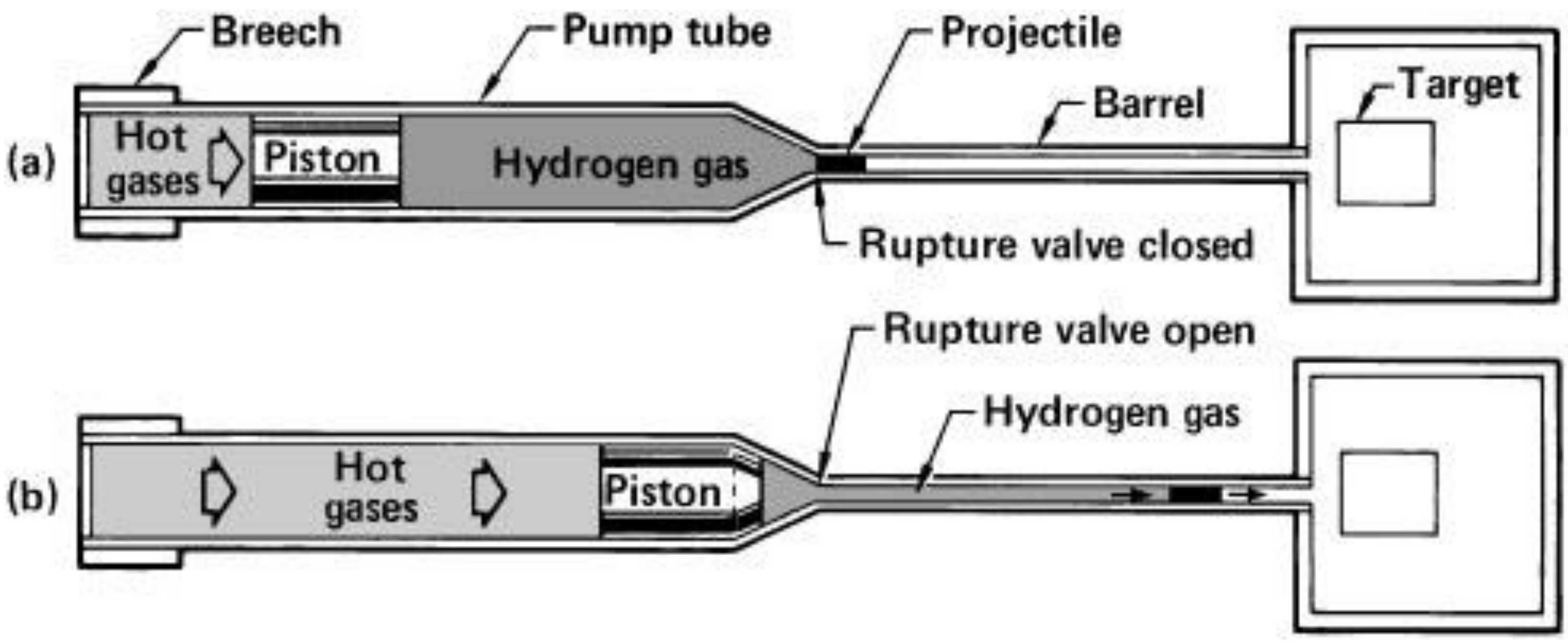

J. Freim, etc., J. Materials Research 11, 112 (1996)

Rochester is known as “The World's Image Center”

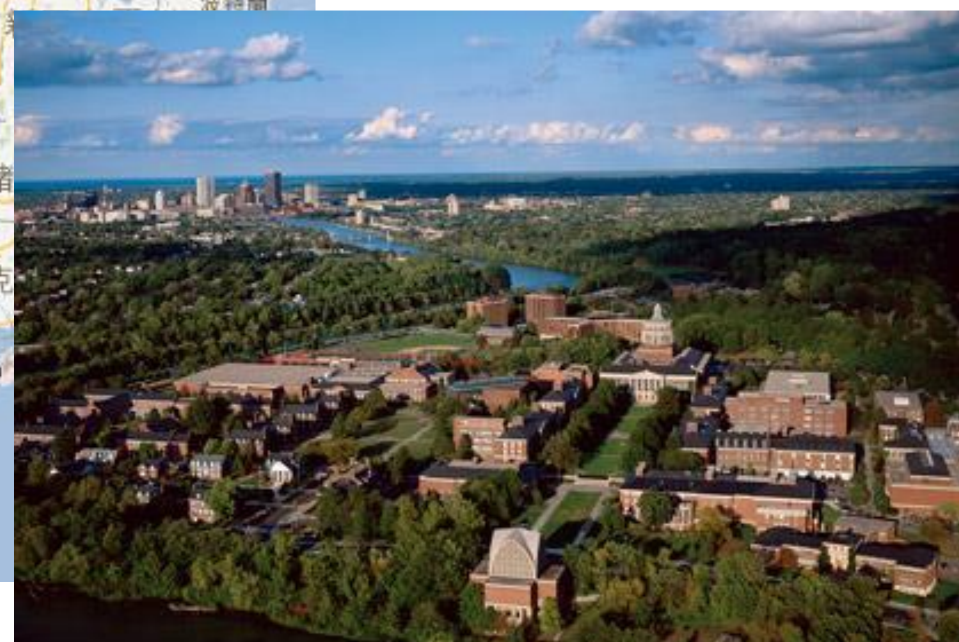

There are many famous optical companies at Rochester

Kodak

xerox ®

Eastman school of music

BAUSCH + LOMB

Laboratory for Laser Energetics, University of Rochester is a pioneer in laser fusion

- **OMEGA Laser System**
  - **60 beams**
  - **>30 kJ UV on target**
  - **1%~2% irradiation nonuniformity**
  - **Flexible pulse shaping**
- **OMEGA EP Laser System**
  - **4 beams; 6.5 kJ UV (10ns)**
  - **Two beams can be high-energy petawatt**
    - **2.6 kJ IR in 10 ps**
    - **Can propagate to the OMEGA or OMEGA EP target chamber**

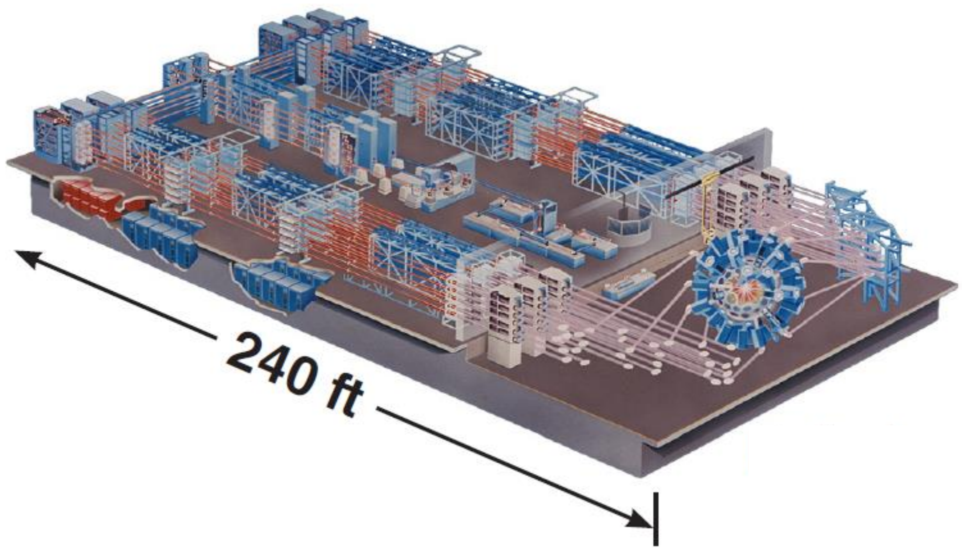

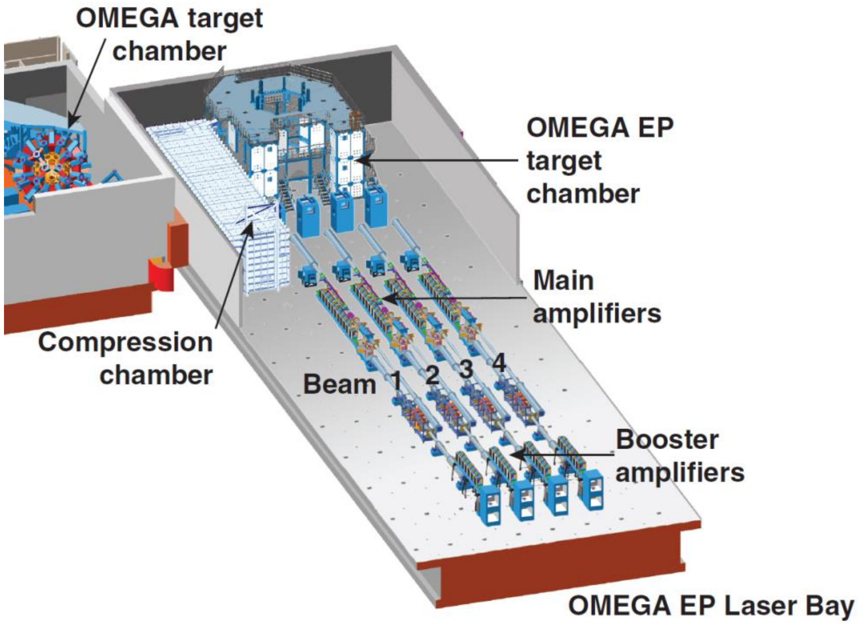

The OMEGA Facility is carrying out ICF experiments using a full suite of target diagnostics

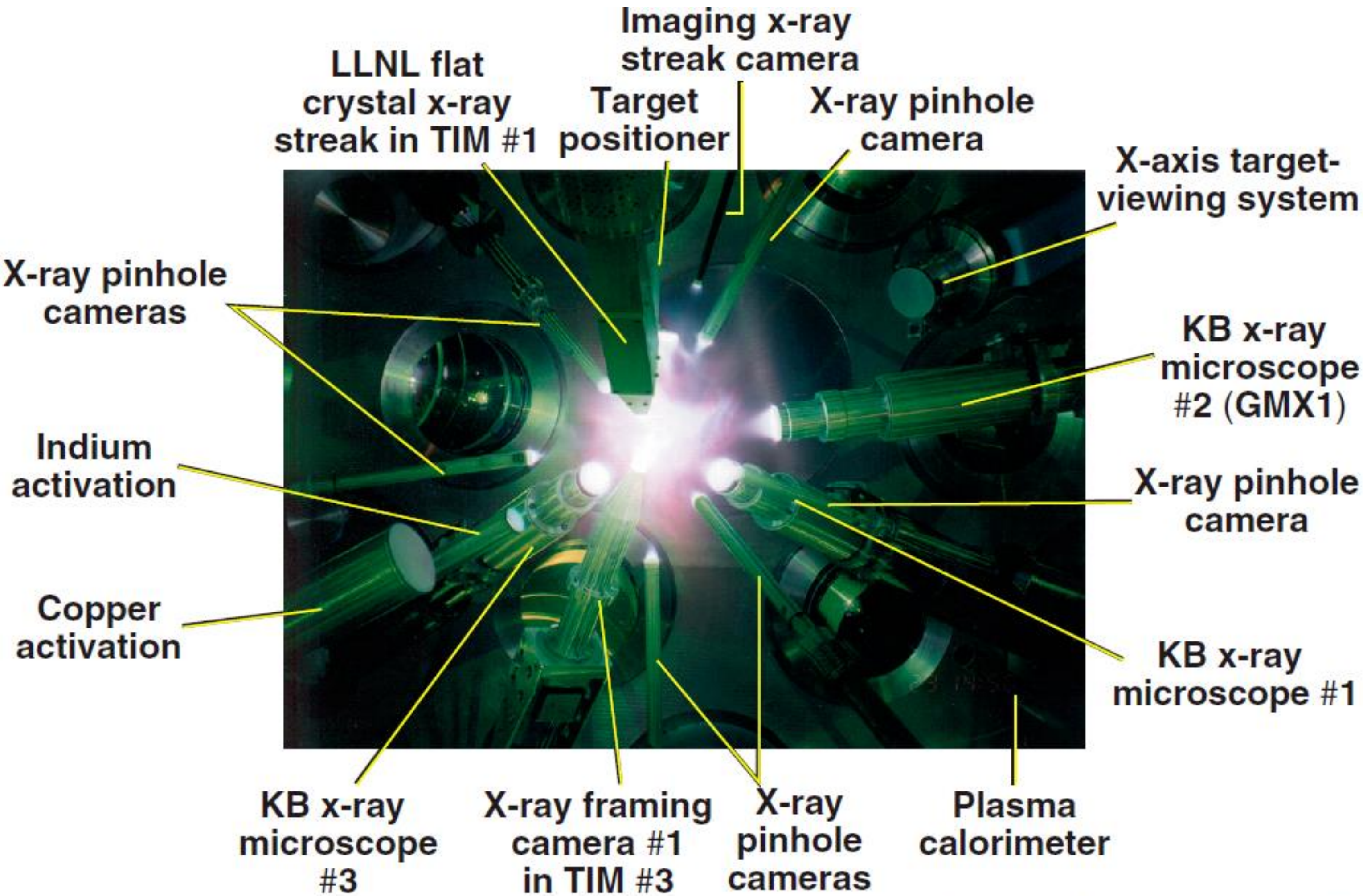

E8012b

Photo taken from port H11B

The 1.8-MJ National Ignition Facility (NIF) will demonstrate ICF ignition and modest energy gain

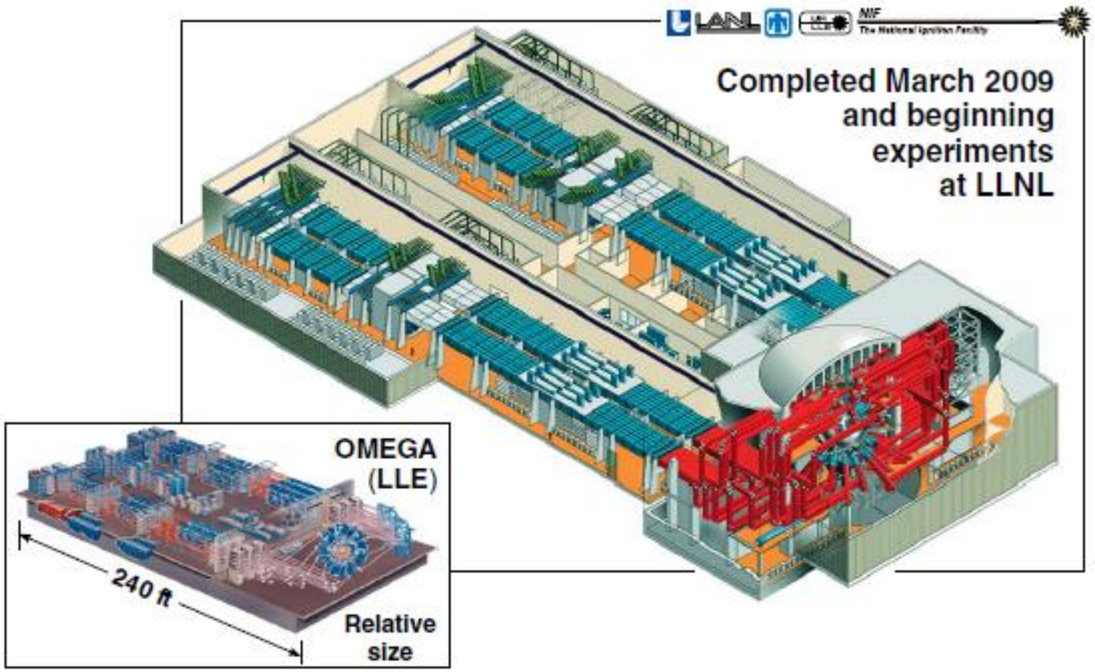

OMEGA experiments are integral to an ignition demonstration on the NIF.

A strong shock can be generated using a high power laser

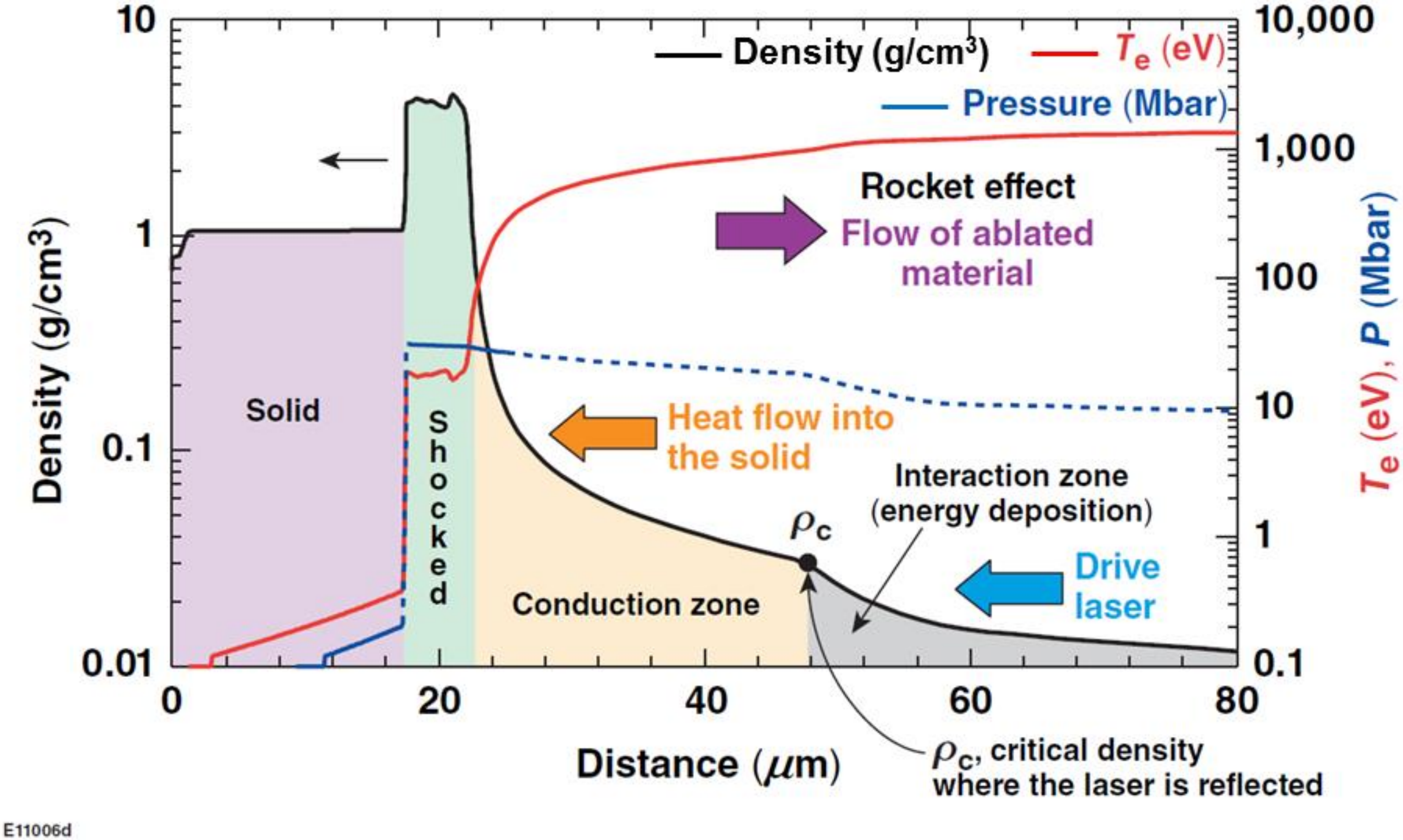

LLE viewgraph database
Danae Nicole Polsin, PhD Thesis, U of Rochester, 2018

The powder x-ray diffraction image plate (PXRDIP) package for studying the shock phenomena

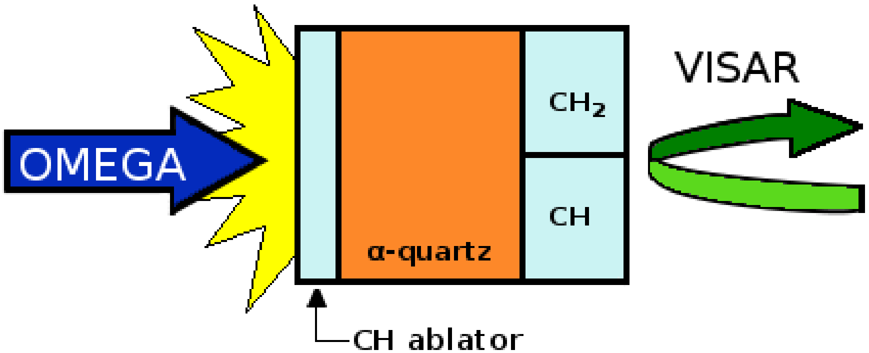

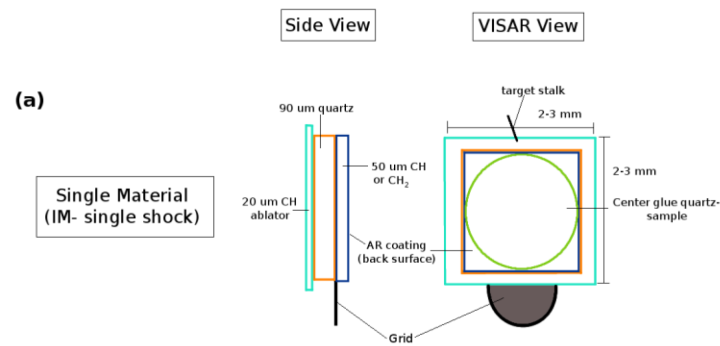

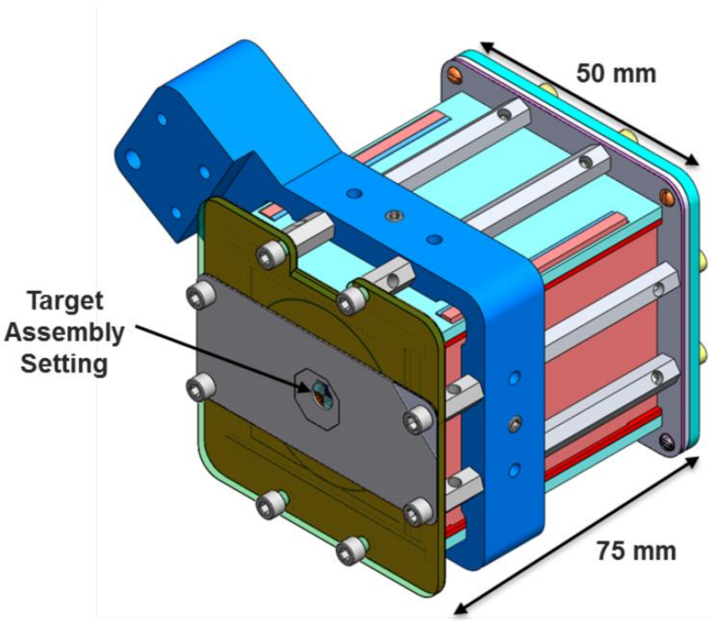

16 Omega beams

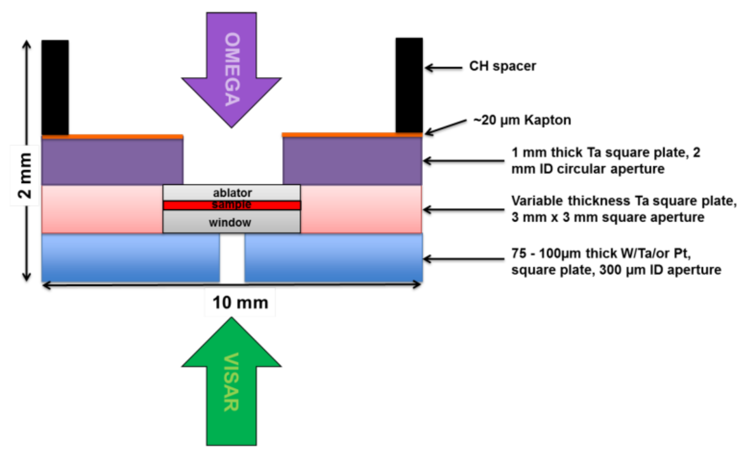

Maria Alejandra Barrios Garcia, PhD Thesis, U of Rochester, 2010
Danae Nicole Polsin, PhD Thesis, U of Rochester, 2018
J. R. Rygg, etc., Rev. Sci. Instrum. 83, 113904 (2012)

The PXRDIP box in the chamber

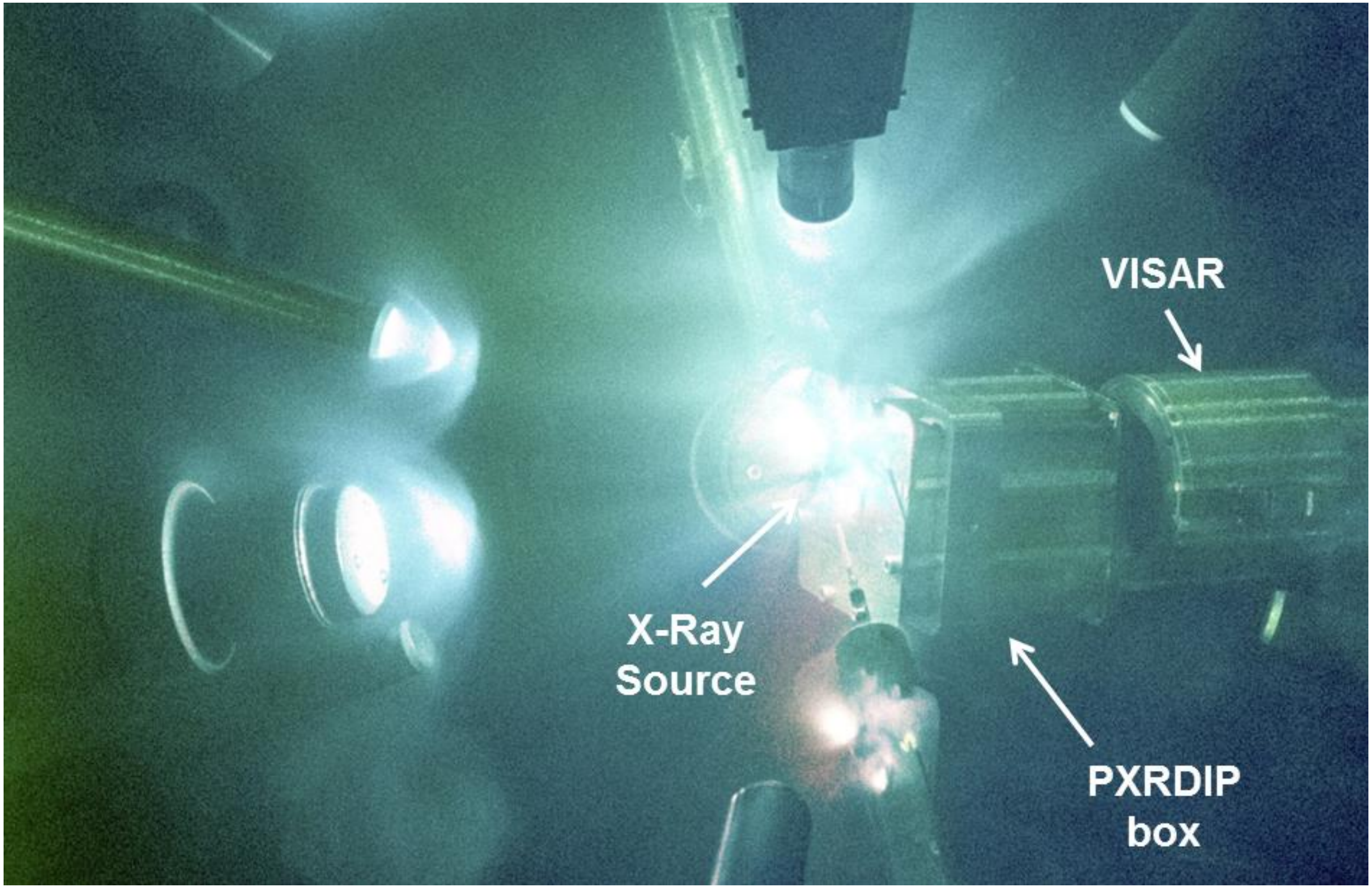

Danae Nicole Polsin, PhD Thesis, U of Rochester, 2018

Interference pattern shifts when a shock breakouts

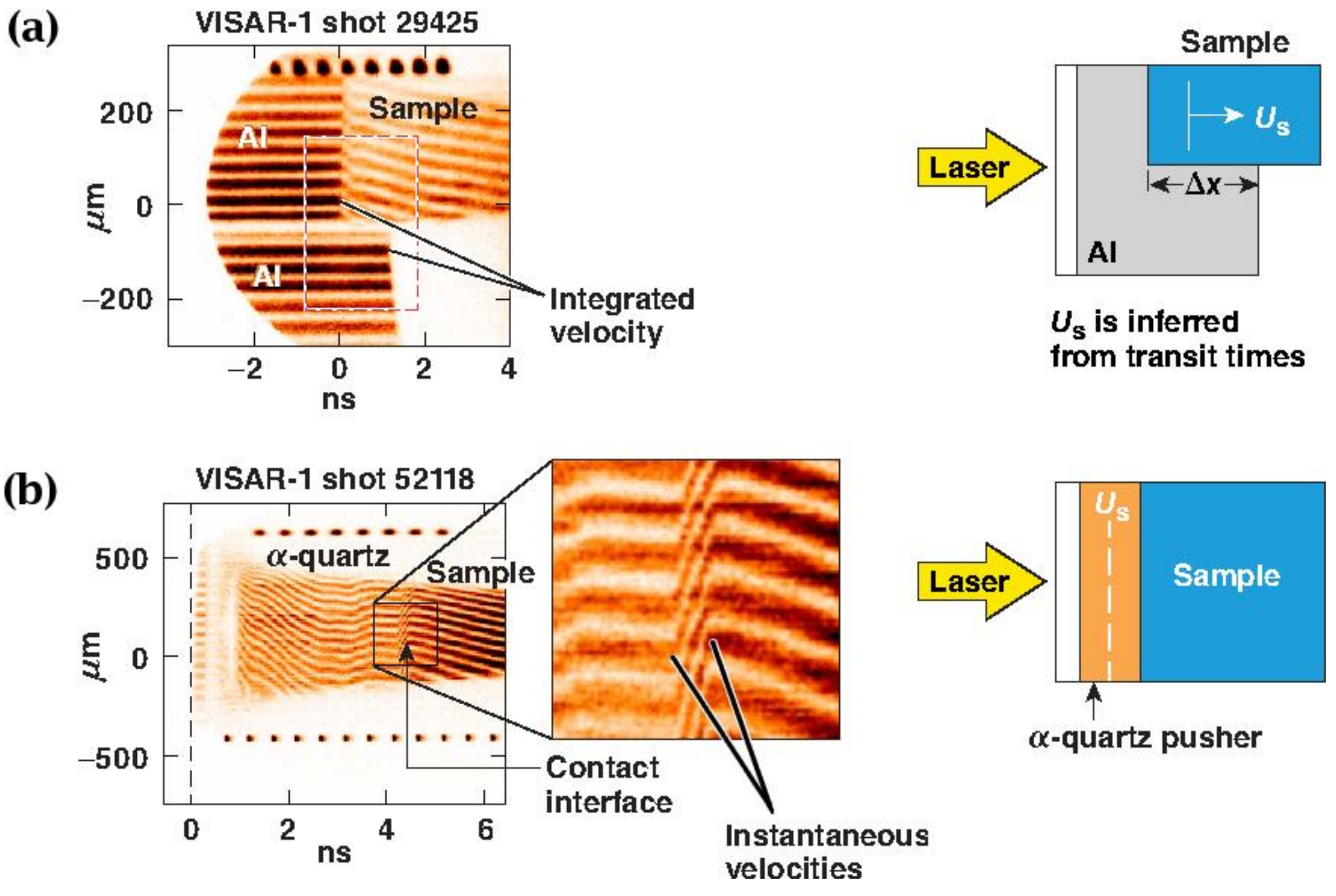

Maria Alejandra Barrios Garcia, PhD Thesis, U of Rochester, 2010

The pressure studied using high-power laser is in the range of 1 TPa (10 Mbar)

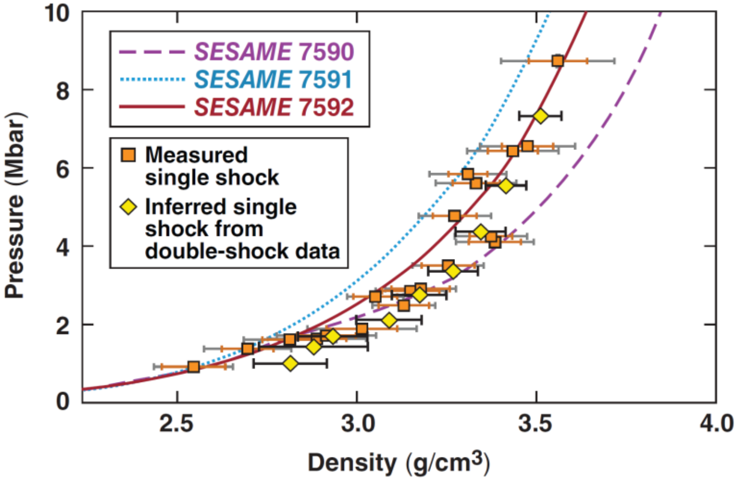

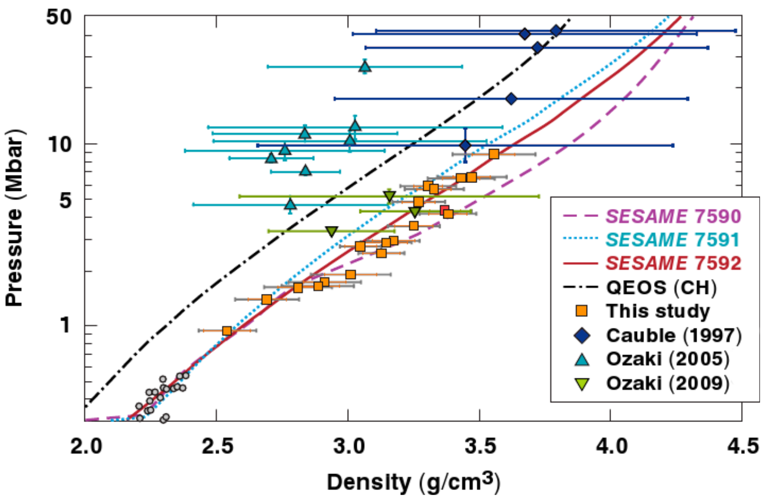

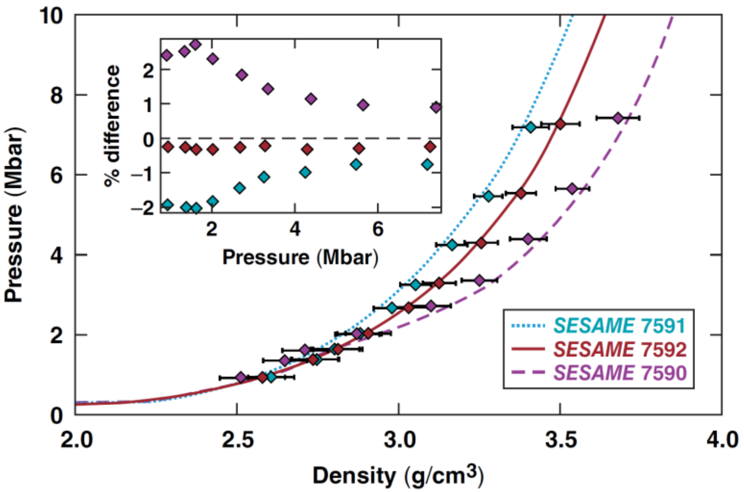

Maria Alejandra Barrios Garcia, PhD Thesis, U of Rochester, 2010

A flyer plate can be used to as the “piston” to generate the shock in a sample

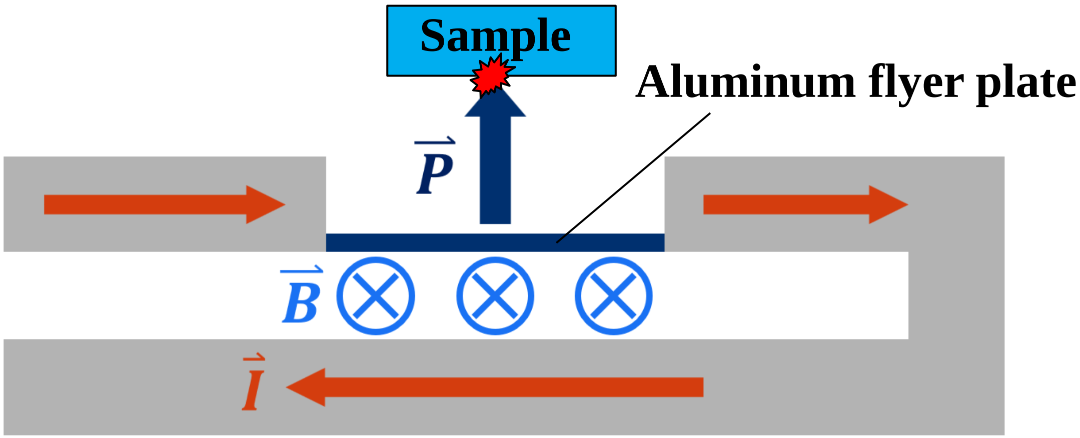

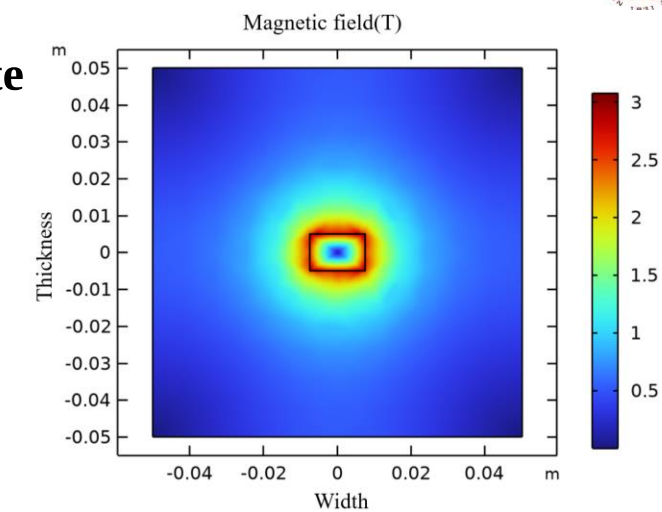

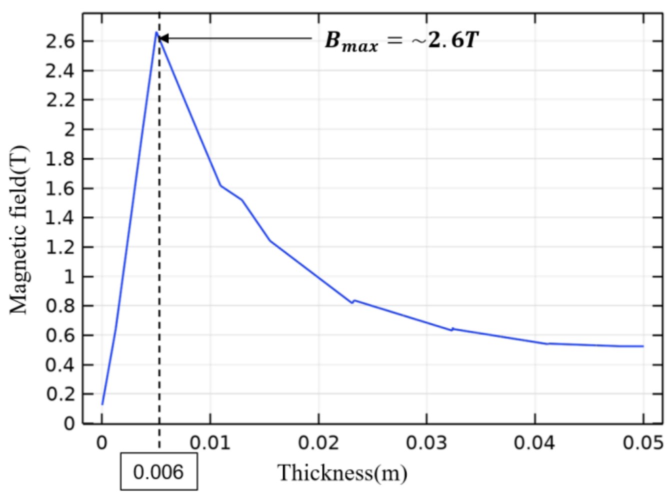

$$B = \frac{\mu_0 I}{w}$$

$$P = \frac{B^2}{2\mu_0} = \frac{\mu_0 I^2}{2w^2}$$

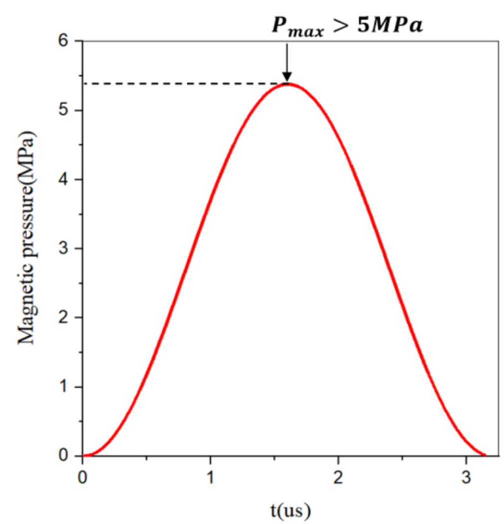

Y.-Z. Pan, Science day, College of Science, NCKU 2023

Sandia's Z machine is the world's most powerful and efficient laboratory radiation source

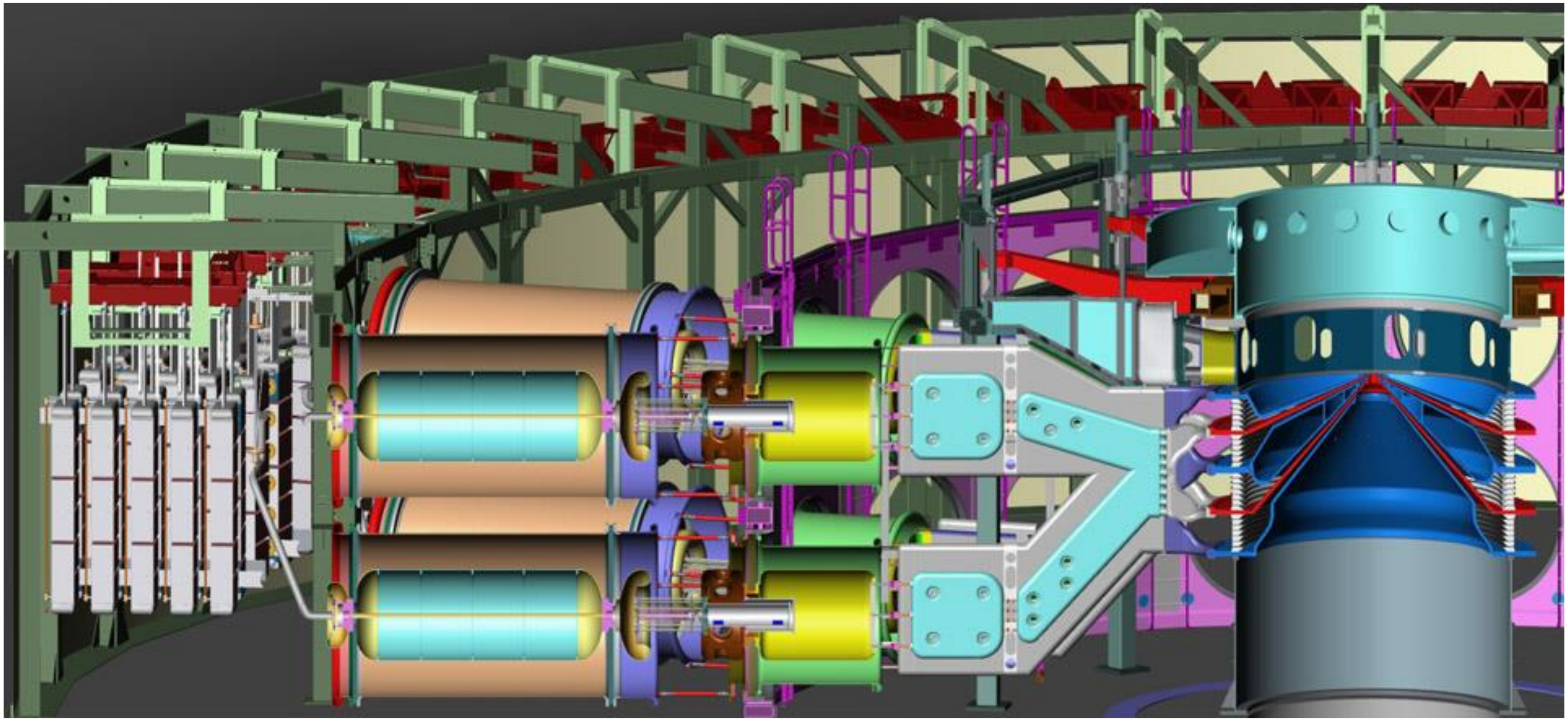

- Stored energy: 20 MJ
- Marx charge voltage: 85 kV
- Peak electrical power: 85 TW
- Peak current: 26 MA
- Rise time: 100 ns
- Peak X-ray emissions: 350 TW
- Peak X-ray output: 2.7 MJ

Z machine discharge

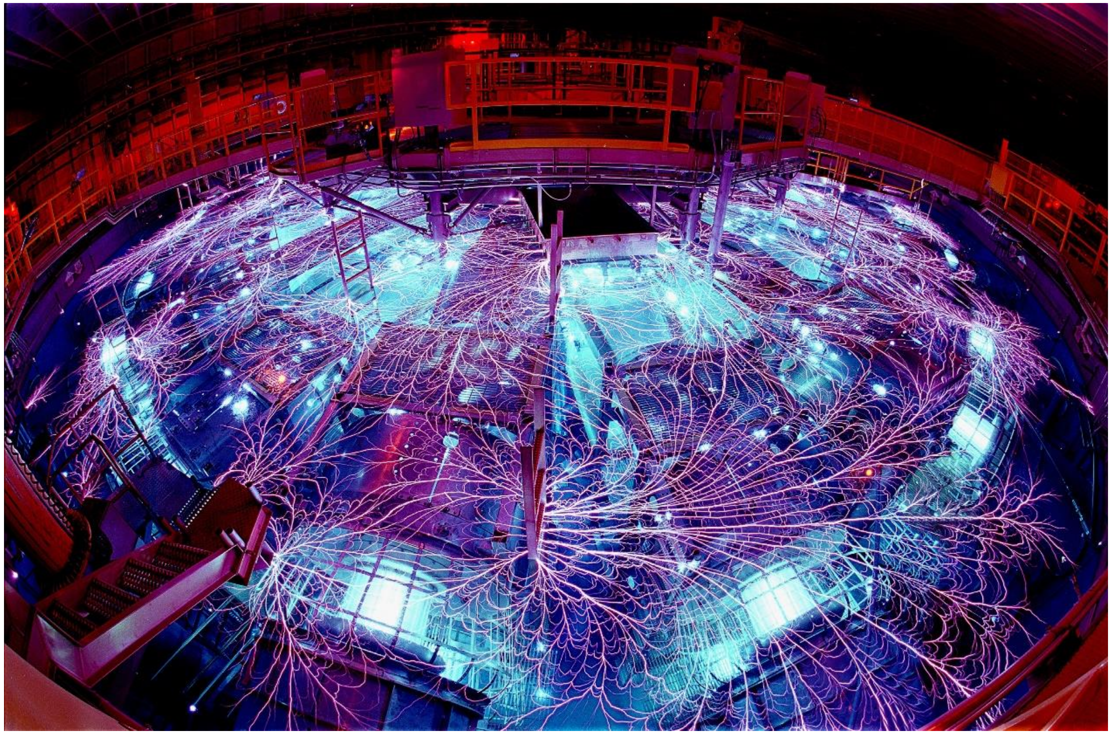

Z machine

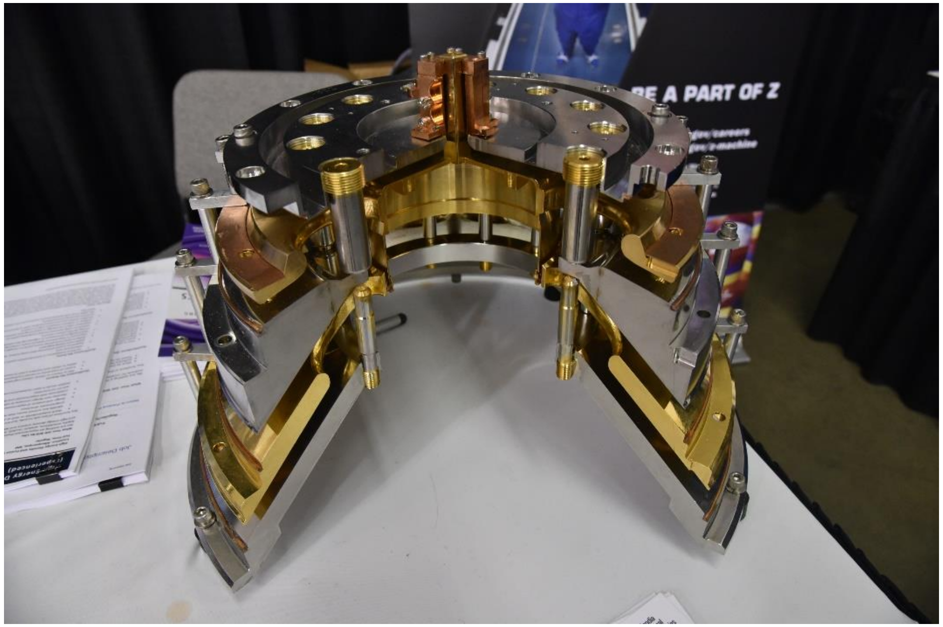

The flyer plate used in the Z machine

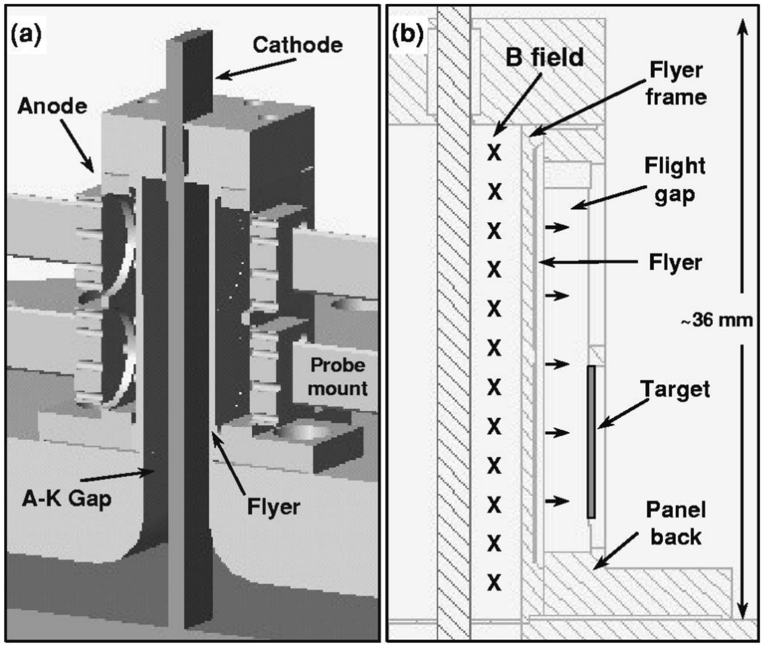

M. D. Knudson, etc., J. Applied Physics 94, 4420 (2003)
https://newsreleases.sandia.gov/releases/2005/nuclear-power/z-saturn.html
Pulsed Power Driven Experiments in the Institute of Shock Physics, by Simon Bland

Before and after shots

- **Before shots**

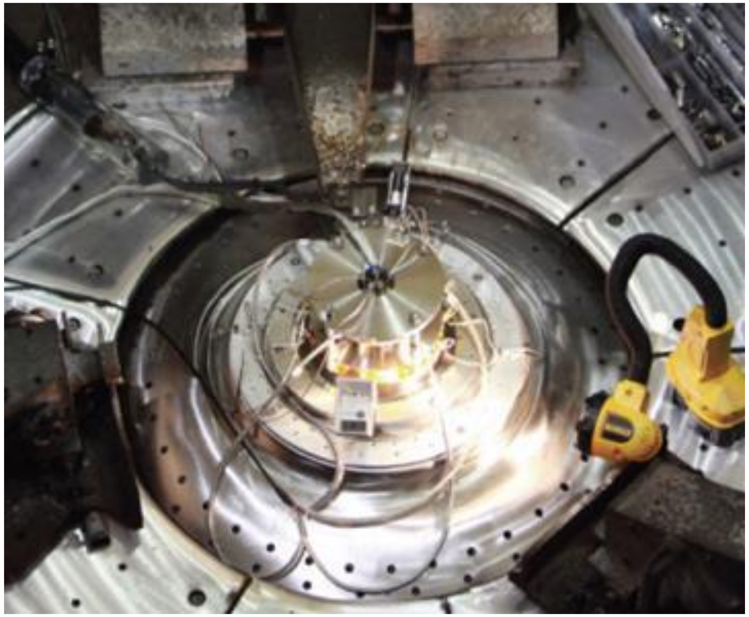

- **After shots**

SAND2017-0900PE_The sandia z machine - an overview of the world's most powerful pulsed power facility.pdf

Imperial College
London

Imperial College MAGPIE facility

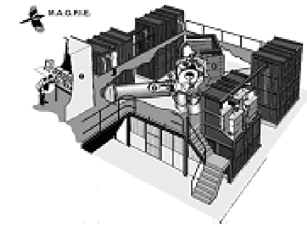

At Imperial the 1.5MA 240 ns MAGPIE generator drives HEDP experiments on a daily basis

Mega
Ampere
Generator for
Plasma
Implosion
Experiments

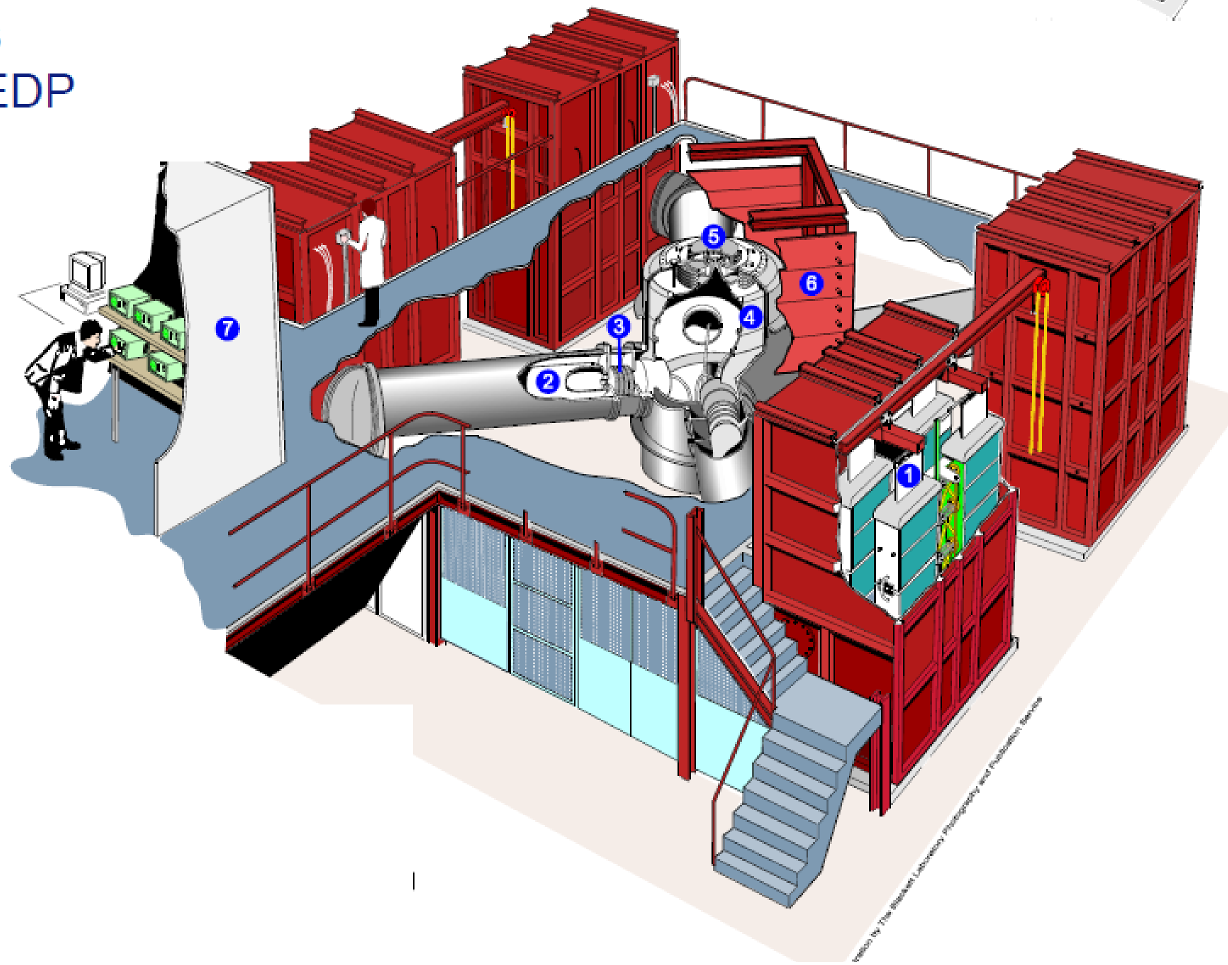

Get experience in magnetically driven isentropic compression experiments

Can also look at shocks in plasmas - e.g. astro relevant radiative shock waves

And using plasma explore new methods of applying high pressures to targets

Imperial College London

Prelude to experiments: new power feed and vacuum chamber

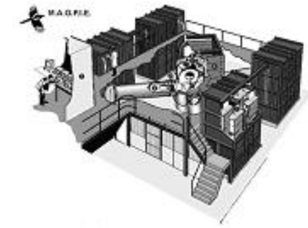

Original vacuum chamber was only ~30cm diameter x 15cm tall

Anode and cathode move by 6mm during vacuum

Water ingress meant vacuum time was 3hrs

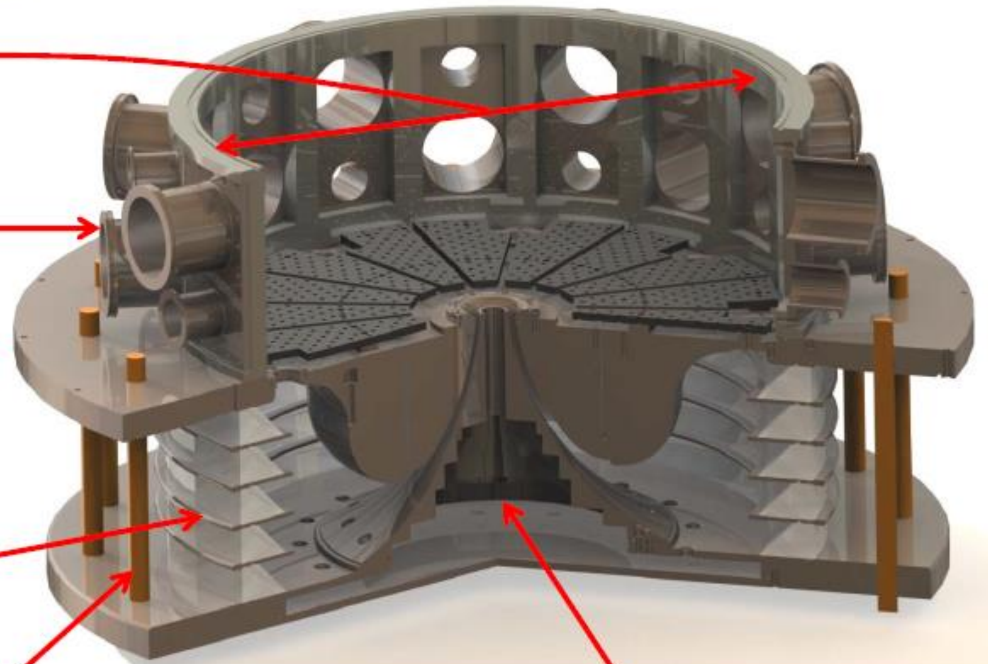

~70cm internal diameter

Chamber surrounded by 16 port plates with ISO100 and ISO 63

Reinforced steel plates to reduce flex

Rexolite diode rings increase strength reduce water absorption

New Torlon bolts don't stretch

Vacuum section below MITL removes force on cathode

Anode and cathode now move ~25um

Vacuum time <1hr

Imperial College London

Initial experiments: Feb 2010

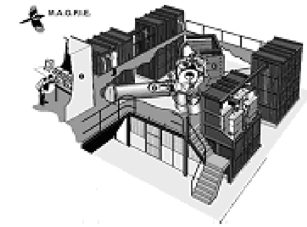

Design and manufacturing issues:

- Will the gap breakdown?
- How uniform is the drive?

EM simulations difficult due to large scale of electrodes c.f. gap in stripline...

=> electrodes designed from simple assumptions and results will serve as test for code

1 – 2 mm gap in stripline

voltages ~200kV

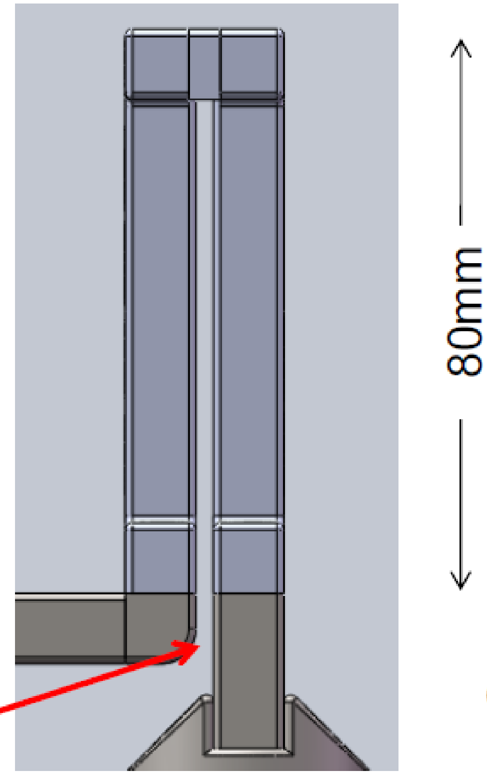

Side view of stripline

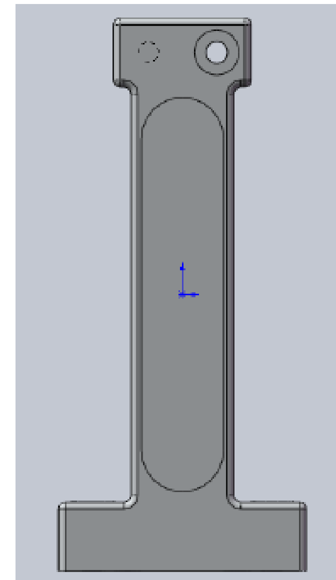

Front view of one electrode with target area outlined

- Need to use a soft material and needs to be easily machined - Copper
- Target thicknesses 1-7mm - shocks expected after ~5mm thickness
- How to support over large areas, polish etc

Imperial College London

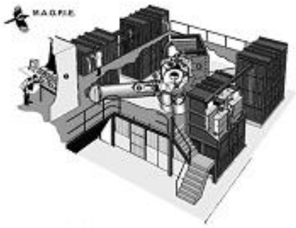

Initial experiments: Feb 2010

Typically for shock experiments:

flatness ~5um, roughness <um via. diamond machining

Overkill for initial experiments (and very expensive)

Tour de Force by Imperial College Instrumentation workshop

2 part ‘glued electrode’ electrode - target area and support

4 axis CNC mill allows fast production of blanks

Precision ground then hand polished – mirror finish ~5um

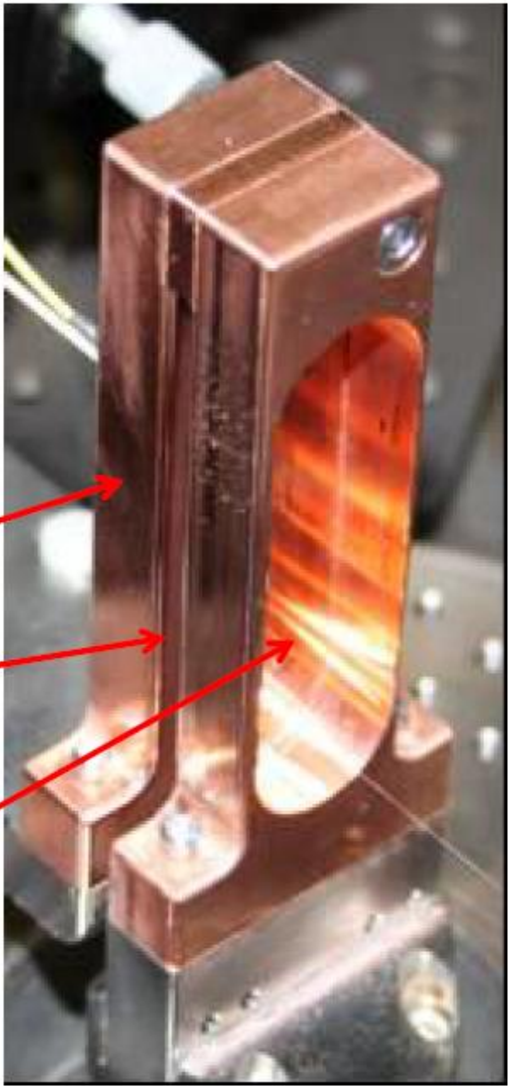

Return electrode

Gap (2mm)

Target area (60x17mm)

Close up of 20mm wide copper strip line in MAGPIE

Imperial College
London

Initial experiments: Feb 2010

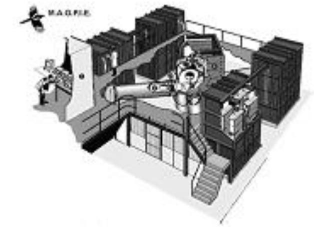

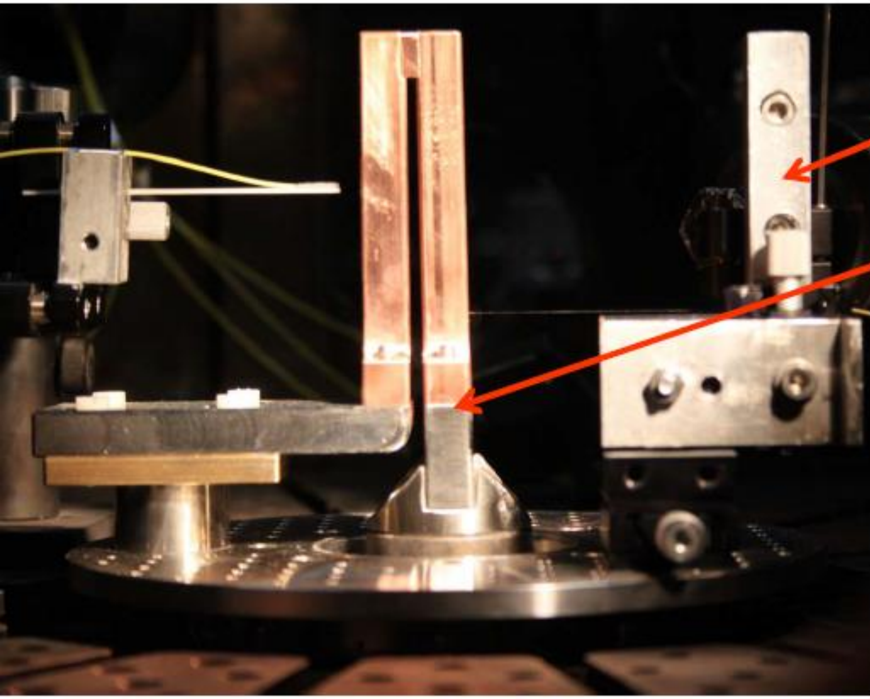

Holder for Het-V probes

Stripline mounted on break away system to prevent damage to MAGPIE

Side view of strip line

Top down view

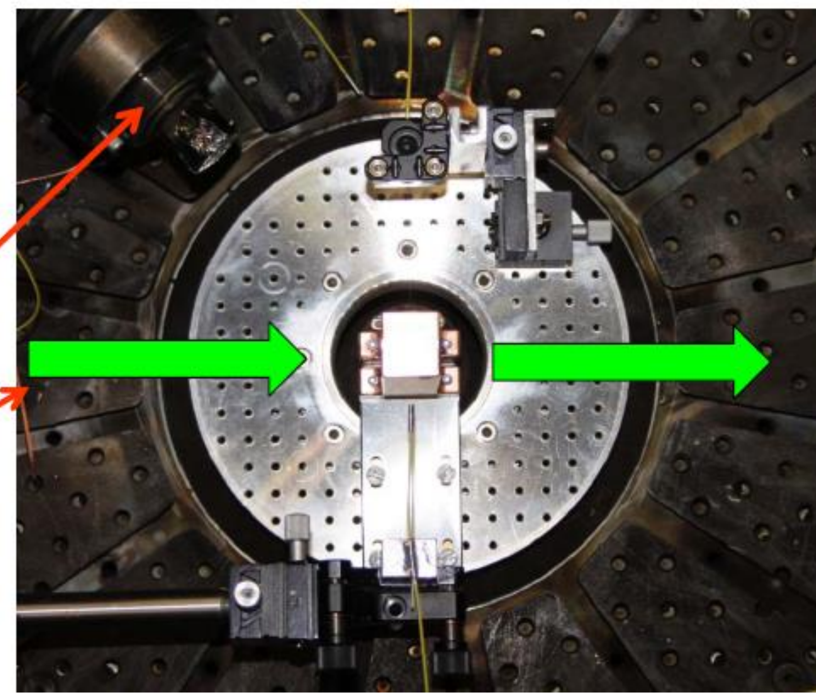

Resistive voltage probe

Path of probing laser

Pulsed Power Driven Experiments in the Institute of Shock Physics, by Simon Bland

½ inch armoured plate top and bottom to 'catch' stripline (not shown)

The design of our flyer-plate launcher

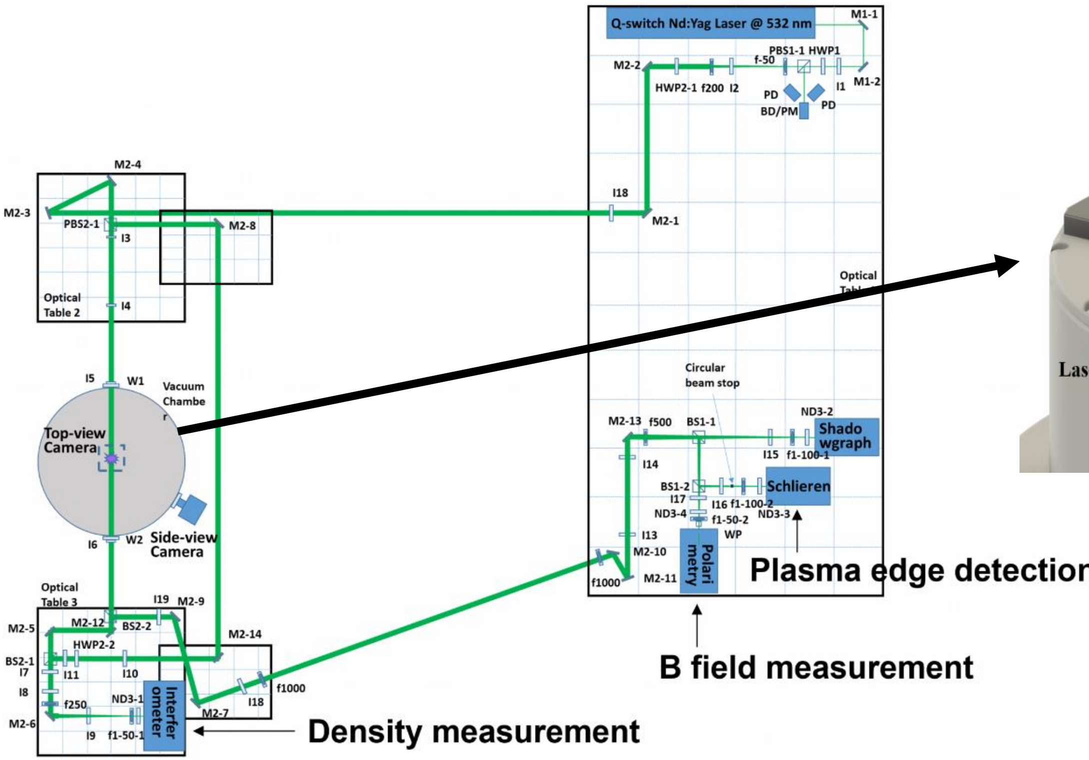

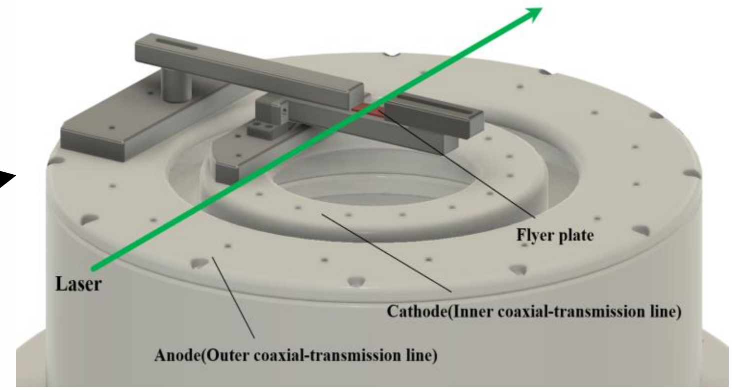

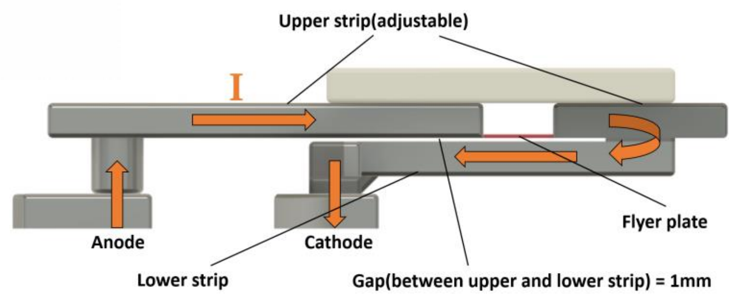

Y.-Z. Pan, Science day, College of Science, NCKU 2023
Y.-Z. Pan, Progress report, Pulsed-Plasma Laboratory 2023

Photos of our flyer-plate launcher

- **Assembly with target**

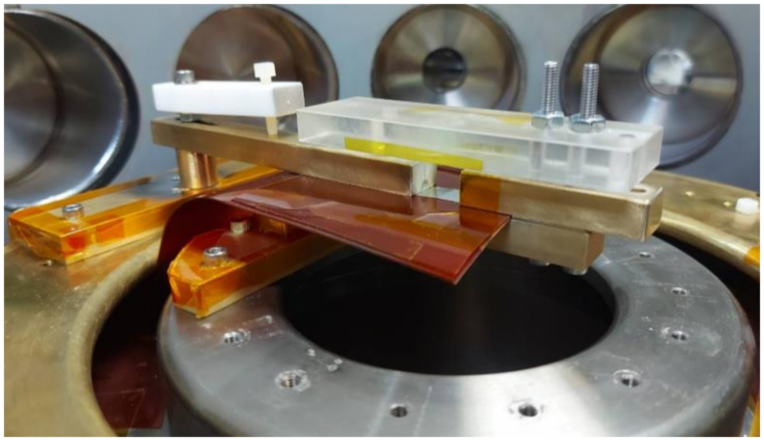

- **Assembly w/o target**

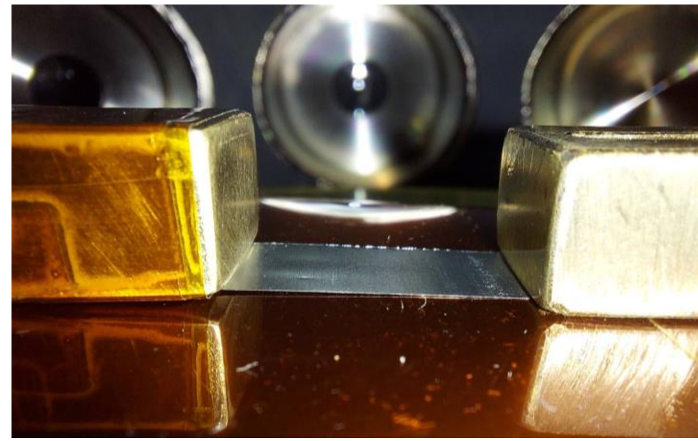

- **Self emission w/o a target**

- **Self emission w/ a target**

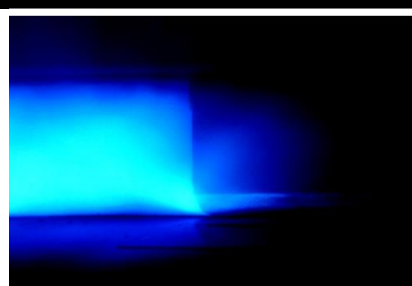

- **After shot**

Y.-Z. Pan, Science day, College of Science, NCKU 2023
Y.-Z. Pan, Progress report, Pulsed-Plasma Laboratory 2023

Velocities of the flyer plate were different when experiments were conducted in 1 atm and in vacuum

- @ ~1 atm

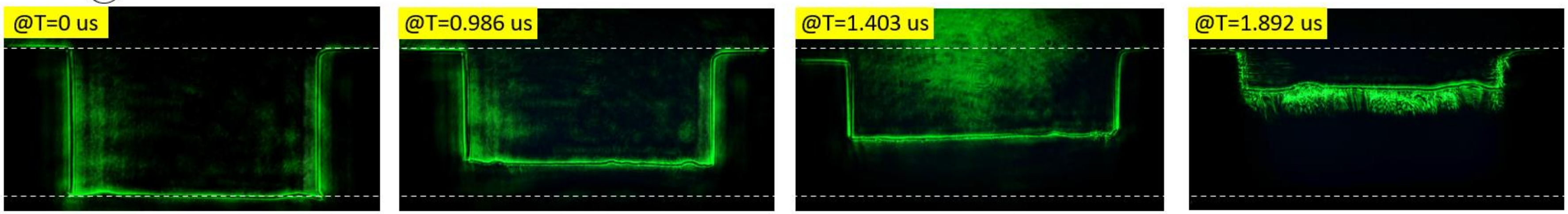

- @ ~10^{-5} torr

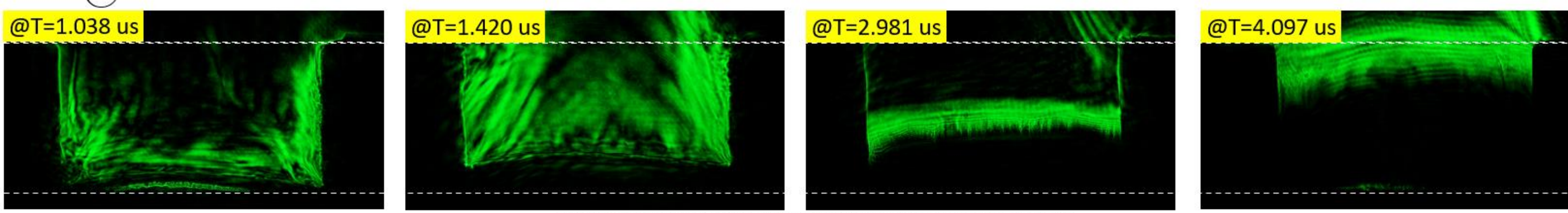

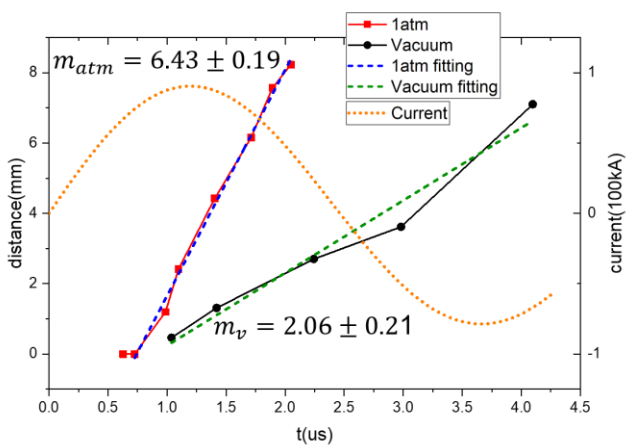

- @ 1 atm

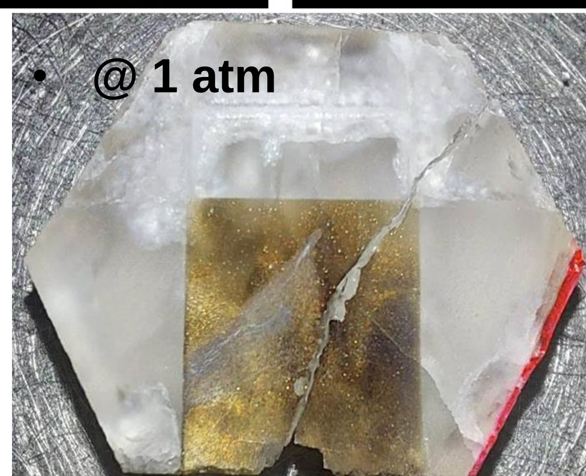

- @ ~10^{-5} torr

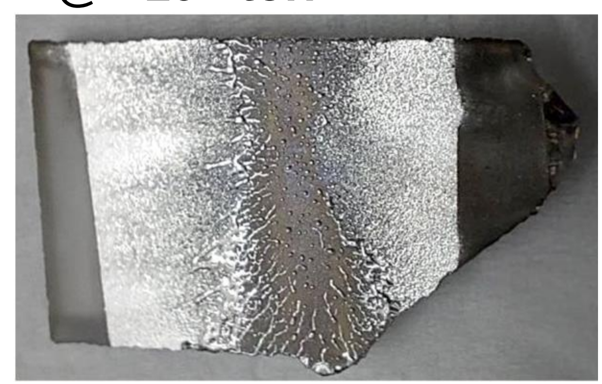

Y.-Z. Pan, Science day, College of Science, NCKU 2023

Raman shift of the SiO2 sample behaved differently after being shocked

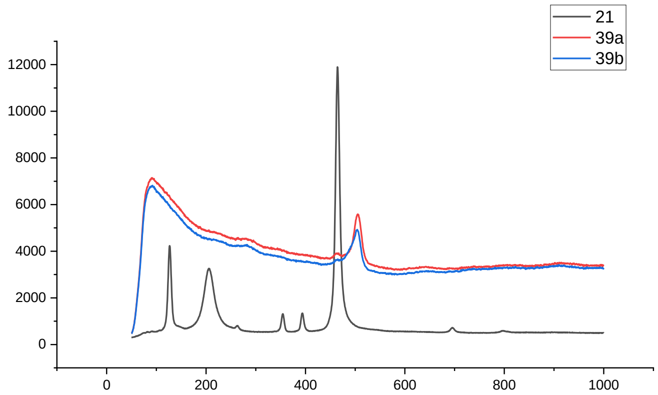

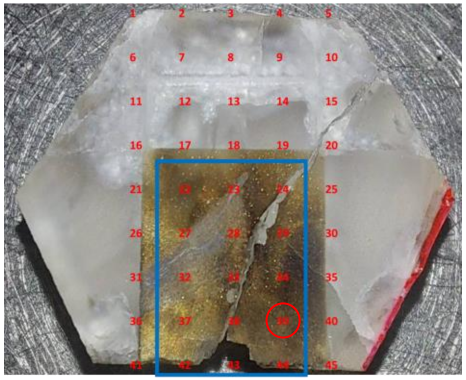

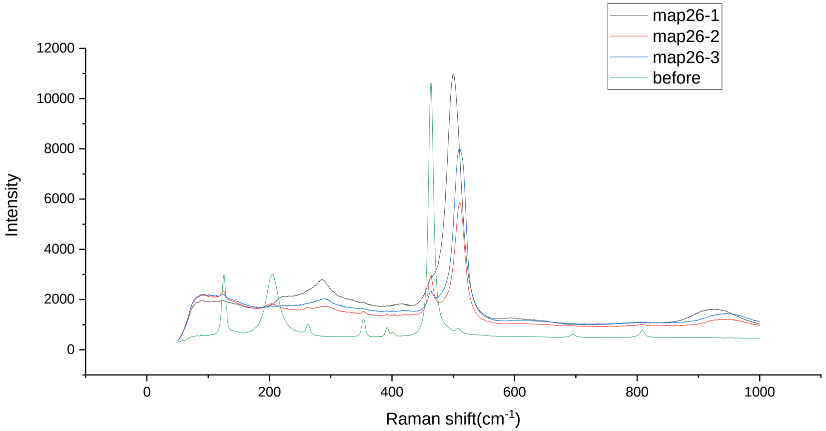

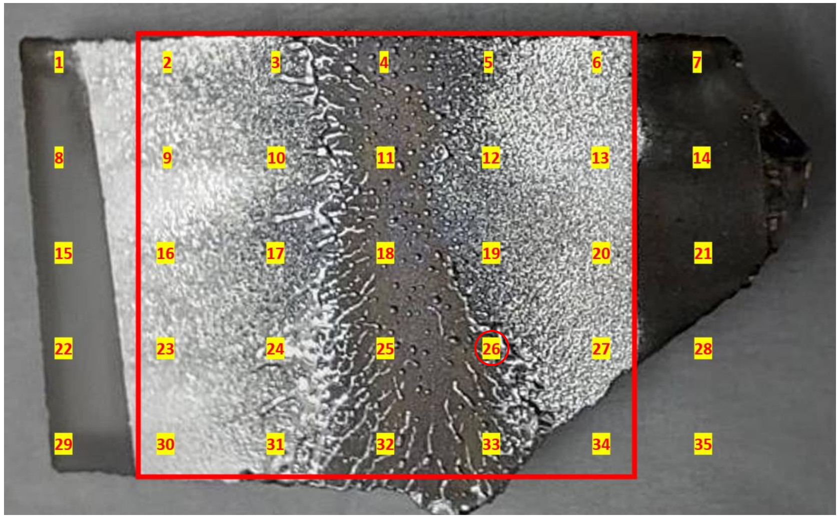

Raman shift of 520 cm-1 was observed suggesting that Coesite was formed

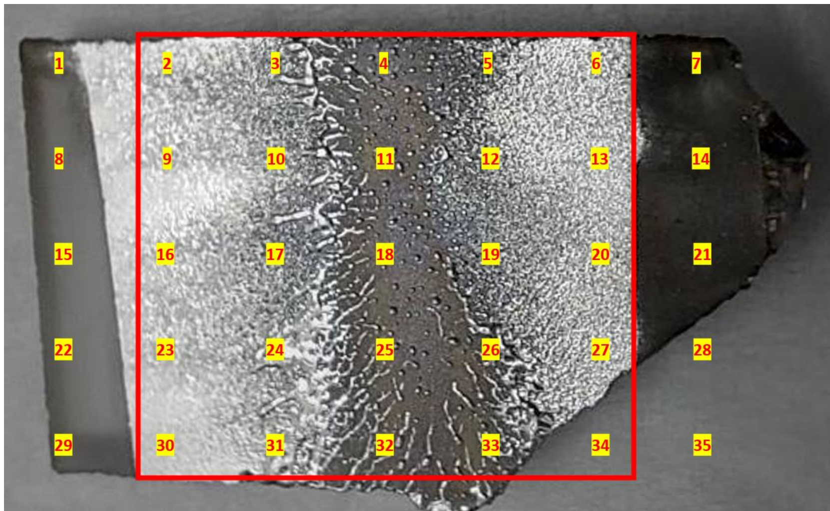

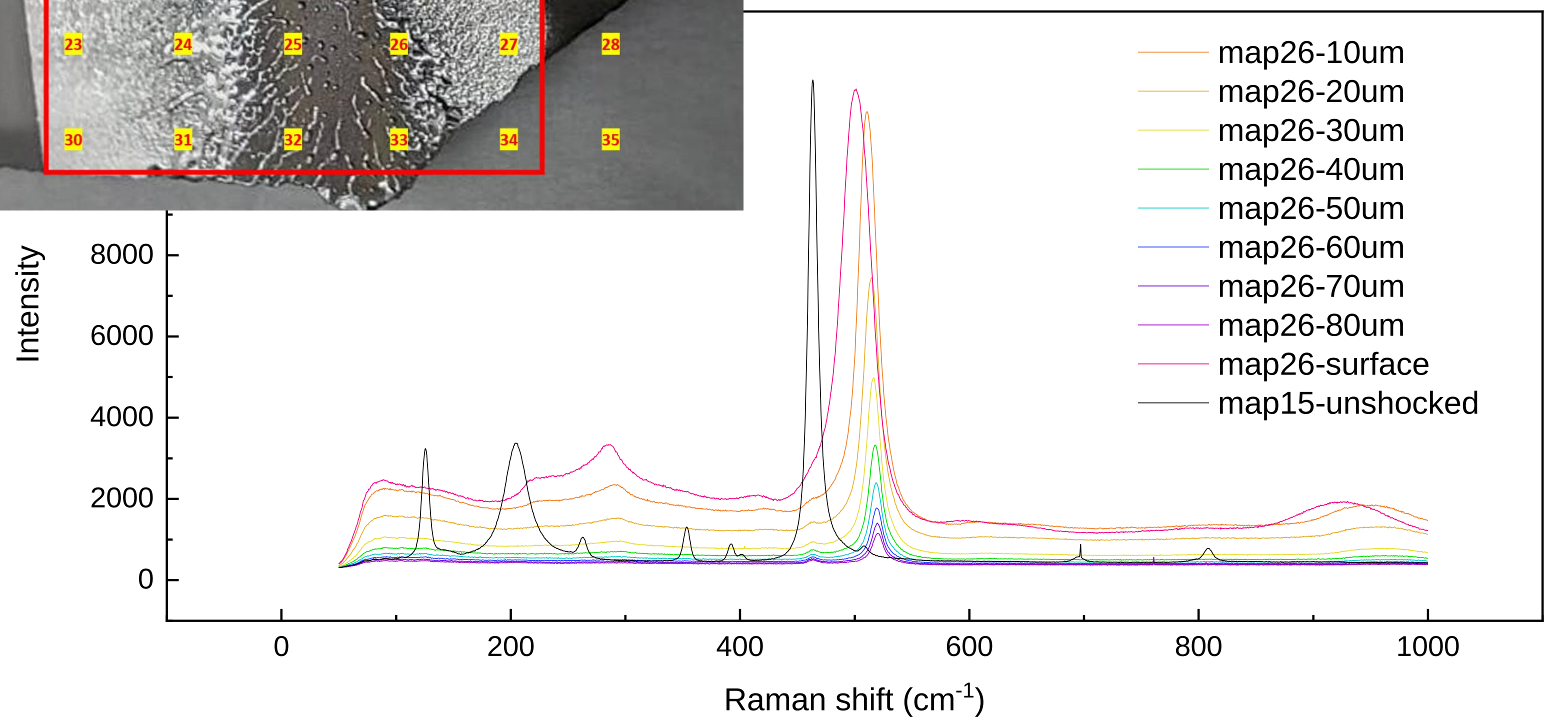

The raman shift indicated that a pressure more than 2 Gpa was generated

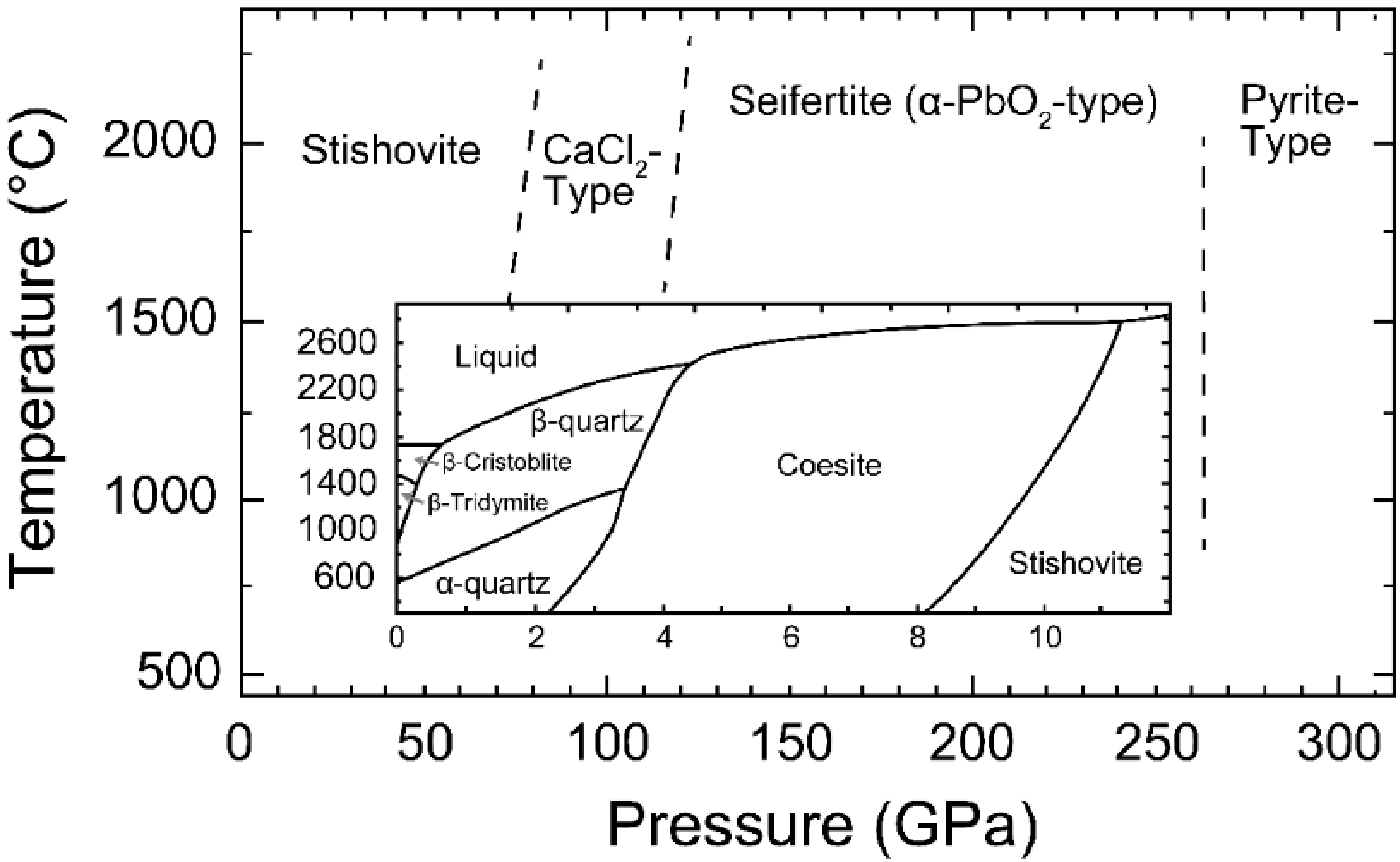

M. Kayama, etc., Minerals 8, 267 (2018)